Human Induced Pluripotent Stem Cells as an *In Vitro* Model for Human Cardiomyocytes to Study Maturation and Metabolism



Heba Hussain A. A. Al-Siddiqi

Merton College

University of Oxford

A thesis submitted for the degree of

Doctor of Philosophy

Trinity 2017

Acknowledgements

First and foremost, I would like to thank my supervisors Professor Carolyn Carr and Dr. Lisa Heather for giving me the opportunity to work on this project and for their guidance and support throughout the course of my D. Phil. Secondly, I would like to thank Qatar Foundation for funding my project. I would also like to thank the head of our research group Professor Kieran Clarke, for her support and for welcoming me in the group.

Second, I would like to thank all the members of the CMRG group for making my time in the lab and office enjoyable. In particular, I would like to thank the Stem Cell group: Dr. Sophia Malandraki-Miller, Dr. Arne A. N. Bruyneel, Dr. Filippo Perbellini, Dr. Khadijeh Pakzad, Colleen Lopez and Rita Alonaizan, for their company in the cell culture room and their friendship, technical help and advice. Next, I would to thank all other group members, Professor Damian Tyler and Drs. Jack Miller, Rhys Evans, Michael Dodd, Brianna Strubbs, Lucia Giles, Cher-Rin Chong, Kerstin Timm and Maria de Luz Fialho, Azrul Bin Abdul Kadir, Vicky Ball, Nicola Dixon, Yvonne Green, Matthew Kerr, and Dragana Savic, for the friendship, advice and the excellent and pleasant working environment.

Third, I would like to thank Dr. Lee Carpentar (NHSBT, John Radcliffe Hospital) and Dr. Sally Cowley (James Martin Stem Cell Facility, University of Oxford) for providing us with the hiPSCs lines and for technical help and support. In addition to Professor Chris Denning and his group (The University of Nottingham) for technical help and support in working with iPS cardiomyocytes. I would also like to thank Colleen Lopez who directly contributed to experiments.

Additionally, I would like to thank all the members of staff in DPAG and other departments for their assistance. In particular, David O'Connor in DPAG, Dr. Alan Wainman of the confocal microscopy facility (Pathology).

Finally, I would like to thank my parents, Hussain Al-Siddiqi and Dawlat Al-Sharkawi for their help and support. I would like to thank my siblings: Haya, Mohammed and Abdullah, my family, and my friends, in particular Dr. Sophia Malandraki-Miller. I would also like to thank Dr. Ayman Bassil, head of research training at Qatar Foundation for his support.

Abstract

This project aimed to generate a mature population of human induced pluripotent stem cell derived cardiomyocytes (hiPSC-CM) which would have the metabolic phenotype of cardiomyocytes in the adult heart as metabolic disorders are strongly linked with cardiovascular disease. Two published differentiation protocols were assessed, and the Wnt-modulation protocol was chosen as it upregulated the gene expression of cardiac genes. In addition, after introducing some alterations, such as transient hypoxia and the addition of Activin A, spontaneously beating human induced pluripotent stem cell derived cardiomyocytes (hiPSC-CMs) were generated.

We characterised the changes in substrate metabolism after differentiation and showed that as hiPSCs are differentiated into beating hiPSC-CMs, there was an increase in both glycolysis and fatty acid oxidation, associated with changes in mRNA expression of glucose and fatty acid metabolism genes. Addition of a PPAR-α agonist (WY14643) to hiPSCs during differentiation did not induce changes in gene expression or substrate metabolism, however addition of the agonist in combination with oleic acid to beating hiPSC-CMs upregulated fatty acid oxidation and respiratory reserve capacity. Interestingly, in beating hiPSC-CM, the addition of oleic acid alone upregulated pyruvate oxidation but not that of oleic acid. There was no change in glycolytic flux with either treatment, suggesting that although activation of PPAR-α increased the capacity of the cells for fatty acid oxidation, they could generate sufficient energy from the high glucose in the culture medium via glycolysis.

In conclusion, as hiPSC-CMs are differentiated there is an upregulation in both glycolysis and fatty acid oxidation. This maturation of metabolism can be further enhanced when

PPAR-α is activated using WY14643 in the presence of fatty acids. This provides a method to metabolically mature hiPSC-CMs, so that they more closely resemble mature cardiomyocytes.

Contents

Contents

1 INTRODUCTION AND LITERATURE REVIEW 2
1.1 CARDIOVASCULAR DISEASE AND REGENERATIVE MEDICINE 2
1.2 BONE MARROW-DERIVED CELLS 3
1.3 ADULT CARDIAC STEM CELLS 4
1.4 HUMAN EMBRYONIC AND HUMAN INDUCED PLURIPOTENT STEM CELLS 5
1.5 HUMAN INDUCED PLURIPOTENT STEM CELL DERIVED CARDIOMYOCYTES 7
1.6 WHY STUDY METABOLISM IN THE HEART? 8
1.7 METABOLISM OF THE HUMAN HEART DURING DEVELOPMENT 10
1.7.1 Metabolism of the Foetal Heart 11
1.7.2 Metabolism of the Neonatal and Adult Heart 12
1.8 SUBSTRATE METABOLISM 14
1.8.1 Fatty Acids 14
1.8.2 Fatty Acid Digestion and Absorption 15
1.8.3 Fatty Acid Oxidation 18
1.8.4 Regulation of Fatty Acid Transport and Oxidation 19
1.8.5 Glucose Metabolism: Glycolysis and Pyruvate Oxidation 21
1.8.6 Glucose Metabolism Regulation 23

AIMS AND HYPOTHESIS OF THESIS 25

2 MATERIALS AND METHODS 27
2.1 CELL CULTURE OF HUMAN INDUCED PLURIPOTENT STEM CELLS 27
2.1.1 Human Induced Pluripotent Stem Cell Lines 27
2.1.2 Maintenance and Expansion of C19 Human Induced Pluripotent Stem Cell Line .. 28
2.1.3 Maintenance and Expansion of OX1-19 Human Induced Pluripotent Stem Cell Line 28
2.2 THE DIFFERENTIATION OF HUMAN INDUCED PLURIPOTENT STEM CELLS INTO BEATING CARDIOMYOCYTES 29
2.2.1 Cardiac Differentiation using Activin A, BMP4 and bFGF[22] 29
2.2.2 Cardiac Differentiation via Small Molecules Modulators of Wnt Signalling[80–82] ... 30
2.3 DISSOCIATION OF BEATING HUMAN INDUCED PLURIPOTENT STEM CELL-DERIVED CARDIOMYOCYTES 31
2.4 CELL COUNTING 32
2.5 RNA EXTRACTION AND CDNA SYNTHESIS 32
2.6 REAL-TIME QUANTITATIVE REVERSE-TRANSCRIPTION POLYMERASE CHAIN REACTION 33
2.6.1 qRT-PCR and TaqMan® Gene Expression Assay 33
2.6.2 qRT-PCR Data Analysis 36
2.6.3 Writing of Gene Symbols 36
2.7 IMMUNOCYTOCHEMISTRY (ICC) AND CONFOCAL IMAGING 36
2.8 MITOCHONDRIAL MEMBRANE POTENTIAL VIA LIVE MITO-TRACKER STAINING 37
2.8.1 Cell Preparation and Staining 37
2.8.2 Imaging and Analysis 38
2.9 OXYGEN CONSUMPTION RATE MEASUREMENTS USING THE CLARK OXYGEN ELECTRODE 38
2.9.1 Reagents, Drugs and Substrate Preparation 38

2.9.2 Cell Preparation ... *38*
2.9.3 Measurement of O_2 Consumption Rate using the Clark Oxygen Electrode ... *39*
2.9.4 Reserve Respiratory Capacity ... *40*
2.10 EXTRACELLULAR GLUCOSE CONSUMPTION AND LACTATE PRODUCTION ... 40
2.11 *IN VITRO* GLUCOSE UTILIZATION USING 5-^{3}H-GLUCOSE ... 40
2.11.1 Reagent Preparation ... *43*
2.11.2 Culturing Cells with [5-^{3}H]–Glucose ... *43*
2.11.3 Dowex Preparation and Scintillation Measurements ... *43*
2.12 STATISTICAL ANALYSIS ... 44

3 DIFFERENTIATION OF HUMAN INDUCED PLURIPOTENT STEM CELLS INTO BEATING CARDIOMYOCYTES ... 46

3.1 ABSTRACT ... 46
3.2 INTRODUCTION ... 47
3.2.1 HEART DEVELOPMENT ... 47
3.2.2 HYPOXIA IN HEART DEVELOPMENT ... 50
3.2.3 HUMAN INDUCED PLURIPOTENT STEM CELLS DIFFERENTIATION INTO BEATING CARDIOMYOCYTES: A COMPARISON OF AVAILABLE PROTOCOLS ... 51
3.2.3.1 Development and Enhancement of EB-Based and Monolayer-Based Protocols *52*
3.2.3.2 Development and Enhancement of Activin A and BMP4-Based Protocols ... *53*
3.2.3.3 Development and Enhancement of Wnt-Based Protocols ... *54*

3.3 AIM OF CHAPTER ... 59

3.4 MATERIALS AND METHODS ... 59
3.4.1 HUMAN INDUCED PLURIPOTENT STEM CELLS ... 59
3.4.2 HUMAN INDUCED PLURIPOTENT STEM CELLS DIFFERENTIATION INTO BEATING CARDIOMYOCYTES ... 60
3.4.2.1 Differentiation using Activin A, BMP4, and bFGF (refered to as Protocol 1) ... *60*
3.4.2.2 Differentiation using Wnt Signalling Modulation (refered to as Protocol 2) ... *60*

3.5 RESULTS ... 61
3.5.1 SIMILARITIES AND DIFFERENCES BETWEEN HUMAN INDUCED PLURIPOTENT STEM CELLS LINES ... 61
3.5.1.1 Culture and Morphology of Human Induced Pluripotent Stem Cells ... *61*
3.5.1.2 Pluripotent Markers of Human Induced Pluripotent Stem Cells ... *62*
3.5.1.3 Metabolism of Human Induced Pluripotent Stem Cells ... *64*
3.5.1.4 Effect of Hypoxia Culture (5% O_2) on Metabolism of Human Induced Pluripotent Stem Cells *64*
3.5.2 HUMAN INDUCED PLURIPOTENT STEM CELLS DIFFERENTIATION INTO BEATING CARDIOMYOCYTES ... 65
3.5.2.1 Differentiation of C19 Line into Beating Human Induced Pluripotent Derived Cardiomyocytes ... *67*
3.5.2.2 The Differentiation of OX1-19 hiPSC line into Beating Cardiomyocytes ... *78*

3.6 DISCUSSION ... 84
3.6.1 SIMILARITIES AND DIFFERENCES BETWEEN HUMAN INDUCED PLURIPOTENT STEM CELL LINES: PLURIPOTENCY AND METABOLISM ... 84
3.6.2 HUMAN INDUCED PLURIPOTENT STEM CELLS DIFFERENTIATION INTO BEATING CARDIOMYOCYTES: C19 LINE ... 86
3.6.2.1 Comparison between Protocol 1 and Protocol 2 ... *86*
3.6.2.2 Alteration 1 to Protocol 2 (Transient Hypoxia) ... *87*

3.6.3 HUMAN INDUCED PLURIPOTENT STEM CELLS DIFFERENTIATION INTO BEATING CARDIOMYOCYTES – THE OX1-19 LINE: OPTIMISATION OF THE ALTERED WNT-MODULATION PROTOCOL 89
3.6.4 IMMATURITY OF HUMAN INDUCED PLURIPOTENT STEM CELL DERIVED BEATING CARDIOMYOCYTES 91

3.7 SUMMARY 91

4 THE METABOLISM IN HUMAN INDUCED PLURIPOTENT STEM CELLS AND THEIR DIFFERENTIATED BEATING CARDIOMYOCYTES 93

4.1 ABSTRACT 93

4.2 INTRODUCTION 94
4.2.1 METABOLISM IN HUMAN PLURIPOTENT STEM CELLS 94
4.2.1.1 Metabolism during Embryogenesis and in Human Embryonic Stem Cells 94
4.2.1.2 Metabolism during the Nuclear Reprogramming of Human Induced Pluripotent Stem Cells 95
4.2.1.3 Metabolism in Human Induced Pluripotent Stem Cells 96
4.2.2 METABOLISM SHIFT IN HUMAN INDUCED PLURIPOTENT STEM CELL-DERIVED CARDIOMYOCYTES 97

4.3 AIM OF CHAPTER 97

4.4 METHODS 98
4.4.1 FATTY ACID UPTAKE AND OXIDATION 98
4.4.2 GLUCOSE UPTAKE AND METABOLISM 99
4.4.3 MITOCHONDRIA MORPHOLOGY AND FUNCTION 100

4.5 RESULTS 101
4.5.1 THE DIFFERENCE IN FATTY ACID METABOLISM IN HUMAN INDUCED PLURIPOTENT STEM CELLS AND THEIR DIFFERENTIATED BEATING CARDIOMYOCYTES 101
4.5.1.1 Fatty Acid Metabolic Gene Expression CD36, ACSL1, CPT1B, and MCAD ... 101
4.5.1.2 Oxygen Consumption Rate Measurement using Fatty Acid (Oleic Acid) as Energy Substrate 102
4.5.2 THE DIFFERENCE IN GLUCOSE UPTAKE AND METABOLISM BETWEEN HUMAN INDUCED PLURIPOTENT STEM CELLS AND THEIR DIFFERENTIATED CARDIOMYOCYTES 104
4.5.2.1 Glucose Metabolism Gene Expression of GLUT1, GLUT4, PFKM, PDHA1, and PDK4 104
4.5.2.2 Oxygen Consumption Rate Measurement using Pyruvate and Malate as Energy Substrates 106
4.5.2.3 Glycolytic Flux using in Vitro ^{3}H-glucose utilization in Human Induced Pluripotent Stem Cells and their Differentiated Cardiomyocytes 107
4.5.2.4 Mitochondria and TCA cycle in Human Induced Pluripotent Stem Cells and their Differentiated Beating Cardiomyocytes 110

4.6 DISCUSSION 113
4.6.1 THE SWITCH IN METABOLISM AS HUMAN INDUCED PLURIPOTENT STEM CELLS ARE DIFFERENTIATED INTO BEATING CARDIOMYOCYTES 113
4.6.2 METABOLISM OF FATTY ACIDS IN HUMAN INDUCED PLURIPOTENT STEM CELLS AND THEIR DIFFERENTIATED BEATING CARDIOMYOCYTES 114
4.6.3 METABOLISM OF GLUCOSE IN HUMAN INDUCED PLURIPOTENT STEM CELLS AND THEIR DIFFERENTIATED BEATING CARDIOMYOCYTES 115
4.6.4 MITOCHONDRIA AND TCA CYCLE IN HUMAN INDUCED PLURIPOTENT STEM CELLS AND THEIR DIFFERENTIATED BEATING CARDIOMYOCYTES 117

4.6.4.1 Mitochondrial Structural and Morphology 117
4.6.4.2 Mitochondrial Bioenergetics Dependent on the Energy Substrate Oxidised 117
4.6.4.3 TCA Cycle 118

4.7 CONCLUSION 119

5 THE EFFECT OF PPAR-A ACTIVATION DURING HUMAN INDUCED PLURIPOTENT STEM CELLS DIFFERENTIATION INTO BEATING CARDIOMYOCYTES 121

5.1 ABSTRACT 121

5.2 INTRODUCTION 122
5.2.1 DEFINITION AND STRUCTURE OF PEROXISOME PROLIFERATOR-ACTIVATED RECEPTORS 122
5.2.2 PPAR ACTIVATION, LIGANDS, AND TARGET GENES 123
5.2.3 PPAR-A IN THE DEVELOPING AND ADULT HEARTS 125
5.2.3.1 PPAR-α Expression, Ligands, and Target Genes in the Heart 125
5.2.3.2 PPAR-α Agonist (WY14643) 126
5.2.4 PPAR-α EXPRESSION AND ACTIVATION DURING CARDIAC DIFFERENTIATION IN MOUSE EMBRYONIC STEM CELLS 126
5.2.5 PPAR-α ACTIVATION IN HEART METABOLISM 127

5.3 AIMS OF CHAPTER 128

5.4 MATERIALS AND METHODS 129
5.4.1 WY14643 TREATMENT DURING THE DIFFERENTIATION OF HUMAN INDUCED PLURIPOTENT STEM CELLS INTO BEATING CARDIOMYOCYTES 129

5.5 RESULTS 131
5.5.1 THE EFFECT OF WY14643 TREATMENT DURING CARDIAC DIFFERENTIATION ON THE EXPRESSION OF *PPARA*, *PGC1A*, AND *PDK4* 131
5.5.2 THE EFFECT OF WY14643 TREATMENT DURING CARDIAC DIFFERENTIATION ON THE EXPRESSION OF CARDIAC GENES 132
5.5.3 THE EFFECT OF WY14643 TREATMENT DURING CARDIAC DIFFERENTIATION ON THE EXPRESSION OF METABOLIC GENES 134
5.5.3.1 Glucose Metabolism 134
5.5.3.2 Fatty Acid Metabolism 136
5.5.3.3 TCA Cycle: 138

5.6 DISCUSSION 140
5.6.1 THE EFFECT OF WY14643 ON THE EXPRESSION OF *PPARA*, *PGC1A*, AND *PDK4* 140
5.6.2 THE EFFECT OF WY14643 ON THE EXPRESSION OF CARDIAC GENES (*MYH6* AND *MYL7*) 141
5.6.3 THE EFFECT OF WY14643 ON THE EXPRESSION OF METABOLIC GENES 142

5.7 CONCLUSION 143

6 METABOLIC MATURATION OF YOUNG BEATING HIPSC-CMS VIA PPAR-A ACTIVATION USING WY14643 AND OLEIC ACID 145

6.1 ABSTRACT 145

6.2 INTRODUCTION 145
6.2.1 MATURATION METHODS OF HUMAN INDUCED PLURIPOTENT STEM CELLS DERIVED CARDIOMYOCYTES 146
6.2.2 OLEIC ACID 151

6.3 AIMS OF CHAPTER 151

6.4 MATERIALS AND METHODS 152

6.4.1 DIFFERENTIATION OF HUMAN INDUCED PLURIPOTENT STEM CELLS INTO BEATING CARDIOMYOCYTES 152

6.4.2 OLEIC ACID TREATMENT 153

6.4.3 WY14643 TREATMENT 153

6.5 RESULTS 154

6.5.1 EFFECT OF OA ALONE OR OA AND WY14643 TREATMENT ON THE ACTIVATION OF PPAR-A IN BEATING HIPSC-CMS BY MEASURING THE RELATIVE GENE EXPRESSION OF *PPARA*, *PGC1A*, *UCP3*, AND *PDK4* 154

6.5.2 EFFECT OF OA ALONE OR OA AND WY14643 TREATMENT ON FATTY ACID OXIDATION IN BEATING HIPSC-CMS 156

6.5.2.1 Relative Gene Expression of Genes Involved in Fatty Acid Oxidation 156

6.5.2.2 Fatty Acid Metabolism in OA alone or OA and WY14643 Pre-Treated Beating Human Induced Pluripotent Stem Cells-Derived Cardiomyocytes using the Clark-Type Oxygen Electrode 159

6.5.3 EFFECT OF OA ALONE OR OA AND WY14643 TREATMENT ON GLUCOSE METABOLISM 161

6.5.3.1 Relative Gene Expression of Genes Involved in Glucose Utilization 161

6.5.3.2 Extracellular Glucose Consumption and Lactate Production 164

6.5.3.3 Glycolytic Flux Measurement via in Vitro ^{3}H-Glucose Utilization 166

6.5.3.4 Pyruvate Oxidation in Pre-Treated Beating Cardiomyocytes 166

6.5.4 EFFECT OF LONG-TERM TREATMENT WITH OA ALONE OR OA AND WY14643 ON METABOLISM IN BEATING HUMAN INDUCED PLURIPOTENT STEM CELLS-DERIVED CARDIOMYOCYTES 168

6.5.4.1 Effect of Long-term Treatment on Fatty Acid Metabolic Gene Expression 168

6.5.4.2 Effect of Long-term Treatment on Glucose Metabolism 170

6.6 DISCUSSION 173

6.6.1 EFFECT OF OA ALONE OR OA AND WY14643 TREATMENT ON BEATING HUMAN INDUCED PLURIPOTENT STEM CELLS-DERIVED CARDIOMYOCYTES 173

6.6.2 EFFECT OF OA ALONE OR OA AND WY14643 TREATMENT ON THE ACTIVATION OF PPAR-α IN BEATING HIPSC-CMS: GENE EXPRESSION OF *PPARA, PGC1A*, *UCP3*, AND *PDK4* 174

6.6.3 EFFECT OF OA ALONE OR OA AND WY14643 TREATMENT ON FATTY ACID METABOLISM 175

6.6.3.1 Gene Expression 175

6.6.3.2 Fatty Acid Metabolism by Measuring Oxygen Consumption Rate using the Clark-Type Oxygen Electrode 177

6.6.4 EFFECT OF OA ALONE OR OA AND WY14643 TREATMENT ON GLUCOSE METABOLISM 178

6.6.4.1 Gene Expression after OA alone or OA and WY14643 Treatment 178

6.6.4.2 Anaerobic Glycolysis and Glycolytic Flux in Young Beating Human Induced Pluripotent Stem Cells Derived Cardiomyocytes 179

6.6.4.3 Pyruvate Oxidation by Measuring Oxygen Consumption Rate using the Clark-Type Oxygen Electrode 179

6.6.5 EFFECT OF LONG-TERM OA ALONE OR OA AND WY14643 TREATMENT (1 WEEK) ON METABOLISM IN BEATING HIPSC-CMS 180

6.8 CONCLUSION 181

7 GENERAL DISCUSSION 182
8 CONCLUSION 186
REFERENCES..... 187

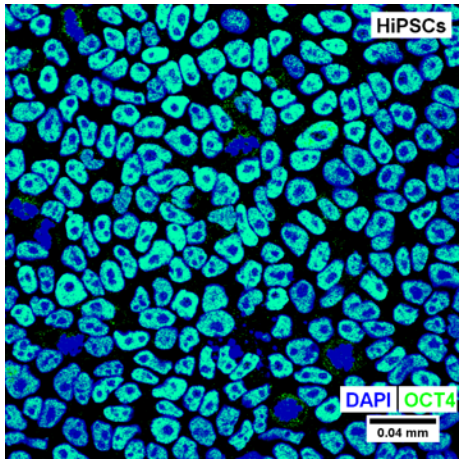
ABBREVIATIONS

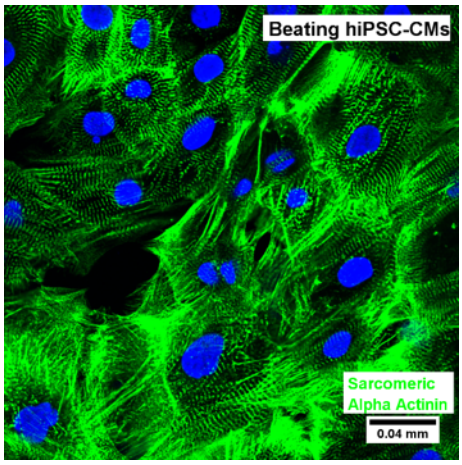
AA	Activin A
ACADM	Acyl CoA dehydrogenase medium-chain
ACADVL	Acyl CoA dehydrogenase very long-chain
ACC	Acyl CoA carboxylase
ACS	Acyl CoA synthetase
ACSL1	Acyl CoA synthetase long-chain 1
ADP	Adenosine diphosphate
AMPK	AMP activated protein kinase
ATP	Adenosine triphophate
bFGF	Basic fibroblast growth factor
βME	β-mercaptoethanol
BMP	Bone morphogenetic protein
BSA	Bovine serum albumin
BTS	N-Benzyl-p-toluenesulfonamide
CAT	Carnitine/acylcarnitine translocase
CD36	CD36 molecule
CDC	Cardiosphere-derived cells
CDS	Cell dissociation solution
CHD	Coronary heart disease
CHIR	Wnt signalling activator
CPT I or II	Carnitine palmitoyl transferase I or II
CPT1 A or B	Carnitine palmitoyl transferase 1 A or B
CS	Citrate synthase
c-kit	Stem cell growth factor receptor
CVD	Cardiovascular diseases
DAPI	Diamidino-2-phenylindole
DMEM/F-12	Dulbecco's modified eagle medium: nutrient mixture F-12

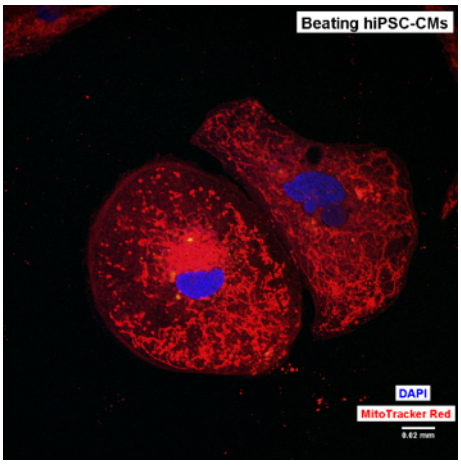
DMSO	Dimethyl sulfoxide
EB	Embryonic body
ECI1	Enoyl-CoA delta isomerase 1
ETC	Electron transport chain
FAO	Fatty acid oxidation
FABP	Fatty acid binding protein
FAT	Fatty acid translocase
FATP	Fatty acid transport protein
$FADH_2$	Flavin adenine dinucleotide
FBS	Fetal bovine serum
FCCP	Carbonylcyanide-p-trifluoromethoxy-phenylhydrazone
GATA4	GATA binding protein - 4
GLUT1	Glucose transporter member 1
GLUT4	Glucose transporter member 4
HADHA	Hydroxyacyl-CoA dehydrogenase, alpha-subunit
Hand 1 or 2	Heart and neural crest derivatives expressed 1 or 2
HEPES	4-(2-hydroxyethyl)-1-piperazineethanesulfonic acid
hESCs	Human embryonic stem cells
hESC-CMs	Human embryonic stem cell-derived cardiomyocytes
HF	Heart failure
HIF 1 α	Hypoxia-inducible factors 1 alpha
hiPSCs	Human induced pluripotent stem cells
hiPSC-CMs	Human induced pluripotent stem cell-derived cardiomyocytes
HK	Hexokinase
ICM	Inner cell mass
IWP	Wnt signaling inhibitor
KDR	Kinase insert domain receptor
LCAD	Long-chain acyl CoA dehydrogenase

LDH	Lactate dehydrogenase
MCD	Malonyl CoA decarboxylase
MESP 1 or 2	Mesoderm posterior 1 or 2
MI	Myocardial infarction
mTOR	Mammalian target of rapamycin
MYH6	Myosin heavy chain 6, alpha
MYH7	Myosin heavy chain 7, cardiac muscle, beta
MYL2	Myosin light chain 2
MYL7	Myosin light chain 7
NADH	Nicotinamide adenine dinucleotide
NKX2.5	NK2 homeobox 5
NR	Nuclear reprogramming
OA	Oleic acid
OCR	Oxygen consumption rate
OGDH	Oxoglutarate (alpha-ketoglutarate) dehydrogenase
PBS	Phosphate-buffered saline
PDH	Pyruvate dehydrogenase
PDHA1	Pyruvate dehydrogenase alpha 1
PDK4	Pyruvate dehydrogenase kinase 4
PFA	Paraformaldehyde
PFK	Phosphofructokinase
PFKM	Phosphofructokinase – muscle isozymes
PGC1A	Peroxisome proliferator-activated receptor gamma, coactivator 1 alpha
PITX2	Paired-like homeodomain transcription factor 2
PK	Pyruvate kinase
PPARA	Peroxisome proliferator-activated receptor alpha
PPP	pentose phosphate pathway
ROCK	Rho associated coil kinase

ROS	Reactive oxygen species
RPMI	Roswell Park Memorial Institute
RRC	Reverse respiratory capacity
RT	Room temperature
qRT-PCR	Real-time quantitative reverse-transcription polymerase chain reaction
SAM	S-adenosyl methionine
Sca-1	Stem cell antigen 1
T2D	Type-2 diabetes
T3	Tri-iodothryonine
TAG	Triacylglycerol
TBX5	T-box transcription factor 5
TCA	Tricarboxylic acid
TDZ	Thiazolidinedione
TGFB	Transforming growth factor beta
TNNT2	Troponin T – type 2
UCP 2 and 3	Mitochondrial uncoupling protein 2 and 3
Wnt	Wnt signalling pathway
Wt1	Wilm's tumor







Chapter 1

Introduction and Literature Review

1 Introduction and Literature Review

1.1 Cardiovascular Disease and Regenerative Medicine

Cardiovascular diseases (CVD) includes diseases of the heart and circulation, and causes more than 26% of all deaths in the UK, with 160,000 deaths a year[1]. In the UK, 7 million people are living with CVD, costing the healthcare system around £9 billion a year[1]. Coronary heart disease (CHD) is the most common type of CVD, with 2.3 million people living with it in the UK and leading to 70,000 deaths a year[1]. It is caused by narrowing of the lumen of the coronary arteries as a result of atherosclerosis and plaque formation, which if not treated eventually lead to blockage of one or more of the arteries that feed the cardiac muscle and myocardial infarction (MI)[2,3]. There is extensive cardiomyocytes loss during the first 24 hours post MI[4]. During the initial ischemic insult, necrosis plays a role in cardiomyocytes death as factors that promote cellular necrosis propagate through gap junctions. Whereas apoptosis, autophagy, and inflammation occur as cardiomyocytes struggle to survive[4]. In the hypoxic cardiomyocytes there is a transition in metabolism from aerobic metabolism to anaerobic metabolism causing acidosis[4]. Removal of hydrogen ions in exchange with Na^+ results in the increase of intracellular Na^+, which is exchanged with Ca^{2+} [4]. Increasing intracellular Ca^{2+} will lead to an increase in H_2O influx and swelling of the mitochondria, which, when ruptured, release cellular compartments that increase apoptosis of cardiomyocytes, which peaks 4.5 hours post MI[4]. In addition, during this hypoxic condition the reduction in ATP levels activates AMP activated protein kinase (AMPK) and inhibits the mammalian target of rapamycin (mTOR) to activate autophagy, which is a process that occurs in healthy cardiomyocytes to remove intracellular proteins and organelles[4]. This results in death of cardiomyocytes, which are replaced by fibroblasts

to form scar tissue[2], followed by remodelling of the heart and thinning of the ventricular wall, affecting contraction and ultimately leading to heart failure (HF). Available pharmacological therapies help by improving the symptoms and delaying the progression of the diseases, however, they do not replace the lost cardiomyocytes. In addition, adult cardiomyocytes are terminally differentiated cells with little or no ability to proliferate and regenerate the heart[5]. It has been shown that in adult cardiomyocytes, cell cycle arrest is induced by the changes in oxygen levels from the low-oxygen hypoxic intrauterine condition to the normoxic environment after birth[6]. Recently it has been reported that adult cardiomyocytes have the ability to re-enter the cell cycle allowing cardiomyocytes proliferation and this re-entry to the cell cycle is induced by the gradual exposure to chronic hypoxia (7 % O_2)[7].

Currently the only available treatment for end-stage heart failure is heart transplantation. The number of donated hearts are limited; therefore, alternative approaches are needed, and cell therapy holds the promise to be used in the clinic to replace the lost cardiomyocytes with new contractile cells[8,9]. A wide range of cells have been tested both in animal models or early-stage human clinical trials in order to find the appropriate source for cell therapy[8,9]. These included bone-marrow derived cells[10–12], cardiac stem or progenitor cells[13–17], human embryonic stem cell-derived cardiomyocytes[18–21], and human induced pluripotent stem cell-derived cardiomyocytes[22,23].

1.2 Bone Marrow-Derived Cells

Bone marrow-derived mesenchymal stem cells were claimed to differentiate into cardiomyocytes that spontaneously beat after 2 weeks in culture[11] or into myotubules that when injected into infarcted hearts stimulated angiogenesis and generated cardiac-like

cells[10]. In addition, others showed that when bone morrow-derived stem cell growth factor receptor positive / linage negative (c-kit$^+$/lin$^-$) cells were injected into infarcted hearts, they generate new cells and remuscularised the infarcted heart[12]. However, later studies showed that bone marrow-derived cells do not trans-differentiated into cardiomyocytes[24,25].

1.3 Adult Cardiac Stem Cells

Another source for *de novo* or new cardiomyocytes are endogenous cardiac progenitor cells. In 2003, a population of cardiac progenitor cells called stem cell growth factor receptor-positive (c-kit$^+$) cells were identified. *In Vitro*, these proliferative cells can self-renew and differentiate into myocytes[13]. When injected into infarcted hearts, c-kit$^+$ cells differentiated into cardiomyocytes resulting in myocardium regeneration and improved heart function[13]. In the same year, another population of cardiac progenitor cells were identified, the stem cell antigen 1 (sca-1$^+$) cells, which were differentiated into myocytes both *in vitro* and *in vivo*[14]. In addition, a population of progenitor cells were derived, via the formation of cardiospheres from cells migrating from adult human and murine heart explants, called cardiosphere-derived cells (CDCs)[15]. It was reported that human CDCs have the ability to self-renew in culture and express the endothelial kinase insert domain receptor (KDR) and CD-31, and stem cell (CD-34, c-kit, and sca-1) markers[15]. Further characterisation of CDCs from neonatal rat hearts showed that these cells express pluripotent markers such as Oct3/4, Sox2, and Klf4[16]. CDC-treatment has been shown to improve function of infarcted hearts[16]. In this study, cardiac function and morphology were measured post myocardial infarction using MRI. In untreated infarcted hearts, cardiac remodelling resulted in a significant reduction in ejection fraction that persisted till week 16 post MI[16]. In CDC-treated hearts, there was reduction in ejection fraction, but this

reduction was significantly lower than untreated hearts[16]. In addition, 16 weeks post MI the size of the infarct was significantly lower in CDC-treated hearts than untreated[16]. The improvement reported in CDC-treated hearts is likely due to the increased paracrine factors that have reduced fibrosis and increased capillary density[16]. In addition, a population of cardiac progenitor cells expressing the embryonic epicardial gene Wilm's tumor (Wt1) migrates from the epicardium in response to thymosin B4 treatment[17], and these progenitor cells have been shown to differentiate to *de novo* cardiomyocytes[17]. A number of different markers have been used to identify endogenous cardiac progenitor cells, however, these cells are rare and they only contribute to low turnover in the heart, therefore, they are not the most suitable cells to use to repair the heart after MI. Although, cardiac progenitor stem cells have been tested extensively, the effect of these cells after MI was limited, and it is believed to be due to a paracrine effect of the injected cells. For these reasons, new sources for cells have been explored. The use of human embryonic stem cells (hESCs) and human induced pluripotent stem cells (hiPSCs) provided more potential opportunities for cardiac cell therapy. These cells expand extensively for large scale production of stem cell-derived cardiomyocytes.

1.4 Human Embryonic and Human Induced Pluripotent Stem Cells

Human embryonic stem cells (hESCs) are derived from the inner cell mass (ICM) of blastocysts from donated fertilised eggs[26]. Human ESCs have the ability to continuously proliferate in an undifferentiated state, and when given the appropriate signals they have the ability to differentiate into any cell type. Human ESCs were the first pluripotent cells to be expanded *in vitro* and these showed promises for drug testing and for cell therapy[26], however, there are ethical concerns using hESCs in clinic.

In 2007, Yamanaka's group were the first to report the reprogramming of human somatic cells into hiPSCs, by overexpression of the following transcription factors: Oct4, Sox2, KLF4, and c-myc[27]. The reprogrammed hiPSCs resembled hESCs and had the ability to self-renew while maintaining pluripotency, which is defined by the capacity of hiPSCs to differentiate into any cell type of the three primary germ layers[27]. Human iPSCs can be produced from patient-specific somatic cells, therefore, overcoming the problem of immune rejection and the ethical concerns of using hESCs. Theoretically, hiPSCs hold a promise towards using them as therapies in regenerative medicine, such as in the infarcted heart[22]. Human ESC-derived cardiomyocytes (hESC-CMs) and hiPSC-derived cardiomyocytes (hiPSC-CMs) were used to improve function of infarcted hearts in rats[18,19,22,23], guinea pigs[20], and non-human primates (pigtail macaques-Macaca nemestrina)[21]. In this last study, one billion hESC-derived CMs were injected into each infarcted heart and showed that cells engrafted properly into the infarcted area and were perfused with host vessels.

The proliferative capacity and the pluripotency that characterise hiPSCs make them a very important tool for a wider range of applications. They have been used extensively as *in vitro* human-cell-based models to study basic biology and development[28], to model diseases[29,30], and to screen for drugs[31]. In addition, hiPSC can be produced from patients with rare genetic mutations known to induce disease phenotypes, opening up a larger field of research. This is particularly important for the heart, since adult cardiomyocytes do not survive *in vitro,* as morphological and functional changes occur in long-term culture[32] and so there has been no easy way to determine whether the effect of genetic mutations or of

drug compounds that were observed in animal models would also be seen in a human cardiomyocyte.

1.5 Human Induced Pluripotent Stem Cell Derived Cardiomyocytes

Initially protocols to differentiate ESCs to cardiomyocytes were used, but over the last 10 years a wide range of protocols have evolved to induce cardiomyocyte differentiation and these will be discussed in detail in chapter 3. Even with all these protocols, differentiated cardiomyocytes were found to be immature[33–37]. Human iPSC-CMs are small and circular in shape, whereas, adult cardiomyocytes are large and rectangular in shape[33,34]. Sarcomeres are disorganised with a length of ≈ 1.6 μm in immature foetal-like hiPSC-CMs, while, sarcomeres in mature adult cardiomyocytes are organised with a length of ≈ 2.2 μm[33,34]. In immature foetal-like hiPSC-CMs, myosin heavy chain α (αMHC) is more dominant than myosin heavy chain β (βMHC) and myosin light chain 2 atrial (MLC2a) is more dominant than myosin light chain 2 ventricular (MLC2v), whereas, the opposite is found in mature adult cardiomyocytes[33,34,36]. Metabolically, there are fewer mitochondria that occupy only a small fraction of the cell volume, forming irregular reticular network in the cytoplasm of immature foetal-like hiPSC-CMs[33–37] whereas, adult mature cardiomyocytes have regular mitochondrial networks that occupy ≈ 20 – 40% of the cell volume. Therefore, the main energy substrate used in immature foetal-like hiPSC-CMs is glucose, whereas adult mature cardiomyocytes depends more on fatty acid oxidation[33,34].

Although immature foetal-like hiPSC-CMs could be used therapeutically[23], it is vital to have an adult cardiomyocyte for modelling pharmacological or genetic changes. Most importantly, it is important to have mature hiPSC-CMs to model and study diseases that present late in life (late-onset diseases) such as cardio-metabolic diseases. For example,

diabetic cardiomyopathy is a complication of type 2 diabetes, and hiPSC-CMs have been used as an *in vitro* cell-based model for drug screening[38]. Diabetic cardiomyopathy can be defined as structural and functional abnormalities of the myocardium of diabetic patients. In the heart of diabetic patients, metabolism is switched towards enhanced fatty acid oxidation and reduced glucose oxidation. In order to use hiPSC-CMs to better model and study diabetic cardiomyopathy, it is very important to study the metabolism of hiPSC-CMs and find ways to metabolically mature hiPSC-CMs. It was found that hiPSC-CMs do mature slowly over a long period of time in culture[39–42]. Techniques to mature hiPSC-CMs more rapidly have focused on inducing mechanical stimuli like stretching or by constraining cells into lines[37,43] but the important role of metabolism in cardiac development has been largely overlooked.

1.6 Why Study Metabolism in the Heart?

Living cells need energy in order to function, the energy source for living cells is in the form of adenosine triphosphate (ATP) [7,18]. ATP is an energy-rich molecule that is generated from the oxidation of energy substrates such as fatty acid, glucose, and protein[7,18]. When ATP is hydrolysed into adenosine diphosphate (ADP), a phosphoanhydride bond is broken and a large amount of free energy is released[7,18]. ATP is synthesised from ADP either via substrate-level phosphorylation or via oxidative phosphorylation[7,18]. Substrate-level phosphorylation occurs during glycolysis and in the tricarboxylic acid (TCA) cycle, and it is important in providing energy in situations where oxygen levels are low[7,18]. In oxidative phosphorylation, ATP is generated in the mitochondria via the electron transport chain (ETC) as electrons are transferred from the reduced form of nicotinamide adenine dinucleotide (NADH) and the reduced form of flavin adenine dinucleotide ($FADH_2$) to

molecular oxygen, therefore, oxygen is required for oxidative phosphorylation[44,45]. The ETC consists of four protein complexes (complex I, II, III, IV) and linked by two soluble membrane proteins (coenzyme Q and cytochrome c). The transport of electrons is coupled with the transport of protons into the intermembrane space creating an electrochemical gradient across the inner membrane. Protons return to the mitochondrial matrix via ATP synthase, which is also located in the inner mitochondrial membrane. Three protons move through the F0-proton channel of the ATP synthase enzyme in order to catalyse ATP synthesis.

The human heart beats around 60 – 100 beats per minute at rest. Around 60 – 70% of the hearts ATP is used for contraction, and the remaining 30 – 40% is used for the sarcoplasmic reticulum Ca^{2+}-ATPase and other ion channels[46]. Around 95% of that ATP is generated via oxidative phosphorylation, and the remaining 5% is generated via substrate-level phosphorylation[46]. From the 95% of ATP generated via oxidation phosphorylation, 60 – 90% of acetyl CoA is generated from fatty acid oxidation, and the remaining 10 – 40% is generated from glucose and lactate oxidation[46]. The heart has a high rate of ATP hydrolysis and a low ATP content, therefore, in order for the heart to keep its ATP content constant there is a link between ATP hydrolysis and oxidative phosphorylation[46]. This is important in stressful situations such as during exercise, when the heart beats faster and therefore requires more ATP to be generated. In addition, the heart has the capability to use a range of different energy substrates, such as fatty acids, carbohydrates, proteins, and ketone bodies. There is a delicate balance between the pathways, which is disrupted in diseases such as type-2 diabetes (T2D) and heart failure. There is an reduction in glucose metabolism and an increase in fatty acid metabolism in rats with T2D[47], whereas, in heart

failure, heart metabolism switches back to a foetal state, increasing glucose metabolism and decreasing fatty acid metabolism[46].

1.7 Metabolism of the Human Heart during Development

There is a shift of metabolism in the heart during development from the foetal, to the neonatal (new-born), and to the adult stage. Metabolism of the foetal heart differs from that of adult hearts in that glucose is the primary source of energy in the foetal heart, whereas fatty acids are the primary source of energy in the adult heart. The reasons for this is the differences in the energy requirements, the availability of the energy substrates at each stage[48–50] and availability of oxygen[49,50]. The adult heart requires an efficient and sustained source of ATP production for muscle contraction (60-100 beat per minute) and, in the presence of oxygen, fatty acids are the main fuel[46]. In contrast, the foetal heart requires a source of ATP production that will be sufficient for development and growth in a hypoxic environment, therefore, glucose and lactate are the major substrates during this stage[48]. During the foetal life and towards the end of gestation, the heart starts to prepare itself for the time immediately after birth by storing glucose in the form of glycogen[48,50]. The stored fuel is used immediately after birth, the time when the heart starts to adapt to the loss of glucose supply from the mother and the increased capacity for oxidative phosphorylation in the presence of oxygen[48,50]. This period is also known as the transition period, where metabolism starts to shift from carbohydrate dependence in the foetal heart to fatty acid dependence in the adult heart. Since the main energy substrates used in the heart are carbohydrates and fatty acids, the metabolic pathways that will be covered here are glycolysis, glucose and lactate oxidation, and fatty acid oxidation.

1.7.1 Metabolism of the Foetal Heart

In the foetal heart, glucose and lactate are the two sources for energy production. Glycolysis is regulated by phosphofructokinase (PFK), which is highly active in the foetal heart and unaffected by inhibitory regulators such as increased levels of ATP and citrate[48,49,51,52]. Glucose is transported into the foetal heart via the GLUT1 transporter, independent of insulin[51,53], and most of the glucose is converted into lactate rather than oxidised[48,49,54]. The reason for this is partly due to the low number and immaturity of the foetal mitochondria, with low activity of TCA and ETC enzymes[49,52]. In addition, it has been reported that the foetal heart stores glycogen at high quantity[49–51], and that glycogen occupies 30% of the cell volume in a foetal heart[53,55] in preparation for the transition period from the foetal to the adult heart[51].

Another important source for energy in the foetal heart is lactate as studies on lactate uptake and oxidation have shown that foetal hearts uptake and oxidise lactate at a greater rate than neonatal or adult hearts[48–51,54]. It has been reported that lactate levels in the foetal circulation are high[48,50–52], and it becomes the major energy substrate during late gestation[48,54] before lactate levels decline just after birth[48,54,56]. The two main sources of lactate to the foetal circulation are the placenta, as it is believed that a large quantity of glucose taken up by the placenta is converted into lactate[48,50,51], and from glycolysis [48,49,54]. In foetal guinea pig hearts, around 75% of glucose is converted into lactate, whereas only 25% is oxidised[49]. Lactate oxidation has been shown to contribute to 60% of ATP production in foetal lambs and 80% of ATP production in foetal pigs[48]. This high level of lactate oxidation mainly during the late stage of foetal life might be due to upregulation of the foetal heart to oxidise substrates as late gestation is marked with decreased glycolytic

flux and increased ability for substrate oxidation, thus preparing the foetus to adapt to the new environment just after birth.

Free fatty acids can transfer across the placenta[50], however the concentration in the foetal circulation is low[48–50] and the capacity of foetal heart to oxidise fatty acid is limited. This limited capacity might be due to low carnitine content and limited activity of carnitine palmitoyl-transferase (CPT)[5758], or might be due to the fact that lactate at its physiological levels exhibits an inhibitory effect on fatty acid uptake and oxidation in the foetal heart[7, 14]. If the foetal heart is given the optimal conditions for fatty acid oxidation in the absence of lactate in isolated foetal pig hearts, fatty acid oxidation still only contributes 30% to ATP production[48].

1.7.2 Metabolism of the Neonatal and Adult Heart

There is a shift in metabolism in the heart soon after birth and the duration of metabolic transition from the foetal to the adult varies between species. What is common about this metabolic shift between species, is that this period is marked by changes in plasma substrate concentrations (glucose, lactate, and free fatty acids). Lactate which is present in the foetal circulation at high concentration, falls within hours of birth to levels that are seen in the adult[48,52]. Immediately after birth, the continuous infusion of glucose from the placenta is lost, therefore in the neonatal circulation (1-2 hours after birth) glucose concentration reaches its lowest level, but then it starts to increase gradually until it stabilises 4-6 hours after birth. When glucose concentrations reach their lowest level, glycogen stored in the liver plays a very important role in maintaining the glucose levels in the neonatal circulation[51]. After birth, neonatal plasma levels of free fatty acid increase rapidly, due to drinking the mother's milk. In addition, it is important to highlight the

change in oxygen availability soon after birth, which plays a major role in this metabolic shift.

This period is regulated by inactivation of hypoxia-inducible factors 1 alpha (HIF1α) signalling and activation of the peroxisome proliferator-activated receptor (PPAR) signalling pathways which are key regulators of substrate metabolism[59]. Immediately after birth, when the foetal levels of oxygen rise, HIF1α is degraded[4,59]. PPAR-α expression is downregulated via HIF1α[60] and immediately after birth as HIF1α is degraded, PPAR-α activation will upregulate fatty acid metabolism in the heart[46,61,62]. In addition, HIF1α degradation results in decreased expression of heart and neural crest derivatives expressed 1 (Hand1), which has been reported to be stimulated in the foetal heart via HIF1α proteins[4,59]. This downregulation in Hand1 expression will result in upregulation of fatty acid metabolism in the heart[4,59]. Breckenridge *et al* showed that when Hand1 expression is prolonged till after birth there is a downregulation in the expression of the fatty acid enzymes, medium-chain acyl CoA dehydrogenase (ACADM), fatty acid binding protein (FABP), and carnitine palmitoyl-transferase 1 alpha (CPT1a)[4].

Mitochondrial maturation from an embryo into an adult heart is a very important aspect of metabolic maturation. During foetal life, there is little or no mitochondrial energy metabolism, but during the transition period (perinatal), there is an increase in mitochondrial oxidation capacity due to a burst of mitochondrial biogenesis at birth. After birth, there is an increase in mitochondrial size and function. In addition, the distribution of mitochondria from foetal into adult differs, in foetal/neonatal cardiomyocytes mitochondria are concentrated around the nucleus whereas in an adult heart the mitochondria are redistributed throughout cardiomyocytes[63]. Peroxisome proliferator-

activated receptor gamma coactivator 1-alpha and beta (PGC1 α and β) play an important role in regulating mitochondrial dynamics and maturation and disruption of PGC1 α and β during heart development causes mitochondrial abnormalities[63].

1.8 Substrate Metabolism

1.8.1 Fatty Acids

Fatty acids are an important source of fuel for energy production (ATP) in many cells. Fatty acids are defined as carboxylic acids with a long hydrocarbon chain (Figure 1.1). They are classified as either saturated (no carbon-carbon double bond) or unsaturated (containing carbon-carbon double bond) and are further classified depending on the number of carbon atoms, from very long-chain (larger than 22 carbon), long-chain (13-21 carbon), medium-chain (6-12 carbon), to short-chain (less than 6 carbon) fatty acids.

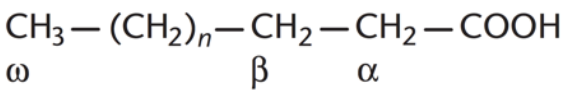


Figure 1.1: Structure of saturated fatty acid[64]. Fatty acids are carbon chains with a methyl group at one end (ω) and a carboxyl group at the other end. The carbon atom next to the carboxyl group is called the α carbon and β carbon represent the carbon atom next to the α carbon. The letter n indicates the number of additional carbons in the chain.

The naturally occurring unsaturated fatty acids have their double bond in the *cis*-configuration and include Oleic Acid (OA), which is a long-chain monounsaturated omega-9 fatty acid (18:1 cis-9) that occurs naturally in plant fats and oils (Figure 1.2). Oleic acid accounts for 92% of dietary monounsaturated fatty acid, and is the major monounsaturated fatty acid in the body[65]. Digestion, absorption, and oxidation of oleic acid

is similar to other fats. However, oxidation of OA is greater than palmitic acid, which is the most common saturated fatty acid[65].

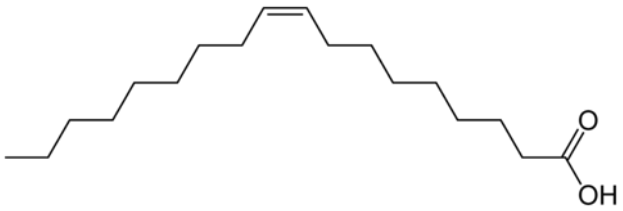


Figure 1.2: Structure of *cis*-oleic acid[66]. Oleic acid has a chain length of 18 carbons and one carbon-carbon double bond with a cis-configuration in the ω-9 position (18:1 ω-9).

1.8.2 Fatty Acid Digestion and Absorption

Most of the fat consumed by adults is in the form of triacylglycerol (TAG)[64,67], which consists of 3 fatty acids and a molecule of glycerol. TAGs are hydrophobic compounds and during intestinal digestion they are hydrolysed by lipase to free fatty acid and monoacyglycerol. Inside the absorptive cells, free fatty acids and monoacylglycerols are re-esterified and TAGs are formed again, packaged with phospholipids to form chylomicrons, which are released to the lymphatic system then to the circulation. In the circulation, TAGs in the chylomicrons are hydrolysed by endothelial lipoprotein lipase, with free fatty acids released to be transported or passively diffused into the cell for oxidation and ATP production (Figure 1.3).

Fatty acids are stored in the body as TAGs in the cytosol of adipose tissue, which can be used during prolonged exercise or between meals[45]. Free fatty acids are released from TAGs stored in adipose tissue by a hydrolysis reaction that is mediated by hormone-sensitive lipase and monoacylglycerol-specific lipase. In the circulation, released fatty

acids bind to plasma albumin for delivery to target tissues, where they enter the cells down the concentration gradient (Figure 1.3). In cardiac muscles, free fatty acids move from a concentration of 500 μmol/l in plasma to 100 μmol/l in cardiac muscles[67].

Fatty acids enter the cells either via passive diffusion using the "flip-flop" movement or via facilitated transporters using cell membrane fatty acid transporters. Fatty acid translocase (FAT)/CD36 and fatty acid transport proteins (FATP) are cell membrane transporters that subsequently transport the FA to fatty acid binding protein in the cytosol, to facilitate fatty acid movement within the cells[67,68] (Figure 1.3).

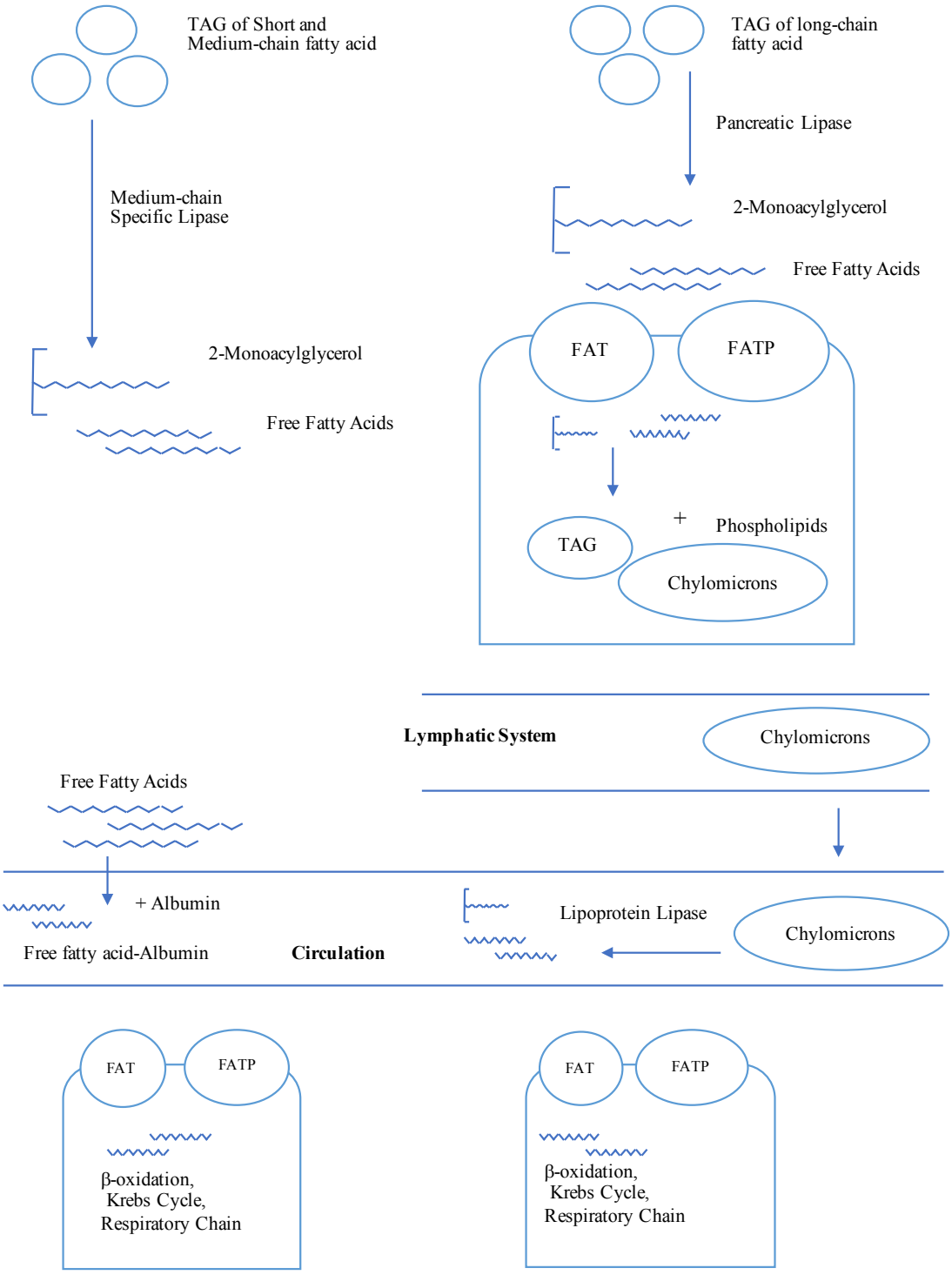


Figure 1.3: Digestion, absorption and uptake of fatty acids by the human body.
TAG: triacylglycerol, FAT: Fatty acid translocase, FATP: fatty acid transport proteins.

1.8.3 Fatty Acid Oxidation

Fatty acid oxidation includes the following steps: activation in the cytosol, uptake by the mitochondria, and beta (β)-oxidation in the mitochondria, to produce 2-carbon molecules that undergo further oxidation in the Krebs cycle and the respiratory chain (Figure 1.4). As fatty acids enter the cell for oxidation, they are activated by attachment to CoA and the formation of fatty acyl CoA, a reaction that is catalysed by acyl CoA synthetase (ACS). Fatty acyl CoA is taken up into the matrix of the mitochondria using the carnitine shuttle, a system that transports activated long-chain fatty acid into the matrix of the mitochondria (Figure 1.4). The carnitine shuttle consists of carnitine/acylcarnitine translocase (CAT), and carnitine palmitoyl transferases I and II (CPTI and CPTII) (Figure 1.4).

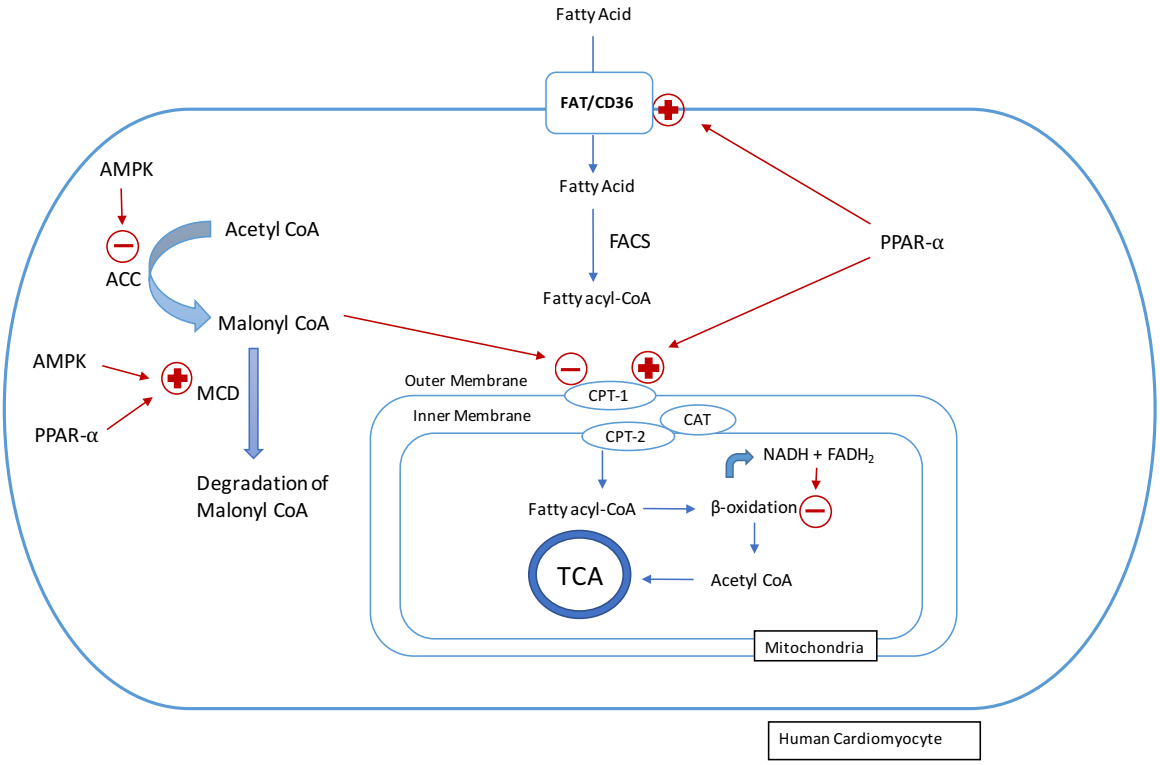


Figure 1.4: Regulation of fatty acid uptake and oxidation. This diagram illustrates fatty acid uptake and esterification inside cells, and uptake and oxidation by the mitochondria. FAT: fatty acid translocase, FACS: fatty acyl CoA synthetase, CPTI: Carnitine palmitoyltransferase I, CPTII: Carnitine palmitoyltransferase II, CAT: Carnitine/acyl Carnitine Translocase, ACC: acetyl CoA carboxylase, MCD: malonyl CoA decarboxylase,

AMPK: AMP-activated protein kinase, PPAR-α: peroxisome proliferator-activated receptors

In the mitochondria, oxidation of fatty acyl CoA occurs in cycles that involve a sequence of reactions: oxidation, hydration, oxidation, and thiolysis. The number of β-oxidation cycles depends on the number of carbon atoms in the fatty acid, with every cycle yielding 2-carbon acetyl CoA. In addition, each cycle generates NADH and $FADH_2$. For example, oleic acid oxidation produces 9 acetyl CoA, 8 NADH, and 7 $FADH_2$[69]. Acetyl CoA will enter the Krebs cycle for further oxidation, with more NADH and $FADH_2$ formed. NADH and $FADH_2$ produced from both mitochondrial β-oxidation and the Krebs cycle are transported to the respiratory chain for oxidation and ATP production. A molecule of oleic acid produces a total of 118.5 ATP[69]. β-oxidation of unsaturated fatty acid is similar to saturated fatty acid until it forms intermediates with the *trans*-configuration.

1.8.4 Regulation of Fatty Acid Transport and Oxidation

The regulation of fatty acid oxidation occurs at various levels: fatty acid release from stored TAGs in adipose tissue, uptake from the blood into cells, rate of mitochondrial β-oxidation[44,45,67]. The release of free fatty acid from TAG in adipose tissue is regulated by hormone-sensitive lipase, which is activated by adrenaline during exercise and inhibited by insulin in the fed state[44,45]. The rate of fatty acid uptake by the heart for oxidation is proportional to the concentration of fatty acid in circulation. In addition, contraction and insulin increase fatty acid transport rates via regulating CD36 translocation from an intracellular pool to the sarcolemmal membrane[62,68,70] (Figure 1.5). In the heart, it is estimated that 50% of the CD36 transporters are stored in intracellular compartments and CD36 appears to recycle between endosomes and the sarcolemma[68].

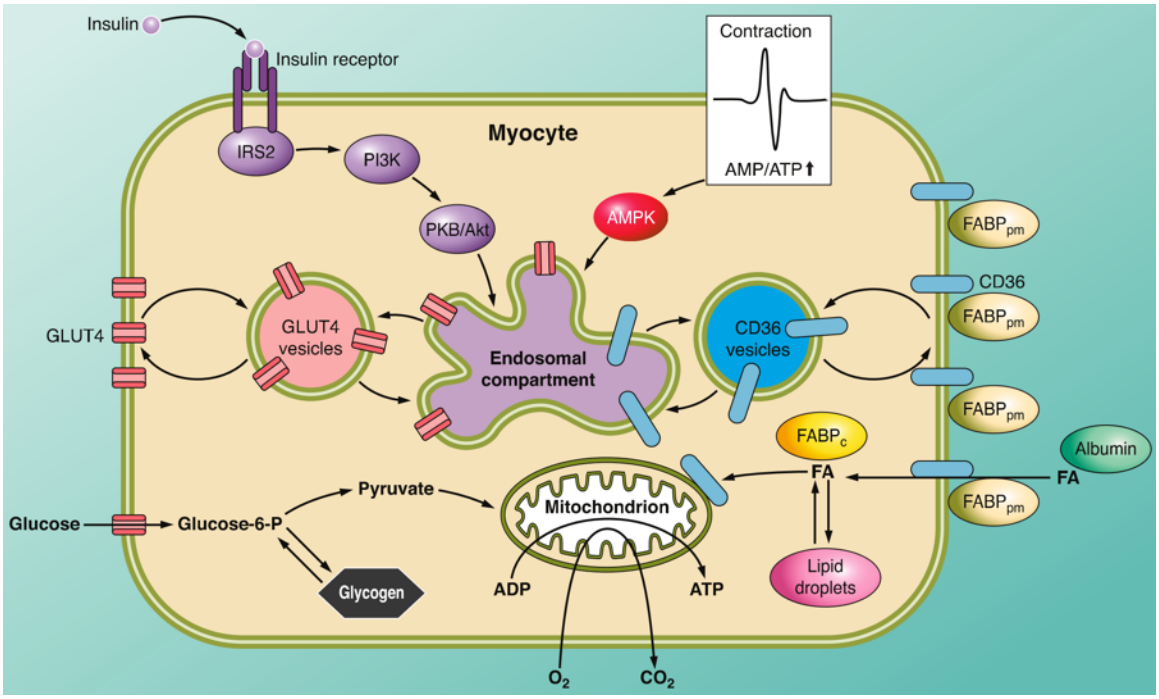


Figure 1.5: Translocation of CD36 and GLUT4 in cardiac cells[68]. Cellular uptake of fatty acids and glucose is regulated via the translocation of fatty acid transporters (CD36) and glucose transporters (GLUT4) from endosomal compartments to the sarcolemma in cardiac cells. In the presence of insulin or as the muscle contracts more, CD36 or GLUT4 is translocated into the sarcolemma membrane to increase cellular uptake of fatty acids or glucose, respectively[68].

The rate of mitochondrial β-oxidation is regulated by the mitochondrial uptake of activated fatty acid via the carnitine shuttle, and by the availability of coenzymes NAD^+ and FAD. Mitochondrial uptake of fatty acyl CoA is controlled by CPT1 which is inhibited by high levels of cardiac malonyl CoA, increased during fatty acid synthesis. Malonyl CoA synthesis is regulated by acetyl CoA carboxylase (ACC), whereas, malonyl CoA degradation is regulated by malonyl CoA decarboxylase (MCD). Gene expression of MCD is controlled by PPAR-α[71]. In addition, mitochondrial β-oxidation is inhibited by high levels of NADH and $FADH_2$ which are generated during β-oxidation from NAD^+ and FAD. The availability of NAD^+ and FAD depends on regeneration via the ETC when ATP is produced, and the competition for their use from dehydrogenase enzymes used in the TCA

cycle[44,45,67] (Figure 1.4). PPAR-α is a major transcriptional regulator of enzymes of fatty acid oxidation such as CD36, acyl CoA synthetase (ACS), CPT1, MCD, long-chain acyl CoA dehydrogenase (LCAD), and medium-chain acyl CoA dehydrogenase (MCAD)[62].

1.8.5 Glucose Metabolism: Glycolysis and Pyruvate Oxidation

Glucose circulates freely in the blood and it enters the cells via facilitated diffusion mediated by glucose transporters[44,45]. Glucose transporters (GLUT) facilitate passive transport of glucose down a concentration gradient. There are 14 isoforms of GLUT, with GLUT1 and GLUT4 expressed in the heart. GLUT1 is present predominantly at the membrane, whereas, GLUT4 moves between the membrane and intracellular vesicles in response to insulin stimulation[44,45,67] (Figure 1.5). Once inside the cell, the six-carbon glucose goes through a series of reactions (10 steps) to form two three-carbon pyruvate molecules[44,45] (Figure 1.6). Pyruvate is either converted into lactate for export, or to acetyl CoA, which enters the TCA cycle for oxidation[44,45]. The first 5 steps in glycolysis are defined as the energy investment phase (uses 2 ATP), whereas, the last five steps are defined as the energy generating phase (makes 4 ATP and 2 NADH) (Figure 1.6)[44,45]. Anaerobic glycolysis gives 2 ATPs, whereas, complete glucose oxidation gives a total of 31 ATP (ATP was calculated here using the modern non-integral P/O ratios of 2.5 ATP for NADH and 1.5 ATP for $FADH_2$)[44,45].

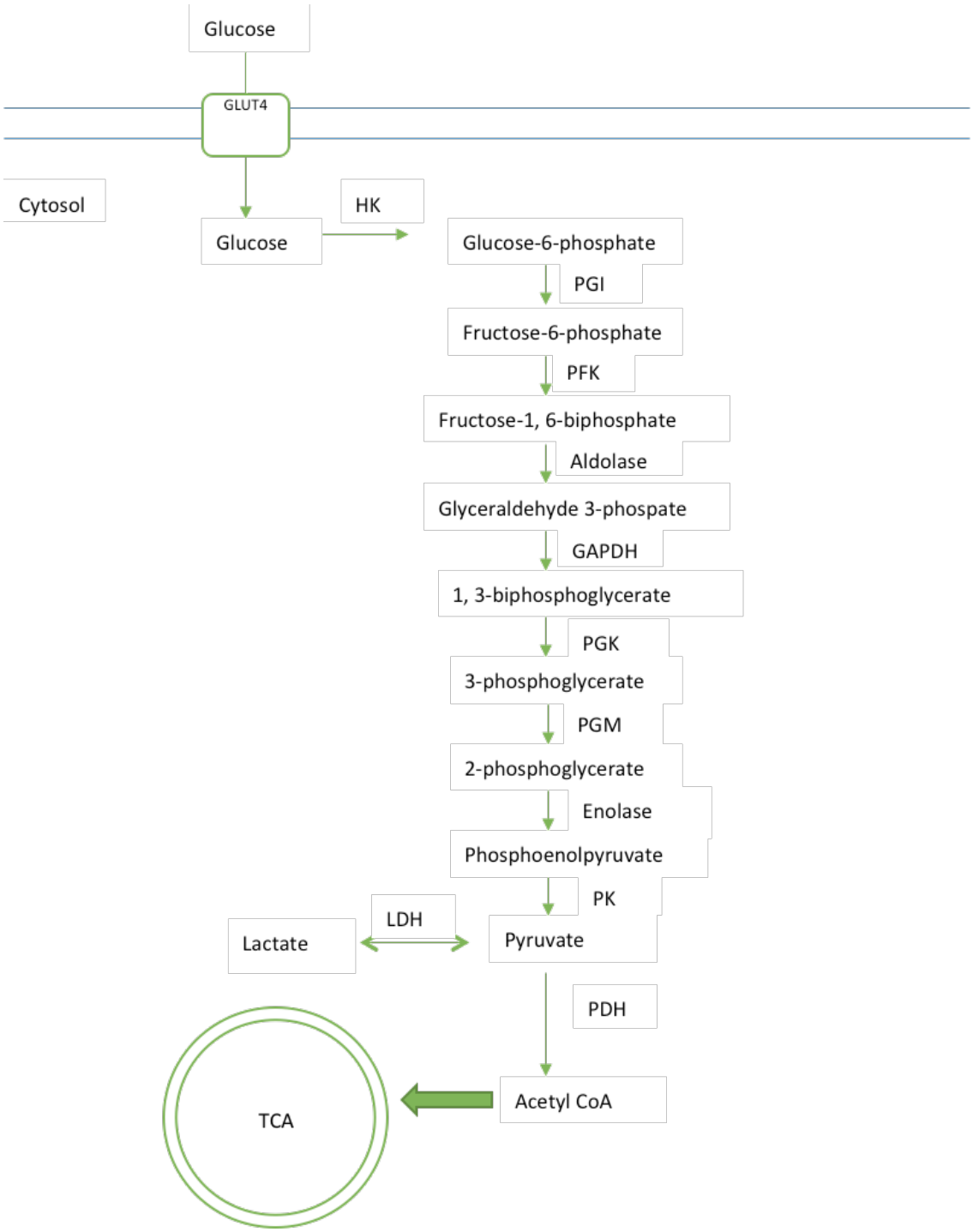


Figure 1.6: Glucose uptake and metabolism. HK: Hexokinase, PGI: Phosphoglucose Isomerase, PFK: Phosphofructokinase, GAPDH: Glyceraldehyde-3-phosphate dehydrogenase, PGK: Phosphoglycerate Kinase, PGM: Phosphoglycerate Mutase, PK: Pyruvate Kinase, LDH: Lactate Dehydrogenase, PDH: Pyruvate Dehydrogenase.

Pyruvate molecules are either converted into lactate or to acetyl CoA, which enters the TCA cycle for oxidation[44,45]. The conversion of pyruvate to acetyl CoA is an irreversible reaction that happens in the mitochondria and is catalysed by pyruvate dehydrogenase (PDH)[44,45]. PDH is a multi-enzyme complex consisting of three enzymes and requires the presence of five coenzymes[45]. PDH is either in its phosphorylated (inactive) form or in its non-phosphorylated (active) form[45]. PDH kinase catalyses the phosphorylation, thus in-activating PDH, and PDH phosphatase catalyses de-phosphorylation, thus activating PDH[45]. PDH kinase is activated by ATP, acetyl CoA, and NADH, whereas PDH phosphatase is activated by Mg^{+}, Ca^{2+}, and insulin[45] (Figure 1.7). This complex system plays an important role in balancing between glucose and fatty acid oxidation.

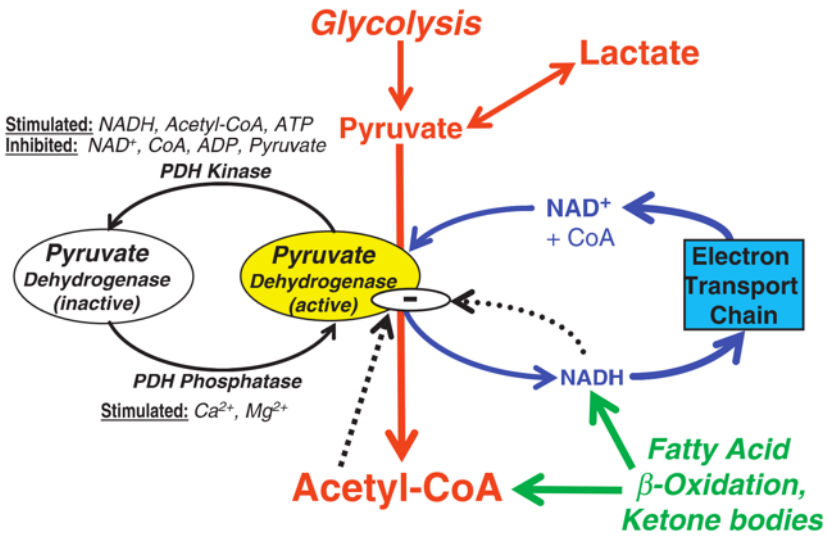


Figure 1.7: Regulation of the oxidation of glucose and lactate by pyruvate dehydrogenase (PDH)[46]. The activity of PDH is inhibited by product inhibition from acetyl- CoA and NADH (dashed arrows), and by phosphorylation by PDH kinase and de-phosphorylation by PDH phosphatase[46].

1.8.6 Glucose Metabolism Regulation

Glycolysis is an important metabolic pathway during times when oxygen is limited, such as in exercising skeletal muscle when oxidative metabolism cannot keep up with increased

energy demand. GLUT4 moves from intracellular stores to the membrane of the cells in respond to insulin signalling (Figure 1.5). Glycolysis is regulated at the irreversible reactions in the glycolysis pathway, steps 1, 3, and 10. These irreversible reactions are catalysed by the following enzymes, hexokinase (HK), phophofructokinase-1 (PFK-1), and pyruvate kinase (PK). Insulin activates HK, PFK-1, and PK, whereas, HK is inhibited by glucose-6-phosphate, PFK-1 is inhibited by citrate and ATP, and PK is inhibited by ATP.

Aims and Hypothesis of Thesis

Human induced pluripotent stem cells (hiPSCs) favour glycolysis over glucose oxidation, and glycolytic rates in hiPSCs are high and sufficient to support fast self proliferation[72–77]. The adult human heart has the capability to use a range of different energy substrates, such as fatty acids, carbohydrates, proteins, and ketone bodies[46,62]. The majority of ATP (> 90%) is produced via mitochondrial oxidative phosphorylation, with the remaining of ATP produced via glycolysis[46,62]. As cardiac metabolism changes fundamentally between the foetal, neonatal and adult heart, it is important to understand the metabolism of hiPSC-CMs before using them as an *in vitro* cell-based model for human cardiomyocytes for disease modelling or drug screening. Current cardiac differentiation protocols focus mainly on the microenvironment of the culture and the signalling pathways involved in heart development. One limitation of these differentiation protocols is that they do not consider the metabolic changes that occur during heart development and during cardiac differentiation the cells are cultured with the same metabolic media throughout the procedure. Although there have been some attempts to purify or enrich hiPSC-CMs via metabolic manipulation (removal of glucose and addition of lactate)[78], however, this still does not represent the metabolic shift that occurs in human heart after birth. Therefore, we sought to first understand the metabolic state of hiPSC-CMs comparing them to the undifferentiated stem cells, and secondly to mature hiPSC-CMs by introducing fatty acids (oleic acid) into the culturing media and activating the PPAR-α pathway, which regulates the metabolic shift during heart development.

1. Differentiation of human induced pluripotent stem cell (hiPSC) lines into spontaneously beating human induced pluripotent stem cell-derived cardiomyocytes (hiPSC-CMs) using the Activin A + BMP4 + bFGF protocol and Wnt-modulation protocol.

2. Characterise changes in substrate metabolism between hiPSCs and differentiated beating hiPSC-CMs.

3. Enhance cardiac differentiation and induce a metabolic shift during the early stages of cardiac differentiation by adding WY14643 to activate PPAR-α

4. Enhance metabolic maturation in immature beating hiPSC-CMs by adding fatty acids into the culture medium and activating PPAR-α using WY14643 at a later stage of cardiac differentiation

2 Materials and Methods

This chapter will cover most materials and methods, and a specific materials and methods section will be included in some of the result chapters.

2.1 Cell Culture of Human Induced Pluripotent Stem Cells

2.1.1 Human Induced Pluripotent Stem Cell Lines

In this project, I have used two human induced pluripotent stem cell (hiPSC) lines, C19 from Dr. Lee Carpentar (NHSBT, John Radcliffe Hospital)[22], and OX1-19 from Dr. Sally Cowley (James Martin Stem Cell Facility)[79]. HiPSC Lines were cultured and expanded under the culturing conditions determined by their lab of origin. The C19 hiPSC line was cultured and maintained in 5% CO_2 and 5% O_2 at 37°C, whereas OX1-19 hiPSC line was cultured and maintained in 5% CO_2 and 21% O_2 at 37°C. Both hiPSC lines were cultured feeder-free on matrigel hESC-qualified matrix (Corning®)-coated plates in the chemically defined medium mTeSR1 (Stem Cell Technologies). Each new stock of hESC-qualified matrix has its own dilution factor based on protein concentration, and every time new aliquots were prepared the new dilution factor was used. To expand hiPSC lines, matrigel-coated plates were prepared in advance using one aliquot of hESC-qualified matrix diluted in Dulbecco's modified eagle medium: nutrient mixture F-12 (DMEM/F-12) basal media in a ratio of (1:100) (Invitrogen). A total of 9 ml of diluted matrigel was used for a 6-well plate (1.5 ml / 9.5 cm^2 growth area) and incubated for a minimum of 2 hours at room temperature or overnight at 4°C. When ready to use, the diluted matrigel was removed and hiPSCs were transferred into the plates in mTeSR1 media supplemented with Y27632 Rho

associated coil kinase (ROCK) inhibitor (10 μM; Calbiochem). HiPSC lines were passaged with a 1:6 split ratio every 4 - 6 days.

2.1.2 Maintenance and Expansion of C19 Human Induced Pluripotent Stem Cell Line

To expand the C19 hiPSC line, matrigel-coated plates were pre-prepared as described above. To dissociate C19 hiPSCs, cells were pre-incubated with Y27632 (10 μM final; Calbiochem) in mTeSR1 for 2 hours. After 2 hours, cells were rinsed with DMEM/F-12 basal media and incubated with 1 ml of dispase solution (1 mg/1 ml; Stemcell Technologies) per 9.5 cm^2 growth area for 10 - 15 minutes at 37°C. Dispase solution was removed and cells were rinsed with DMEM/F-12 basal media to dilute away any remaining dispase. Using dispase solution, hiPSC colonies remained attached to the plate, therefore cells were further dissociated using a cell scraper. Dissociated hiPSCs colonies were mechanically dispersed into clumps of 10 – 20 cells, which were transferred into the pre-prepared matrigel-coated plates and cultured with mTeSR1 supplemented with 10 μM Y27632. The following day, the medium was replaced with mTeSR1 alone, and from this point then media was refreshed on a daily basis.

2.1.3 Maintenance and Expansion of OX1-19 Human Induced Pluripotent Stem Cell Line

To dissociate OX1-19 hiPSCs, cells were rinsed with phosphate-buffered saline (PBS) and incubated with 1 ml of TrypLE™ Express Enzyme (1X) (Gibco), per 9.5 cm^2 growth area for 5 minutes at 37°C. Using TrypLE™ Express, almost all seeded hiPSCs will dissociate from the plates. Dissociated hiPSCs were neutralised with mTeSR1 and PBS, collected in falcon tubes, and centrifuged at 1200 rpm for 5 minutes. Supernatant was removed and the

hiPSC pellet was re-suspended with mTeSR1 supplemented with 10 μM Y27632. HiPSCs in mTeSR1 were transferred into the pre-prepared matrigel-coated plates. The following day, the medium was replaced with mTeSR1 alone, and from this point then media was refreshed on a daily basis.

2.2 The Differentiation of Human Induced Pluripotent Stem Cells into Beating Cardiomyocytes

To differentiate hiPSCs, matrigel-coated plates were prepared in advance using one aliquot of matrigel basement membrane matrix growth factor reduced (GFR-matrigel) (Corning®) diluted in DMEM/F-12 basal media in a ratio of (1:100) (Invitrogen). A total of 9 ml of diluted matrigel was used for a 12-well plate (750 μl / 3.8 cm^2 growth area) and incubated for a minimum of 2 hours at room temperature or overnight at 4°C. When ready to use, the diluted matrigel was removed and hiPSCs were seeded (80-90% confluence) into the plates in mTeSR1 media supplemented with 10 μM Y27632 (day -4 of differentiation). The following day (day -3 of differentiation) change of medium was performed with fresh 1 ml mTeSR1 per well of the 12-well plate. On day -2 of differentiation (90-95% confluence) cells were cultured with 1 ml mTeSR1 supplemented with GFR-matrigel (1:100) in preparation to start cardiac differentiation.

2.2.1 Cardiac Differentiation using Activin A, BMP4 and bFGF[22]

On day 0 of differentiation (98-100% confluence), cells were cultured with 1ml Stem Pro-34 serum-free complete medium (10639; Gibco) supplemented with 50 ng/ml Activin A (338-AC; R&D Systems) for 4 hours, followed by culturing them with fresh Stem Pro-34 SFM supplemented with GFR-matrigel (1:100), 5 ng/ml Activin A, 10 ng/ml bone

morphogenetic protein 4 (BMP4) (314-BP; R&D Systems) and 5ng/ml basic fibroblast growth factor (bFGF) (AA 10-155; Gibco) for 2 days (Figure 2.1). On day 2 of differentiation, cells were cultured with Stem Pro-34 SFM supplemented with fresh 5ng/ml Activin A, 10 ng/ml BMP4 and 5 ng/ml bFGF (Figure 2.1). Starting from day 4 until the end of differentiation, cells were cultured every second day with Stem Pro-34 SFM alone (Figure 2.1)[22].

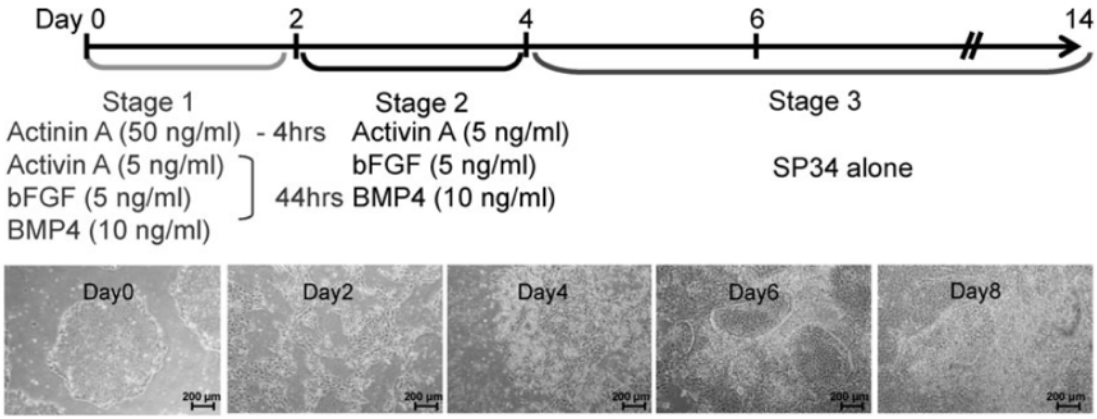


Figure 2.1: Timeline of cardiac-directed differentiation using Activin A, BMP4, and bFGF[22].

2.2.2 Cardiac Differentiation via Small Molecules Modulators of Wnt Signalling[80–82]

On day 0 of differentiation, cells were cultured with 2 ml of Roswell park memorial institute (RPMI) 1640 medium (500ml; Gibco), supplemented with B27 supplement, minus insulin (10 ml; Gibco), and 12 μM of CHIR-99021 (S2924; Selleckchem). The following day a medium exchange was performed with RPMI 1640, supplemented with B27 minus insulin alone. On day 3 of differentiation, cells were cultured with RPMI 1640, supplemented with B27 minus insulin and 5 μM of the Wnt inhibitor IWP4 (04-0036;

Stemgent). A media change was performed on day 5 with RPMI 1640, supplemented with B27 minus insulin alone. On day 7, cells were cultured with 2 ml RPMI 1640 medium (500ml; Gibco), supplemented with B27 supplement (50x), serum free (10 ml; Gibco). Starting from day 7 a media change with RPMI 1640 medium (500ml; Gibco), supplemented with B27 supplement (50x), serum free (10 ml; Gibco) was performed every three days until the end of differentiation[80–82] (Figure 2.2).

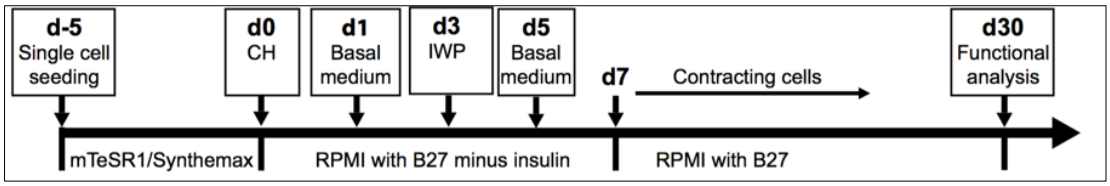


Figure 2.2: Timeline of cardiac-directed differentiation using small molecule modulators of Wnt signaling[80] (CH: CHIR-99021; IWP: IWP4)

2.3 Dissociation of Beating Human Induced Pluripotent Stem Cell-Derived Cardiomyocytes

Human induced pluripotent stem cell-derived beating cardiomyocytes (hiPSC-CMs), younger than 1 month were dissociated using cell dissociation solution (CDS), comprising 40% cell dissociation buffer, 40% RPMI media, and 20% trypsin-EDTA (0.05%). Cells were rinsed with PBS, and then incubated with 1 ml CDS for 6 minutes at 37°C. Cells were neutralised with fetal bovine serum (FBS), collected, and centrifuged at 2000 rpm for 2 minutes. Human induced pluripotent stem cell-derived cardiomyocytes older than 1 month, were dissociated using collagenase II (200 U/ml) in combination with 1 mM HEPES, 10 μM Y-27632, and 30 μM N-Benzyl-p-toluenesulfonamide (BTS). Cells were incubated with 1.5 ml of the above dissociation solution per 9.5 cm^2 growth area for 3.5 hours at

37°C. Cells were neutralised with RPMI supplemented with DNAse (500:1), collected, and centrifuged at 800 rpm for 15 minutes.

2.4 Cell Counting

Cells were counted using Countess® automated cell counter (C10227; Invitrogen). In Eppendorf tubes, 10 µl of the dissociated cell suspension was mixed with 10 µl of trypan blue (0.4%) (T10282; Life Technologies). To count the cell number, 10 µl of the mixture was used per chamber of the Countess® Cell Counting Chamber Slides (C10228; Invitrogen). For each sample, cells were counted in duplicate and an average of the cell count was used.

2.5 RNA extraction and cDNA synthesis

Ribonucleic acid (RNA) from hiPSCs and hiPSC-derived cardiomyocytes were extracted and purified using RNeasy mini kit (Qiagen). Around $5x10^6$ – $1x10^7$ cells were disrupted using 600 µl buffer RLT (included in the kit) and 6 µl β-mercaptoethanol (βME). Cells were homogenised using RNase-free disposable pellet pestles (12141368; Fisher Scientific), and 600 µl of 70% ethanol was added to the homogenised lysate. The homogenised lysate was transferred into the RNeasy spin column. Total RNA binds to the silica-based membrane of the column, while contaminants are washed away using buffer RW1 and buffer RPE. Finally, RNA was eluted using RNase-free water. The RNA yield and purity was determined using the NanoDrop. Total RNA (1 µg) was converted to complementary DNA (cDNA) via Oligo (dT), using the Superscript™ III First-Strand kit (18080051; Invitrogen). Complementary DNA synthesis was divided into two reactions. For the first reaction, total RNA, 50 µM oligo $(dT)_{20}$, and annealing buffer were incubated

in a thermal cycler at 65°C for 5 minutes. In reaction two, the product from reaction one was incubated with 2X first-strand reaction mix and super-script III enzyme mix in a thermal cycler at 50°C for 50 minutes followed by 85°C for 5 minutes.

2.6 Real-Time Quantitative Reverse-Transcription Polymerase Chain Reaction

2.6.1 qRT-PCR and TaqMan® Gene Expression Assay

Real time PCR amplification was carried out using the StepOne Plus (Applied Biosystems) with TaqMan® Gene Expression Assays (Invitrogen) and TaqMan® Fast Advanced PCR Master Mix (2x) (Invitrogen).

Table 2.1: TaqMan® assays used for quantitative RT-PCR:

Genes	Full Name	Function	TaqMan® Gene Expression Assay ID
UBC	Ubiquitin C	Housekeeping gene	Hs00824723_m1
B2M	Beta-2-microglobulin	Housekeeping gene	Hs99999907_m1
KDR	Kinase insert domain receptor	Mesoderm marker	Hs00911700_m1
GATA4	GATA binding protein - 4	Cardiac progenitor marker	Hs00171403_m1
TNNT2	Troponin T – type 2	Cardiac marker	Hs00943911_m1
MYH6	Myosin Heavy Chain 6, alpha	Cardiac marker	Hs 01101425_m1
MYH7	Myosin Heavy Chain 7, beta	Cardiac marker	Hs01110632_m1
MYL2	Myosin Light Chain 2	Cardiac marker	Hs00166405_m1
MYL7	Myosin Light Chain 7	Cardiac marker	Hs00221909_m1
PPARA	Peroxisome proliferator-activated receptor alpha	Cardiac metabolism	Hs00947536_m1
PGC1A	Peroxisome proliferator-activated receptor gamma, coactivator 1 alpha	PPAR-α coactivator	Hs01016719_m1
UCP3	Mitochondrial uncoupling protein	PPAR-α target gene	Hs01106052_m1
GLUT1	Glucose transporter member 1	Glucose transport	Hs00892681_m1
GLUT4	Glucose transporter member 4	Glucose transport	Hs00168966_m1

PFKM	Phosphofructokinase – muscle isozymes	Glycolysis	Hs00175997_m1
PDK4	Pyruvate dehydrogenase kinase 4	Pyruvate oxidation	Hs01037712_m1
PDHA1	Pyruvate dehydrogenase complex E1 alpah 1	Pyruvate oxidation	Hs01049345_g1
CD36	CD36 molecule	Fatty acid uptake	Hs01567185_m1
ACSL1	Acyl CoA synthetase, long-chain	Fatty acid activation	Hs00960561_m1
CPT1B	Carnitine palmitoyltransferase 1B (muscle-type)	Mitochondrial fatty acid uptake	Hs03046298_s1
HADHA	Hydroxyacyl-CoA dehydrogenase, alpha-subunit	Fatty acid oxidation	Hs00426191_m1
ACADVL	Acyl CoA dehydrogenase, very long-chain	Fatty acid oxidation	Hs00825606_g1
ACADM	Acyl CoA dehydrogenase, medium-chain	Fatty acid oxidation	Hs00936584_m1
ECI1	Enoyl-CoA delta isomerase 1	Unsaturated fatty acid oxidation	Hs00157239_m1
CS	Citrate synthase	TCA enzyme	Hs02574374_s1
OGDH	Oxoglutarate (alpha-ketoglutarate) dehydrogenase	TCA enzyme	Hs01081865_m1

2.6.2 qRT-PCR Data Analysis

Expression levels of target genes were normalised to house-keeping genes. The method used to analyse the data is the comparative C_T Method ($\Delta\Delta C_T$). Analysis conducted using the following steps:

1. Calculate the standard deviation of the replicates from the C_T-values of the housekeeping genes (KHG) and target genes (TG).
2. Calculate ΔC_T = C_T of TG - C_T of HKG
3. Calculate $\Delta\Delta C_T$ = ΔC_T of test sample - ΔC_T of control sample
4. Calculate the fold change (FC) = $2^{-\Delta\Delta CT}$

2.6.3 Writing of Gene Symbols

In this project, gene symbols that refer to human, were written all upper case and italicised, and the use of roman numbers and Greek letters was avoided, for example, peroxisome proliferator-activated receptor alpha, referred to as *PPARA*.

2.7 Immunocytochemistry (ICC) and Confocal Imaging

Cells were either cultured on glass slides or on Ibidi imaging plates (Ibidi). Cells were washed with PBS, and then fixed using 4% paraformaldehyde (PFA) for 15 minutes at room temperature (RT). Fixed cells were washed three times with PBS for 5 minutes, then permeabilised using PBS with 0.25% Triton-X-100 for 10 minutes at RT. Cells were blocked using 5% donkey serum in PBS for one hour at RT. The primary antibody used (Table 2.2) was diluted in the blocking solution and kept overnight at 4°C. The following day, primary antibody was removed and the cells were washed three times with PBS for 5

minutes. Cells were incubated with blocking buffer containing the secondary antibody (Alexa Fluor®; Thermo-Fisher Scientific) for 45 minutes at RT, and then washed three times with PBS for 5 minutes. Cells were incubated with Diamidino-2-phenylindole (DAPI) diluted in PBS for 10 minutes at RT. Cells were kept in PBS in the dark at 4°C until ready to be used for imaging. Images were taken using Olympus Confocal Microscope.

Table 2.2: Primary antibody

Name	Antibody Code	Ratio used
OCT4	Sc-9081	1:50
Connexin 43	Cell signaling-3511S	1:50
Anti-Sarcomeric-Alpha Actinin	ab9465	1:100
Anti-Cardiac Troponin T (1F11)	ab10214	1:50
Anti-Myosin Light Chain 2 (EPR3741)	ab92721	1:100
Anti-Heavy Chain Cardiac Myosin (3-48)	Ab15	1:100

2.8 Mitochondrial Membrane Potential via live Mito-tracker Staining

MitoTracker®Red CMXRos dye (M7512; Invitrogen) diffuses passively across the mitochondria plasma membrane in live cells and accumulates in active mitochondria, depending on the mitochondrial membrane potential. The dye is retained in the cells after fixation.

2.8.1 Cell Preparation and Staining

Human iPSCs and beating hiPSC-CMs were incubated with pre-warmed incubation media with 100 nM or 250 nM MitoTracker®Red CMXRos dye for 30 minutes at 37°C[83]. Then cells were washed several times and fixed with 4% PFA at 37°C for 10-15 minutes. After fixation, cells were washed several times. If permeabilisation was required, cells were incubated with 0.25% Triton® X-100 in PBS for 10 minutes at RT.

2.8.2 Imaging and Analysis

Fixed cells were imaged using an Olympus Confocal Microscope. Image J was used to analyse the intensity of MitoTracker®Red CMXRos dye in hiPSCs and beating hiPSC-CMs. The level of fluorescence of a given area was measured by selecting stained areas and unstained areas (background). Corrected total cell fluorescence (CTCF) was calculated using the following equation[84]:

$$CTCF = Integrated\ Density - (Area\ of\ selected\ cell \times Mean\ fluorescence\ of\ background)$$

2.9 Oxygen Consumption Rate Measurements using the Clark Oxygen Electrode

The rate of mitochondrial oxygen consumption (OCR) was measured using the Clark-type oxygen electrode[85–88].

2.9.1 Reagents, Drugs and Substrate Preparation

Table 2.3: Solution preparation for OCR.

Solution	Contents
Washing Solution (KME)	100 mM KCl 50 mM MOPS 0.5 mM EGTA
Respiration Solution (gimish)*	100 mM KCl 50 mM MOPS 1 mM EGTA 5 mM KH_2PO_4 1 mg/ml BSA

*Prepared fresh on the day of the experiment

2.9.2 Cell Preparation

On the day of the experiment, cells were rinsed with PBS and dissociated into single cells using the relevant dissociation solution. For hiPSCs, cells were dissociated into single cells via incubation with 1 ml of TrypLE per 9.5 cm^2 growth area for 5 minutes at 37°C. Beating

hiPSC-derived cardiomyocytes were dissociated to single cells as described before (2.3). After dissociation, cells were counted, two million cells were transferred into 15 ml falcon tubes and centrifuged at 1200 rpm for 5 minutes. Supernatant was removed and the cell pellet was washed with KME (Table 2.3). Cells were centrifuged again at 1200 rpm for 5 minutes. KME was removed and replaced with 600 µl respiration solution (Table 2.3).

2.9.3 Measurement of O_2 Consumption Rate using the Clark Oxygen Electrode

To measure O_2 consumption rate, the Clark-type oxygen electrode was used[85,86,88,89]. The electrodes were embedded in the reaction chambers, and the chamber's temperature was set at 37°C. When cells were ready to be measured, 500 µl of respiration solution containing the two million cells was transferred to the respiratory chambers. Respiration was measured under baseline un-stimulated conditions, following the addition of the energy substrate of interest (pyruvate; 10 mM, malate; 5 mM, or oleic acid 400 µM), the ATP synthase inhibitor oligomycin (2 mM), and the metabolic uncoupler, carbonylcyanide-p-trifluoromethoxy-phenylhydrazone (FCCP; 10 mM).

Table 2.4: Stage of mitochondrial respiration recorded by the Clark-type oxygen electrode.

Stage	Treatment
Baseline Respiration	None
Respiring on energy substrate	Pyruvate (10 mM) and Malate (5 mM) or Oleic Acid (400 µM)
ATP synthase inhibitor	Oligomycin (2 mM)
Maximal Respiration Capacity	FCCP (10 mM)
FCCP biphasic	None
Maximal Respiration Capacity	FCCP (10 mM)
FCCP2 biphasic	None

2.9.4 Reserve Respiratory Capacity

Using the Clark-type oxygen electrode, OCR was measured at baseline and maximal respiration while respiring on pyruvate and malate or oleic acid. Reserve respiratory capacity (RRC) was determined as the difference in OCR at maximal respiration and baseline (Equation).

$$Reserve\ Respiratory\ Capacity = OCR\ at\ Maximal\ Respiration - OCR\ at\ baseline$$

2.10 Extracellular Glucose Consumption and Lactate Production

Glucose and lactate levels were determined using ABX Pentra 400 Chemistry Analyser (Horiba Ltd. USA). Cell culture medium was collected after the experiment and ran through ABX Pentra with lactate reagent (A11A01721, Horiba Ltd.). Reagents provided to be used with this analyser bound to glucose or lactate molecules present in the medium and fluoresced. The analyser detected the signal and analysed the concentration of glucose and lactate. Glycolysis yields two molecules of pyruvate, which can be converted to either lactate or acetyl CoA. Therefore, a ratio of glucose consumption to lactate production that equals two was used as an indicator of exclusively anaerobic glycolysis, whereas, a ratio less than two was used as an indicator of some utilisation of pyruvate in oxidative metabolism.

2.11 *In Vitro* Glucose Utilization using 5-^{3}H-Glucose

Glycolytic flux was measured in cultured cells, hiPSCs and beating hiPSC-CMs, using the rate of ^3H_2O production from ^{3}H-glucose[90,91,100,92–99]. ^3H_2O is released in the ninth step of glycolysis, which is catalysed by enolase (Figure 2.3). The measurement of glycolytic flux using ^{3}H-glucose in isolated working hearts is well established[90,94–96,99,100], but not in

cultured beating hiPSC-CMs, therefore, we adapted the method and applied it to cultured hiPSCs and beating hiPSC-CMs. In preparation, hiPSC were cultured as previously described (section 3.1.1), and differentiated using the preferred differentiation protocol (section 3.2.2).

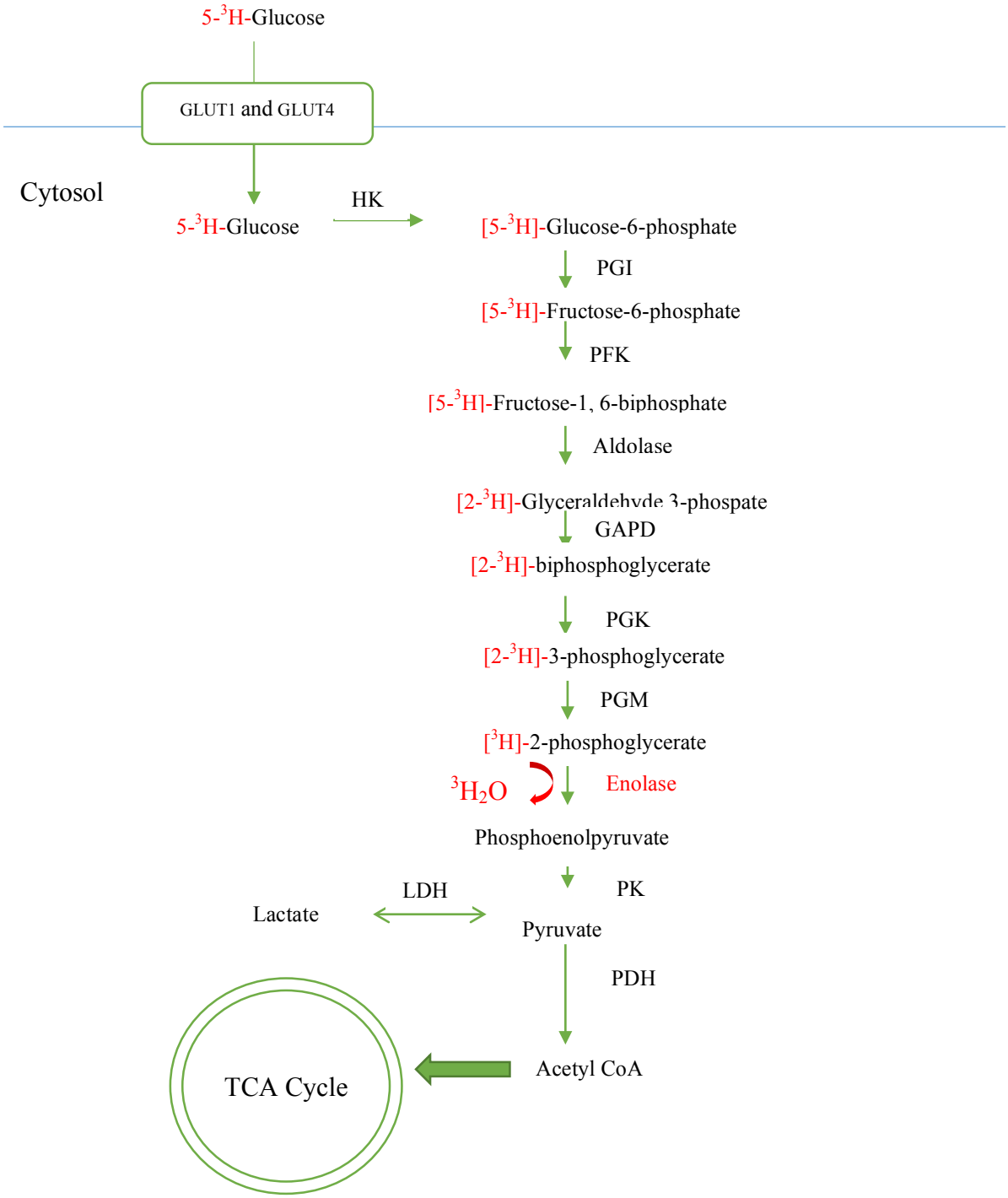


Figure 2.3: Outline of uptake and utilisation of ^{3}H-glucose and release of $^{3}H_2O$ at step nine of glycolysis. HK: Hexokinase, PGI: Phosphoglucose Isomerase, PFK: Phosphofructokinase, GAPDH: Glyceraldehyde-3-phosphate dehydrogenase, PGK: Phosphoglycerate Kinase, PGM: Phosphoglycerate Mutase, PK: Pyruvate Kinase, LDH: Lactate Dehydrogenase, PDH: Pyruvate Dehydrogenase.

2.11.1 Reagent Preparation

Cells were cultured with incubation media that contained 0.00074 MBq of Glucose, D-[5-^{3}H(N)] (PerkinElmer) per 1 ml of incubation media. Two types of incubation media were used either a low-glucose media (5.5 mmol/L) or the culturing media in which the cells were routinely cultured, which is known to be high-glucose media. HiPSCs are routinely cultured in mTeSR1 that contains 17.7 ± 0.01 mmol/L glucose, whereas, beating hiPSC-CMs are cultured with RPMI + B27 media that contains 13.3 ± 0.01 mmol/L glucose.

2.11.2 Culturing Cells with [5-^{3}H]–Glucose

On the day of the experiment, culture media was removed and cells were rinsed with PBS, and then cultured with 2 ml of the incubation media containing 0.00148 MBq of [5-^{3}H]-glucose (Glucose, D-[5-^{3}H(N)], PerkinElmer) per well of a 6-well plate (2 ml per 9.5 cm^{2} growth area). Cells were cultured in 5% CO_2 and 21% O_2 at 37°C for various time points. Incubation time varies depending on the experiment, but in all experiments, there will be a zero-hour time point, and end points of experiments for example, 8 hours and 24 hours. During incubation, $^{3}H_2O$ was released into the incubation media, which was collected at the end of the experiment. The remaining [5-^{3}H]-glucose was separated from $^{3}H_2O$ in the incubation media using the ion-exchange chromatography separation method[91,96–98].

2.11.3 Dowex Preparation and Scintillation Measurements

Dowex was prepared by adding 250 g of Dowex® 1x4 chloride form (Sigma) to 1 L dH_2O, containing 50 g NaOH, and 100g boric acid. Glass Pasteur pipettes (VWR 612-1701) were prepared with glass wool at the bottom, and then filled up to 2/3 with Dowex (Diagram 1). Scintillation vials were filled with 10 ml of scintillation fluid (CytoScint), and placed under each glass Pasteur pipette for collecting samples (Diagram 1). From the collected

incubation media, 200 µl of each sample was added to the Dowex column, and after 15 minutes, the Dowex was washed twice with 1 ml of ddH_2O. Scintillation vials were read using the Tri-Carb 2800TR Liquid Scintillation Analyzer (PerkinElmer).

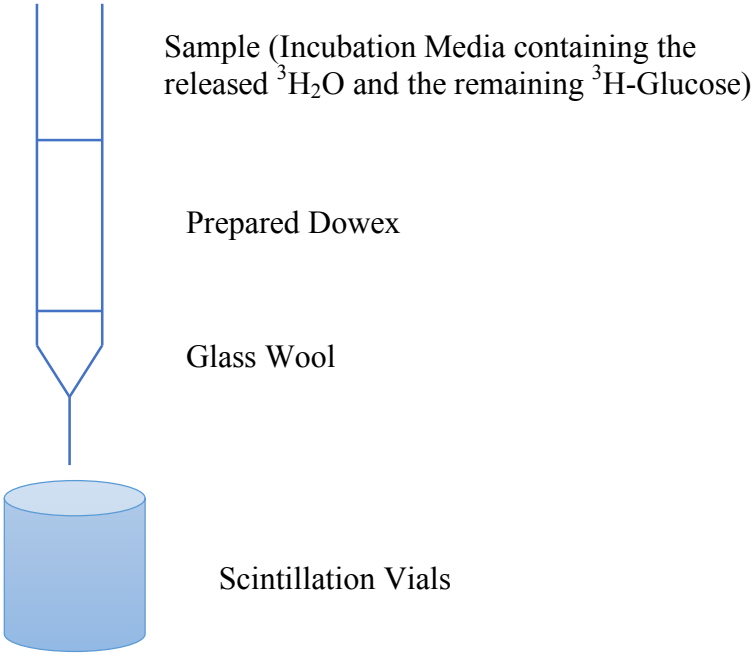
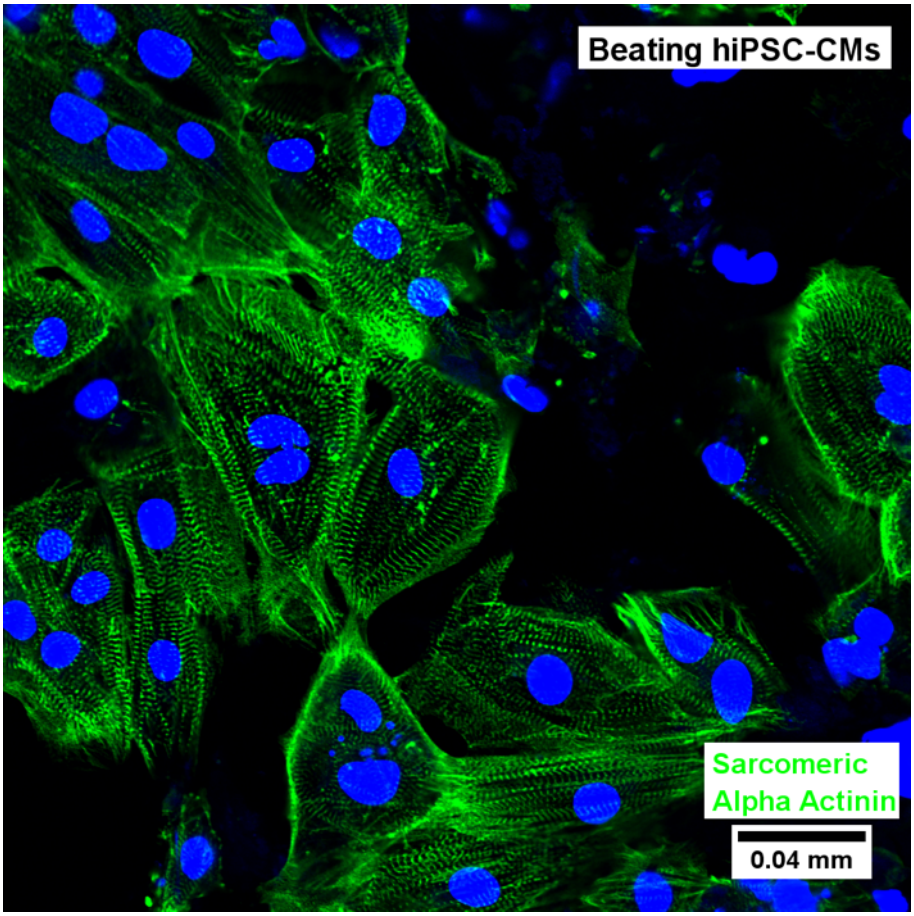


Diagram 1: Dowex columns and scintillation vials. Glass Pasteur pipettes with 1/3 glass wool and 2/3 Dowex. Scintillation vials filled with 10 ml of scintillation fluid were placed under each glass Pasteur pipette for collecting samples.

2.12 Statistical Analysis

Data are expressed as means +/- standard error of the mean (SEM). Data were analysed using unpaired t-test, one-way or two-way analysis of variance (ANOVA) via GraphPad Prism 6. A p value of < 0.05 was taken as the level of statistical significance.



Chapter 3

Differentiation of Human Induced Pluripotent Stem Cells into Beating Cardiomyocytes

3 Differentiation of Human Induced Pluripotent Stem Cells into Beating Cardiomyocytes

3.1 Abstract

Human induced pluripotent stem cells (hiPSCs) need to be differentiated into beating cardiomyocytes (hiPSC-CMs) to be used as an *in vitro* cell-based model to study human cardiomyocytes or for drug screening. In addition, hiPSC-CMs hold the potential to be used in the field of regenerative and personalised medicine. The main aim of this chapter was to find a differentiation protocol that was reproducible, efficient, and produced spontaneously beating cardiomyocytes. Two published protocols were used to differentiate hiPSCs (C19 line) into cardiomyocytes, the Activin A + BMP4 + bFGF protocol[22], and the Wnt-modulation protocol[80]. Gene expression of *KDR*, *GATA4*, *TNNT*, and *MYH6* were upregulated in hiPSC-CMs that were differentiated using the Wnt-modulation protocol, however, no sign of spontaneously beating was observed. Alterations to the Wnt-modulation protocol were introduced, including differentiating cells under transient hypoxia (5% O_2) and the addition of Activin A in combination with CHIR on day 0 of the differentiation. These alterations resulted in spontaneously beating hiPSC-CMs and upregulation in the gene expression of *GATA4*, *MYH6*, and *MYL7*. Due to instability in the C19 cell line, an alternative cell line, OX1-19, was taken forward using the altered Wnt-modulation protocol to differentiate hiPSC-CMs into sheets of spontaneously beating hiPSC-CMs, that expressed cardiac markers such as sarcomeric alpha actinin myosin heavy chain, myosin light chain, and connexin 43. In conclusion, the efficiency of a cardiac

differentiation protocol varies depending on the hiPSC line used, therefore, various optimisation steps were required in order to find a successful protocol.

3.2 Introduction

3.2.1 Heart Development

The heart is one of the early organs to develop and function in the embryo, by the middle of week 3 in the human embryo. The heart first beats around day twenty-one and it starts to pump blood around day twenty-four. This occurs when the embryo has grown so that it can no longer satisfy its nutritional and oxygen requirement by simple diffusion[101–103]. The key steps of heart development include establishment and migration of cardiac progenitor cells, formation of the two lateral endocardial tubes, formation of the primary heart tube, beating of the primary heart tube, looping of the primary heart tube, septation and formation of the four-chambered heart, and formation of the vascular system (Figure 3.1).

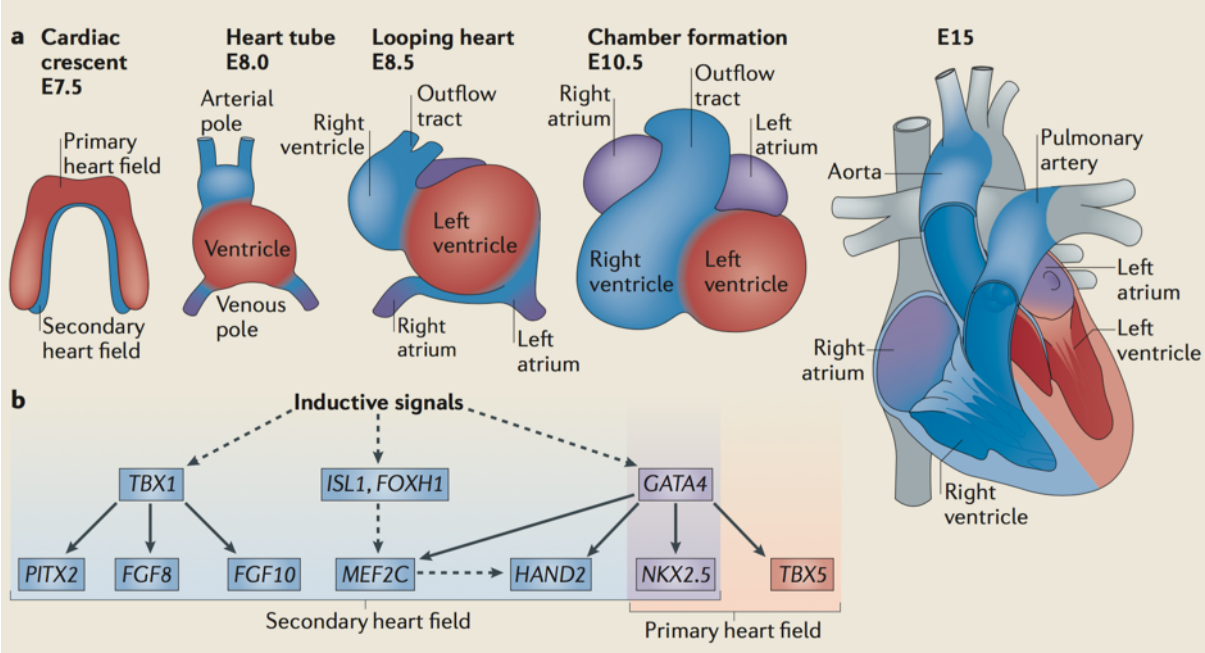


Figure 3.1: Developmental stages of the mouse embryonic heart[104]. Heart development starts with the establishment of cardiac progenitor cells in the primitive streak. Cardiac progenitor cells migrate forming the two lateral mesoderm plates, which fuse in the middle forming the cardiac crescent (the primary heart field). Medial to the primary heart field is the secondary heart field. As the embryo grows, the heart will undergo looping and the formation of the four chambers of the heart.

In the blastula, the appearance of the primitive streak marks the beginning of gastrulation. The primitive streak folds inward and enlarges to create the gastrula, which contains the 3 germ layers (endoderm, mesoderm, and ectoderm). Cardiogenesis starts with the induction of mesoderm in the primitive streak as gastrulation begins. Mesoderm induction in the primitive streak is regulated by Activin/NODAL signalling to induce the secretion of BMP4 from the anterior endoderm and the lateral plate mesoderm[101,102] (Figure 3.2). In addition, Wnt signalling induces the expression of the mesoderm marker Brachyury T, which induces the expression of mesoderm posterior 1 (Mesp1)[105,106] (Figure 3.2). Inhibition of Wnt signalling regulates the specification of mesoderm towards a cardiac linage[106]. Around week 2 of human gestation, naïve cardiogenic mesoderm cells migrate in to the anterior lateral area of the primitive streak to form the cardiac crescent, regulated the transient expression of mesoderm posterior 1 and 2 (Mesp1 and Mesp2)[101,105,106]. The cardiac crescent has two populations: the first-heart field gives rise to the atria, left ventricle, and the nodal conduction system. The second-heart field gives rise to the right ventricle, outflow tract, and parts of the atria[106]. The net effect of BMP signalling activation and Wnt signalling inhibition from anterior endoderm is to upregulate the expression of NK2 homeobox 5 (NKX2.5) in the lateral plate mesoderm[101,102,105,106] which, in turn, upregulates expression of other cardiac transcription factors such as T-box transcription factor 5 (TBX5), paired-like homeodomain transcription factor 2 (PITX2), HAND1, and HAND2 (Figure 3.2). At week 3, the first-heart field cardiac crescent fuses at the middle

and give rise to the linear heart tube[101–103,106]. Around week 4, the linear heart tube start to beat spontaneously and undergo rightward looping, septation, and rapid growth[106]. PITX2 expression in the lateral plate mesoderm is upregulated by NKX2.5 and it plays a role in deposition of extracellular matrix molecules and looping of the heart[102,103]. TBX5 is shown to play an important role in septation of the developing heart[102]. As development proceeds, the linear heart tube undergoes further expansion by cell proliferation and recruitment of additional cells. NKX2.5 regulates the expression of HAND1 and HAND2, which play an important role in the expansion and differentiation of the left and right ventricles, respectively[102,107]. By day 32, the four chambers of the developing heart are well defined[101,106] and by week 8, the foetal heart is connected to the pulmonary truck and the aorta[101,106].

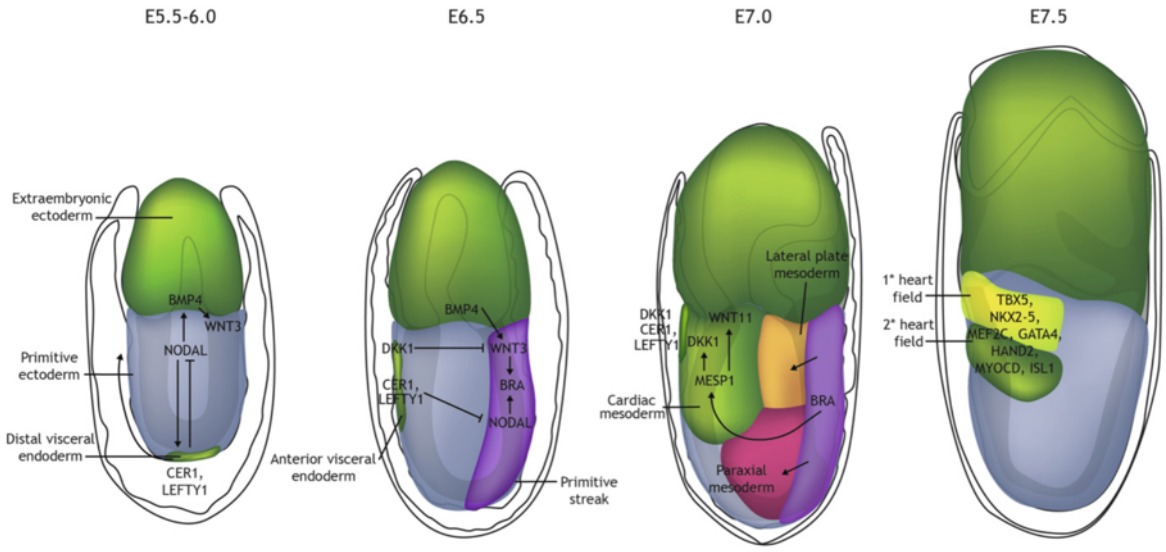


Figure 3.2: The mouse as a model for human cardiogenesis[108]. Cardiogenesis starts with mesoderm induction in the primitive streak mediated via NODAL signalling. The mesoderm state is maintained via BMP signalling and WNT signalling. The expression of mesoderm posterior (Mesp) drives the migration of cardiac progenitor cells to the lateral mesoderm plates, which later forms the primary heart tube.

3.2.2 Hypoxia in Heart Development

Hypoxia is defined as reduced partial pressure of oxygen (pO_2) in arterial blood and it is shown to have an important role in embryogenesis and foetal heart development[109–111]. In humans, oxygen tension varies from 100 mmHg in alveolar arteries to 40-20mmHg in tissue[110,112]. In adult cardiomyocytes, pO_2 is between 5 to 20mmHg (~ 3% O_2) [3]. In adult tissue, physiological hypoxia is when oxygen tension is lower than physiological levels and the demand for oxygen exceeds the supply available and it ranges from 20 to 7 mm Hg[110]. To mimic hypoxia during cell culture, researchers used between 1% (7 mmHg) to 3% (21 mm Hg) O_2[110]. In the uterus oxygen concentration ranges 0.5 to 30 mm Hg[109] and normal foetal arterial blood pO_2 ranges from 20 to 30mm Hg (~ 3-5% O_2). Therefore what is considered to be hypoxia in adult tissues is considered "normoxia" during foetal development[110, 111]. To mimic the oxygen levels during foetal heart development researchers used 3-5% O_2 for cardiac differentiation *in vitro*[113,114]. Although human embryonic stem cells proliferate at a similar rate both under hypoxia 3-5% O_2 and normoxia 21% O_2, hypoxia was shown to be required to maintain the pluripotency of hESCs in culture[115]. The response to hypoxia is mediated by hypoxia-inducible factor-1 (HIF-1), which is an oxygen-sensor transcriptional activator[111,116]. Under normoxic conditions (21% O_2), genes that encode HIF-1α are transcribed and translated but HIF-1α protein is unstable and is rapidly degraded in the presence of sufficient O_2 levels [116–118]. The oxygen-dependent degradation domain of HIF-1α is hydroxylated and tagged for degradation. Under hypoxic conditions, hydroxylation of the oxygen-dependent degradation domain of HIF-1α is blocked and degradation of HIF-1α is inhibited, therefore, HIF-1α protein levels are increased, stabilised and translocated into the nucleus where the

protein activates target genes[111,116–118]. When cells were re-oxygenated after being in hypoxia, HIF-1 α proteins start to degrade in less than 5 minutes[116–118].

During heart development, cardiac progenitor cells (myocardial and endocardial) move from the primitive streak towards forming the heart tube (E7.75 - E8.25), which undergoes looping and chamber formation (E8.5 - E12.0). Between E12.5 and E15 (remodelling stages), division of heart chambers is completed by septation and formation of the heart valves, ensuring unidirectional blood flow[109]. Studies showed that the early embryo heart develops in an hypoxic environment[119]. In addition, HIF-1α was broadly present in the myocardium between E8 and E10.5[120], yet from E13.5 its presence was restricted to the outflow tract, interventricular septum and atrioventricular cushions[109]. Therefore, timed activation and deactivation of HIF is important to cardiac differentiation.

3.2.3 Human Induced Pluripotent Stem Cells Differentiation into Beating Cardiomyocytes: A comparison of available protocols

During heart development, signalling pathways from adjacent areas induce the expression of cardiac transcription factors in specific areas at specific times. The signalling pathways that are activated or inhibited in most experimental differentiation protocols represent the very early stages of cardiac development, such as the establishment of cardiac progenitor population and linage specification to cardiac cells.

In order to use hiPSC-CMs as an *in vitro* cell-based model for drug screening or cell therapy, it is vital to develop a reproducible and efficient differentiation protocol. Cardiac-directed differentiation protocols can be divided into two main groups, the Embryonic Bodies (EB)-based method[114,121] and monolayer-based method[22,80–82,122]. Although cardiac differentiation protocols vary, most involve stage-specific activation and inhibition of

signalling pathways that control heart development, replicating the early cardiac developmental stages in the early embryo (mesoderm induction, mesoderm cardiac specification, and generation of cardiomyocytes). The signalling pathways that are involved in most directed cardiac differentiation protocols are Activin/Nodal and bone morphogenetic proteins (BMP) signalling[114], which are members of the transforming growth factor beta (TGFB) signalling pathway, in addition, to the fibroblast growth factors (FGF)[22,114], and the Wnt signalling pathway[80–82,122]. Activin A, BMP4, and Wnt3a induce the mesoderm, and upregulate the expression of Brachy T, whereas, inhibition of Wnt signalling at later stages of differentiation was shown to induce mesoderm cardiac specification (KDR and platelet-derived growth factor receptor alpha (PDGFR-α) positive cells). Following these steps, cells are generally cultured with media in the absence of growth factors, to allow cardiomyocyte generation and spontaneous beating.

3.2.3.1 Development and Enhancement of EB-Based and Monolayer-Based Protocols

Differentiation protocols were first developed using hESCs and then were translated to iPSCs. Table 3.1 summarises and compares some of the published differentiation protocols from 2001 to 2013 and show a shift from the EB-based model using hESCs to the monolayer-based model using hiPSCs, which is the commonly model used currently. Figure 3.3 shows the timeline of some of the published cardiac differentiation. In the past 5 years, the focus of research has shifted towards maturing hESC or hiPSC-derived cardiomyocytes rather than finding new differentiation protocols.

In general, spontaneously beating EBs are generated from cells in suspension using a serum-based media to induce cardiac differentiation[121,123,124]. In 2001, Kehat et al, used

hESCs in suspension to generate spontaneously beating EBs (8%), which contained 30% cardiac-specific troponin I-positive cells[121]. In 2002, Xu et al reported that 25% of EBs generated using the serum-induction method beat spontaneously. The efficiency of differentiation was enhanced by using 5-aza-2'-deoxycytidine in a stage-dependent manner as the positive effect of 5-aza-2'-deoxycytidine was only reported when it was added from day 6 to 8 of the differentiation. Dimethyl sulfoxide (DMSO) and all-trans retinoic acid had no effect on the efficiency of differentiation[123].

3.2.3.2 Development and Enhancement of Activin A and BMP4-Based Protocols

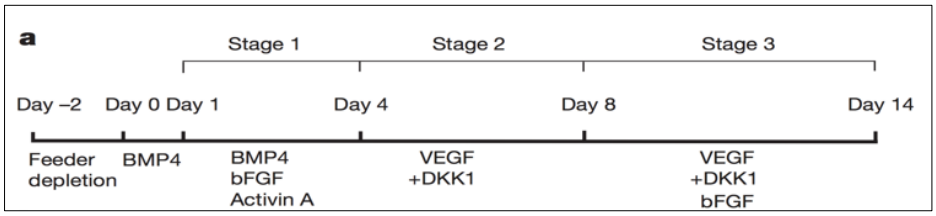
Laflamme et al, played a role in the enhancement of cardiac differentiation protocols by shifting from the serum-induced EB-based differentiation protocol that generated 10-15% spontaneously beating EBs[124] to the serum-free monolayer-based differentiation generating > 30% cardiomyocytes using Activin A and BMP4[18]. In 2008, Yang et al, used Activin A and BMP4 to induce cardiac differentiation and used kinase insert domain protein (KDR) as a marker for cardiac progenitors, representing early stage in mesoderm cardiac specification[125]. They highlighted the importance of the activation and inhibition of Activin/Nodal/TGF-B, BMP4 and Wnt signalling in a stage-specific manner that recapitulated key steps of heart development[125]. Cardiac differentiation was divided into 3 main stages, induction of primitive-streak-like population and mesoderm, cardiac mesoderm specification, and cardiomyocyte generation[125]. In addition, they showed that plating KDR-positive cells in a monolayer caused enrichment in cells expressing cardiac-specific troponin T from around 40 to 60%[125]. In 2011, Kattman et al, generated spontaneously beating EBs containing cells expressing both KDR and platelet-derived growth factor receptor alpha (PDGFR-α) using Activin A and BMP4. KDR and PDGFR-

α cells were sorted and cultured as monolayer producing 80% cardiac-specific troponin T-positive cells[114]. This protocol was further optimised by Carpenter *et al* in 2012[22].

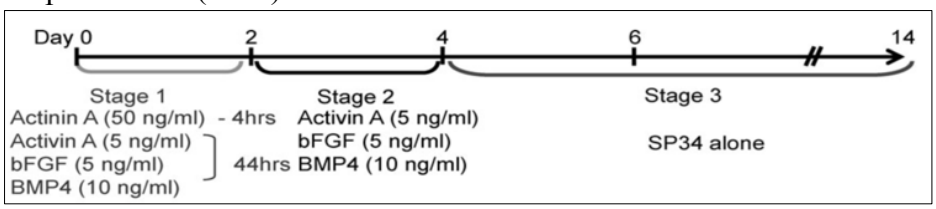
3.2.3.3 Development and Enhancement of Wnt-Based Protocols

Canonical Wnt/B-catenin signalling plays an important role during heart development. It is activated early in heart development during the time of mesoderm induction, then it is inhibited later during specification of mesoderm towards cardiac linage. During cardiac differentiation, the effect of Wnt activation at an early stage was shown to enhance the differentiation[122], and inhibition at a later stage, during cardiac mesoderm specification, also enhanced cardiac differentiation[80,125].

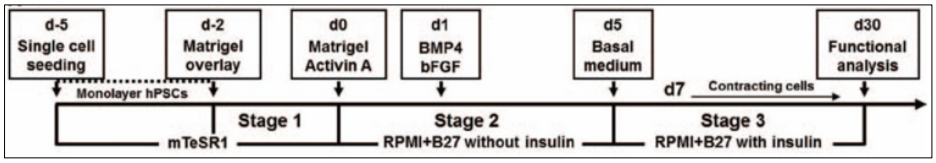
Yang et al (2008):



Carpenter et al (2012):



Zhang et al (2012):



Lian et al (2012):

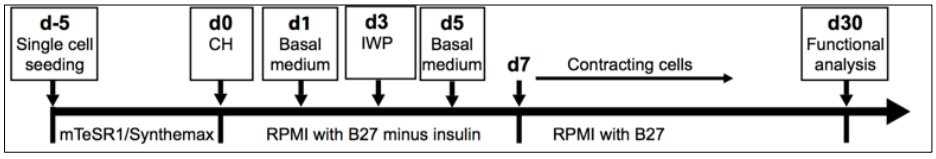


Figure 3.3: Timeline of some published direct cardiac differentiation[22,80,125,126]. A summary of the development of some to the published cardiac differentiation protocols**.** Protocols are divided into stages, recapitulating specific stages during heart development.

In each stage, activation or inhibition of specific signalling pathway is induced by addition of growth factors or small molecules.

Table 3.1: Comparison of direct cardiac differentiation protocols.

Differentiation Method	Cell Type	Growth Factors or Small Molecules	Culture Media	% of cardiac markers	Paper
EB-Method	hESCs	Cells in suspension	80% KO-DMEM, 1 mmol/L L-glutamine, 1.1 mmol/L B-mercaptoethanol, 1% NEAA 20% FBS	• 8.1% spontaneously beating EBs • In beating EBs, 29.4% $cTnI^+$ cells	Kehat et al (2001)[121]
EB-Method	hESCs	Cells in suspension and differentiated with serum-based media To enhance differentiation, addition of DMSO, all-trans retinoic acid (RA), or 5-aza-2'-deoxycytidine.	80% KO-DMEM, 1 mmol/L L-glutamine, 1.2 mmol/L B-mercaptoethanol, 1% NEAA 20% FBS	• 25% spontaneously beating EB by day 8 and 70% by day 16 of differentiation • 5-aza-2'-deoxycytidine enhanced levels of cardiac alpha-MHC	Xu et al (2002)[123]
EB-Method	hESCs	Cells in suspension in Serum-based media		• 10 to 15% positive for sarcomeric MHC	Laflamme et al (2005)[124]
Monolayer	hESCs	h-Activin A h-BMP4	RPMI+B27	• > 30% CMs • Differentiated cells underwent Percoll gradient centrifuge for CMs enrichment (69±10% CMs)	Laflamme et al (2007)[18]

EB-Method	hESCs	h-Activn A h-BMP4 h-bFGF h-VEGF h-DKK1	StemPro-34 (Base) + [L-glutamine, ascorbic acid, monothioglycerol (MTG), P/S]	• KDR^+ cells represent early stage in mesoderm specification to the cardiac lineage • 35±6% $CTNT^+$ cells, enriched to 57±4% when monolayer plated • Wnt signalling inhibition day 4 of differentiation (using DKK1) 2-fold enrichment of $CTNT^+$ cells	Yang et al (2008)[125]
EB-method	hESCs	h-Activin A h-BMP4 h-bFGF h-VEGF h-DKK1	StemPro-34 (Base) + [L-glutamine, ascorbic acid, monothioglycerol (MTG), P/S]	• $KDR^+/PDGFRA^+$ progenitor cells represent cardiac specific mesoderm linage • Upregulated gene expression of MESP1 and NKX2.5 • In beating EBs, 50-70% $CTNT^+$ cells • Enrichment to 80% $CTNT^+$ cells by monolayer culture of day 5 $KDR^+/PDGFRA^+$ cells	Kattman et al (2011)[114]
Monolayer	hESCs	h-Activin A h-BMP4 h-Wnt3a (when applicable)	RPMI+B27	• Early activation of Wnt signalling (using wnt3a in combination with Activin A) enhanced cardiac differentiation	Paige et al (2010)[122]

		h- DKK1 (when applicable)		• Increase in sarcomeric MHC^+ cells from 4 to 27%	
Monolayer	hESCs hiPSCs	h-Activin A h-BMP4 h-bFGF + Extracellular Matrix (Matrigel)	RPMI+B27(-insulin) [d0-6 of differentiation] RPMI+B27 [start from d7 of differentiation]	• Addition of Matrigel (day -2 and 0 of differentiation generated 80% cTnT+ Cells	Zhang et al (2012)[126]
Monolayer	hiPSCs	h-Activin A h-BMP4 h-bFGF	StemPro-34 + [L-glutamine, monothioglycerol (MTG), ascorbic acid, P/S]	• Spontaneously beating sheets of CMs • 40±15% CMs	Carpenter et al (2012)[22]
Monolayer	hESCs hiPSCs	CHIR99021 IWP4/IWP2	RPMI+B27(-insulin) [d0-6 of differentiation] RPMI+B27 [start from d7 of differentiation]	• Spontaneously beating sheets of CMs • 87% $cTNT^+$ CMs	Lian et al (2012)[80] Lian et al (2013)[81] Lian et al (2013)[82]

EB: Embryonic Bodies, hESCs: Human Embryonic Stem Cells, hiPSCs: Human induced Pluripotent Stem Cells, CMs: Cardiomyocytes, NEAA: non-essential amino acids, FBS: fetal bovine serum, cTnI: cardiac troponin I, cTnT: cardiac troponin T, MHC: myosin heavy chain, KDR: kinase Insert Domain Receptor, PDGFRA: platelet-derived growth factor receptor alpha, DKK1: Dickkopf-related protein 1, MESP1: mesoderm posterior 1, DMSO: Dimethyl sulfoxide, BMP4: Bone morphogenetic protein 4, bFGF: Basic fibroblast growth factor, VEGF: Vascular endothelial growth factor, IWP4: Wnt Inhibitor 4, IWP2: Wnt Inhibitor

3.3 Aim of Chapter

The aim of this chapter was to optimise the process of differentiating hiPSC's into beating cardiomyocytes

This chapter will:

1. Highlight similarities and differences between different hiPSCs lines
2. Compare different protocols, to find a differentiation protocol that fits well with our hiPSC lines
3. Overcome difficulties and differences in differentiation efficiency as a result of using different hiPSC lines
4. Modulate Activin A, CHIR, oxygen levels, and cell density to improve differentiation
5. Investigate gene and protein expression of cardiac markers in hiPSCs and beating cardiomyocytes

3.4 Materials and Methods

3.4.1 Human Induced Pluripotent Stem Cells

At the beginning of this chapter, I used the C19 hiPSC line from Dr. Lee Carpenter (NHSBT, John Radcliffe Hospital). After having difficulties culturing the C19 hiPSC line, I used the OX1-19 hiPSC line from Dr. Sally Cowley (James Martin Stem Cell Facility). The maintenance and expansion of the two hiPSC lines is explained in detail in the material and method chapter. Briefly, the C19 hiPSC line was cultured in hypoxia (5% O_2), whereas, the OX1-19 hiPSC line was cultured in normoxia (21% O_2). Both hiPSC lines were

cultured and expanded using pre-prepared hESC-qualified extracellular matrix-coated plates and fed with mTeSR1.

3.4.2 Human Induced Pluripotent Stem Cells Differentiation into Beating Cardiomyocytes

3.4.2.1 Differentiation using Activin A, BMP4, and bFGF (refered to as Protocol 1)

The first differentiation protocol used was based on the differentiation protocol published in 2012 by Lee Carpenter[22] (Figure 3.4).

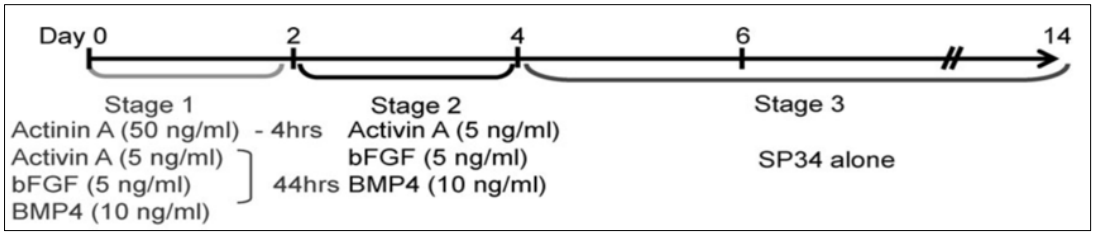


Figure 3.4: Timeline of cardiac differentiation with protocol 1 (Taken from Carpenter, et al)[22].

3.4.2.2 Differentiation using Wnt Signalling Modulation (refered to as Protocol 2)

The second differentiation protocol used in the thesis was based on a protocol published in 2012 by Lian[80] (Figure 3.5). Alterations to this protocol were introduced in order to enhance the efficiency of cardiac differentiation and generate spontaneously beating hiPSC-CMs. Details about the alterations will be introduced before the corresponding result section to make the results easier to follow.

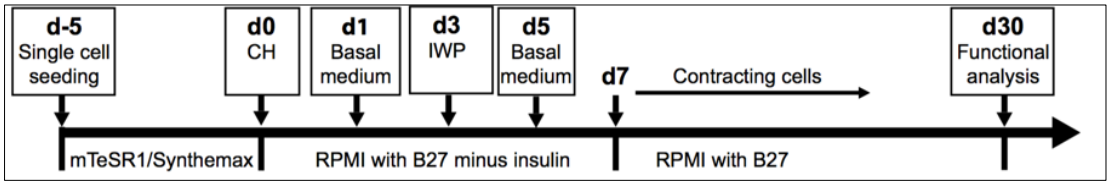


Figure 3.5: Timeline of cardiac differentiation with protocol 2 (Taken from Lian, et al)[80].

3.5 Results

3.5.1 Similarities and Differences between Human Induced Pluripotent Stem Cells Lines

3.5.1.1 Culture and Morphology of Human Induced Pluripotent Stem Cells

The two hiPSC lines used in this project, the C19 and the OX1-19, had different culturing conditions. Therefore, it was important to test the effect of this difference on the pluripotency of the lines. Microscopic Images showed that hiPSCs formed colonies of small cells with a high nucleus-to-cytoplasm ratio (Figure 3.6). Both cell lines were positive for pluripotent markers such as OCT4 (Figure 3.7 and 3.8).

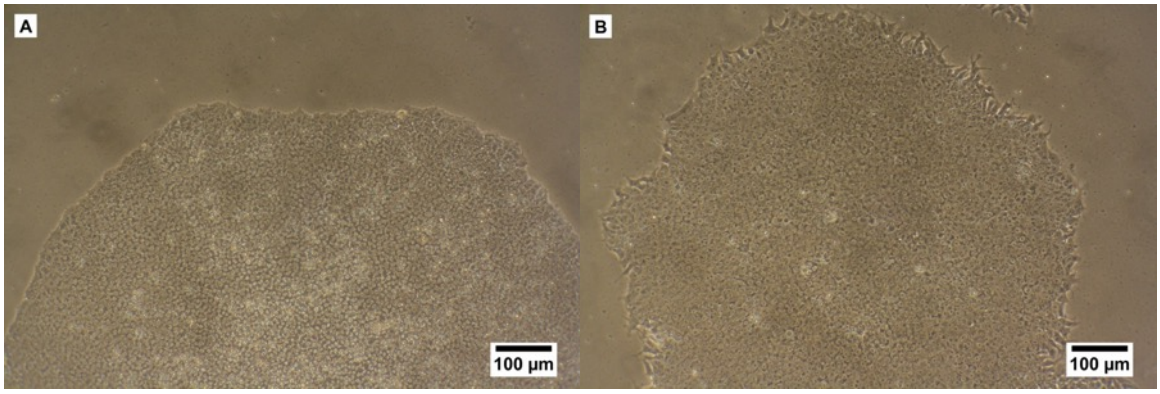


Figure 3.6: Human induced pluripotent stem cell colony. Microscopic images of a colony of the C19 hiPSC line in low magnification (A) and higher magnification (B).

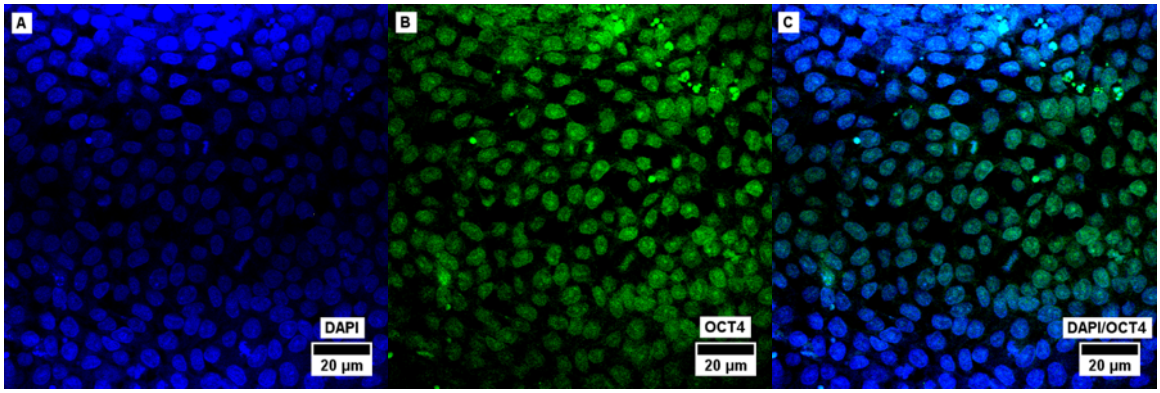


Figure 3.7: Immunocytochemistry of pluripotent marker (OCT4) in C19 hiPSCs. Confocal images of DAPI (A), OCT4 (B), and OCT4 and DAPI (C). **DAPI**: 4′,6-diamidino-2-phenylindole, **OCT4**: octamer-binding transcription factor 4.

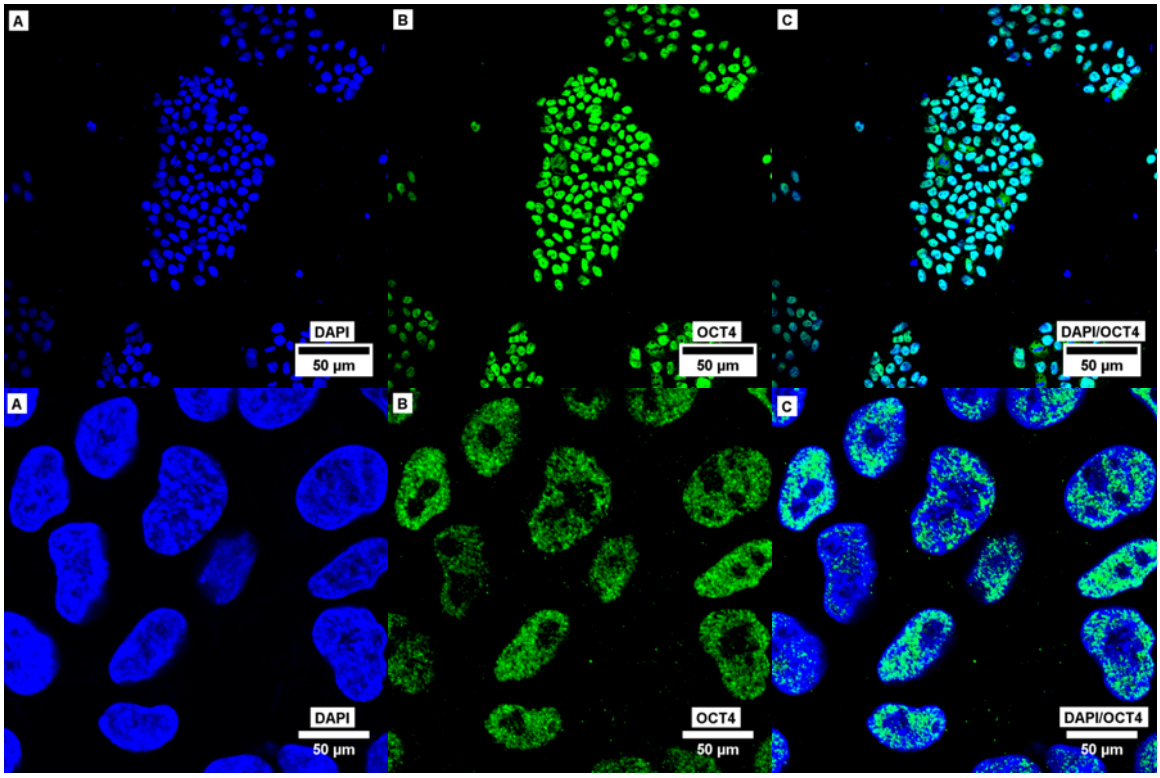


Figure 3.8: Immunocytochemistry of pluripotent marker (OCT4) in OX1-19 hiPSCs. Confocal images of DAPI (A), OCT4 (B), and OCT4 and DAPI (C) at low-magnification (20x) lower row and high-magnification (60x) second row. **DAPI**: 4′,6-diamidino-2-phenylindole, **OCT4**: octamer-binding transcription factor 4.

3.5.1.2 Pluripotent Markers of Human Induced Pluripotent Stem Cells

The relative gene expression of the pluripotent markers *OCT4* and *NANOG* were measured in the two hiPSC lines and data showed no significant difference between the 2 cell lines (Figure 3.9). C19 hiPSCs are routinely cultured in physiological hypoxia (5% O_2), whereas OX1-19 hiPSCs are routinely cultured in normoxia (21% O_2). Therefore, the effect of hypoxia on the expression of pluripotent markers in the OX1-19 hiPSC line was tested after culturing the cells in physiological hypoxia (5% O_2) for 24 hours. Hypoxic culture for 24

hours did not change the relative gene expression of pluripotent markers *OCT4* and *NANOG* (Figure 3.10).

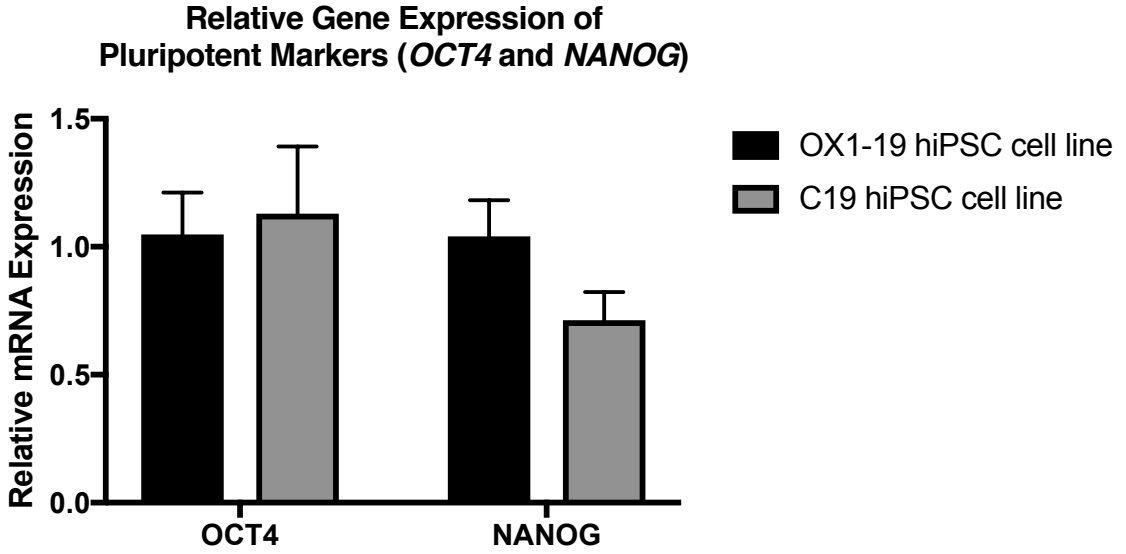


Figure 3.9: The relative gene expression of pluripotent markers, OCT4 and NANOG, in OX1-19 and C19 hiPSC cell lines using qRT-PCR. The expression of pluripotent markers, OCT4 and NANOG, was measured in C19 and OX1-19 hiPSC cell lines. Data were analysed using two-way ANOVA test (n=5).

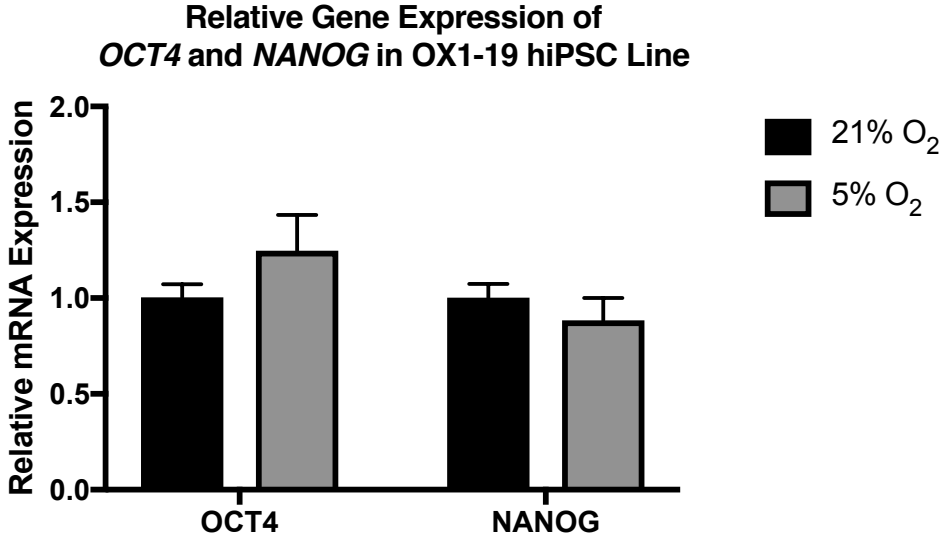


Figure 3.10: The relative gene expression of pluripotent markers in OX1-19 hiPSC line using qRT-PCR. The gene expression of pluripotent markers, *OCT4* and *NANOG*, were measured in OX1-19 hiPSC line cultured in either normoxia (21% O_2) or hypoxia (5% O_2) for 24 hours. Data were analysed using two-way ANOVA test (n=3).

3.5.1.3 Metabolism of Human Induced Pluripotent Stem Cells

Glucose is an important energy substrate for hiPSCs, therefore, the relative gene expression of glucose transporters, *GLUT1* and *GLUT4*, in the two hiPSC lines were measured. The expression of *GLUT1* was 5-fold higher in the C19 cell line compared to the OX1-19 cell line (Figure 3.11). The expression of *GLUT4* and of *PFK* were also significantly higher in C19 cell line compared with OX1-19 cell line (Figure 3.11).

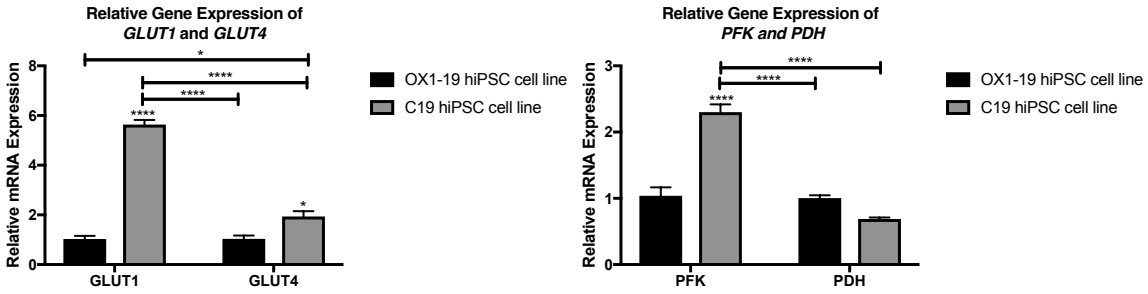


Figure 3.11: The relative gene expression of glucose transporters, *GLUT1* and *GLUT4*, *PFK*, and *PDH* in OX1-19 and C19 hiPSC cell lines using qRT-PCR. *GLUT1*, *GLUT4*, *PFK*, and *PDH* relative gene expression were measured in C19 and OX1-19 hiPSC lines. Abbreviations: GLUT1; glucose transporter 1; GLUT4: glucose transporter 4; PFK: phosphofructokinase; PDH: pyruvate dehydrogenase. Data were analysed using two-way ANOVA test with a p-value ≤ 0.05 (*) and ≤ 0.0001 (****) (n=5).

3.5.1.4 Effect of Hypoxia Culture (5% O_2) on Metabolism of Human Induced Pluripotent Stem Cells

After 24 hours of hypoxia (5% O_2), OX1-19 hiPSCs showed a significant 3.5-fold increase in *GLUT1* relative gene expression compared with normoxia (Figure 3.12). However, there was no change in expression of *GLUT4* or *PFK* (Figure 3.12).

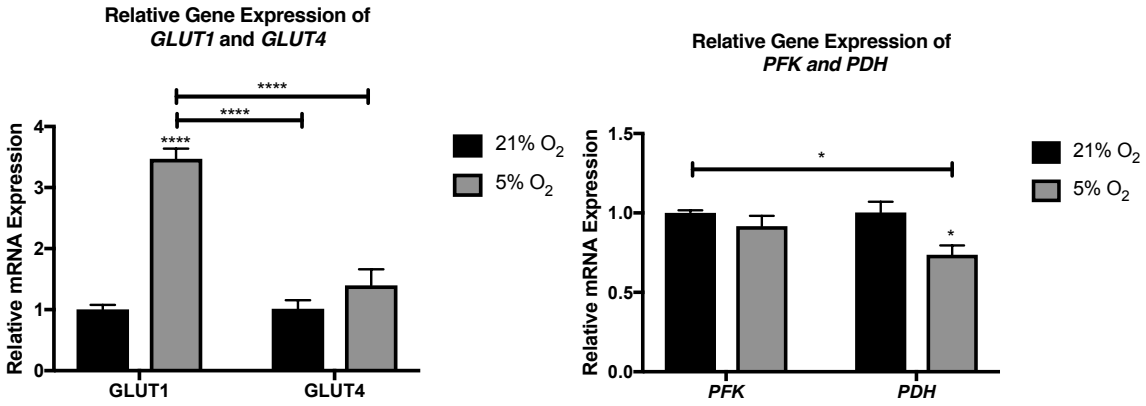


Figure 3.12: The relative gene expression of glucose transporters, *GLUT1*, *GLUT4*, *PFK*, and *PDH* in OX1-19 hiPSC line using qRT-PCR. *GLUT1*, *GLUT4*, *PFK*, and *PDH* relative gene expression were measured in OX1-19 hiPSC cell line cultured in normoxia (21% O_2) and hypoxia (5% O_2) for 24 hours. Abbreviations: GLUT1; glucose transporter 1; GLUT4: glucose transporter 4; PFK: phosphofructokinase; PDH: pyruvate dehydrogenase. Data were analysed using two-way ANOVA test with a p-value ≤ 0.05 (*) and ≤ 0.0001(****) (n=3).

3.5.2 Human Induced Pluripotent Stem Cells Differentiation into Beating Cardiomyocytes

The differentiation of hiSPCs into spontaneously beating hiPSC-CMs involved many optimisation steps, which are summarised below including all the difficulties encountered over time. In summary, two hiPSC lines, C19 and OX1-19, were used at different time points during this project. In addition, two differentiation protocols were tested, looking for spontaneously beating hiPSC-CMs as a first sign of a successful differentiation protocol.

Described here are the many optimisation steps that were investigated in this chapter. This is provided here as a summary, to make the subsequent results easier to follow.

Steps to optimise the cardiac differentiation initially using the C19 hiPSC line, followed by the OX1-19 line:

1. Using the C19 hiPSCs Line:

a. Comparison of Activin A-based verses the Wnt-modulation protocol in normoxia
b. Effect of transient hypoxia on the Wnt-modulation protocol, and comparing it with normoxia – this step was introduced because C19 hiPSCs were routinely cultured under hypoxia
c. Effect of addition of 10 ng/ml of AA to the Wnt-modulation protocol in both normoxia and transient hypoxia – since I started to have more difficulties with the C19 line and wanted to enhance differentiation in hypoxia
d. Effect of higher concentration of AA to the Wnt-modulation protocol in transient hypoxia only – testing whether more enhancement can be achieved
e. Found the optimal conditions for efficient differentiation for the C19 line

2. Using the OX1-19 hiPSC Line:

As the C19 hiPSC line was expanded to higher passages, it was difficult to keep the cells in their stemness state (in terms of morphology) and more cells start to spontaneously differentiation during hiPSCs culture

Using the altered differentiation with the OX1-19 hiPSC line

a. Test the effect of normoxia on the optimised protocol above
b. Find the optimal concentration of CHIR using the optimised differentiation
c. Find the optimal cell-density using the optimised differentiation
d. Test whether transient hypoxia is better than normoxia with CHIR concentrations and cell-density

3.5.2.1 Differentiation of C19 Line into Beating Human Induced Pluripotent Derived Cardiomyocytes

At the beginning of this project, the C19 hiPSCs cell line was used for the differentiation of hiPSCs into beating cardiomyocytes. Two differentiation protocols were tested on this cell line, the Activin A + BMP4 + bFGF protocol (protocol 1)[22] and the Wnt-modulation protocol (protocol 2)[80]. Cardiomyocytes differentiated using protocol 1 had been used by our laboratory previously and were injected into infarcted rat hearts[22]. However, this protocol did not transfer well to our lab and did not result in the generation of spontaneously beating cardiomyocytes. After several attempts, we thought to try another protocol, the Wnt-modulation protocol, which had been reported to generate a high yield of spontaneously beating cardiomyocytes[80]. However, no sign of spontaneously beating cardiomyocytes was observed. Therefore, we decided to directly compare the phenotype of the non-beating hiPSC-CMs from these 2 protocols.

3.5.2.1.1 A Comparison between Protocol 1 (Activin A + BMP4 + bFGF) and Protocol 2 (Wnt-Modulation Protocol)

The gene expression of cardiac markers that represent different stages of heart development, such as *KDR* representing cardiac mesoderm, *GATA4* representing cardiac progenitor cells, *TNNT2*, *MYH6,* and *MYL7* representing cardiomyocytes, and in some cases expression of *MYH7* and *MYL2* were used to investigate differentiation into ventricular or mature cardiomyocytes. Non-beating day-15 hiPSC-CMs were collected to measure the relative mRNA expression of cardiac markers *KDR*, *GATA4*, *TNNT2*, *MYH6*, and *MYL2*. There was an apparent increase in the relative gene expression of *KDR*, *GATA4* and *TNNT2* in the Wnt-differentiated day-15 hiPSC-CMs compared with day-15 hiPSC-

CMs differentiated using protocol 1 (Figure 3.13 A-D). However statistical differences could not be assessed because we had difficulties expanding sufficient numbers of C19 hiPSCs to test.

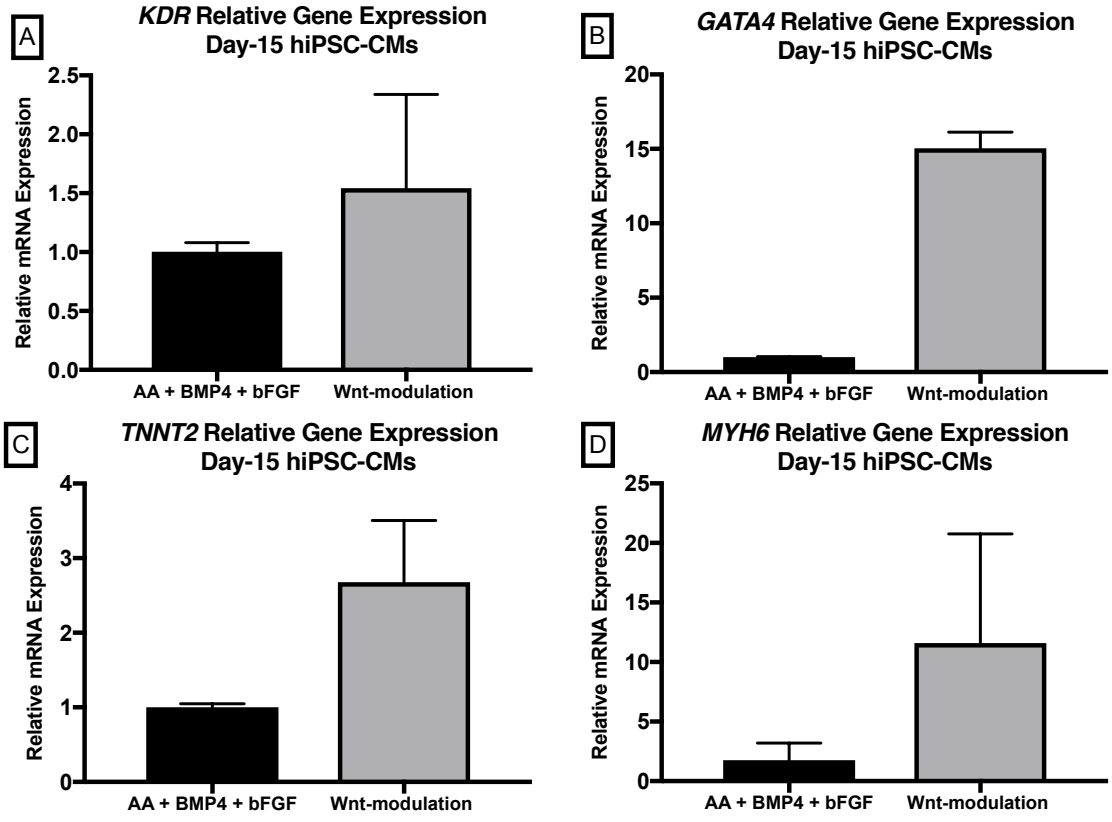


Figure 3.13: Comparison of the relative mRNA expression of cardiac markers in Day-15 hiPSC-CMs. C19 hiPSCs were differentiated using protocol 1 (AA+BMP4+bFGF) and protocol 2 (Wnt-modulation). On Day 15 of differentiation, hiPSC-CMs were collected for analysis (n=2). Abbreviations: KDR: kinase insert domain receptor; GATA4: GATA binding protein 4; TNNT2: troponin T, type 2; MYH6: myosin heavy chain 6.

The differentiated hiPSC-CMs expressed cardiac markers, such as myosin heavy chain in hiPSC-CMs differentiated using protocol 1 (Figure 3.14) and myosin light chain in hiPSC-CMs differentiated using protocol 2 (Figure 3.15). Differentiated hiPSC-CMs using protocol 1 and 2 were further cultured for up to 30 and 60 days, and still failed to produce spontaneously beating cardiomyocytes.

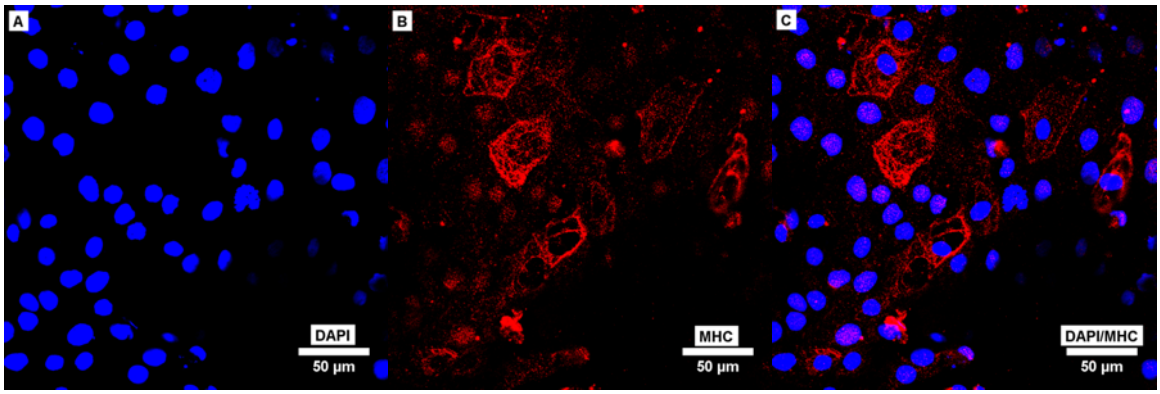


Figure 3.14: Immunocytochemistry of cardiac markers in hiPSC-CMs. Confocal images of DAPI (A), myosin heavy chain (MHC) (B), and DAPI and MHC (C) in C19 hiPSC-CMs differentiated using protocol 1 (AA+BMP4+bFGF). **DAPI**: 4′,6-diamidino-2-phenylindole, **MHC:** myosin heavy chain.

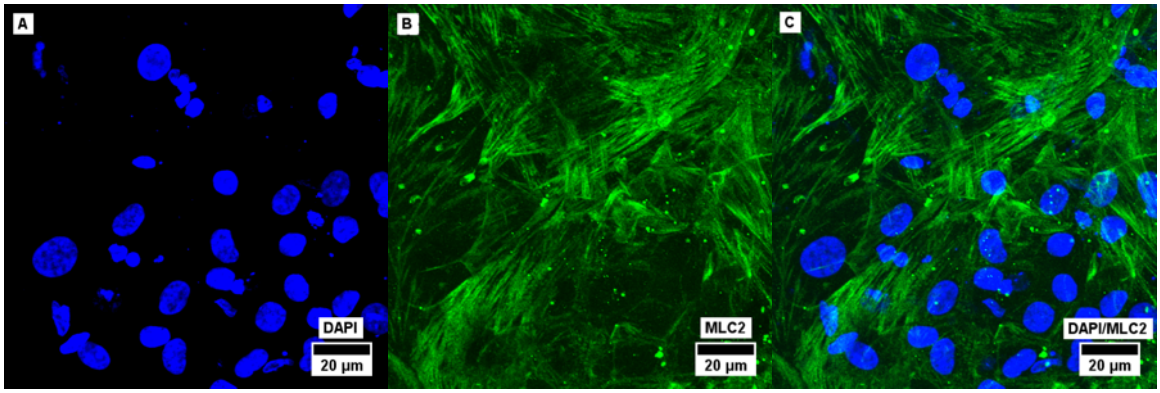


Figure 3.15: Immunocytochemistry of cardiac markers in hiPSC-CMs. Confocal images of DAPI (A), myosin light chain 2 (MLC2) (B), and DAPI and MLC2 (C) in C19 hiPSC-CMs differentiated using protocol 2 (Wnt-modulation). **DAPI**: 4′,6-diamidino-2-phenylindole, **MLC2**: myosin light chain 2.

3.5.2.1.2 Alteration 1 to Protocol 2 (Transient Hypoxia)

C19 hiPSCs are routinely cultured under hypoxia (5% O_2) and the Wnt-modulation protocol is done under normoxia (21% O_2), therefore the protocol was altered to fit with the culturing conditions of the C19 hiPSC cell line. C19 hiSPCs were kept in hypoxia (5% O_2) for the first week of the differentiation until day 7, when they were transferred into normoxia (21% O_2) (Figure 3.16). The differentiation was carried out up to day 15, by which time the hiPSC-CMs showed no sign of spontaneously beating cardiomyocytes in either condition.

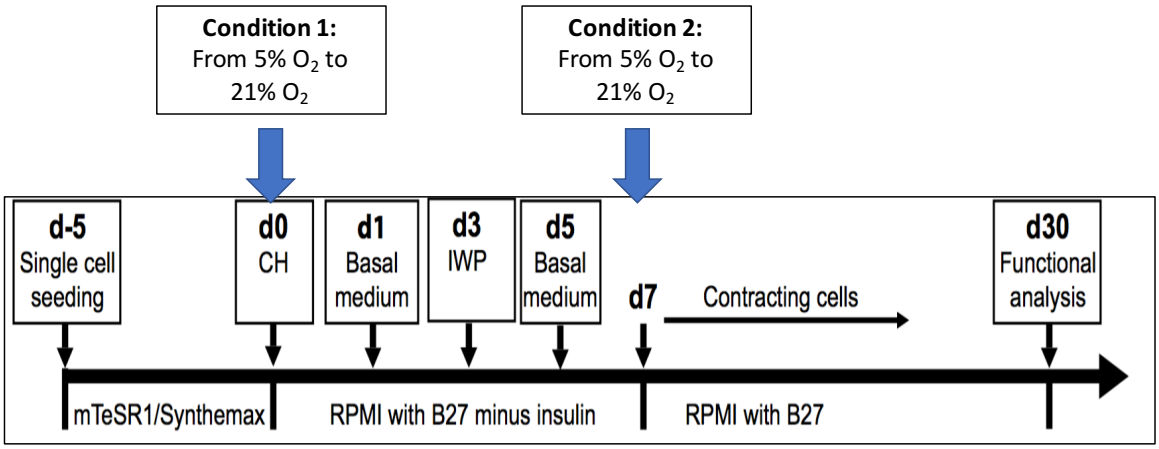


Figure 3.16: Alteration introduced to the Wnt-modulation cardiac differentiation protocol[80]. Condition 1: No alteration to the Wnt-modulation protocol, but C19 hiPSCs were removed from their hypoxic culture in preparation for the cardiac differentiation. Condition 2: The alteration introduced by keeping the C19 hiPSCs in hypoxia (5% O_2) during the first week of differentiation and on day 7, cells were transferred into normoxia (21% O_2) for the rest of their time in culture.

The relative expression of *KDR*, *GATA4*, *TNNT2*, *MYH6*, *MYH7*, *MYL7*, and *MYL2* in day-15 hiPSC-CMs differentiated under normoxia (21% O_2) or transient hypoxia (5% O_2) was measured. There was no difference in the relative mRNA expression of *KDR* (Figure 3.17 A), but a reduction in the relative mRNA expression of *GATA4* in Day-15 hiPSC-CMs differentiated under transient hypoxia (5% O_2) when compared to normoxia (21% O_2) (Figure 3.17 B). There was no difference in *TNNT2*, *MYH6*, *MYH7* or *MYL7* (Figure 3.17 C-F). Gene expression of *MYL2* was undetectable in hiPSC-CMs differentiated using either culture condition.

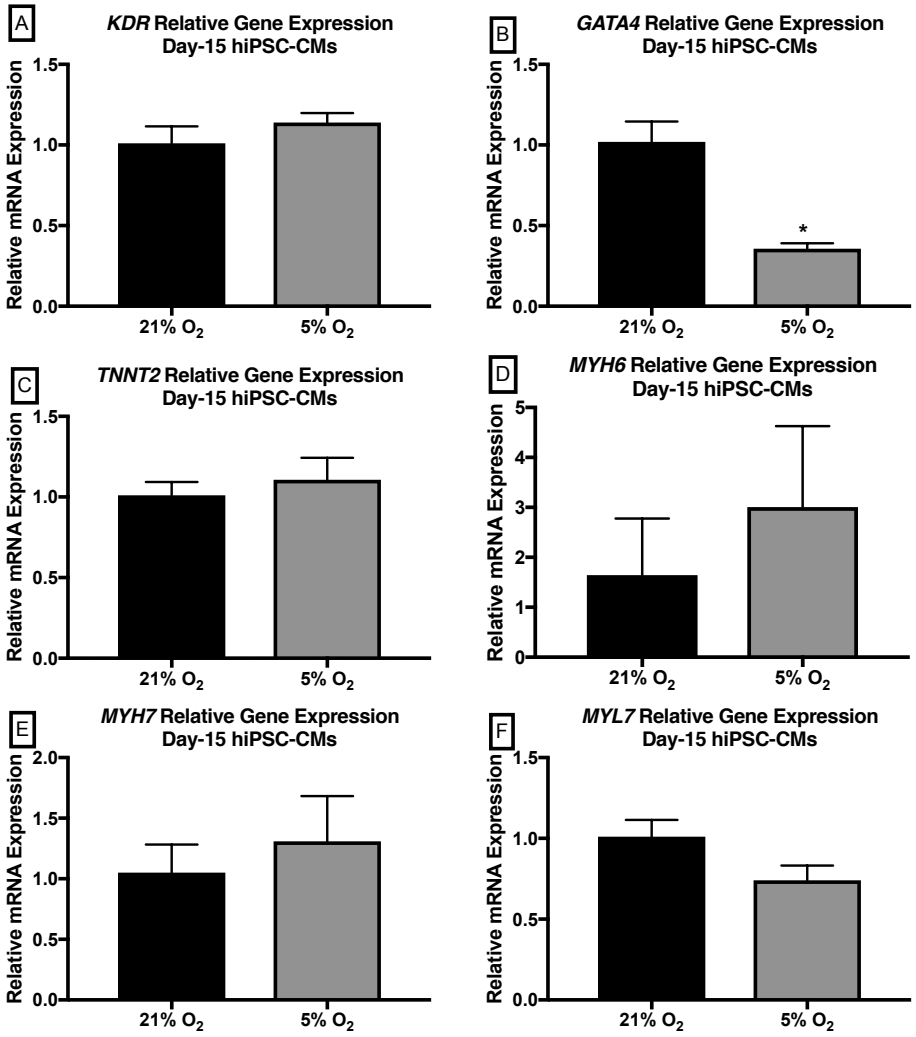


Figure 3.17: The relative mRNA expression of cardiac markers in day-15 hiPSC-CMs differentiated under 21% O_2 verse 5% O_2. C19 hiPSCs were differentiated using protocol 2, under either normoxia (21% O_2) or transient hypoxia (5% O_2). HiPSC-CMs were cultured up to 15 days of each differentiation. Abbreviations: KDR: kinase insert domain receptor; GATA4: GATA binding protein 4; TNNT2: troponin T, type 2; MYH6: myosin heavy chain 6; MYH7: myosin heavy chain 7; MYL7: myosin light chain 7. Data were analysed using an unpaired, two-tailed t-test with a p-value = 0.003 (*) (n=3).

3.5.2.1.3 Alteration 2 to Protocol 2 (Addition of Activin A)

The team that developed the Wnt-modulation protocol showed that the addition of Activin A (AA) at a concentration of 10 ng/ml increased the efficiency of differentiation by increasing the percentage of TNNT2-postive cells and promoting early beating[127]. Therefore, C19 hiPSCs were differentiated using protocol 2 with addition of AA treatment

on day 0 of the differentiation. For condition 1, C19 hiPSCs were differentiated under normoxia from day 0 and cells were treated with 10 ng/ml AA in combination with CHIR (Figure 3.18). In a parallel experiment, C19 hiPSCs were differentiated under transient hypoxia and treated with 10 ng/ml Activin A in combination with CHIR on day 0 of the differentiation, called condition 2 (Figure 3.18). For the first time, spontaneous beating was observed in day-15 hiPSC-CMs differentiated under condition 2.

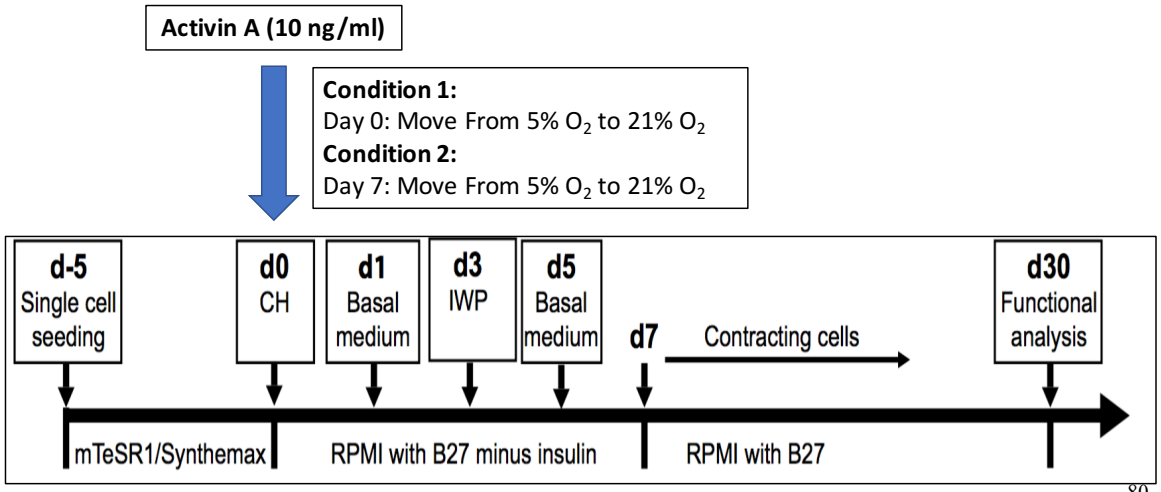


Figure 3.18: Alteration to the Wnt-modulation cardiac differentiation protocol[80]. Condition 1: Alteration 2 was introduced to the Wnt-modulation protocol, which was the addition of adding Activin A (10 ng/ml) on day 0 of differentiation in combination with CHIR. Condition 2: Alteration 1 and alteration 2 were introduced to the Wnt-modulation protocol, the differentiation was started while C19 hiPSCs were in hypoxia and Activin A (10 ng/ml) was added in combination with CHIR on day 0 of the differentiation. Cells were transferred to normoxia on day 7 of the differentiation.

Day-15 hiPSC-CMs from the two conditions were collected to study the effect of the addition of 10 ng/ml AA on the relative mRNA expression of *KDR*, *GATA4*, *TNNT2*, *MYH6*, *MYH7*, *MYL7*, and *MYL2*. Although, these cells showed significant reduction in the relative mRNA expression of *KDR* (p-value 0.0002) (Figure 3.19 A), the relative mRNA expression of *GATA4* (Figure 3.19 B), and *MYL7* (Figure 3.19 F) was significantly higher. However, the addition of 10 ng/ml in combination with CHIR under transient

hypoxia differentiation did not significantly upregulate the relative gene expression of *TNNT2* (Figure 3.19 C), *MYH6* (Figure 3.19 D) and *MYH7* (Figure 3.19 E). The expression of *MYL2* was undetectable in both conditions.

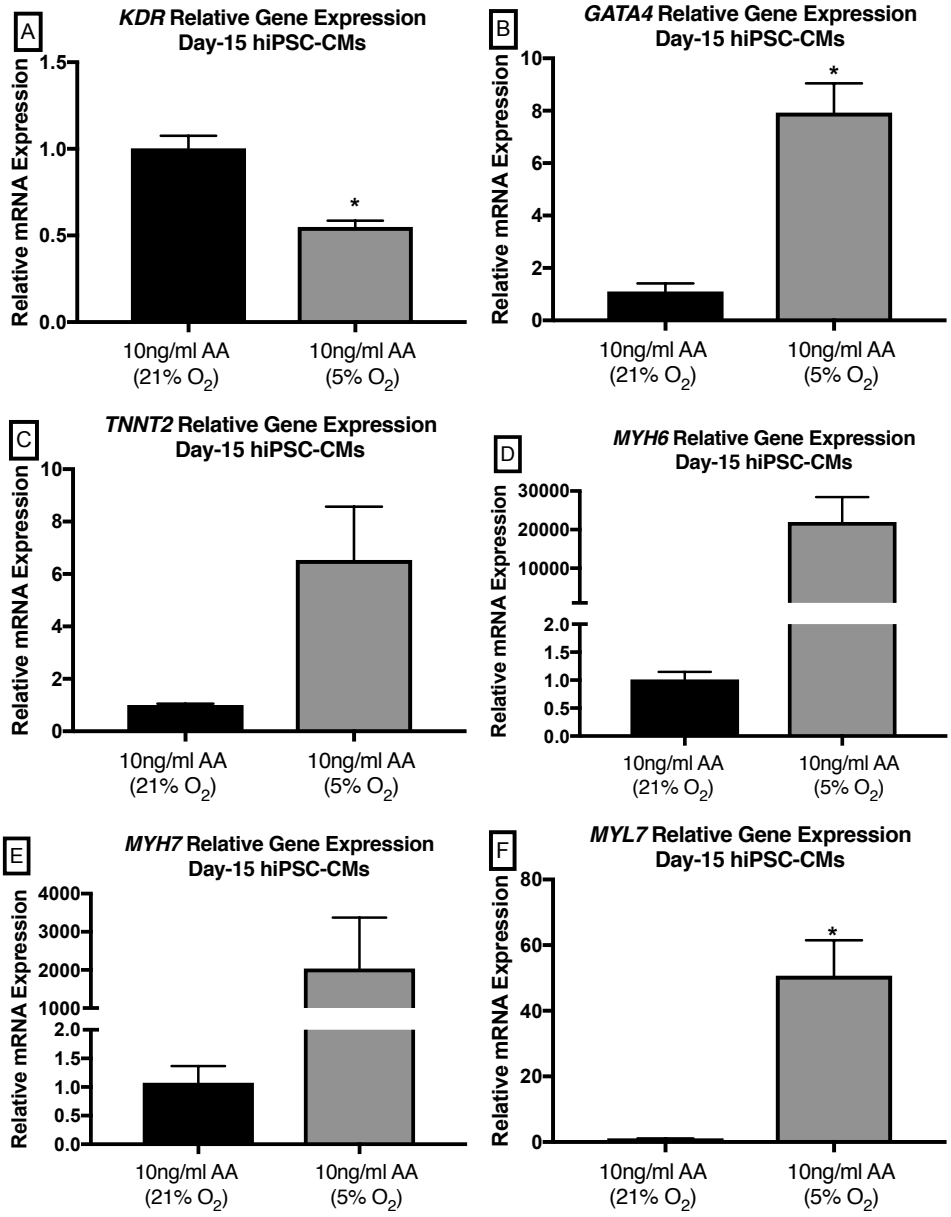


Figure 3.19: The effect of Activin A in day-15 hiPSC-CMs differentiated using the Wnt-modulation protocol under normoxia (21% O_2) or transient hypoxia (5% O_2). The relative mRNA expression of *KDR* (A), *GATA4* (B), *TNNT2* (C), *MYH6* (D), *MYH7* (E), and *MYL7* (F) in day-15 hiPSC-CMs differentiated using the Wnt-modulation protocol in the addition of 10ng/ml Activin A (AA). Abbreviations: KDR: kinase insert domain receptor; GATA4: GATA binding protein 4; TNNT2: troponin T, type 2; MYH6: myosin

heavy chain 6; MYH7: myosin heavy chain 7; MYL7: myosin light chain 7. Data were analysed using unpaired, two-tailed t-test with a p-value ≤ 0.05 (*) (n=3).

The above data showed that transient hypoxia (5% O_2) for the first week of differentiation resulted in an efficient differentiation that gave rise to spontaneously beating hiPSC-CMs on day 11 of the differentiation, when 10 ng/ml AA was added on day 0 of the differentiation. We tested whether a higher concentration of AA (100 ng/ml) would further enhance hiPSC-CMs differentiation by differentiating cells under transient hypoxia and 3 conditions, CHIR alone, CHIR + 10 ng/ml AA, and CHIR + 100 ng/ml (Figure 3.20).

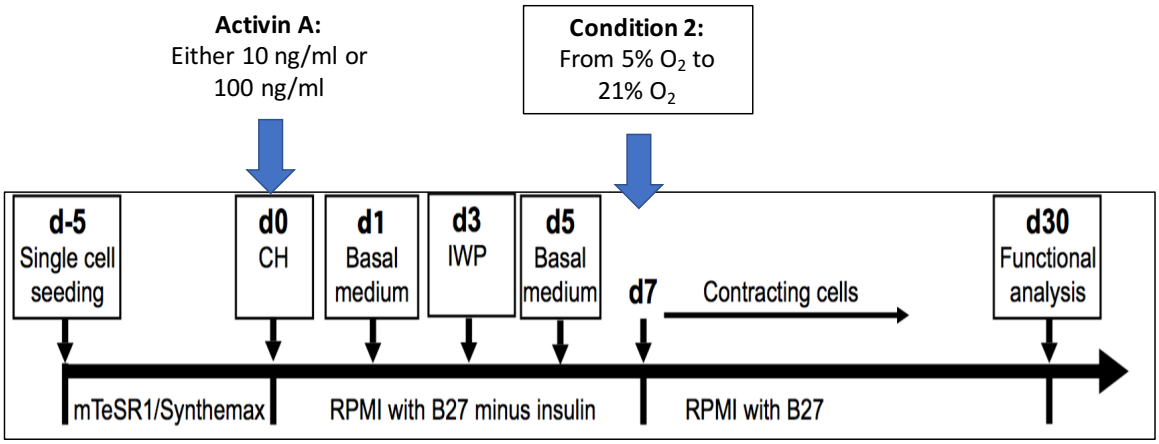
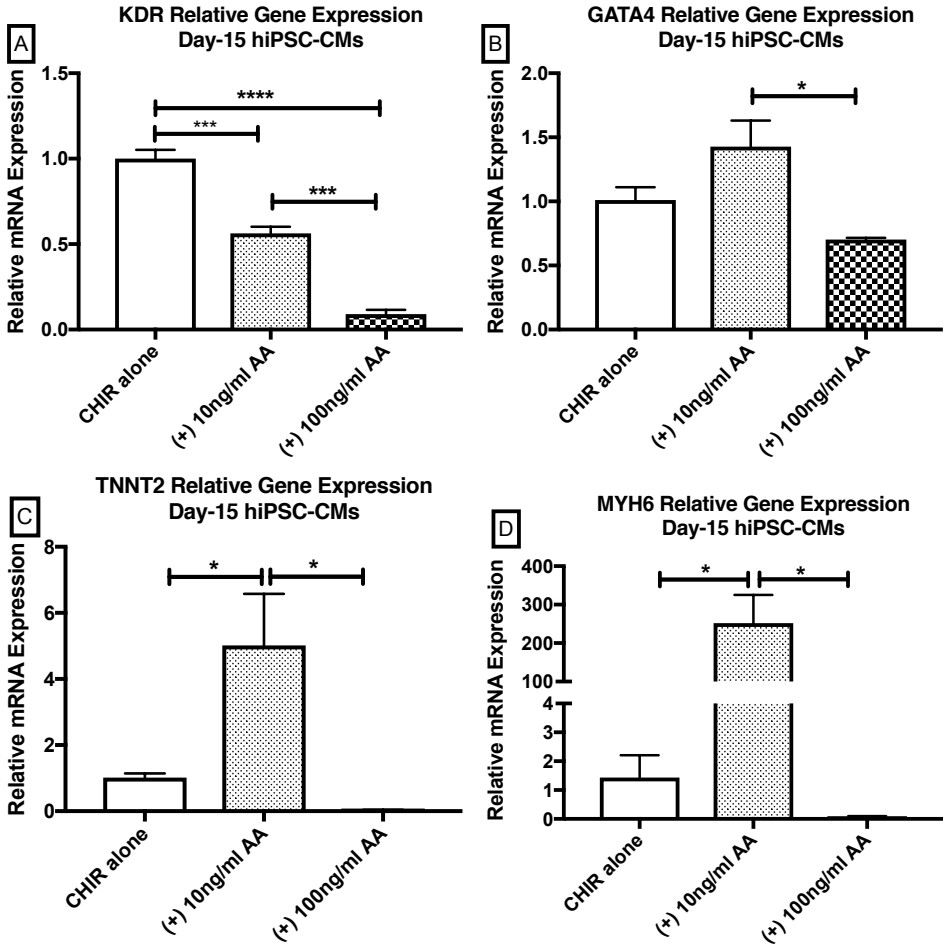


Figure 3.20: More alterations to the Wnt-modulation cardiac differentiation protocol[80]. Alteration 1: the first week of cardiac differentiation using the Wnt-modulation protocol, was conducted under hypoxia, and cells were back to normoxia on day 7 of the differentiation. Alteration 2: on day 0 of the differentiation cells were treated with CHIR alone, CHIR + 10 ng/ml AA, or CHIR + 100 ng/ml AA.

The relative gene expression of *KDR*, *GATA4*, *TNNT2*, *MYH6*, *MYH7*, *MYL7*, and *MYL2* were measured in day-15 hiPSC-CMs, differentiated under transient hypoxia (5% O_2) in the absence of AA or presence of 10 ng/ml AA or 100 ng/ml AA in combination with CHIR. The addition of 10 ng/ml AA in combination with CHIR, significantly upregulated the relative gene expression of *TNNT2* (Figure 3.21 C), *MYH6* (Figure 3.21 D), and *MYL7* (Figure 3.21 F) compared with no AA. Whereas, the treatment of 100 ng/ml AA + CHIR

resulted in a significant reduction in the relative gene expression of *KDR*, *GATA4*, *TNNT2*, *MYH6*, and *MYL7* when compared to hiPSC-CMs treated with only 10 ng/ml AA + CHIR (Figure 3.21 A-F). The relative gene expression of *MYL2* was undetected in all cells. In addition, only in the 10 ng/ml AA + CHIR-treated hiPS-CMs was spontaneous beating observed, as CHIR-treated and 100 ng/ml AA + CHIR-treated hiPSC-CMs showed no sign of spontaneous beating.



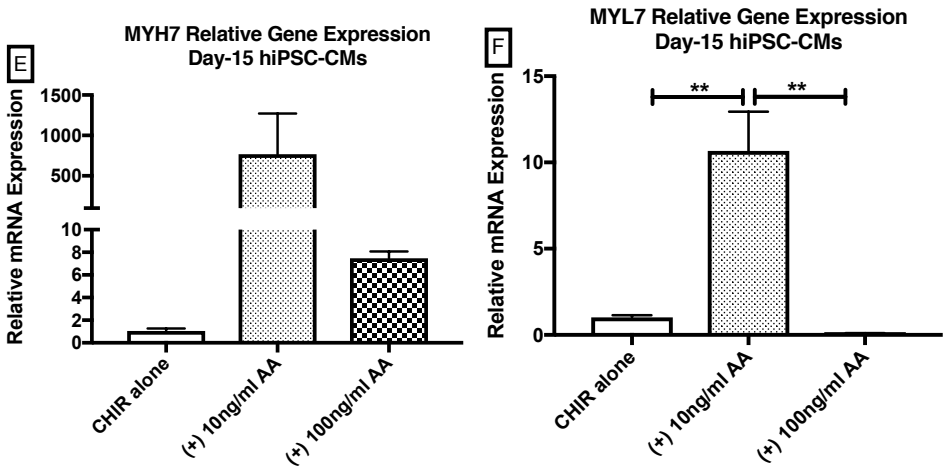


Figure 3.21: Effect of different concentration of Activin A on the relative mRNA expression in day-15 hiPSC-CMs differentiated using the altered Wnt-modulation protocol. HiPSCs were differentiated using the altered Wnt-modulation protocol differentiated, under transient hypoxia, in the absence or addition of either 10 ng/ml Activin A (AA) or 100 ng/ml AA. The relative expression of the following genes *KDR* (A), *GATA4* (B), *TNNT2* (C), *MYH6* (D), *MYH7* (E), and *MYL7* (F). Abbreviations: KDR: kinase insert domain receptor; GATA4: GATA binding protein 4; TNNT2: troponin T, type 2; MYH6: myosin heavy chain 6; MYH7: myosin heavy chain 7; MYL7: myosin light chain 7. Data were analysed using a one-way ANOVA with a Tukey post-hoc test with p-value ≤ 0.05 (*), p≤ 0.01 (**), and p≤ 0.0001 (****) (n=3).

Both beating (CHIR + 10 ng/ml Activin A) and non-beating (CHIR alone) hiPSC-CMs were cultured for up to 30 days, and hiPSC-CMs were positive to the following cardiac markers, myosin light chain ((Figure 3.22), myosin heavy chain, and connexin 43 (Figure 3.23).

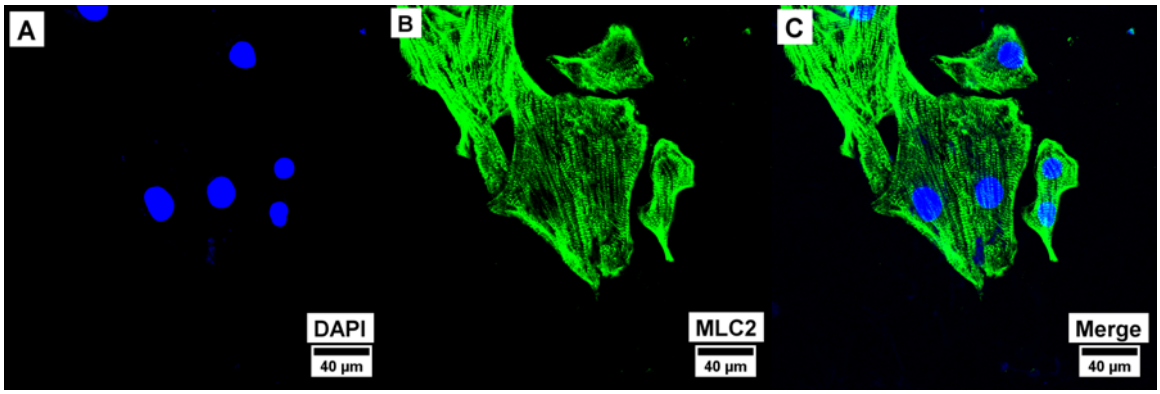


Figure 3.22: Confocal images of Day-30 hiPSC-CMs using the altered Wnt-modulation differentiation. Day-30 hiPSC-CMs differentiated with CHIR in combination with 10 ng/ml Activin A. (A) DAPI, (B) myosin light chain 2, and (C) DAPI and MLC2 in

OX1-19 hiPSC-derived beating cardiomyocytes. **DAPI**: 4′,6-diamidino-2-phenylindole, **MLC2**: myosin light chain 2.

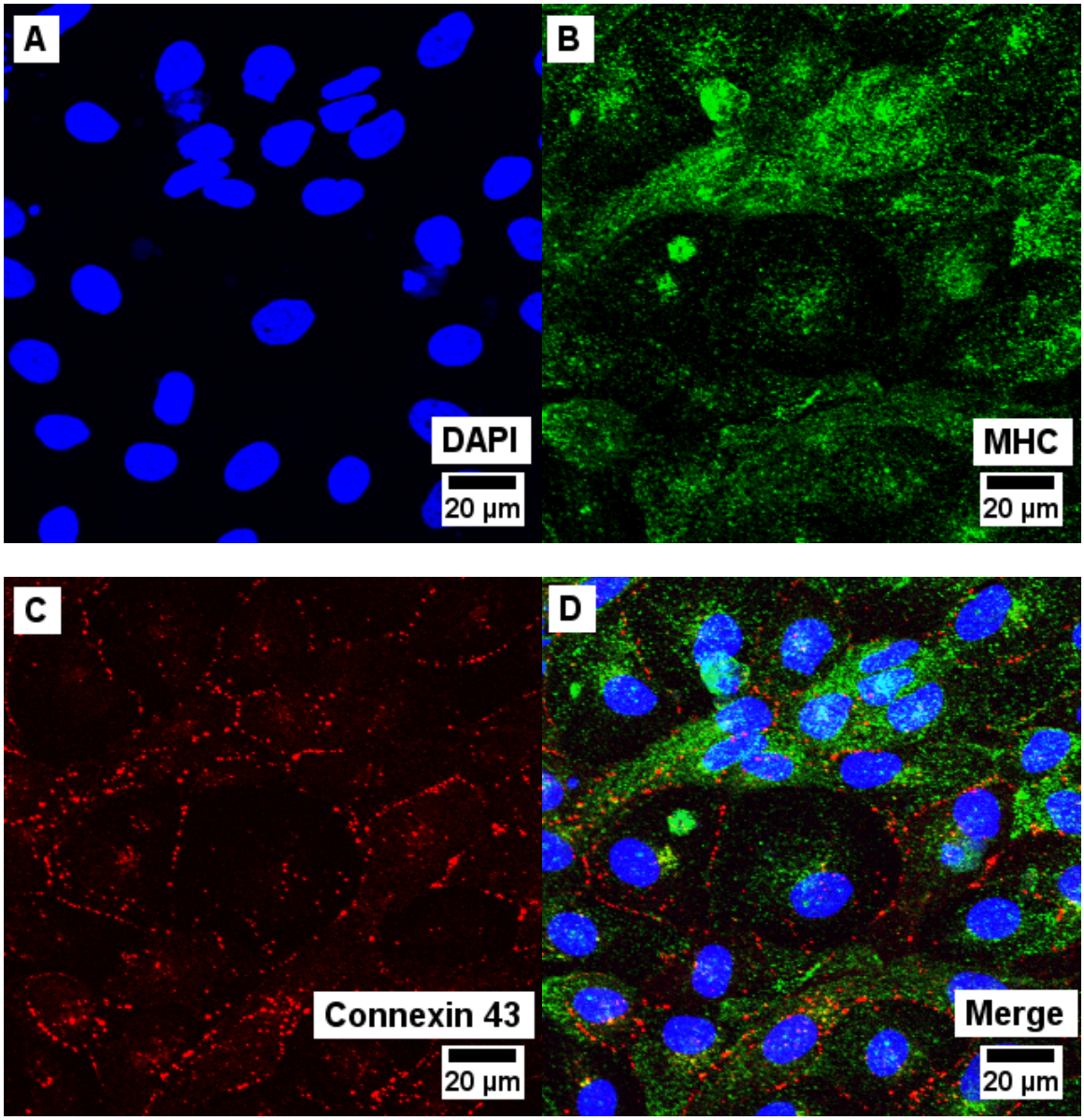


Figure 3.23: Confocal images of Day-30 hiPSC-CMs using the altered Wnt-modulation differentiation. Day-30 hiPSC-CMs differentiated with CHIR in combination with 10 ng/ml Activin A. **DAPI**: 4′,6-diamidino-2-phenylindole and **MHC**: myosin heavy chain.

3.5.2.2 Difficulties Culturing and Expanding the C19 hiPSC Line

Although, the Wnt-protocol with the addition of Activin A resulted in spontaneously beating hiPSC-CMs, I was having difficulties maintaining the stem cell morphology of the C19 hiPSC cell line during passages (Figure 3.24). In addition, the C19 hiPSC cell line started to grow slowly and failed to produce the cell numbers required. It was vital to have a hiPSC cell line that proliferated rapidly and maintained the stemness phenotype. Therefore, I obtained the OX-19 hiPSC cell line from Dr Sally Cowley at the James Martin Stem Cell Facility. The differentiation protocol used for these cells was the Wnt-modulation protocol with the alterations described previously that resulted in spontaneously beating hiPSC-CMs in the C19 hiPSC cell line.

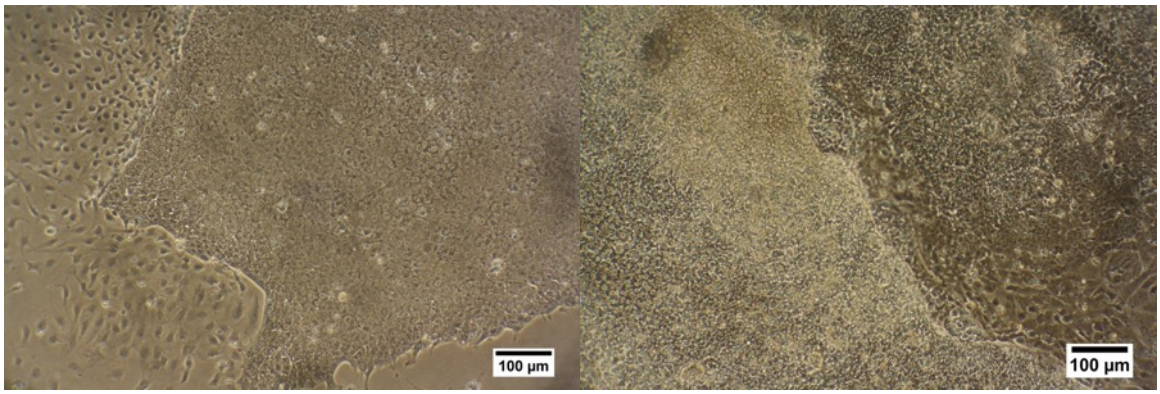


Figure 3.24: C19 human induced pluripotent Stem Cell Line. As C19 hiPSCs were expanded and passaged, the morphology of the cells start to change and fibroblast-like cells appeared in the culture.

3.5.2.2 The Differentiation of OX1-19 hiPSC line into Beating Cardiomyocytes

3.5.2.2.1 Alteration 1 and 2 to Protocol 2 (Wnt-Modulation Protocol)

To test the efficiency of the optimised Wnt-modulation protocol using the new hiPSCs cell line, OX1-19, the relative gene expression of the cardiac markers *TNNT2* and *MYH6* were measured. Data showed a significant increase in the relative gene expression of the two cardiac markers in beating OX1-19 hiPSC-CMs that were differentiated using the

optimised Wnt-modulation protocol, with addition of 10 ng/ml AA + CHIR of day 0 of the differentiation and transient hypoxia for the first week of differentiation (Figure 3.25).

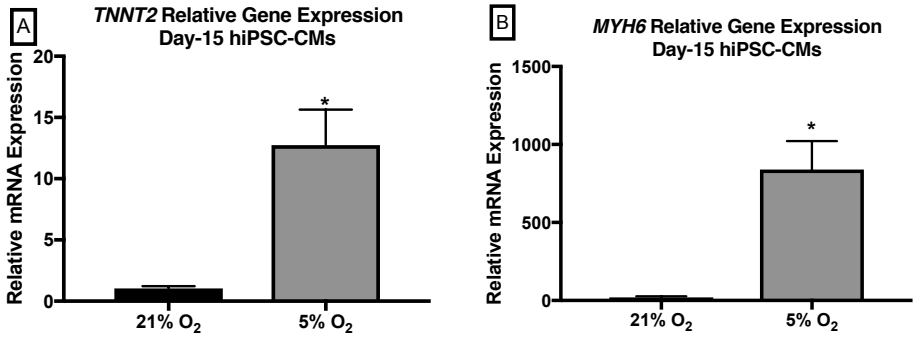


Figure 3.25: The Relative mRNA expression of *TNNT* and *MYH6* in day-15 hiPSC-CMs using OX1-19 Cell Line. HiPSC-CMs were differentiated using the OX1-19 hiPCs and the Wnt-modulation protocol under normoxia (21% O_2) and hypoxia (5% O_2). Day-15 hiPSC-CMs were collected and the relative gene expression of *TNNT2* (A) and *MYH6* (B). Abbreviations: TNNT2: troponin T, type 2; MYH6: myosin heavy chain 6. Data were analysed using an unpaired, two-tailed t-test with a p-value = 0.02 and 0.01, respectively (n=3).

3.5.2.2.2 Optimal CHIR Concentration and Cell Density for the Altered Wnt-Modulation Protocol

Using the transient hypoxia (5% O_2) differentiation, the effect of different CHIR concentrations (8 µM, 12 µM, and 16 µM) was assessed at two different hiPSC seeding-densities (125,000 and 250,000 / 0.32cm^2 growth area). In the low cell-density differentiation (Figure 3.26 A-E), there was a significant increase in the relative mRNA expression of *MYH6* in the 12 µM and 16 µM CHIR-treated hiPSC-CMs compared with 8 µM CHIR-treated hiPSC-CMs (Figure 3.26 B). However, no difference was in the relative mRNA expression of *TNNT2*, *MYH7*, *MYL2* and *MYL7* in the 12 µM and 16 µM CHIR-treated hiPSC-CMs (Figure 3.26 C-D). In addition, 8 µM CHIR failed to differentiate spontaneously beating hiPSC-CMs, whereas both 12 µm and 16 µM CHIR was sufficient to generate spontaneously beating hiPSC-CMs.

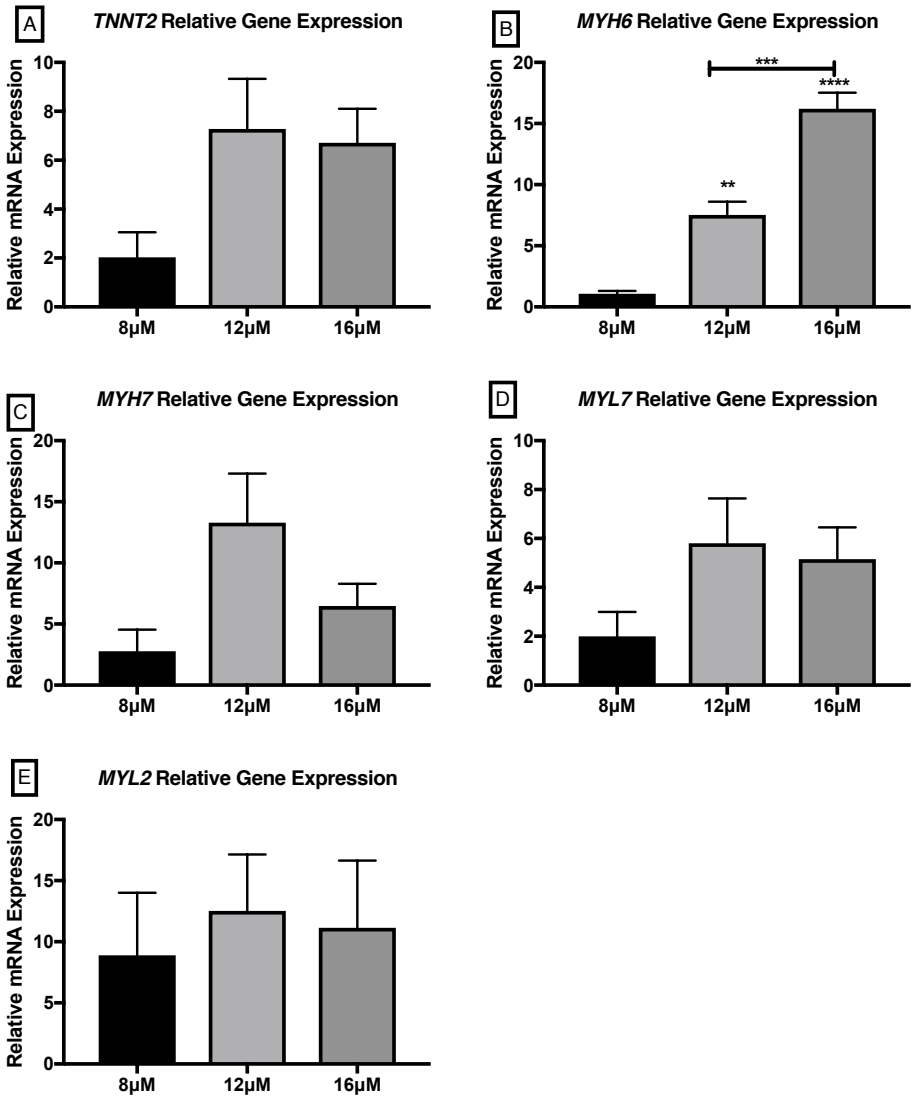


Figure 3.26: The relative mRNA expression of cardiac genes using 8 μM, 12 μM, and 16 μM CHIR in the low cell-density hiPSCs. HiPSC-CMs were differentiated using the OX1-19 hiPCs and the altered Wnt-modulation protocol. Day-30 hiPSC-CMs were collected and the relative gene expression of *TNNT2* (A), *MYH6* (B), *MYH7* (C), *MYL2* (D), and *MYL7* (E) was measured. Abbreviations: TNNT2: troponin T, type 2; MYH6: myosin heavy chain 6; MYH7: myosin heavy chain 7; MYL2: myosin light chain 2; MYL7: myosin light chain 7. Data were analysed using a one-way ANOVA with a Tukey post-hoc test with a p-value ≤ 0.01 (**) and p ≤ 0.001 (***) (n=4).

When a larger population of hiPSCs were used at the start of the differentiation, 12 μM CHIR was not sufficient to increase the relative mRNA expression of *TNNT2*, *MYH6*, *MYH7*, *MYL2*, and *MYL7*, whereas 16 μM of CHIR significantly increased the expression

of *MYH6* (Figure 3.27 F-J). In addition, 8 µM CHIR failed to differentiate spontaneously beating hiPSC-CMs, whereas both 12 µm and 16 µM CHIR was sufficient to differentiate OX1-19 hiSPCs into spontaneously beating hiPSC-CMs.

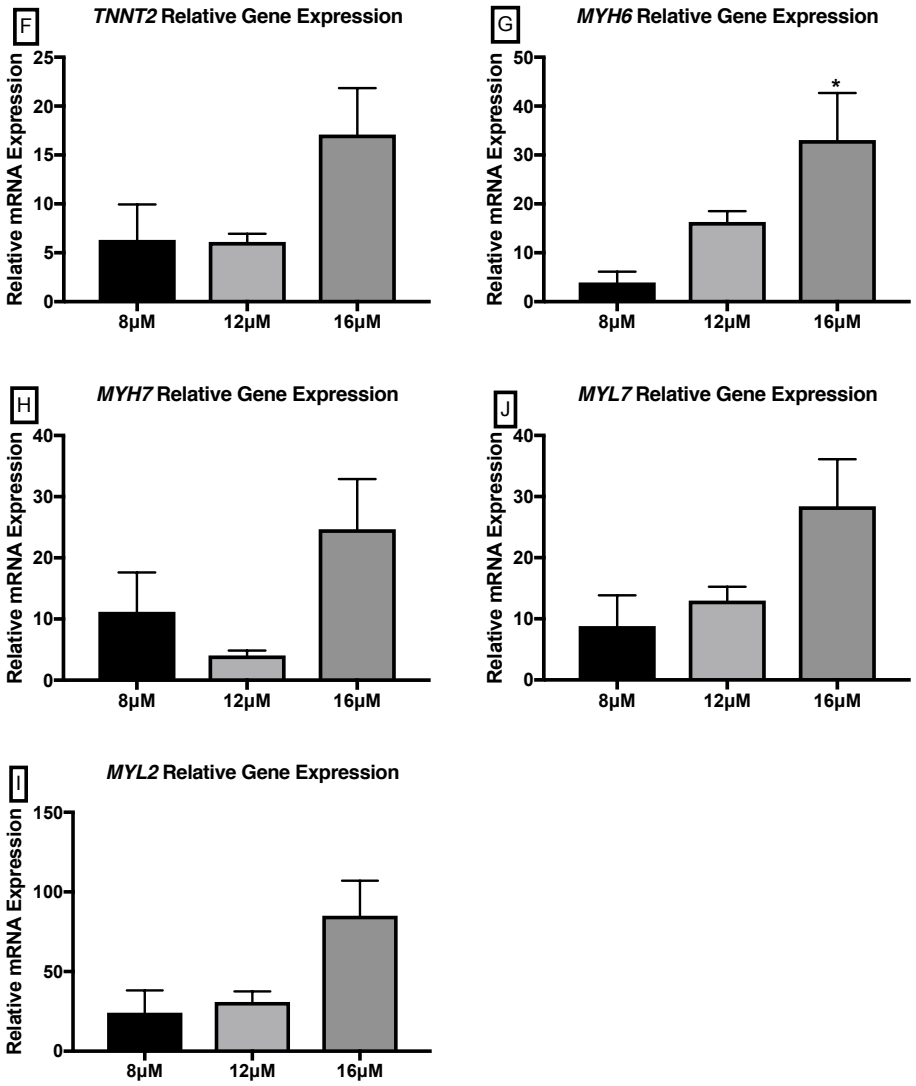
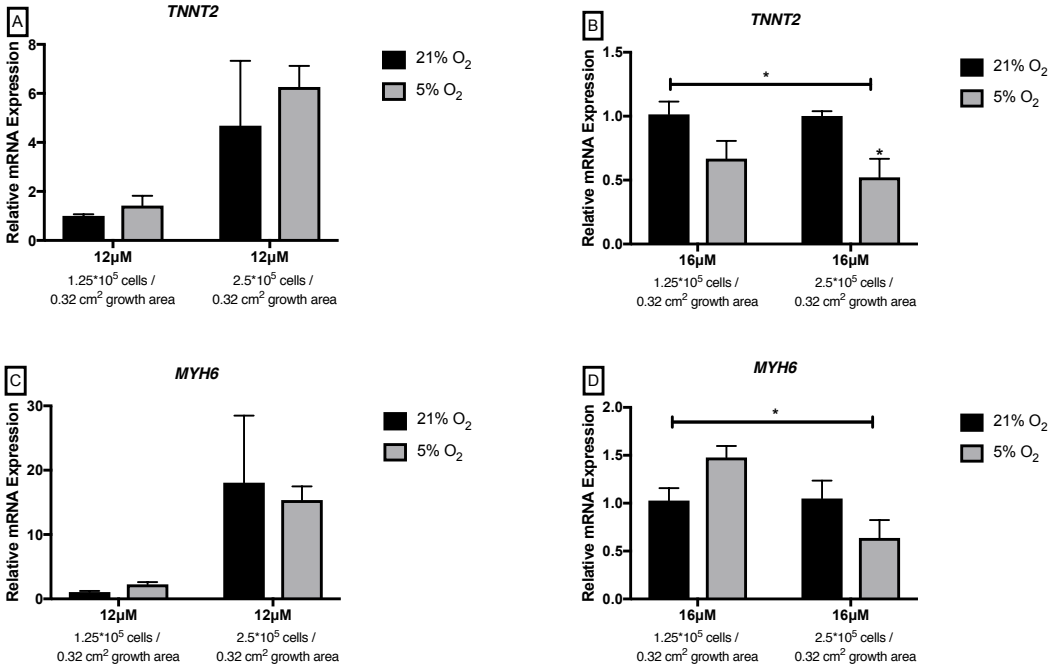


Figure 3.27: The relative mRNA expression of cardiac genes using 8 µM, 12 µM, and 16 µM CHIR in the high cell-density hiPSCs. HiPSC-CMs were differentiated using the OX1-19 hiPCs and the altered Wnt-modulation protocol. Day-30 hiPSC-CMs were collected and the relative gene expression of TNNT2 (A), MYH6 (B), MYH7 (C), MYL2 (D), and MYL7 (E). Abbreviations: TNNT2: troponin T, type 2; MYH6: myosin heavy chain 6; MYH7: myosin heavy chain 7; MYL2: myosin light chain 2; MYL7: myosin light chain 7. Data were analysed using a one-way ANOVA with a Tukey post-hoc test with a p-value ≤ 0.05 (*) (n=4).

The above data, showed the effect of different CHIR concentrations on the expression levels of cardiac genes using the altered Wnt-modulation protocol (transient hypoxia and the addition of 10 ng/ml AA) on two different cell-densities. Here we tested whether differentiating the cells under normoxia + 10 ng/ml AA using the different cell-densities and 12 µM and 16 µM CHIR would increase expression of cardiac genes. The relative mRNA expression of *TNNT2, MYH6, MYH7, MYL2, and MYL7* were measured using qRT-PCR (Figure 3.28 A-J). It was found that when cells were treated with 12 µM CHIR, transient hypoxia (5% O_2) enhanced the differentiation of 250,000 hiPSCs per 0.32cm^2 into spontaneously beating cardiomyocytes with upregulation of *MYL2 and MYL7* compared with differentiation under normoxia (Figure 3.28). When cells were treated with 16 µM CHIR there was no significant benefit from culturing cells under transient hypoxia.



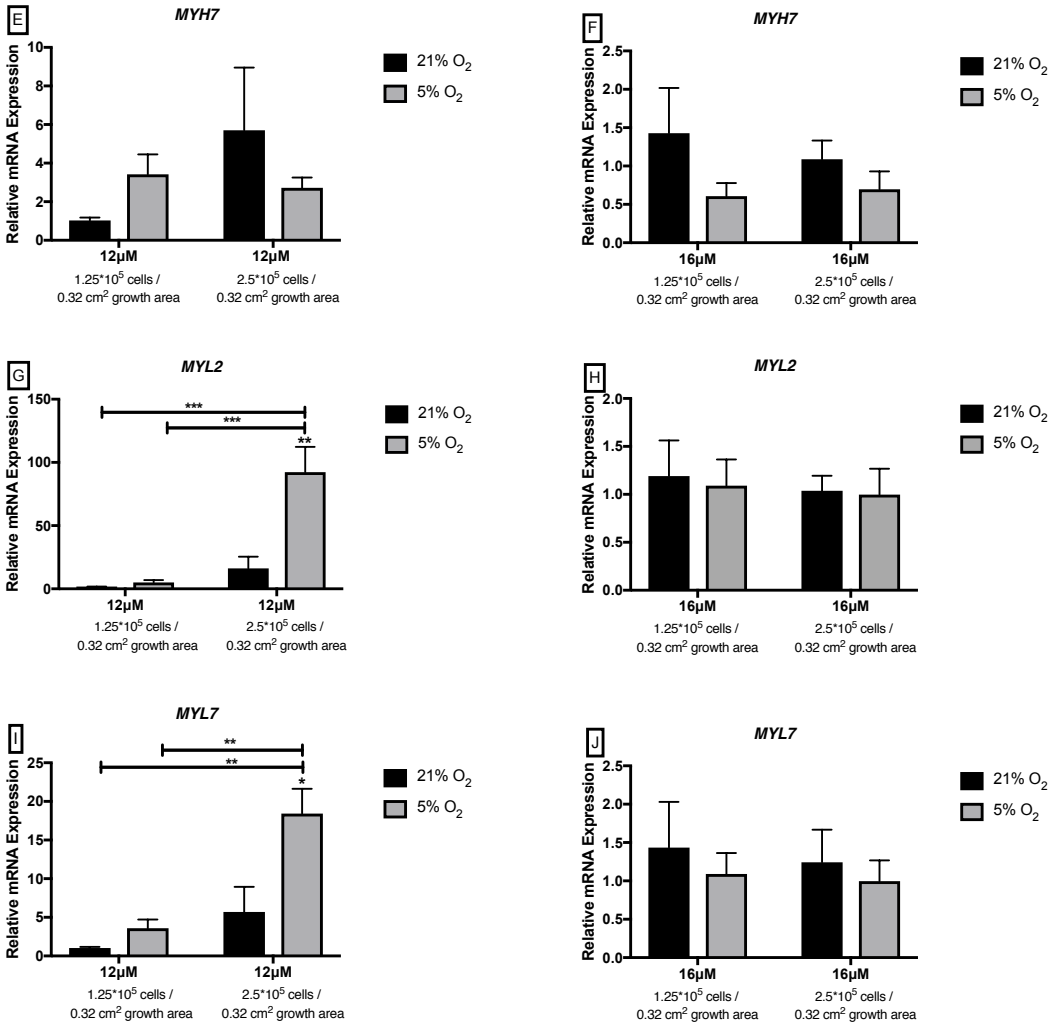


Figure 3.28: The relative mRNA expression for cardiac markers in Day-30 hiPSc-CMs differentiated under transient hypoxia (5% O_2) and normoxia (21% O_2) using 12 µM and 16 µM CHIR. HiSPC-CMs were differentiated under transient hypoxia (A, C, E, G, and I) and normoxia (B, D, F, H, J) using 12 µM and 16 µM CHIR on either low-density seeding (125, 000 / 0.32 cm^2) or high-density seeding (250,000 / 0.32 cm^2). The expression levels of TNNT2 (A-B), MYH6 (C-D), MYH7 (E-F), MYL2 (G-H), and MYL7 (I-J) were measured using qRT-PCR. Abbreviations: TNNT2: troponin T, type 2; MYH6: myosin heavy chain 6; MYH7: myosin heavy chain 7; MYL2: myosin light chain 2; MYL7: myosin light chain 7. Data were analysed using a two-way ANOVA with a Tukey post-hoc test with a p- value ≤ 0.05 (*), ≤ 0.01 (**), and ≤ 0.001 (***) (n=4).

3.6 Discussion

3.6.1 Similarities and Differences between Human Induced Pluripotent Stem Cell Lines: Pluripotency and Metabolism

Although both hiPSC cell lines used in this project showed no difference in the relative gene expression of pluripotent markers *OCT4* and *NANOG*, in practice there were differences working with each hiPSC line. The C19 hiPSC line was more difficult to expand and keep in a stemness state as the cells spontaneously differentiated during expansion. A line-to-line variation has frequently been reported by others[128–130]. Differences between hiPSC lines might be due to differences in the reprogramming method used to induce pluripotency, the origin of the somatic cell reprogrammed or the culturing conditions[129,130]. Also, it has been reported that some hiPSCs lines retain transcriptional memory of the original cells, due to incomplete DNA methylation, mainly in low-passage hiPSCs[130]. Both C19 and OX1-19 lines were reprogrammed from human skin fibroblasts using a retrovirus reprogramming method, therefore, differences between the two lines is unlikely to be due to differences in the reprogramming method or origin of cells. In addition, both lines had a similar passage number (11 to 13) when they were provided to us, therefore, it is unlikely that the difference between the two lines is due to retained transcriptional memory of the original cells. An important factor that might have caused this difference in stemness and proliferation rate is the culturing conditions, since C19 hiPSCs are cultured under hypoxia (5% O_2), whereas, OX1-19 hiPSCs are cultured under normoxia (21% O_2). Previously, it has been reported that human embryonic stem cells proliferate at a similar rate both under hypoxia 3-5% O_2 and normoxia 21% O_2, but it was reported that under hypoxia hESCs showed reduced tendency to spontaneous

differentiation[115]. However, under comparable culturing conditions, still there was no difference in the relative gene expression of *OCT4* and *NANOG* and in the OCT4-postive stain. However, there was a difference in the relative gene expression of metabolic markers between the two lines. Our data showed that the relative gene expression of glucose transporters *GLUT1* and *GLUT4* were higher in the C19 hiPSC line compared it with the OX1-19 hiPSC line. In addition, *PFK* gene expression was increased in C19 compared to OX1-19. This would suggest that C19 hiPSCs may be more glycolytic than OX1-19 hiPSCs, possibly due to the fact that the C19 hiPSC line is routinely cultured under physiological hypoxia (5% O_2), whereas the OX1-19 hiPSC line is routinely cultured under normoxia (21% O_2). There are studies that showed an increase expression of *GLUT1* mRNA in hypoxia via HIF-1α transcriptional control[73,131,132]. The effect of hypoxia on upregulating *GLUT1* expression was confirmed when the OX1-19 hiPSC line was cultured under hypoxia for 24 hours.

As C19 hiPSCs are cultured under hypoxia and showed significant upregulation in glucose metabolism markers compared with OX1-19 hiPSCs, one might expect that C19 hiPSCs would have a higher proliferation rate, but that was not the case. During expansion of the hiPSC lines, using the same split ratio of 1:6, the C19 hiPSC line required passaging after 6 - 7 days from the previous split, whereas the OX1-19 hiPSC line was passaged within 4 days of the previous split, suggesting that the OX1-19 hiPSC line used substrates other than glucose to fuel proliferation, such as glutamine[133].

The difference between the two hiPSC lines was more pronounced when the cells were differentiated into cardiomyocytes as the C19 hiPSC line was much more difficult to differentiate into beating cardiomyocytes than the OX1-19 hiPSC line. Differences in

differentiation capacity between different human embryonic stem cell lines (HUES) has been reported previously[128]. Osafune *et al* compared thirteen HUES lines and showed no difference in the expression of pluripotent markers between the lines, however, when the HUES lines were differentiated there was difference in the tendency to differentiate into specific linages. For example spontaneous and induced cardiac differentiation showed higher levels of cardiac markers NKX2-5 and cTnT in the HUES3 cell line wherease the HUES1 was the most difficult line to differentiate into the cardiac linage[128].

3.6.2 Human Induced Pluripotent Stem Cells Differentiation into Beating Cardiomyocytes: C19 Line

At the beginning of the project we had two main challenges, difficulties in culturing and expanding the C19 hiPSC line and finding the best cardiac differentiation protocol. However, we managed to establish a reproducible and efficient protocol yielding spontaneously beating hiPSCs after comparing different differentiation protocols and introducing alterations to published protocols.

3.6.2.1 Comparison between Protocol 1 and Protocol 2

From all available protocols, the AA + BMP4 + bFGF protocol (protocol 1) was used initially because it is a protocol that was established by the same group that provided us with the C19 hiPSC line, and had successfully generated beating hiPSC-CMs that were used to improve heart function in infarcted rat heart[22]. However, it failed to produce spontaneously beating cardiomyocytes in our laboratory. HiPSC-CMs were cultured and monitored for up to 60 days, but there was no sign of spontaneously beating cardiomyocytes at any time point of the differentiation. It was not clear what might have

caused this failure, taking into account that both the differentiation protocol and the cell line were provided form the same group.

After several unsuccessful attempts to differentiate C19 hiPSCs using protocol 1, and discussion with members in the field, the Wnt-modulation protocol[80] (protocol 2), was used as it showed promising results and high success in various laboratories. Although, Wnt-modulation did not generate spontaneously beating hiPSC-CMs in our hands, there was an increase in the relative gene expression of *KDR*, *GATA4*, *TNNT2*, and *MYH6*. A comparison between the two protocols was conducted in a different laboratory and they showed a preference to the Wnt-modulation protocol[78]. The gene expression of *MYL2* was undetectable in both groups and that might be due to the fact that *MYL2* expression is used as a mature cardiac marker[134], and it is unlikely for day-15 hiPSC-CMs to be mature.

3.6.2.2 Alteration 1 to Protocol 2 (Transient Hypoxia)

The first alteration introduced to the Wnt-modulation protocol was that of transient hypoxic culture (5% O_2). The reasons behind this alteration included the fact that C19 hiPSCs are routinely cultured under hypoxia, the early embryo heart develops in hypoxia[109–111,120,135], and reports showed that hypoxia promotes cardiac differentiation of embryonic stem cells[113,136,137]. During mouse heart development HIF-1α is broadly present in the myocardium between E8 and E10.5[120], yet from E13.5 its presence is restricted to the myocardium of the outflow tract, interventricular septum and atrioventricular cushions[109]. In addition, depletion of HIF-1α downregulates early cardiac markers such as nkx2.5, gata4, tbx5, hand1, and hand2[135]. Normal foetal arterial blood pO_2 ranges from 30 to 20 mmHg (~ 5-3% O_2) [110, 111], and the myocardium has a pO_2 range from 5 to 20 (~ 3% O_2) mmHg[3], therefore, researchers used 3% O_2 for 24 hours or 5% O_2 for 10-12 days for cardiac

differentiation *in vitro* to mimic the oxygen levels during foetal heart development [113,114]. It has been reported that transient hypoxia (24 hours in 3% O_2) during *in vitro* cardiac differentiation upregulated the Wnt signalling pathway, by increased expression of the endogenous Wnt proteins, wnt3, wnt3a, wnt9a, and wnt11, which was lost when cells were transferred back to normoxia, which resulted in an increased expression of cardiac markers such as Isl-1 and troponin C[113]. In addition, Kattman *et al* used 5% O_2 for the first 10-12 days of *in vitro* hESCs and hiPSCs cardiac differentiation[114]. Others used exogenous HIF-1α cDNA transduced mouse embryonic stem cells and differentiated the cells into beating embryonic bodies [136]. The sustained presence of HIF-1α during differentiation resulted in the upregulation of early cardiac markers such as GATA4, NKX2.5 and late cardiac markers such as MHC-A, MHC-B, and MLC-2V in the HIF-1α cDNA treated EBs[136].

After C19 hiPSCs were transferred to normoxia, the morphology of the hiPSCs changed from small round with high nucleus-to-cytoplasm ratio cells to larger, longitudinal cells. This is an indication of spontaneous differentiation in the C19 hiPSCs, as a result of stress caused by sudden change in oxygen levels, therefore, by undertaking the first stage of differentiation under hypoxia, C19 hiPSCs are kept in a stemness state until cardiac differentiation was started. The cells were transferred into normoxia on day 7 of the differentiation, when all cytokines were removed and insulin was introduced into the culturing condition. Alteration 1 did not result in spontaneously beating hiSPC-CMs and resulted in the downregulation of the relative gene expression of *GATA4*, with no change in the relative gene expression of *TNNT2*, *MYH6*, *HYH7*, and *MYL7,* contrary to the improvement other groups have reported on the positive effect of hypoxia culture on enhancement of cardiac differentiation[113,135–137]. However, the positive effect of transient

hypoxia was observed when 10 ng/ml of Activin A was added on day 0 of differentiation and, for the first time, spontaneous beating hiPSC-CMs were observed with an associated upregulation of the relative gene expression of *GATA4*, *MYH6*, and *MYL7*. Activin A has been reported to induce cardiac mesoderm during heart development[101,102] and in a previous study, the first 10 days of cardiac differentiation using Activn A and BMP4 under hypoxia showed this increased KDR and PDGFR- α cells, which are used as markers for cardiac mesoderm[114,125]. In our hiPSC-CMs *KDR* gene expression was significantly downregulated which might be due to the fact that Day-15 hiPSC-CMs are already committed to become cardiac cells as shown by the significant upregulation of cardiac markers that represent later stages of cardiac development, such as *TNNT*2 and *MYH6*. A higher concentration of Activin A either caused cell death or significant reduction in cardiac markers. It has been reported by others that 100 ng/ml inhibit cardiogenesis[127] and induce definitive endoderm differentiation[138–142].

3.6.3 Human Induced Pluripotent Stem Cells Differentiation into Beating Cardiomyocytes – the OX1-19 Line: Optimisation of the Altered Wnt-Modulation Protocol

In general, the C19 hiPSC line was more difficult to culture and maintain than the OX1-19 hiPSC line, therefore, C19 was eliminated after several differentiations attempts, and OX1-19 hiPSC cell line was used. As both lines had similar levels of gene expression of *OCT4* and *NANOG*, it was expected that both lines would have a similar tendency towards cardiac differentiation. However, that was not the case, in general OX1-19 hiPSC line had a better tendency to differentiate into spontaneously beating cardiomyocytes.

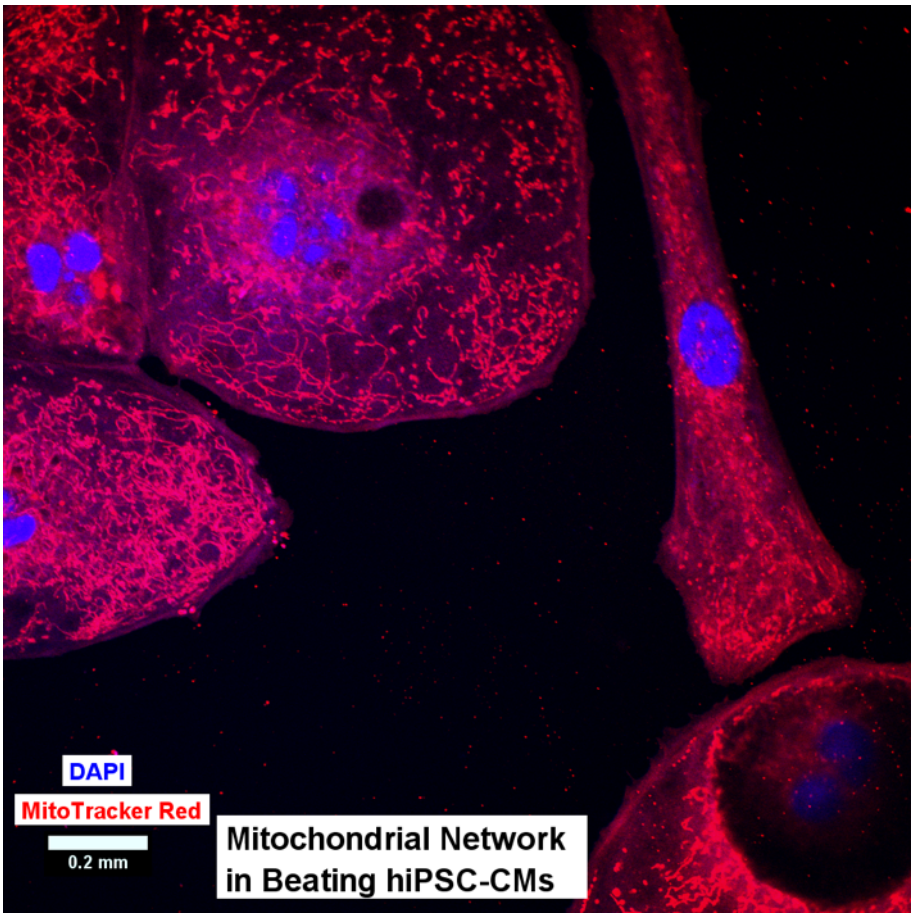
In the published protocol, CHIR was used at a concentration of 12 μM, but, it was important to find the optimal concentration of CHIR using the OX1-19 hiPSC line. Our data showed that both 12 and 16 μM CHIR upregulated gene expression of cardiac genes such as *MYH6* in the low-density seeding condition, whereas, 16 μM of CHIR was required to upregulate cardiac gene (*MYH6*) at high density seeding. We decided that 12 μM of CHIR in low-density seeding seemed to be the optimal condition for cardiac differentiation. Although, some would argue that it would be expected that a lower CHIR concentration is better for the low-density cells, and the higher CHIR concentration is better for the high-density cells, since the 2 conditions generated spontaneously beating hiPSC-CMs that expressed *MYH6*, it is more efficient to use lower cell numbers and fewer reagents, therefore, we decided to use this condition for future differentiations. In the final experiment, we compared culture in normoxia and hypoxia, as well as seeding density, at the two CHIR concentrations. The data from the higher CHIR concentration were inconclusive and confirmed our decision that 12 uM CHIR was the best to use. As before, cells cultured under transient hypoxia had higher expression of cardiac markers than those cultured under normoxia (Figure 3.25). From figure 3.28 the higher seeding density did give increased expression of cardiac markers compared with the lower seeding density. However, this experiment was performed in 96 well plates and we suspect that this increased differentiation was partly driven by the fact that a substantial proportion of the cells would have been growing against the sides of the wells. We and others have observed that the cells behave differently against the walls of culture vessels. By this point in the project we had successfully produced beating sheets of cells in larger flasks using the lower seeding density and decided to continue with that for the future experiments.

3.6.4 Immaturity of Human Induced Pluripotent Stem Cell Derived Beating Cardiomyocytes

In vitro cardiac differentiation produced a heterogeneous population of beating hiPSC-CMs that have different beating patterns in culture. This might be due to the difference in the type of hiPSC-CMs generated such as atrial or ventricular cardiomyocytes[33,108]. Beating hiPSC-CMs have irregular shapes, some are round and others are more longitudinal, with the length and diameters varying. All these features have been reported previously and have been used as a sign of immature cardiomyocytes, when compared to adult cardiomyocytes[34,143,144]. Therefore, we concluded that our differentiation protocol including our alterations generates immature hiPSC-CMs.

3.7 Summary

Human induced pluripotent stem cells are a very important tool in the field of regenerative medicine. HiPSCs are used as an *in vitro* cell-based model to study human cells that were very difficult to study in the past such as the heart and brain. Using hiPSCs, a direct differentiation into human cardiomyocytes was achieved. Although, the differentiated human cardiomyocytes are usually immature, finding a reproducible and efficient protocol to differentiate hiPSCs is a vital step towards enhancing the quality of the differentiated human cardiomyocytes. The Wnt-modulation protocol with some alterations was efficient in producing spontaneously beating human cardiomyocytes. Therefore, the Wnt-modulation protocol has been used going forward in this project.



Chapter 4

The Metabolism in Human Induced Pluripotent Stem Cells and their Differentiated Beating Cardiomyocytes

4 The Metabolism in Human Induced Pluripotent Stem Cells and their Differentiated Beating Cardiomyocytes

4.1 Abstract

Metabolic diseases have been strongly linked to cardiovascular diseases, therefore, it is important to study the metabolism of beating hiPSC-CMs, if we intend to use them as an *in vitro* cell-based model of human cardiomyocytes. It is known that in pluripotent stem cells (PSCs) glycolysis supplies sufficient energy (ATP) to support rapid self-proliferation[72–76,145], whereas, in adult beating cardiomyocytes, glycolysis alone is not sufficient to supply the energy demand for contraction, therefore, in the healthy adult heart fatty acid oxidation plays the major role in supplying energy (ATP)[46,62,146,147]. In addition, the differentiation of stem cells into beating cardiomyocytes is accompanied by a shift in metabolism towards more oxidative phosphorylation[148,149]. Therefore, we hypothesised that as hiPSCs are differentiated into beating cardiomyocytes, there should be an upregulation in fatty acid metabolism. We found that as hiPSCs were differentiated into beating cardiomyocytes, there was a significant increase in both fatty acid oxidation and glucose metabolism in beating hiPSC-CMs. In addition, glycolytic flux, measured using ^{3}H-gluocse utilisation and mitochondrial oxygen consumption were higher in hiPSC-CMs. These results demonstrate that hiPSCs differentiation into beating hiSPC-CMs is accompanied with mitochondrial metabolic maturation.

4.2 Introduction

4.2.1 Metabolism in Human Pluripotent Stem Cells

4.2.1.1 Metabolism during Embryogenesis and in Human Embryonic Stem Cells

The one-cell embryo (zygote) uses pyruvate oxidation for ATP production over glycolysis, and the glycolysis rate in the zygote is low[73,74]. Although zygotes metabolise pyruvate, they have immature mitochondria with a low oxygen consumption rate[72,73]. Before implantation into the uterus, the zygote undergoes cell division, which leads to a reduction in mitochondria DNA copy number (mtDNA) and mitochondrial density. In addition, there is an increase in glucose uptake and glycolysis rate to support the rapid cell replication. The zygote forms a blastocyst which has an outer layer of cells (trophoblast) and an inner cell mass (ICM). As the blastocyst implants into the uterus, glycolysis increases to maximal rates[72–74]. The ICM becomes the embryo, and as it differentiates into the 3 germ layers there is a small shift from glycolysis towards oxidation phosphorylation[72,74] in differentiated cells. Human embryonic stem cells (hESCs) are derived from the ICM of blastocysts from donated fertilised eggs and have a high glycolytic rate[72–74,150] and increased flux through the pentose phosphate pathway (PPP)[74,150]. They have low mtDNA copy number and immature mitochondria with a low oxygen consumption rate[72–74,150,151].

In this project, human induced pluripotent stem cells (hiPSCs) have been used, and it was important to understand whether the metabolic profile of hiPSC resembles that of hESCs. Overall the metabolic profile of hiPSCs and hESCs has been reported to be similar[152], but differences do exist[129]. Metabolomics studies showed differences in the levels of unsaturated fatty acid and metabolites involved in DNA methylation. Levels of w-6 and w-

3 fatty acids were lower in hiPSCs compared to hESCs, whereas the levels of metabolites involved in the S-adenosyl methionine (SAM) cycle, which is involved in methylation reactions, were higher in hiPSCs compared to hESCs[152].

4.2.1.2 Metabolism during the Nuclear Reprogramming of Human Induced Pluripotent Stem Cells

During nuclear reprograming (NR), from somatic cell to induced-pluripotent stem cell by the overexpression of pluripotent markers, there is a shift in metabolism from oxidative phosphorylation towards glycolysis[72–77]. In addition, it has been reported that reprogramming was improved by upregulating glycolysis[153]. Reprogrammed pluripotent stem cells showed an upregulation in glycolytic enzymes such as GLUT1, hexokinase (HK), phosphofructokinase (PFK) and lactate dehydrogenase (LDH)[75–77]. In addition, NR is accompanied by mitochondrial remodelling at a structural and functional level. Mitochondrial morphology changes from elongated, tubular-shaped with well-developed electron-dense cristae in somatic cells, to spherical with small-undeveloped cristae in hiPSCs[72,75–77,151]. In addition, there is a transition in the location of mitochondria within the cells from extensive cytoplasmic networks in somatic cells, to a predominantly peri-nuclear location in hiPSCs[76,77,151]. Functionally, there is a downregulation in the expression and activity of the electron transport chain (ETC) complexes and in oxygen consumption rates (OCR)[72,75–77].

4.2.1.3 Metabolism in Human Induced Pluripotent Stem Cells

4.2.1.3.1 Glycolysis in Human Induced Pluripotent Stem Cells

Human iPSCs are characterised as self-renewing and rapidly proliferating cells, therefore, they require a metabolic state that supports these properties. Human iPSCs favour glycolysis over glucose oxidation, and glycolytic rates in hiPSCs are high and sufficient to support fast self proliferation[72–77]. In addition, hiPSCs have increased levels of intracellular glucose-6-phosphate, which feeds into the pentose phosphate pathway (PPP)[72,74–76,145]. Therefore, there is an increase activity in the PPP in hiPSCs to generate the reducing factor nicotinamide adenine dinucleotide phosphate (NADPH), which is used for biosynthesis of fatty acids[72–76,145,150]. In addition, as the PPP is activated, ribose 5-phosphate is formed, which is used for nucleotide synthesis necessary for the rapid proliferation in hiPSCs[72–74].

4.2.1.3.2 Mitochondria in Human Induced Pluripotent Stem Cells:

Mitochondrial DNA content and copy number is low in hiPSCs[72,73,77,154] and mitochondria in hiPSCs have an immature morphology with a spherical or round shape, and poorly developed cristae[72,73,75,76,149–151,154]. There is a controversy about the expression and activity of the ETC complexes and the rate of oxygen consumption (OCR) at baseline and maximal respiration in hiPSCs. Some studies reported that the ETC complexes I to V are assembled and functional in hiPSCs and that OCR at baseline is similar in hiPSCs and fibroblasts[73,149]. Others showed that the protein expression of complexes II, III, and V are higher in hiPSCs than in fibroblasts[76,151,155]. This increase in protein expression was not reflected by the rate of oxygen consumption in hiPSCs, which was lower in hiPSCs compared to their differentiated fibroblasts[76,155]. Another group showed that hiPSCs had a reduction in the levels of expression and activity in complex IV[151,156], which donates

electrons to oxygen, and they suggested that this reduction in COX expression and activity might limit mitochondrial respiratory capacity in hiPSCs[75,76,88,151,155,156]. In addition, it has been reported that in hiPSCs glycolysis is uncoupled from mitochondrial respiration by a mechanism that is mediated by increased uncoupling protein 2 (UCP2) expression in hiPSCs[77,149,157]. Also, it has been reported that reactive oxygen species (ROS) production is low in hiPSCs, which may play a protective role in these highly-glycolytic fast proliferation cells when cultured in hypoxia[73,76,77,149,150,157].

4.2.2 Metabolism Shift in Human Induced Pluripotent Stem Cell-Derived Cardiomyocytes

There have been few studies into the metabolism of human induced pluripotent stem cell-derived cardiomyocytes (hiPSC-CMs). A study comparing hiPSC-CMs to hiPSCs, showed an increase in mitochondrial relative abundance and activity (mitochondria membrane potential) as a result of cardiac differentiation[41] and that additional mitochondrial maturation in hiPSC-CMs could be achieved by long-term culture (3 months)[41]. With the aim of maturing mitochondrial metabolism over a shorter time period, I first sought to characterise the shift in metabolism during hiPSCs differentiation to beating hiPSC-CMs.

4.3 Aim of Chapter

The aim of this chapter was to study the metabolic maturation when hiPSCs are differentiated into beating hiPSC-CMs.

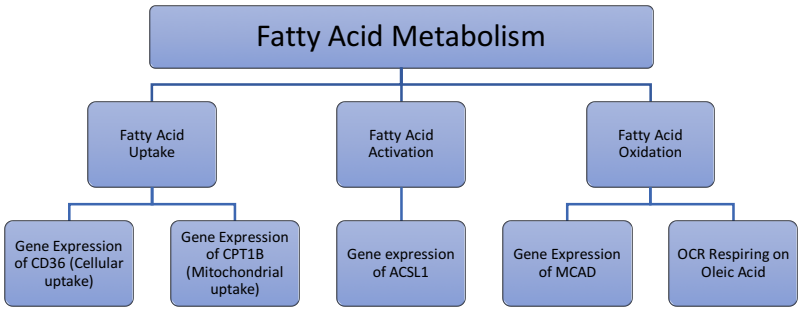
This chapter will:

1. Study the difference in metabolism between hiPSCs and beating hiPSC-CMs by measuring the levels of gene expression of metabolic markers

2. Study glucose metabolism by measuring the glycolytic flux using ^{3}H-glucose
3. Study the oxidative capacity of hiPSC and beating hiPSC-CMs by measuring the rate of oxygen consumption while cells respire on pyruvate and oleic acid
4. Investigate the mitochondrial network formation as hiPSCs are differentiated into beating hiPSC-CMs using the MitoTracker®Red CMXRos dye

4.4 Methods

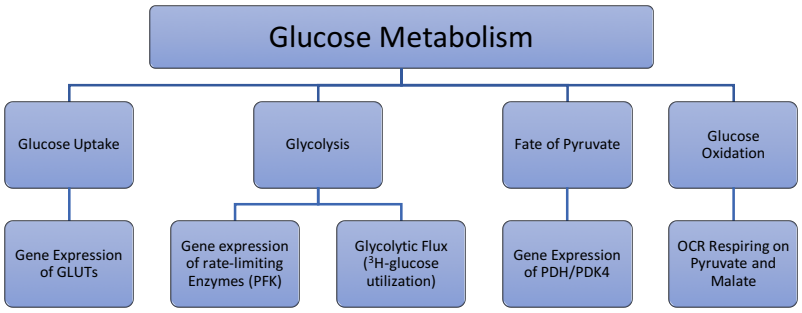
4.4.1 Fatty acid Uptake and Oxidation



The chart above show the methods used to study fatty acid metabolism in hiPSCs and beating hiPSC-CMs. The relative gene expression of *CD36* was measured as a marker for fatty acid uptake as it is known to play a role in the uptake of long-chain fatty acid into cardiac cells[46,62,68,95,146,147,158]. In addition, the metabolism of fatty acids inside the cytosol was studied by measuring the relative gene expression of long-chain acyl-CoA synthetase (*ACSL1*), which catalyses the conversion of free long-chain fatty acid into fatty acyl-CoA esters, which are transported into the mitochondria for oxidation. The transport of long-chain fatty acyl-CoA into the mitochondria occurs using a special transport system the 'carnitine shuttle'. The carnitine shuttle is made of 3 enzymes (translocase, CPT1 and

CPT2)[44,45]. The relative gene expression of carnitine palmitoyltransferase 1B (*CPT1B*) was measured because it is known to be a rate-controlling enzyme of long-chain fatty acid oxidation in muscle mitochondria[46,62,68,146,147]. Medium-chain acyl-CoA dehydrogenase (*MCAD*) relative gene expression was measured as an indicator for mitochondrial oxidation of fatty acid in cardiomyocytes[46,62]. Oxygen consumption was measured with fatty acid (oleic acid) as substrate, to measure the total fatty acid oxidative pathway.

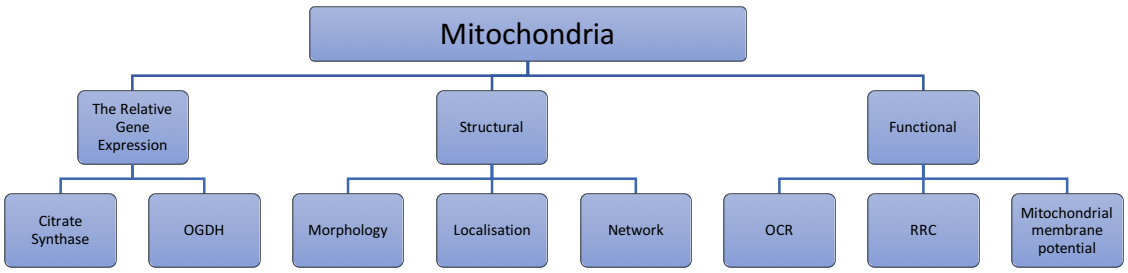
4.4.2 Glucose Uptake and Metabolism



The chart above shows the techniques used to study glucose uptake and metabolism in cultured cells. The genes chosen for analysis included, glucose transporters (*GLUT1* and *GLUT4*), phosphofructokinase, muscle-type (*PFKM*) the enzyme that catalyse irreversible rate-limiting step in glycolysis, pyruvate dehydrogenase, E1 alpha-subunit (*PDHA1*) and pyruvate dehydrogenase kinase 4 (*PDK4*) enzymes that regulate the fate of pyruvate, which is the end-product of glycolysis. *GLUT1* is reported to be expressed in human pluripotent stem cells[74,75,145,159] and cardiomyocytes[53,160–162], whereas *GLUT4* is expressed in adult hearts[53,160–162]. In anaerobic glycolysis, pyruvate, the end-product of glycolysis is converted into lactate via lactate dehydrogenase, whereas, in complete glucose oxidation, pyruvate is irreversibly converted into acetyl CoA via pyruvate dehydrogenase (PDH).

Acetyl CoA is further oxidised in the TCA cycle generating NADH and $FADH_2$. Therefore, PDH plays an important role in linking glycolysis to TCA cycle. PDH is a multi-enzyme complex that catalyses the irreversible reaction of acetyl CoA formation from pyruvate. PDH is inactivated by PDK, and PDK isoform 4 is expressed in the heart[163,164]. The rate of glycolytic flux was studied by measuring the release of ^3H_2O from [5-^{3}H]-glucose[91–95,99,100]. However, one limitation of this method is that it does not represent the complete conversion of glucose to pyruvate, since tritium is removed at step 9 of glycolysis as ^3H_2O (Figure 2.3), therefore the fate of pyruvate cannot be determined by this method. Therefore, the rate of O_2 consumption (OCR) was measured while the cells were respiring on pyruvate and malate, to measure the capacity of the mitochondria to uptake and oxidise pyruvate, as an indicator of glucose oxidation in the mitochondria of hiPSCs and beating hiPSC-CMs.

4.4.3 Mitochondria Morphology and Function



The chart above shows the methods used to characterise mitochondrial function. Acetyl CoA formed from glucose or fatty acids enters the TCA cycle and the acetyl group attaches to oxaloacetate in an irreversible rate-limiting reaction that is catalysed by citrate synthase (CS). Oxoglutarate dehydrogenase (OGDH) catalyses the conversion of α-ketoglutatrate to succinyl CoA. The relative gene expression of these TCA enzymes was measured. Confocal imaging of the MitoTracker®Red CMXRos dye was used to indicate the

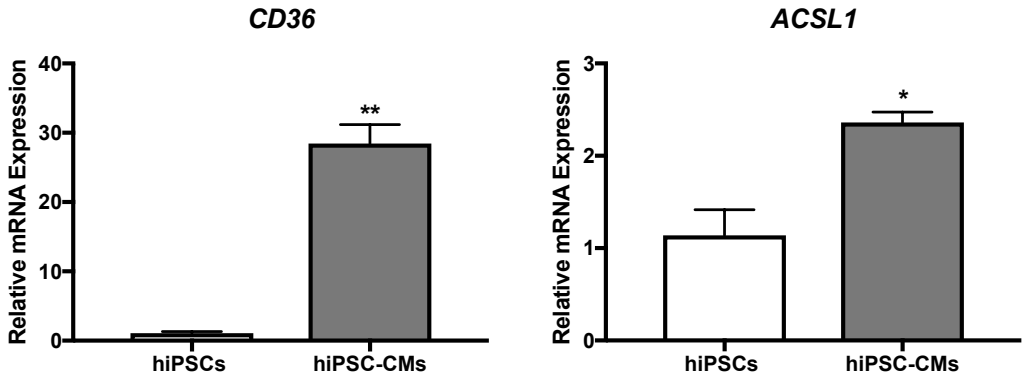
mitochondrial membrane potential and networks of the cells[88,165] whilst oxygen consumption measurements characterised mitochondrial function.

4.5 Results

4.5.1 The Difference in Fatty Acid Metabolism in Human Induced Pluripotent Stem Cells and their Differentiated Beating Cardiomyocytes

4.5.1.1 Fatty Acid Metabolic Gene Expression *CD36*, *ACSL1*, *CPT1B*, and *MCAD*

The expression of enzymes involved in fatty acid uptake and oxidation were measured using qRT-PCR. Expression of the fatty acid uptake gene, *CD36*, was significantly increased by around 30-fold in beating hiPSC-CMs compared with hiPSCs (Figure 4.1). In addition, long-chain acyl CoA synthase 1 (*ACSL1*) and carnitine-palmitoyl transferase 1 (*CPT1B*) relative gene expression was significantly higher in beating hiPSC-CMs than hiPSCs by 3-fold and 10-fold, respectively. However, there was no difference in the relative gene expression of medium-chain acyl CoA dehydrogenase (*ACADM*) between hiPSCs and beating hiPSC-CMs.



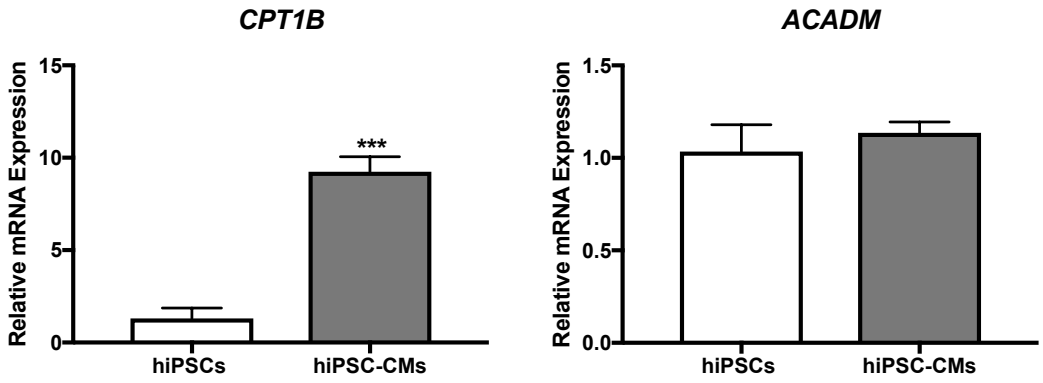


Figure 4.1: Relative gene expression of fatty acid metabolism markers in hiPSCs and beating hiPSC-CMs. Abbreviations: CD36: cluster of differentiation 36 (fatty acid transporter); ACSL1: long-chain acyl CoA synthase; CPT1B: carnitine-palmitoyl transferase 1, the muscle-type; and ACADM: acyl CoA dehydrogenase, medium-chain. Data are presented as mean ± SEM and analysed using unpaired, two-tailed t-test with a p-value = 0.002 (**), 0.02 (*), and 0.0004 (***), respectively (n=4).

4.5.1.2 Oxygen Consumption Rate Measurement using Fatty Acid (Oleic Acid) as Energy Substrate

HiPSCs and beating hiPSC-CMs were cultured under their normal culturing conditions. Two million hiPSCs and two million hiPSC-CMs were collected to measure the rate of O_2 consumption (OCR) using the Clark-type oxygen electrode, respiring with 400µM oleic acid. In hiPSCs, OCR at baseline was 0.4 nmol/min/10^3 cells and increased to 2.8 nmol/min/10^3 cells when stimulated to maximum respiration with FCCP (Figure 4.2). In beating hiPSC-CMs at baseline respiration was 0.8 nmol/min/10^3 cells and increased to 4.5 nmol/min/10^3 cells when stimulated to maximal respiration with FCCP. There was no significant difference in OCR at baseline between the 2 cell types, whereas OCR was significantly increased in beating hiPSC-CMs during maximal respiration, by around 2-fold, indicating that mitochondria in beating hiPSC-CMs are more mature with a higher oxidation capacity than hiPSCs. This was confirmed by calculation of the reserve respiratory capacity (RRC), defined as the difference in OCR between maximal respiration

and baseline respiration. RRC in beating hiPSC-CMs was around 2-fold higher than hiPSCs (Figure 4.3).

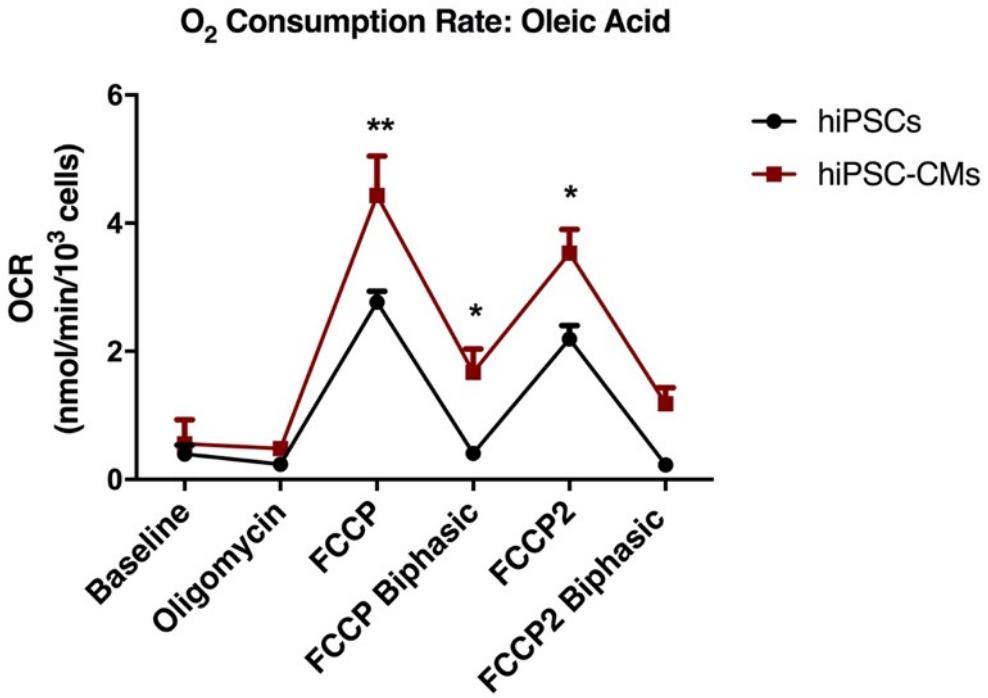


Figure 4.2: O_2 consumption rate (OCR) in hiPSCs and beating hiPSC-CMs respiring on Oleic Acid. Two million hiPSCs (black line) and beating hiPSC-CMs (red line) were collected and supplemented with 400 μM oleic acid and OCR was measured using the Clark oxygen electrode. Measurement was conducted at baseline, after oligomycin treatment, after FCCP treatment, and after allowing cells to rest from FCCP treatment. Data are presented as mean ± SEM and were analysed using unpaired, two-tailed t-test, p-value ≤ 0.05 (*) and ≤ 0.01 (**) (n=4).

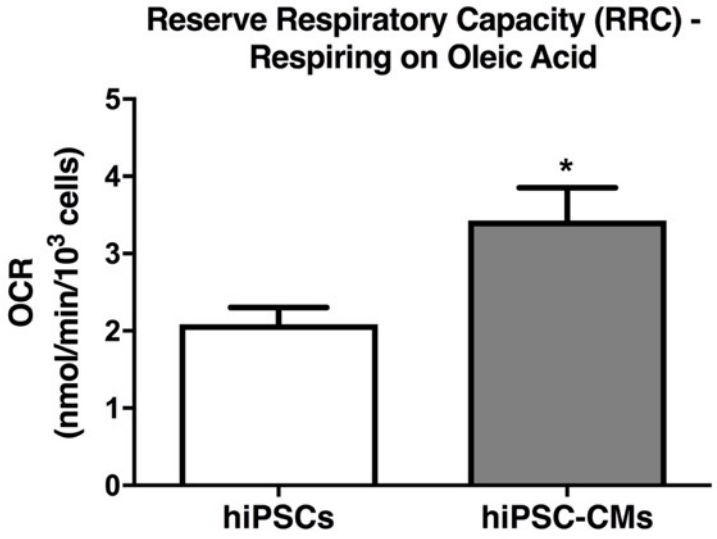


Figure 4.3: Reserve respiratory capacity (RRC) in hiPSCs and beating hiPSC-CMs. Using the Clark-type oxygen electrode, OCR was measured at baseline and maximal respiration (induced via FCCP treatment). RRC was calculated by subtracting maximal from baseline respiration (FCCP – Baseline). Data are presented as mean ± SEM, and were analysed using an unpaired, two-tailed t-test, p value ≤ 0.05 (*) (n=4).

4.5.2 The Difference in Glucose Uptake and Metabolism between Human Induced Pluripotent Stem Cells and their Differentiated Cardiomyocytes

4.5.2.1 Glucose Metabolism Gene Expression of *GLUT1*, *GLUT4*, *PFKM*, *PDHA1*, and *PDK4*

Beating hiPSC-CMs showed no change in *GLUT1* relative gene expression compared with hiPSCs (Figure 4.4). In addition, *GLUT4* relative gene expression was not significantly changed after differentiation, despite a trend to being increased (Figure 4.4). The relative gene expression of phosphofructokinase (*PFKM*), the enzyme that catalyses the second irreversible rate-limiting step in glycolysis, was measured in both cell types. Beating hiPSC-CMs showed a significant 2-fold increase in *PFKM*'s relative gene expression compared with hiPSCs (Figure 4.5). The relative gene expression of *PDHA1* and *PDK4* were significantly increased in beating hiPSC-CMs by around 2-fold and 3-fold compared with hiPSCs (Figure 4.5).

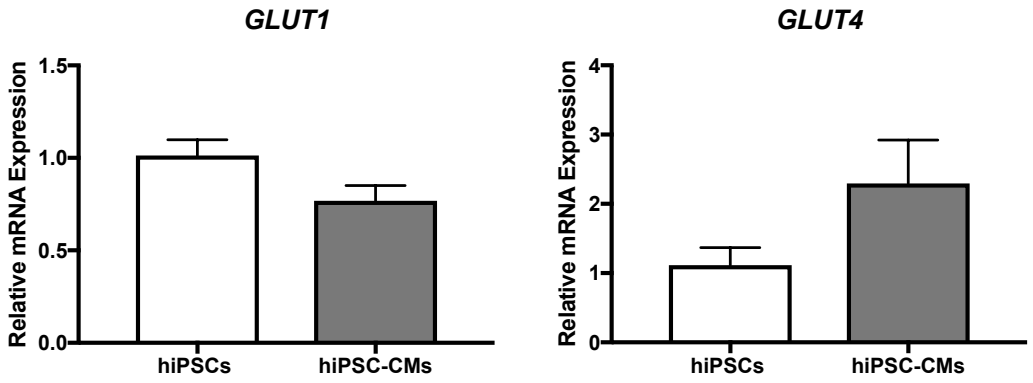


Figure 4.4: Relative gene expression of glucose transporters (*GLUT1* and *GLUT4*) in hiPSCs and beating hiPSC-CMs. GLUT1: glucose transporter 1; GLUT4: glucose transporter 4. Data are presented as mean ± SEM, and were analysed using an unpaired, two-tailed t-test (n=4).

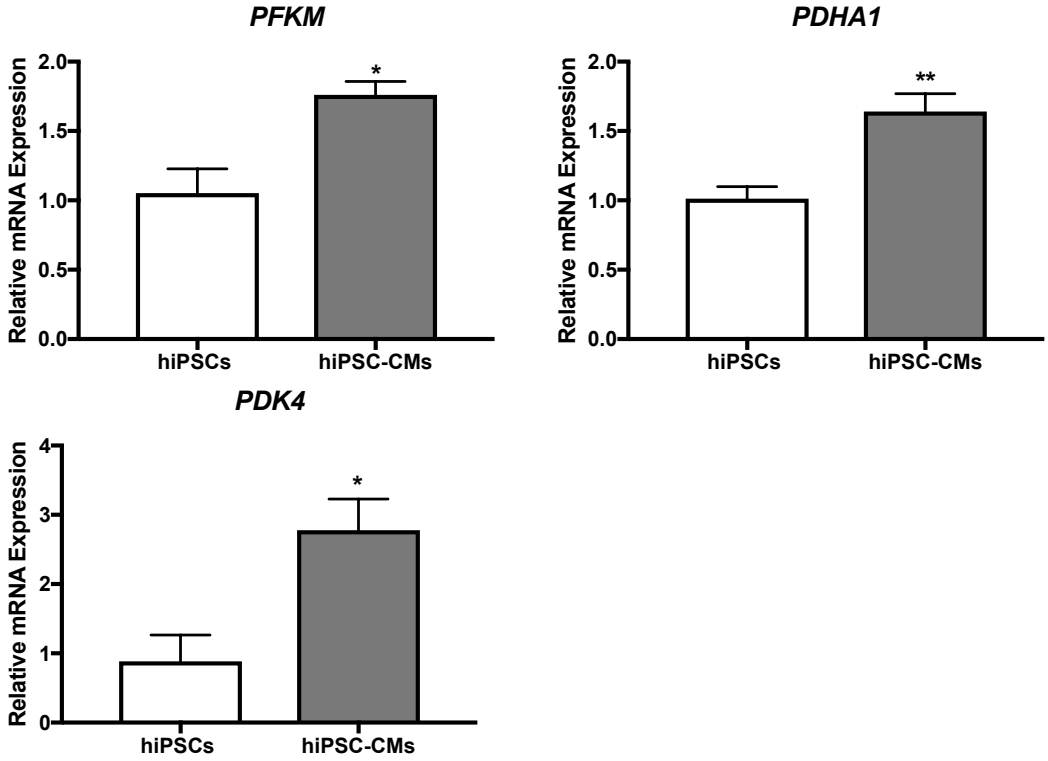


Figure 4.5: Relative Gene Expression of *PFKM*, *PDH*, and *PDK4* in hiPSCs and Beating hiPSC-CMs. Abbreviations: PFKM: phosphofructokinase, muscle-type; PDH: pyruvate dehydrogenase, E1 alpha-subunit; and PDK4: pyruvate dehydrogenase kinase 4. Data are presented as mean ± SEM, and were analysed using an unpaired, two-tailed t-test with a p-value = 0.02 (*), 0.01 (**), and 0.03 (*) respectively (n=4).

4.5.2.2 Oxygen Consumption Rate Measurement using Pyruvate and Malate as Energy Substrates

Two million hiPSCs and two million beating hiPSC-CMs were collected to measure the rate of O_2 consumption (OCR) respiring on pyruvate and malate. There was no significant difference in OCR between hiPSCs and beating hiPSC-CMs at any stage, while respiring on pyruvate and malate as substrates (Figure 4.6). Baseline respiration was 0.70 and 0.80 nmol/min/10^3 cells, respectively, and increased to around 2.5 nmol/min/10^3 cells at maximal respiratory capacity in both cell types. In addition, there was no difference in the reserve respiratory capacity between hiPSCs and beating hiPSC-CMs, while respiring on pyruvate and malate (Figure 4.7).

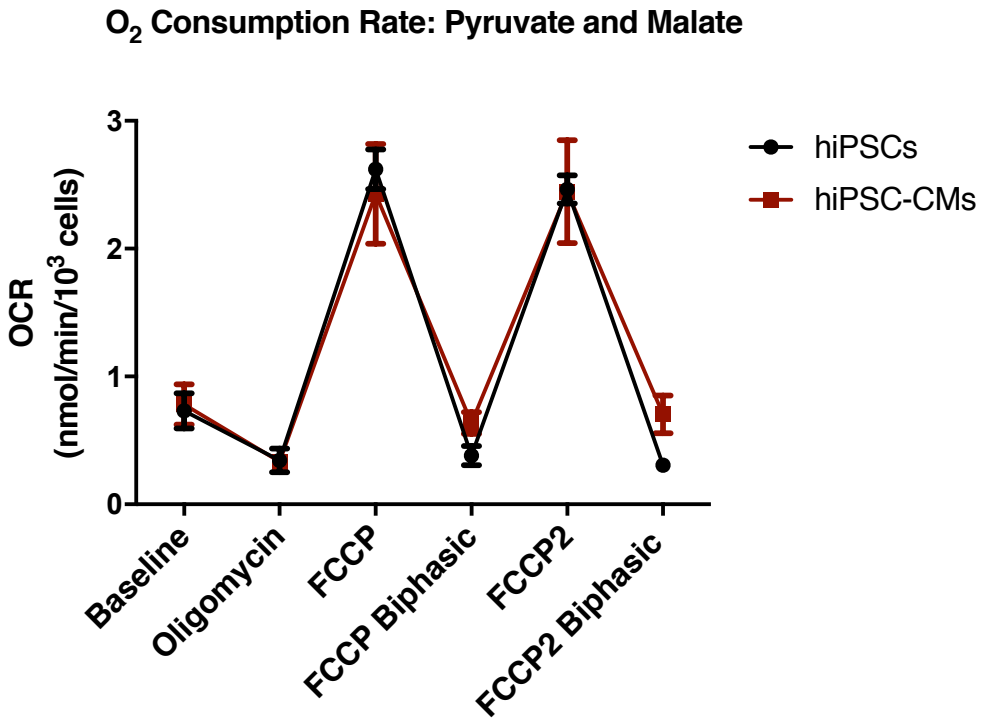


Figure 4.6: O_2 consumption rate (OCR) in hiPSCs and beating hiPSC-CMs respiring on pyruvate and malate. Two million hiPSCs (black line) and beating hiPSC-CMs (red line) were collected and supplemented with (10 mM) pyruvate and (5 mM) malate. Measurement was conducted at base line, after oligomycin treatment, after FCCP treatment, and after allowing cells to rest from FCCP treatment. FCCP treatment was

applied twice. Data are presented as mean ± SEM and were analysed using an unpaired, two-tailed t-test (n=4).

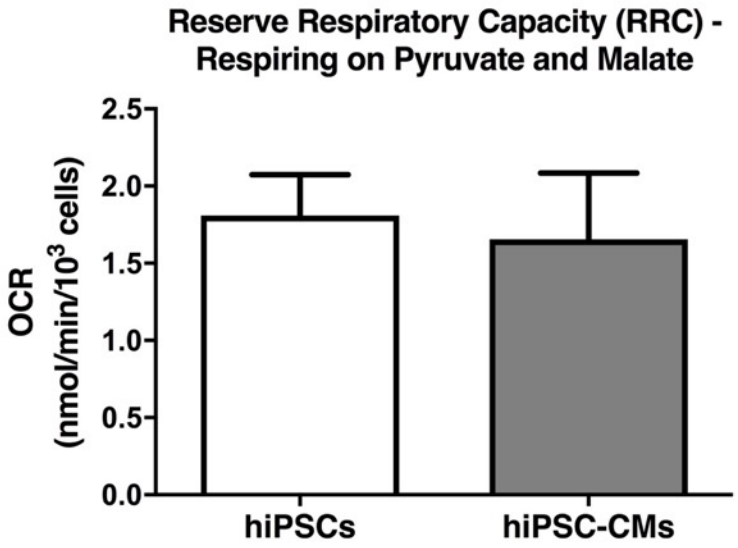


Figure 4.7: Reserve respiratory capacity (RRC) in hiPSCs and beating hiPSC-CMs. Using the Clark-type oxygen electrode, OCR was measured at baseline and maximal respiration (induced via FCCP treatment). RRC was calculated by subtracting maximal from baseline respiration (FCCP – Baseline). Data are presented as mean ± SEM, and were analysed using an unpaired, two-tailed t-test (n=4).

4.5.2.3 Glycolytic Flux using *in Vitro* ^{3}H-glucose utilization in Human Induced Pluripotent Stem Cells and their Differentiated Cardiomyocytes

4.5.2.3.1 Under Normal Culturing Conditions for 8 hours

HiPSCs are routinely cultured with mTeSR1, which contains 17.7 ± 0.01 mmol/L glucose. Beating hiPSC-CMs are routinely cultured in RPMI + B27 media that contains 13.3 ± 0.01 mmol/L glucose. To measure the glycolytic flux in these cells under normal conditions, hiPSCs were cultured with mTeSR1 + 2.5 µl ^{3}H-glucose and beating hiPSC-CMs were cultured with RPMI+B27 + 2.5 µl ^{3}H-glucose. Cells were incubated for 8 hours under 21% O_2 at 37°C. After 8 hours of culture, beating hiPSC-CMs had significantly higher glycolytic rates (0.7 nmoles/10^4 cells) than hiPSCs (0.3 nmoles/10^4 cells) (Figure 4.8).

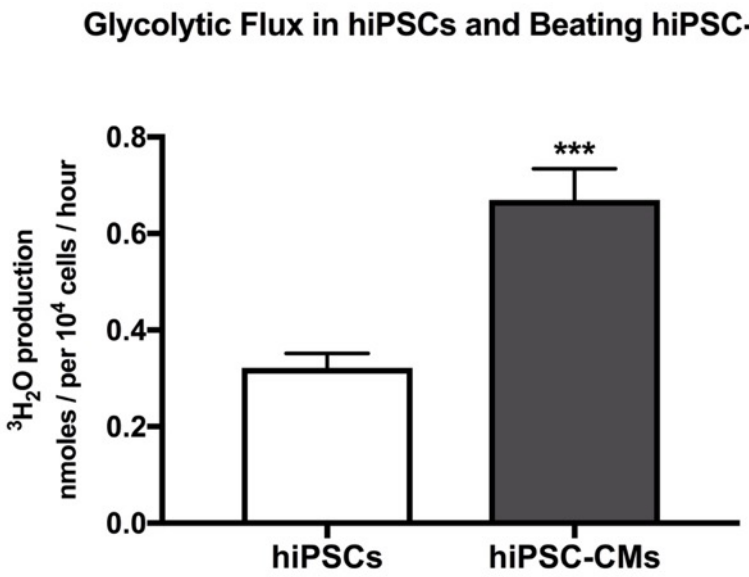


Figure 4.8: Glycolytic flux in hiPSCs and beating hiPSC-CMs cultured in their standard media for 8 hours. Cells were incubated with their standard, high-glucose culture media. HiPSCs were cultured in mTeSR1, which contains 17.7 ± 0.01 mmol/L glucose, whereas, beating hiPSC-CMs were cultured in RPMI + B27 media that contains 13.3 ± 0.01 mmol/L glucose. Data are presented as mean ± SEM, and were analysed using an unpaired, two-tailed t-test with a p-value of 0.0007 (***) (n=6).

4.5.2.3.2 Under Low-Glucose Culturing Conditions for 8 and 24 hours

HiPSC and hiPSC-CMs were cultured with low-glucose (5.5 mmol/L) medium and 2.5µl ^{3}H-glucose. After 8 hours incubation, beating hiPSC-CMs had a higher glycolytic rate (0.6 nmoles/10^4 cells) than hiPSCs (0.2 nmoles/10^4 cells) (Figure 4.9 A). After 24 hours of incubation with low-glucose media, glycolytic flux in hiPSCs was reduced to 0.05 nmol/10^4 cells, whereas in beating hiPSC-CMs it stayed at 0.6 nmol/10^4 cells (Figure 4.9 B).

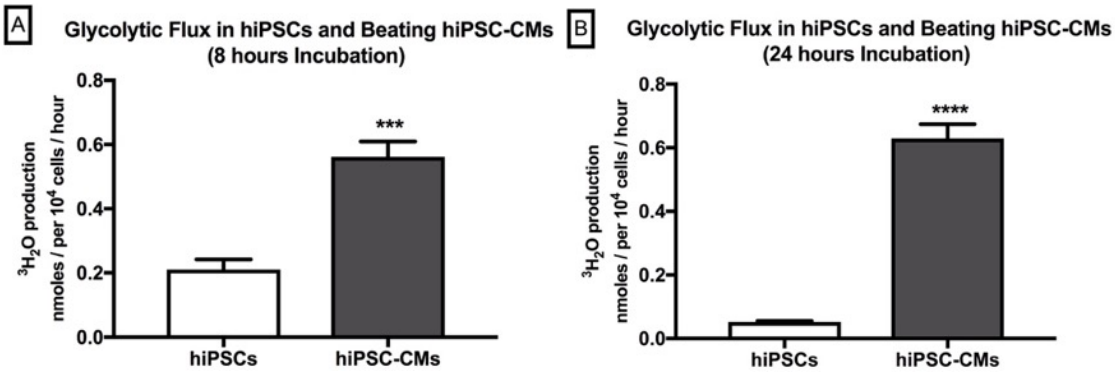


Figure 4.9: Glycolytic flux in hiPSCs and beating hiPSC-CMs cultured with low-glucose media for 8 and 24 hours. HiPSCs and beating hiPSC-CMs were incubated with low-glucose (5.5 mmol/L) incubation media for 8 hours (A) and 24 hours (B). Data are presented as mean ± SEM and were analysed using an unpaired, two-tailed t-test with a p-value ≤ 0.001 (***), and ≤ 0.0001 (****), respectively (n=6).

The cell number of hiPSCs and beating hiPSC-CMs was calculated after 8 and 24 hours culture in low-glucose media. With time, hiPSCs continued to proliferate in low-glucose media, whereas, beating hiPSC-CMs did not proliferate (Figure 4.10). Although hiPSCs continued to proliferate in low-glucose media, glycolytic flux was reduced (Figure 4.11).

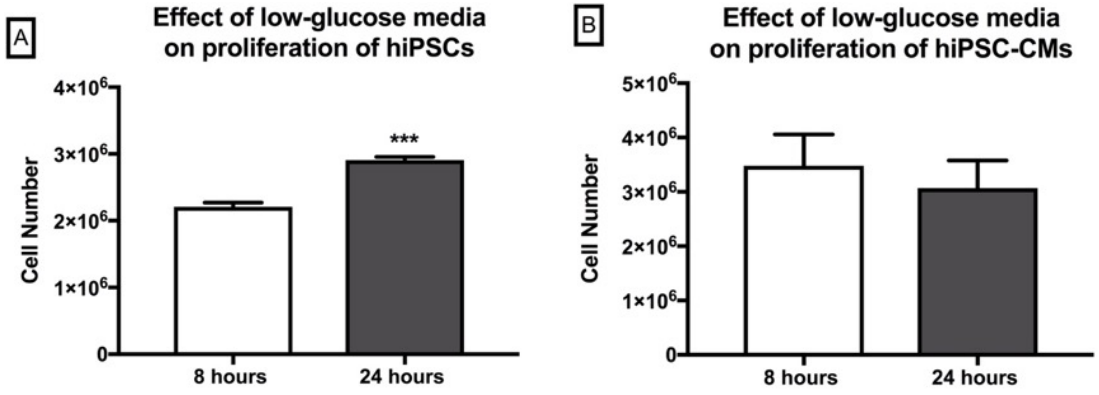


Figure 4.10: Cell number of hiPSCs and beating hiPSC-CMs cultured in low-glucose media for 8 and 24 hours. HiPSCs (A) and beating hiPSC-CMs (B) were incubated with low-glucose (5.5 mmol/L) media. Data are presented as mean ± SEM, using unpaired, two-tailed t-test with a p-value ≤ 0.001 (***) (n=6).

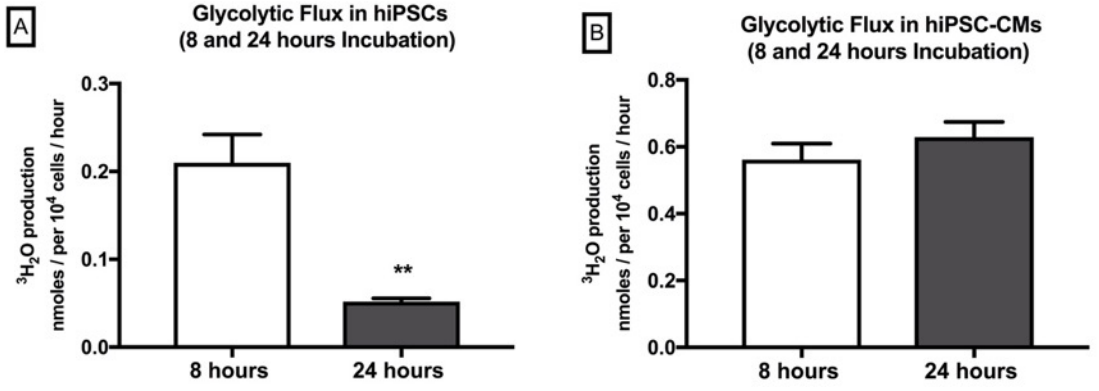


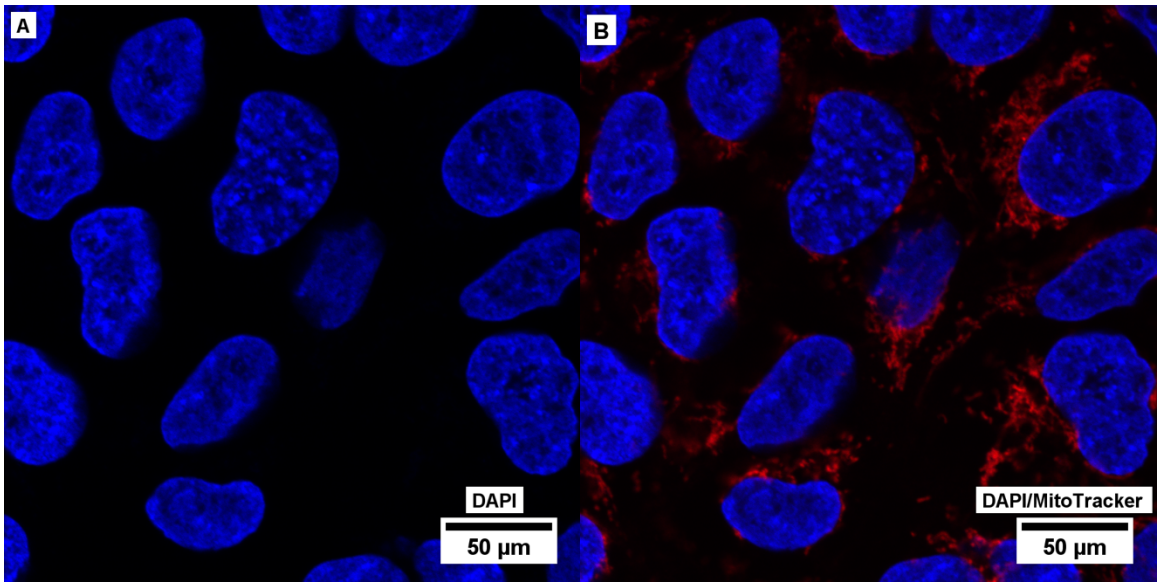
Figure 4.11: The effect of incubation time on the glycolytic flux in hiPSCs and beating hiPSC-CMs cultured in low-glucose media for 8 and 24 hours. HiPSCs (A) and beating hiPSC-CMs (B) were incubated with low-glucose (5.5 mmol/L) media containing 0.00148

MBq of [5-^{3}H]-glucose. Data are presented as mean ± SEM, using unpaired, two-tailed t-test with a p-value ≤ 0.01 (**) (n=6).

4.5.2.4 Mitochondria and TCA cycle in Human Induced Pluripotent Stem Cells and their Differentiated Beating Cardiomyocytes

4.5.2.4.1 Mitochondrial Morphology and Localisation

MitoTracker®Red CMXRos dye was used to label mitochondria in live hiPSCs and beating hiPSC-CMs. HiPSCs were able to take up and retain MitoTracker®Red CMXRos dye, therefore hiPSCs do have active mitochondria (Figure 4.12). However, mitochondrial networks were better developed in beating hiPSC-CMs (Figure 4.12). In addition, in beating hiPSC-CMs the mitochondrial networks were distributed throughout the cytoplasm.



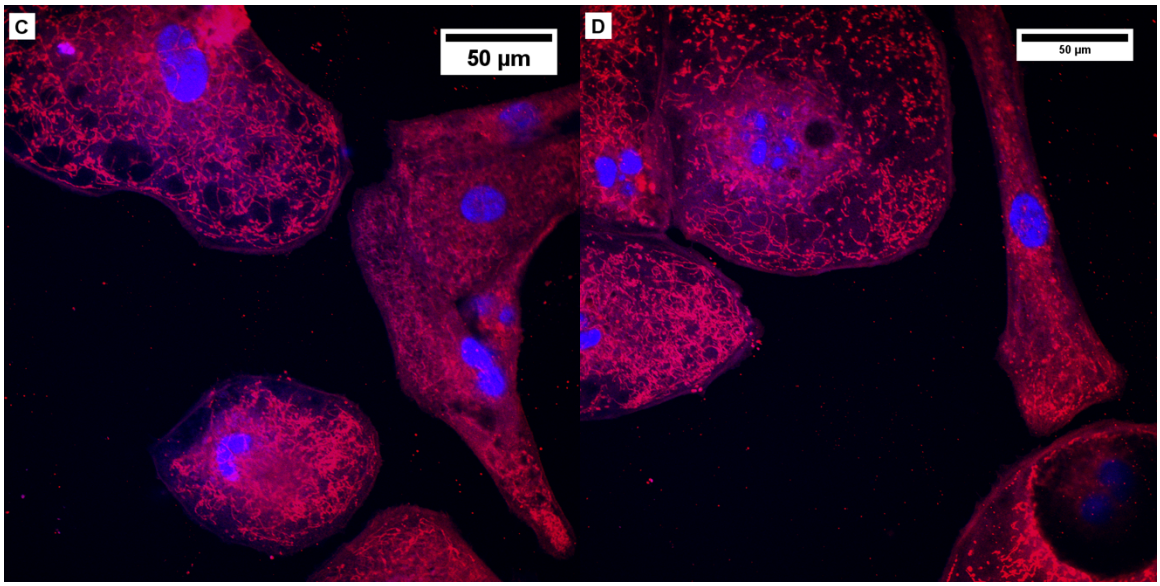


Figure 4.12: Confocal images of MitoTracker®Red CMXRos dye in hiPSC (first row) and beating hiPSC-CMs (second row). HiPSCs and beating hiPSC-CMs were incubated with 100nM MitoTracker®Red CMXRos dye. (A) hiPSCs stained with DAPI, (B) hiPSCs stained with DAPI and MitoTracker Red, (C-D) beating hiPSC-CMs (Day-45) stained with DAPI and MitoTracker Red. **DAPI**: 4′,6-diamidino-2-phenylindole.

4.5.2.4.2 Intensity of MitoTracker®Red CMXRos

The intensity of MitoTracker®Red CMXRos dye was measured in hiPSCs and beating hiPSC-CMs. Two concentrations of mitochondrial dye were used 100 nM and 250 nM. The intensity of the mitochondrial dye was higher in beating hiPSC-CMs compared with hiPSCs at both concentrations (Figure 4.13). Beating hiPSC-CMs had a higher total cell fluorescence than hiPSCs (Figure 4.13).

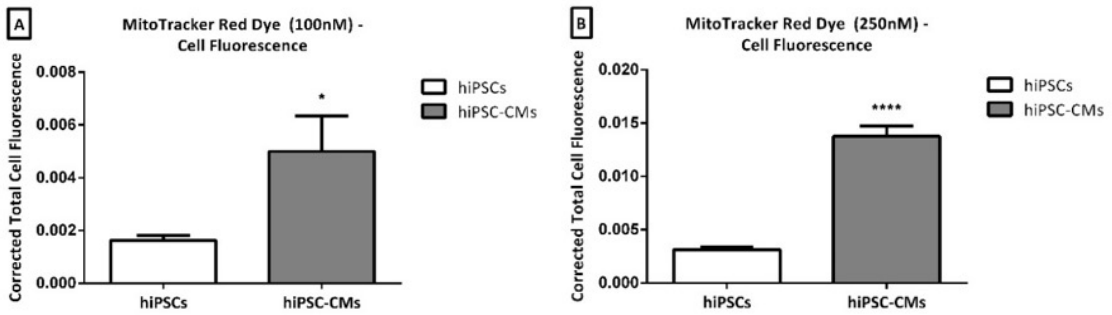


Figure 4.13: Corrected total cell fluorescence (CTCF) of MitoTracker red dye in hiPSCs and beating hiPSC-CMs. (A) MitoTracker Red Dye was used at a concentration of 100 nM and (B) at a concentration of 250 nM. Data are presented as mean ± SEM, using unpaired, two-tailed t-test with a p-value ≤ 0.05 (*) and ≤ 0.0001 (****), respectively (n=8).

4.5.2.4.3 Relative gene expression of TCA enzymes

The relative gene expression of TCA enzymes citrate synthase (*CS*) and oxoglutarate dehydrogenase (*OGDH*) were measured in hiPSCs and beating hiPSC-CMs. There was no difference in the relative gene expression of citrate synthase between the two cell groups (Figure 4.15). However, oxoglutarate dehydrogenase was significantly downregulated in beating hiPSCs-CMs compared with hiPSCs (Figure 4.15)

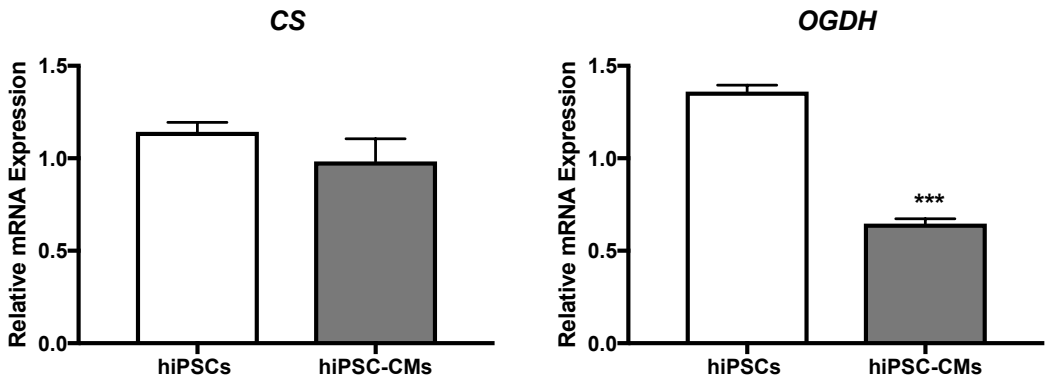


Figure 4.15: Relative gene expression of *CS* and *OGDH*. The relative gene expression of TCA enzymes, Citrate Synthase and oxoglutarate dehydrogenase, was measured in hiPSCs and beating hiPSC-CMs. Abbreviations: CS: citrate Synthase; OGDH: oxo-glutarate dehydrogenase. Data are presented as mean ± SEM, and were analysed using an unpaired, two-tailed t-test with a p-value = 0.0001 (***) (n=3).

4.6 Discussion

4.6.1 The Switch in Metabolism as Human Induced Pluripotent Stem Cells are Differentiated into Beating Cardiomyocytes

In stem cells, glucose is the major energy substrate for ATP production[72–77], whereas adult cardiomyocytes have the ability to use all classes of energy substrates; glucose, fatty acids, ketone bodies, and amino acids[46,146,147]. This flexibility plays an important role during stress and disease conditions. Under normal conditions, fatty acids are the major energy substrate for ATP production in the heart[46,146,147]. Therefore, it was hypothesised that the differentiation of hiPSCs into beating hiPSC-CMs would be associated with metabolic switch towards more fatty acid oxidation (FAO). Taken together, our data showed increases in fatty acid uptake and oxidation in beating hiPSC-CMs at a transcriptional and functional level. It is important to highlight that as the metabolism in beating hiPSC-CMs is shifted towards fatty acid oxidation, it does not necessarily mean that glucose uptake and utilization would be reduced as a result of the differentiation alone without metabolic manipulation. The differentiated beating hiPSC-CMs are immature and have foetal-like morphology and metabolic state. This has been shown in this project as beating hiPSC-CMs had a higher glycolytic rate than hiPSCs. At a transcriptional level, beating hiPSC-CMs had upregulated gene expression of *PFK* and *PDH*. Previously, it has been reported that murine cardiac differentiation is associated with rearrangement of the glycolytic network and not reduction in glucose metabolism[166]. In the mature heart when fatty acid oxidation is increased, glycolysis is reduced, based on the Randle Cycle theory[2] and it has been reported that differentiated beating hiPSC-CMs lack the metabolic maturity that is seen in adult cardiomyocytes. But *in vitro* differentiation of hiPSCs into beating hiPSC-

CMs was accompanied by an increase in both glycolysis and fatty acid oxidation. This is likely due to an increase in energy (ATP) demand to support the differentiation and contraction of the generated hiPSC-CMs, leading to an increase in total metabolism. This explanation is supported by our gene expression and glycolytic flux data.

4.6.2 Metabolism of Fatty Acids in Human Induced Pluripotent Stem Cells and their Differentiated Beating Cardiomyocytes

Transcriptional and function data showed that fatty acid uptake and metabolism was higher in beating hiPSC-CMs than hiPSCs. The relative gene expression of genes involved in fatty acid uptake and oxidation (*CD36*, *ASCL1*, and *CPT1B*) were higher in beating hiPSC-CMs. Similar increases in the relative gene expression of *CPT*, *ACADvl* and *ACADl* were reported during differentiation of murine ESCs into cardiomyocytes[148]. From previous studies, it is well know that PPAR-α has a major role in regulating cardiac metabolism[61,167,176–178,168–175] and that CD36, ASCL1, CPT1B are PPAR-α target genes[61,168–170,175,176,179], therefore it is likely that PPAR-α activation during cardiac differentiation upregulated the expression of fatty acid uptake and oxidation genes, which in turn increased fatty acid oxidation in beating hiPSC-CMs. Our data showed that OCR while respiring on oleic acid was significantly higher in beating hiPSC-CMs than hiPSCs at maximal respiration. Similar data has been reported in studies comparing hESCs, hiPSCs, hiPSC-CMs and human fibroblasts[41,88,155]. They showed that differentiated cells, either human fibroblasts or hiPSC-CMs, had a higher OCR than hESCs and hiPSCs[41,88,155]. In addition, beating hiPSC-CMs had a higher RRC than hiPSCs, suggesting that beating hiPSC-CMs have more mature mitochondria than hiPSCs.

4.6.3 Metabolism of Glucose in Human Induced Pluripotent Stem Cells and their Differentiated Beating Cardiomyocytes

GLUT1 is known to be the major glucose transporter isoform in fertilized eggs and it found to be highly expressed in pre-implantation embryos[159]. During organ formation, GLUT1, has been shown to play an important role in supplying glucose to the cell during differentiation[159]. However, after birth GLUT1 levels are reduced[159]. However, our data showed no significant difference in *GLUT1* expression in beating hiPSC-CMs compared with hiPSCs. In addition, *GLUT4* expression was not significantly changed in beating hiPSC-CMs compared with hiPSCs, although there was a trend to increased expression. It has been reported that both GLUT1 and GLUT4 are present in the foetal heart with GLUT4 being the predominate isoform in adult hearts[53,147,160].

Beating hiPSC-CMs had a higher glycolytic flux than hiPSCs when cultured using standard culture media or in low glucose media. Standard culture media for both hiPSCs and beating hiPSC-CMs are high in glucose, and if the energy demand for each cell type was taken into consideration, it not surprising that beating hiPSC-CMs would uptake glucose and utilize it at high rates to fit with its energy demand for contraction, particularly as there is not sufficient fatty acid present in the culturing media for the beating cardiomyocytes to use, if they adopted the metabolism of adult cardiomyocytes[46,62]. Whereas, in the fast, self-proliferating hiPSCs glycolysis is favoured over mitochondrial oxidative phosphorylation[72–77] and glutamine has been reported to be used for proliferation[133]. Glycolytic flux did not change with time in the beating hiPSC-CMs, whereas a reduction in flux was seen in hiPSCs, although this may be influenced by the change in cell number over the 24 hours. Given that hiPSCs proliferate and beating hiPSC-CMs do not, one can

deduce that hiPSCs principally used glucose for proliferation, whereas, beating hiPSC-CMs used glucose for contraction.

The relative gene expression of *PFK* was significantly upregulated in beating hiPSC-CMs compared with hiPSCs. It is known that PFK catalyses the first irreversible rate-limiting step after glucose becomes committed to glycolysis, therefore this supports our findings of increased glycolytic flux in hiPSC-CMs. The low expression level of PFK in hiPSCs might be due to glucose being diverted away from glycolysis and instead in to the PPP, though flux measurements through the PPP would be needed to confirm this. However, it has been reported that in hiPSCs PPP is active and used to supply hiPSCs with metabolic intermediates used for nucleotide biosynthesis[72–76,145].

At the end of glycolysis, pyruvate can either be converted into lactate via lactate dehydrogenase (LDH) or can be converted into acetyl CoA via pyruvate dehydrogenase (PDH). Therefore, PDH plays an important role in linking glycolysis to TCA cycle, and our data showed significant upregulation in *PDH* gene expression in beating hiPSC-CMs when compared with hiPSCs, which suggests that more pyruvate would be oxidised in the mitochondria. However, we saw no significant difference in pyruvate oxidation between beating hiPSC-CMs and hiPSCs. This is most likely due to the upregulated expression of *PDK4* in beating hiPSC-CMs. It has been reported that PDK4 is highly expressed in oxidative cells such as cardiomyocytes[163,164], and is a well know PPAR-α target gene[163,164,180–183]. Our data suggests that although the capacity for oxidative metabolism is increased during differentiation, sufficient ATP for contraction can be generated by glycolysis in the high glucose medium and therefore PDH flux is inhibited by PDK4 or the production of acetyl CoA or NADH.

4.6.4 Mitochondria and TCA Cycle in Human Induced Pluripotent Stem Cells and their Differentiated Beating Cardiomyocytes

4.6.4.1 Mitochondrial Structural and Morphology

Previous studies reported that mitochondria in pluripotent stem cells are perinuclear[75–77,148]. Our images showed active mitochondria distributed throughout the cells space although the small cell size of hiPSC made it difficult to confirm the location of active mitochondria. In contrast, in the beating hiPSC-CMs which have a large cytoplasmic area, it was clear that mitochondria formed networks and were distributed throughout the cytoplasm. Similar data has been reported previously, mitochondrial network are formed and distributed throughout the cytoplasm in differentiated cardiomyocytes[75,148,155]. This morphological data suggests that beating hiPSC-CMs have more mature mitochondria than hiPSCs.

4.6.4.2 Mitochondrial Bioenergetics Dependent on the Energy Substrate Oxidised

It has been reported that human pluripotent stem cells (hPSCs) have a fragmented mitochondrial network with a disorganised under-developed cristae, which suggest less functional mitochondria[149]. Here, we tested the function of mitochondria by measuring OCR in hiPSCs and beating hiPSC-CMs, while respiring on pyruvate and malate or on oleic acid. OCR at baseline and after oligomycin treatment were the same in both cell types regardless of the energy substrate used. Similar data was reported when hiPSCs were compared with human fibroblasts[88,149]. However, when maximal respiration was induced by the chemical uncoupler, FCCP, beating hiPSC-CMs consumed oxygen at a higher rate than hiPSCs, while respiring on oleic acid but not pyruvate and malate. Our data suggest that the capacity of mitochondria in beating hiPSC-CMs to increase oxidative respiration

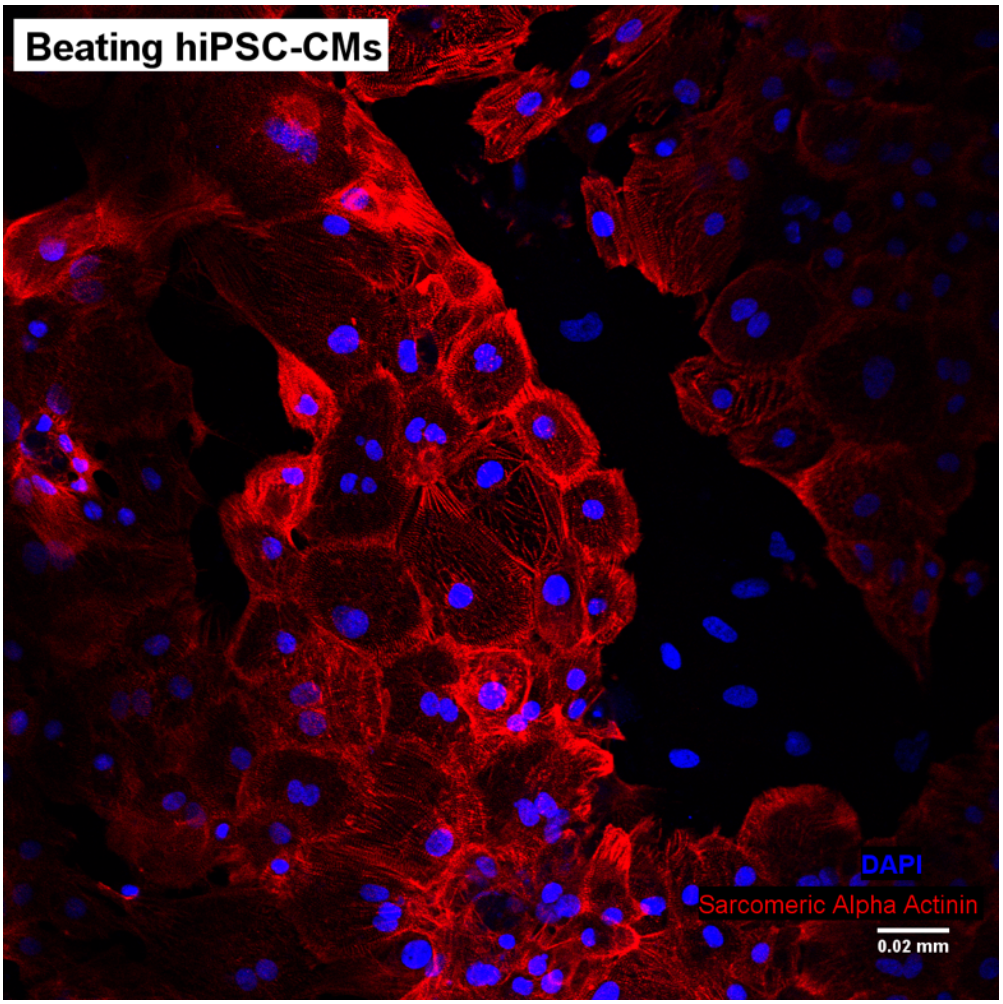
depends on the energy substrate available. Similar data has been reported when beating hiPSC-CMs were respiring on either glucose or palmitate[184]. These data fit with findings in the human adult heart, where fatty acid respiration is preferred over pyruvate respiration, as fatty acids are a more energy dense fuel. The increased RRC in our beating hiPSC-CMs, might be used as an indicator for mitochondria maturity in the differentiated cells compared with hiPSCs.

4.6.4.3 TCA Cycle

As hiPSCs favour anaerobic glycolysis[72–77], it was expected that TCA enzymes would be expressed less in hiPSCs than beating hiPSC-CMs, however, our data did not support this hypothesis. Data showed no difference in the relative gene expression of citrate synthase between hiPSCs and beating hiPSC-CMs. Similar data was reported previously, there was no difference in citrate synthase between hESCs, hiPSCs, and human fibroblasts[155]. Interestingly, our data showed that relative gene expression of *OGDH* was higher in hiPSCs than beating hiPSC-CMs. The high gene expression of TCA enzymes in hiPSCs indicates that TCA cycle in hiPSCs is active. It has been reported that fast proliferating cells such as hiPSCs use TCA cycle metabolic intermediates for biosynthesis of nucleotides and lipids[72–74,185]. For example, citrate is used for lipid synthesis, and oxaloacetate or α-ketoglutarate can be used for amino acid synthesis[72–74,185]. Therefore, we hypothesise that the TCA cycle is active in both hiPSCs and beating hiPSC-CMs, however, the purpose for its activation varies. In hiPSCs, TCA cycle is active to supply the cells with metabolic intermediates for the biosynthesis of nucleotides and lipids necessary for proliferating cells. Whereas, in beating hiPSC-CMs TCA cycle is used for complete substrate oxidation supplying ETC for the generation of ATP.

4.7 Conclusion

There is a switch in metabolism as hiPSCs are differentiated into beating hiPSC-CMs, from glucose-dependence in hiPSCs to glucose and fatty acid-dependence in beating hiPSC-CMs. The upregulation in the capacity for fatty acid oxidation in beating hiPSC-CMs was achieved by upregulation of genes involved in fatty acid uptake and oxidation and an increased mitochondrial reserve respiratory capacity. In addition, glucose uptake and metabolism was increased and glycolytic flux was higher in beating hiPSC-CMs when compared with hiPSCs, accompanied by an upregulation in glucose genes such as *PFK* and *PDH*. Therefore, it can be suggested that the differentiation of beating hiPSC-CMs is associated with mitochondrial maturation and enhanced glucose metabolism and fatty acid oxidation.



Chapter 5

The Effect of PPAR-α Activation during Human Induced Pluripotent Stem Cells Differentiation into Beating Cardiomyocytes

5 The Effect of PPAR-α Activation during Human Induced Pluripotent Stem Cells Differentiation into Beating Cardiomyocytes

5.1 Abstract

PPAR-α is expressed during cardiac differentiation in murine and mouse embryonic stem cells[186–188]. In addition, the PPAR-α agonist (WY14643) enhanced cardiac differentiation from mouse embryonic stem cells by upregulating cardiac gene expression[188]. Therefore, we hypothesised that PPAR-α activation during human induced pluripotent stem cell differentiation into beating cardiomyocytes (hiPSC-CMs) would enhance differentiation by upregulating the expression of PPAR-α target genes. PPAR-α agonist (WY14643) was added at different time points during the differentiation, but no significant difference was reported between treated and untreated hiPSC-CMs. In addition, it is well known that PPAR-α plays an important role in the metabolic shift from glycolysis towards fatty acid oxidation during heart development. Our findings demonstrate that PPAR-α activation by WY14643 during the differentiation process had a negligible effect and did not upregulate the expression of fatty acid oxidation nor TCA markers. We conclude that this may be due to differentiation not being the appropriate time point for this treatment.

5.2 Introduction

5.2.1 Definition and Structure of Peroxisome Proliferator-Activated Receptors

Peroxisome proliferator-activated receptor (PPAR) is a transcription factor that belongs to the ligand-activated nuclear hormone receptor superfamily. Three isoforms of PPAR were identified PPAR-α, PPAR-β/δ, and PPAR-γ. They share structural and functional features (Figure 5.1) but they differ in their tissue distribution (Table 5.1) and their response to activation. PPARs consist of four active domains: the ligand-independent activation domain (A/B), the DNA binding domain (C), the cofactors domain (D), and the ligand-dependent domain (E/F)[189–194] (Figure 5.1). PPARs regulate the rate of gene transcription controlling development, homeostasis, and metabolism in various organs of the body[189–194].

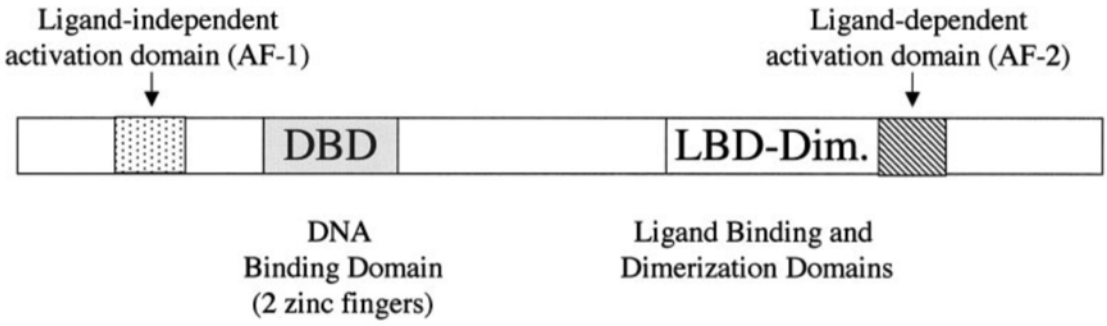


Figure 5.1: The structure of PPARs[190]. PPAR isoforms share structural features.

Table 5.1: Tissue distribution of PPARs isoforms.

PPAR Isoform	Organs
PPAR-α	Liver[179,189–197], Heart[179,189–197], Kidney[179,189,190,193–197], Skeletal Muscles[179,189–192,194–197], Brown Adipose tissue[179,189,192,193,195], Intestine[179,195–197]
PPAR-β/δ	Ubiquitous[189–193,196,197], Brain[191,194], Adipose tissue[191,192], Skin[191], Intestine[192,194], Kidney[192,194]
PPAR-γ	Adipose tissue[189–193,196,197], Intestine[189,190,192,194], Immune system[189,190]

5.2.2 PPAR Activation, Ligands, and Target genes

PPAR distribution in the body differs, however the mechanism of action consists of common steps, summarised in Figure 5.2. The binding of either an endogenous (natural) or an exogenous (synthetic) ligand to the ligand-dependent domain (LDD) of the PPAR induces the heterodimerisation of the PPAR with the common nuclear receptor binding partner, retinoid X receptor (RXR), which itself is activated by 9-cis retinoic acid. This will result in the dissociation of the co-repressor protein and the recruitment of co-activators, followed by the binding of the PPAR:RXR heterodimer complex to the peroxisome proliferator response element (PPRE) in the promoter region of target genes, which will induce gene transcription[61,179,199–203,189–195,198]. There are different isoforms for the RXR (RXR-α, -β/δ, -γ)[186,194], which have different organ distribution, just like PPARs. The specific PPAR:RXR complex binds to the specific sequence (PPRE) in the promoter region of the target gene[194].

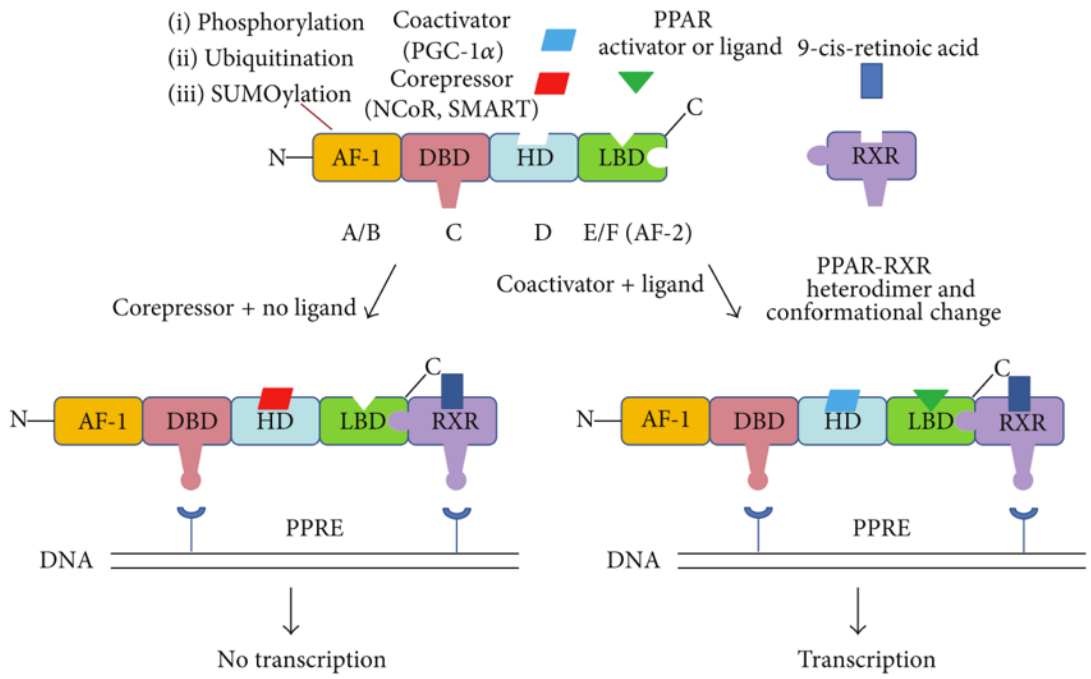


Figure 5.2: PPARs activation and gene transcription[203].

PPARs have a ligand-binding cavity that is 3-4 times larger than other nuclear receptors. This feature gives PPARs the capability to bind a wide range of natural ligands such as fatty acids and eicosanoids, and synthetic ligands such as hypo-lipidemic agents[192]. Natural ligands such as fatty acid bind to all isoforms of PPARs, but with different binding affinities. For example, PPAR-α prefers unsaturated fatty acid to saturated fatty acids[199–202] whereas PPAR-β/δ is activated by polyunsaturated fatty acids[199,200,202], but only weakly activated by saturated fatty acids[200]. PPAR-γ is activated by polyunsaturated fatty acids[199–201], but weakly activated by monounsaturated fatty acids[200,201] and saturated fatty acids[201]. Fibrates act as synthetic ligands for PPAR-α[179,189,190,192,195,199,201] and PPAR-β/δ[199], whereas thiazolidinedione (TDZ) agents act as synthetic ligands for PPAR-γ[189,190,192,193]. Some PPAR ligands that have been reported in literature are shown in table 5.2, and in table 5.3 are some of the target genes reported.

Table 5.2: PPARs natural and synthetic ligands.

Isoforms	Natural Ligands	Synthetic Ligands
PPAR-α	Saturated Fatty Acid[189,192,194,200,201] Unsaturated Fatty Acid[179,189,202,203,190,192–195,199–201] Eicosanoids[179,194,195,199,201,202]	WY-14643[168,179,189,194,195,199,202] Fibrates[179,189,190,192,194,195,199,201] GW231[201]
PPAR-β/δ	Unsaturated Fatty Acid[189,192–194,199,200,202,203] Eicosanoids[194,199]	L-165041[168,189] GW501516[168,192,203] GW0742[167] Fibrates[194,199]
PPAR-γ	Unsaturated Fatty Acid[189,190,192–194,199–201,203] Prostaglandin J2[189,192–194,199,201]	Thiazolidinedione (TZD)[189,190,192–194,203] Fibrates[194,199] GW231[201]

Table 5.3: PPARs target genes and their effect upon activation.

Isoforms	**Target Gene**	**Effect of Target Gene**
PPAR-α	L-FABP, CD36[203] Fatty Acid β-oxidation[203]	Increase fatty acid uptake and oxidation[203]
PPAR-β/δ	Fatty acid uptake[203]	Increase fatty acid oxidation[203]
PPAR-γ	FABP (aP2), CD36[203] Carboxykinase[203] Phosphoenolpyruvate[203]	Glucose homeostasis[203] Lipid Storage[203]

5.2.3 PPAR-α in the Developing and Adult Hearts

5.2.3.1 PPAR-α Expression, Ligands, and Target Genes in the Heart

During embryogenesis, the expression levels of PPAR-α change dependent on the embryonic day[196,197]. The PPAR-α is first detected between E13.5 – E15.5 in rodent hearts[197] and is highly expressed in adult hearts[46,62,198,189–194,196,197]. PPAR-α target genes that have been shown to be upregulated in the heart include genes involved in fatty acid oxidation such as acyl-CoA oxidase (ACO-A), long-chain acyl-CoA synthetase (LCAS), carnitine palmitoyl-transferase-I (CPTI), carnitine palmitoyl-transferase-II (CPTII), medium-chain acyl-CoA dehydrogenase (MCAD), long-chain acyl-CoA dehydrogenase

(LCAD), and malonyl-CoA decarboxylase[167,168,178,179,169,170,172–177]. In addition, PPAR-α regulates the transcription of the uncoupling proteins, UCP2 and UCP3[167,178,179,204,205] and pyruvate dehydrogenase kinase isoform 4 (PDK4) in the heart[163,167,178,179,181,182,206]. It has been reported that starvation, diabetes, high-fat diet and hyperthyroidism, all cause increases in heart PDK4 expression as a result of PPAR-α activation by high levels of free fatty acids in the plasma[178,181,182,206].

5.2.3.2 PPAR-α Agonist (WY14643)

WY14643, which is a 2-pyrimidinylthioacetic acid derivative, was first reported to act as a potent antihypercholestrolemic agent in 1974[207]. It has been shown that WY14643 reduces serum cholesterol in a dose-dependent manner[207]. WY14643 binds and activates human PPAR-α[208,209] and has a higher potency to activate PPAR-α than PPAR-β/δ or PPAR-γ, with EC_{50} values of 5.386 μM, 26 mM, and 17 mM, respectively[209].

5.2.4 PPAR-α Expression and Activation during Cardiac Differentiation in Mouse Embryonic Stem Cells

In previous studies, it has been shown that all isoforms of PPAR are expressed at different time points during cardiomyocyte differentiation from mouse embryonic stem cells[186–188]. The expression of PPAR-α peaked twice during mouse cardiomyocytes differentiation, at day 12 and day 20 and was correlated with the peak of α-MHC[188], α-actinin[186], and troponin T[186,187] expression. In addition, they showed that treatment with the PPAR-α agonist (WY14643) during differentiation increased the expression of cardiogenic transcription factors (GATA4, Nkx2.5, DTEF-1, and MEF2C) and increased the expression of cardiac genes (MHC-β, MHC2*a*, and MLC2*v*). Also, WY14643 increased

the number of spontaneously beating embryonic bodies, and the size of the beating area[188]. Inhibition of PPAR-α using the PPAR-α antagonist (GW6471) reduced the number of beating cells, reduced the expression of cardiac genes (α-MHC and MLC2v), and reduced the expression of α-actinin and troponin T[186,187]. Each research group proposed a mechanism for which PPAR-α activation occurs during cardiomyocyte differentiation. One possible mechanism involves the p38 MAPK signalling pathway[186], another possible mechanism involves ROS and NADPH oxidase activity[188].

5.2.5 PPAR-α Activation in Heart Metabolism

From previous studies, it is well know that PPAR-α has a major role in regulating cardiac metabolism[61,167,176–178,168–175]. In knockout PPAR-α mouse models (PPAR-$\alpha^{-/-}$), cardiac fatty acid oxidation is reduced[178], whereas PPAR-α activation in the heart results in the increase of fatty acid oxidation via upregulating FAO genes[61,148,175–177,210,167–174]. It has been shown that PPAR-α activates genes that represent various steps of fatty acid oxidation: cellular transport and esterification[61,168,169,174,175], mitochondrial uptake[61,170–172], and mitochondrial oxidation[61,172,173,178]. It has been reported that PPAR-α knockout mice had 30-60% reduction in gene expression of cardiac MCAD, LCAD, and VLCAD[172] whilst the PPAR-α agonist (WY14643) has been shown to upregulate the expression of LCAD[168]. Alteration in glucose metabolism in the heart has also been reported to be regulated by PPAR-α[168,175,178,210]. In PPAR-$\alpha^{-/-}$ mouse model, an increase in glycolysis in the heart has been reported[178] whereas a reduction in GLUT4 expression has been reported as a result of PPAR-α activation via natural[168,175] or synthetic ligands[210]. In addition, WY14643 treatment downregulated PFK expression[210]. Another important PPAR-α target gene that

regulates glucose metabolism is PDK4[163,164,167,178,180,181,210]. In the PPAR-$\alpha^{-/-}$ mouse model, PDK4 expression was downregulated[178], whereas, using WY14643 to activate PPAR-α increased expression of PDK4 in the heart[181,210] and neonatal cardiomyocytes[167]. Another target gene of PPAR-α activation in the heart is UCP3[178,179,204,205]. A study of WY14643 treatment, on wild-type animal models showed elevated levels of UCP3[179,204], whereas, in PPAR-$\alpha^{-/-}$ mouse model UCP3 is downregulated[178,204]. Also, it is important to point out that PGC1α gene expression, which is a PPAR-α co-activator in the heart, is induced by increased fatty acid levels in the circulation[194].

5.3 Aims of Chapter

The aim of this chapter is to investigate whether pharmacological PPAR-α activation, using WY14643 during differentiation of hiPSCs into beating hiPSC-CMs was benefical for cardiomyocytes maturation

This Chapter:

1. Used WY14643 treatment at various time points of the differentiation and at different concentrations to try to promote differentiation
2. Tested the effect of WY14643 treatment on the relative gene expression of cardiac markers as a sign for cardiac differentiation enhancement
3. Tested the effect of WY14643 treatment during cardiac differentiation on the metabolic shift from glycolysis towards fatty acid oxidation in hiPSC-CMs, by measurement of gene expression of glucose and fatty acid metabolism markers as a sign of metabolic maturity

5.4 Materials and Methods

5.4.1 WY14643 Treatment during the Differentiation of Human Induced Pluripotent Stem Cells into Beating Cardiomyocytes

HiPSCs were differentiated into beating cardiomyocytes using the optimised Wnt-modulation protocol. PPAR-α was activated using WY14643 at various time points during the differentiation, and at different concentrations. WY14643 (Stratech Scientific) at 6 μM, 60 μM, and 120 μM was added from either day 5, 7, or 10 of the differentiation and continued until collection day (Figure 5.3). Cells were cultured with RPMI+B27 media supplemented with WY14643. Media was changed every 2 days, and in treated groups cells were supplemented with fresh WY14643 every time the media was changed. In total, there were nine different WY14643-treated conditions and an untreated control group. Untreated and WY14643-treated hiPSC-CMs were collected on day 15 of differentiation for further analysis.

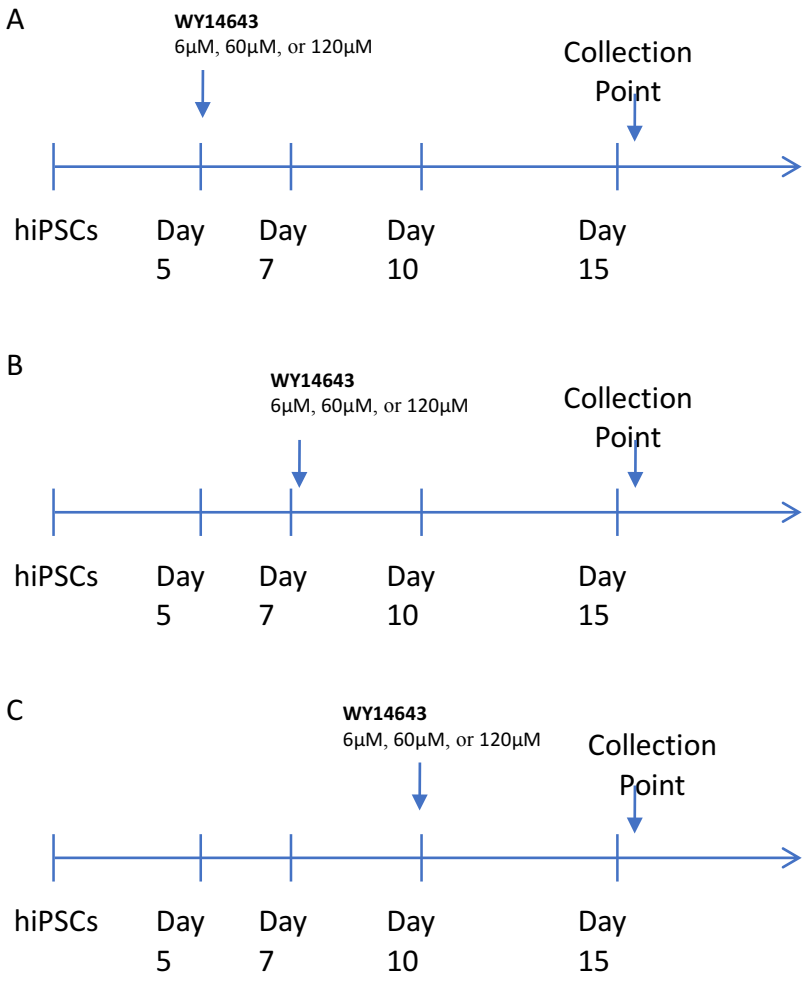
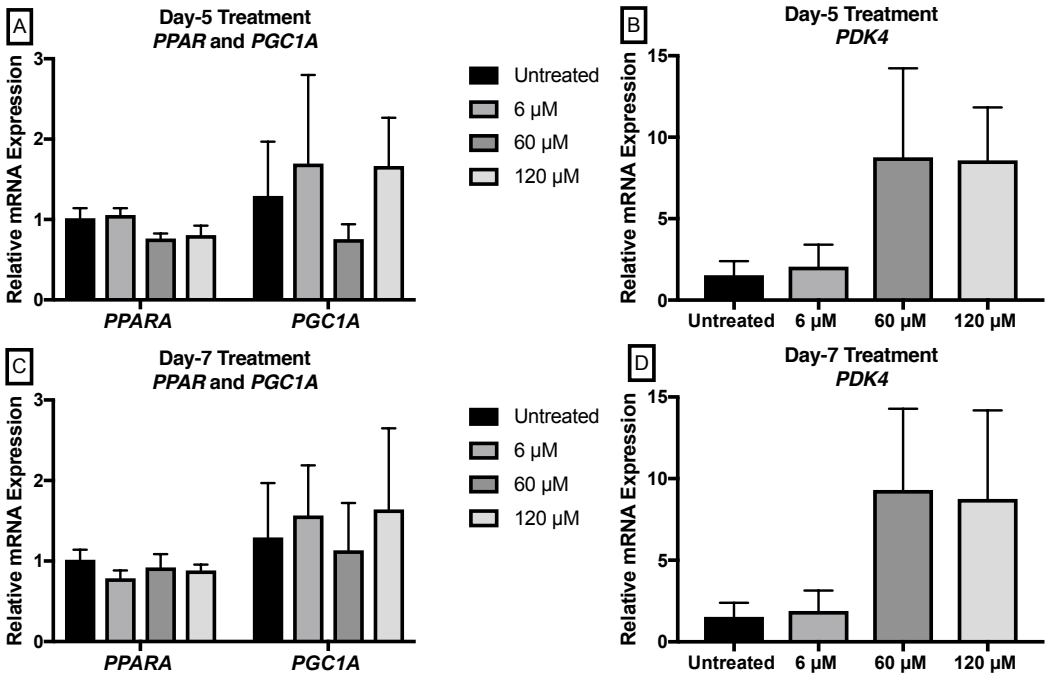


Figure 5.3: WY14643 treatment during hiPSC-CMs differentiation. Outline of the differentiation of hiPSC-CMs and the addition of WY14643 into the media at different time points. (A) Treatment with WY14643 at 6 µM, 60 µM, and 120 µM on day 5 of hiPSC-CMs differentiation. In this condition, RPMI+B27(-insulin) media with WY14643 was changed again on day 7 and 10 of the differentiation. (B) Treatment with WY14643 at 6µM, 60µM, and 120µM on day 7 of hiPSC-CMs differentiation. In this condition, RPMI+B27 media with fresh WY14643 was changed again on day 10 of the differentiation. (C) Treatment with WY14643 at 6 µM, 60 µM, and 120 µM on day 10 of hiPSC-CMs differentiation. Untreated and WY14643-treated hiPSC-CMs were collected on day 15 of the differentiation and untreated hiPSC-CMs were used as control.

5.5 Results

5.5.1 The Effect of WY14643 Treatment during Cardiac Differentiation on the Expression of *PPARA*, *PGC1A*, and *PDK4*

HiPSCs were differentiated into beating hiPSC-CMs using the Wnt-modulation protocol and WY14643 was added into the culturing media at day 5, 7 or 10 of the differentiation protocol, in order to activate PPAR-α. WY14643-treated and untreated hiPSC-CMs were collected on Day 15 of the differentiation, and the relative expression of PPARA, PGC1A (PPAR-α co-activator), and PDK4 (PPAR-α target gene) were measured. There was no difference in the relative expression of PPARA and PGC1A between WY14643-treated and untreated hiPSC-CMs at any time point (Figure 5.4 A, C, E). In addition, there was no difference in the relative expression of PDK4, which is PPAR-α target gene and was used here as a marker of PPAR-α activation (Figure 5.4 B, D, F).



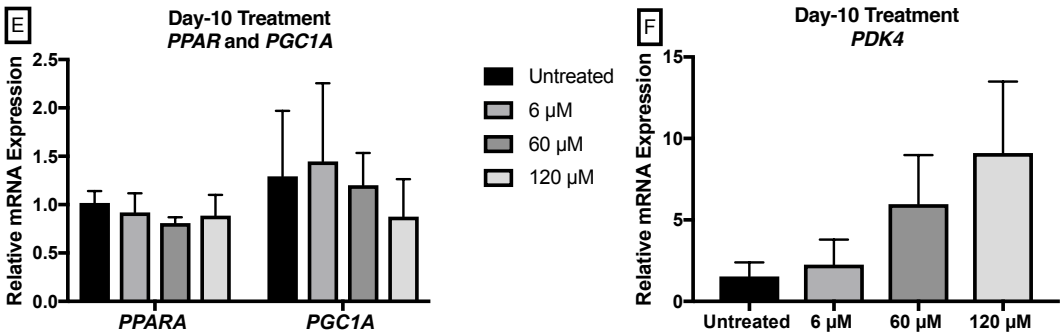
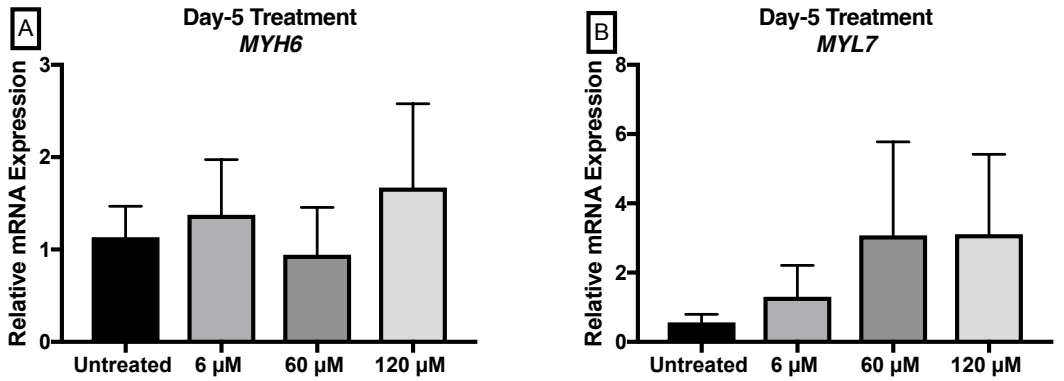


Figure 5.4: The Relative mRNA Expression of *PPARA*, *PGC1A*, and *PDK4*. (A, C, E) the relative mRNA expression of *PPARA* and *PGC1A*, and (B, D, F) the relative mRNA expression of *PDK4*. WY14643 was added either on day 5, 7, or 10 of the differentiation. In each of these time points, different concentration of WY14643 was tested (6 µM, 60 µM, 120 µM). Abbreviations: PPARA: Peroxisome proliferator-activated receptor alpha, PGC1A: Peroxisome proliferator-activated receptor gamma, coactivator 1 alpha, PDK4: pyruvate dehydrogenase kinase 4. Data are present as mean ± SEM, and data were analysed using a one-way ANOVA with Tukey post hoc test (n=3).

5.5.2 The Effect of WY14643 Treatment during Cardiac Differentiation on the Expression of Cardiac Genes

The effect of PPAR-α activation using WY14643 on the relative mRNA expression of cardiac markers (*MYH6* and *MYL7*) was measured. There was no difference in the relative mRNA expression of *MYH6* and *MYL7* between WY14643-treated and untreated hiPSC-CMs (Figure 5.6). Therefore, PPAR-α activation during hiPSCs differentiation into beating hiPSC-CMs using WY14643 did not enhance cardiac differentiation.



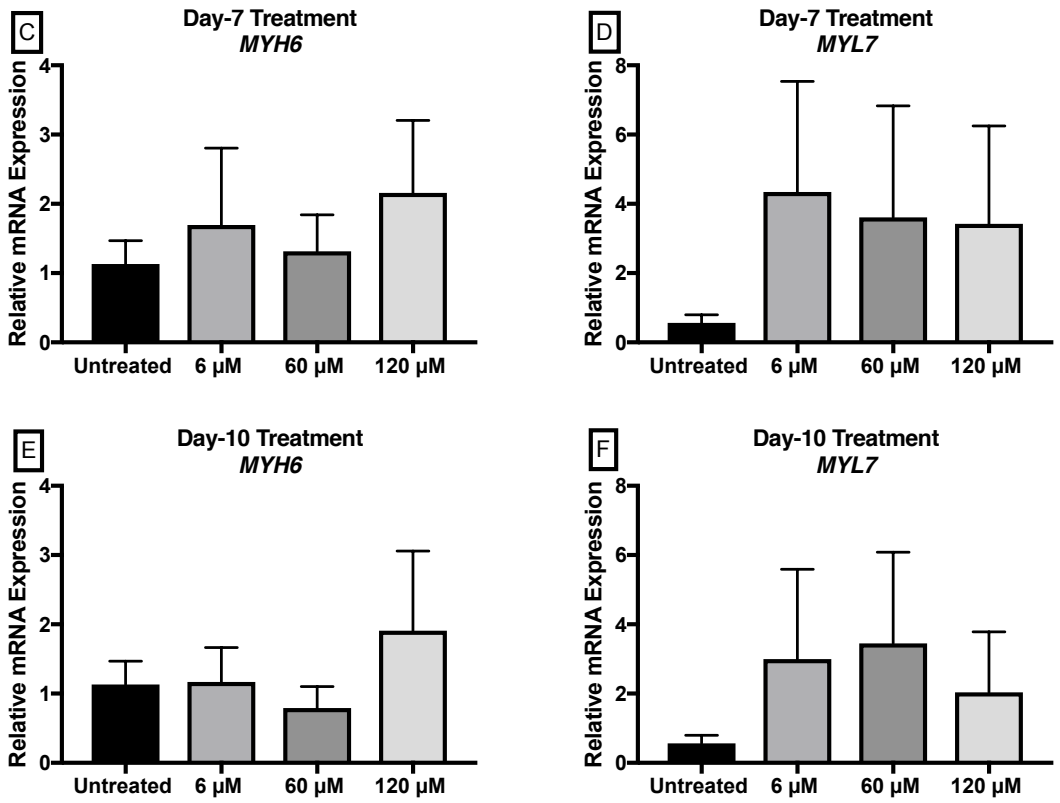
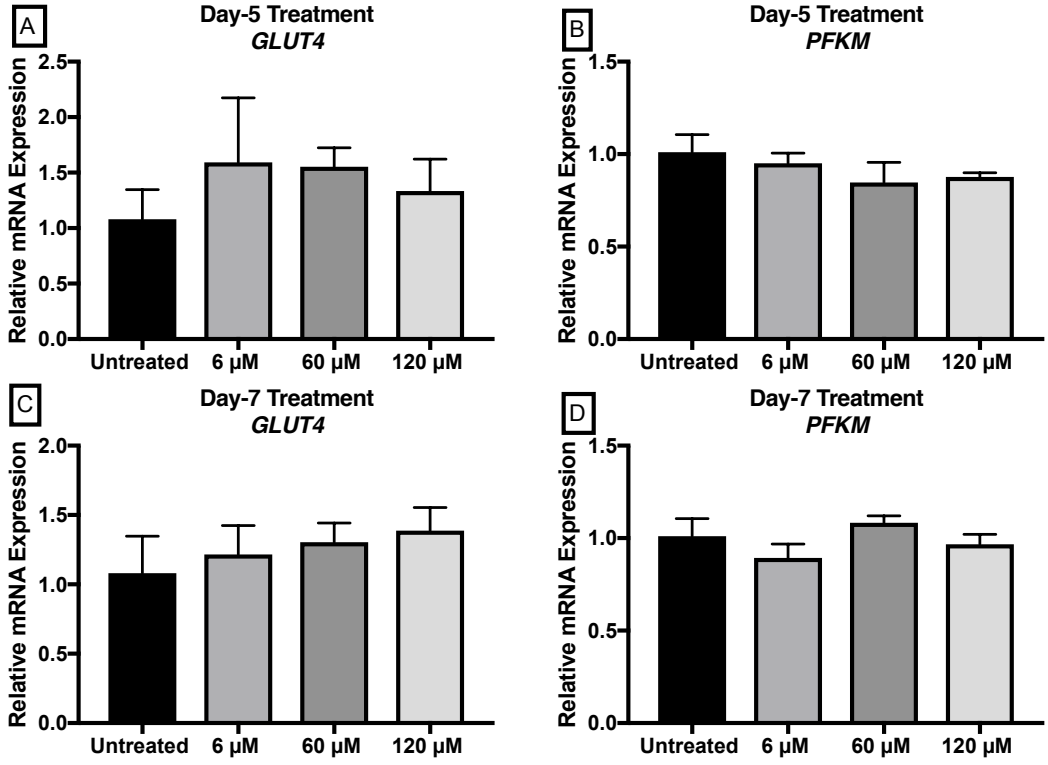


Figure 5.6: The Relative Gene Expression of *MYH6* and *MYL7*. (A, C, E) the relative gene expression of *MYH6* and (B, D, F) the relative gene expression of *MYL*7. WY14643 was added either on day 5, 7, or 10 of the differentiation. In each of these time points, different concentration of WY14643 was tested (6 µM, 60 µM, 120 µM). Abbreviations: MYH6: myosin heavy chain 6, MYL7: myosin light chain 7. Data are present as mean ± SEM, and analysed using a one-way ANOVA with Tukey post hoc test (n=3).

5.5.3 The Effect of WY14643 Treatment during Cardiac Differentiation on the Expression of Metabolic Genes

5.5.3.1 Glucose Metabolism

The relative gene expression of glucose transporter, *GLUT4*, was measured and there was no significant difference between WY14643-treated and untreated cells (Figure 5.7 A, C, E). In addition, there was no significant difference in the relative gene expression of *PFKM* at any time point (Figure 5.7 B, D, F).



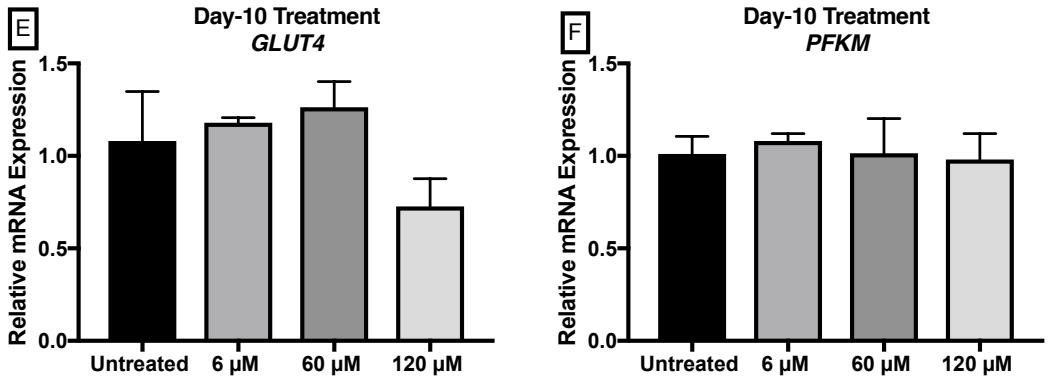
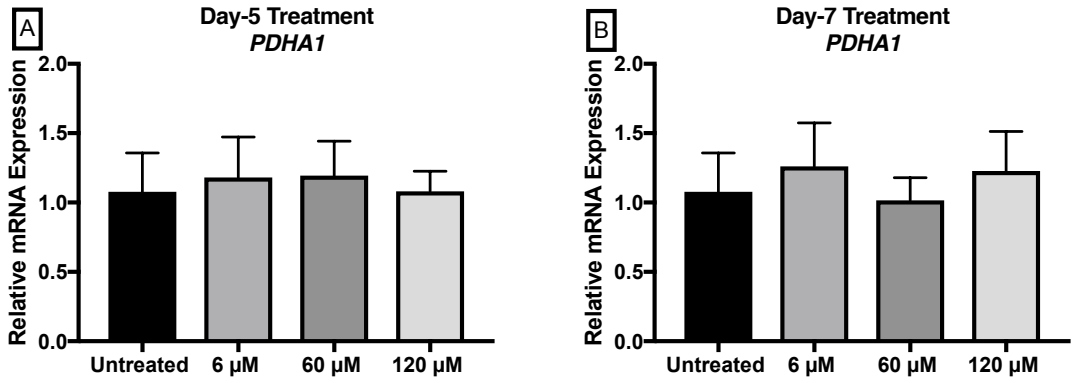


Figure 5.7: The relative gene expression of *GLUT4* and *PFKM*. (A, C, E) the relative gene expression of *GLUT4* and (B, D, F) the relative gene expression of *PFKM*. WY14643 was added either on day 5, 7, or 10 of the differentiation. In each of these time points, different concentration of WY14643 was tested (6 µM, 60 µM, 120 µM). Abbreviations: GLUT4: glucose transporter 4, PFKM: phosphofructokinase, muscle-type. Data are present as mean ± SEM, and analysed using a one-way ANOVA with (Tukey post hoc) test (n=3).

We measured the relative expression of *PDHA1* in WY14643-treated and untreated hiPSC-CMs. Our data showed no significant difference between WY14643-treated and untreated day-15 hiPSC-CMs (Figure 5.8).



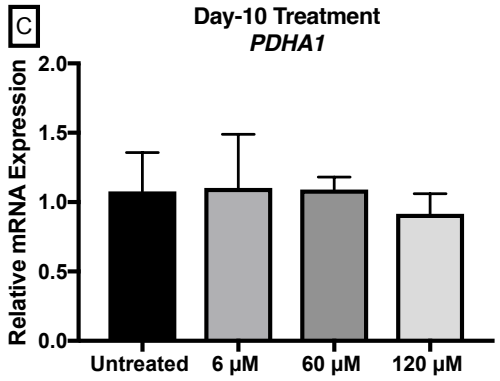
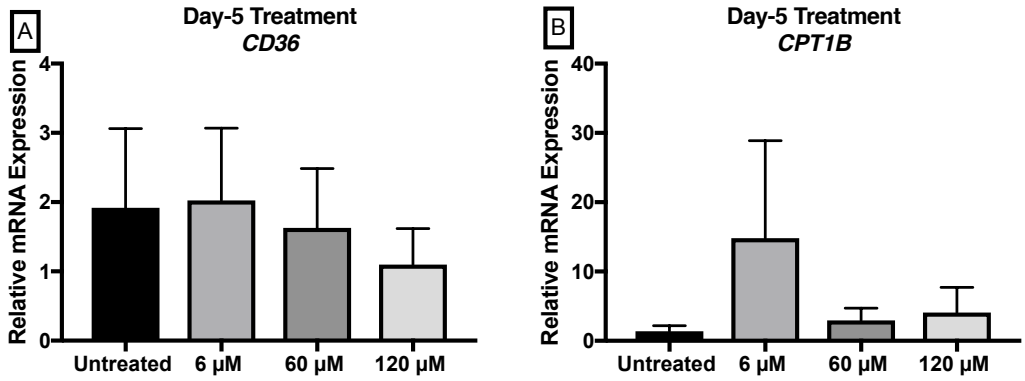


Figure 5.8: The relative gene expression of *PDHA1*. WY14643 was added either on day 5 (A), 7 (B), or 10 (C) of the differentiation. In each of these time points, different concentration of WY14643 was tested (6 µM, 60 µM, 120 µM). Abbreviations: PDHA1: pyruvate dehydrogenase, alpha 1. Data are present as mean ± SEM, and analysed using a one-way ANOVA with Tukey post hoc test (n=3).

5.5.3.2 Fatty Acid Metabolism

There was no significant difference in the relative expression of *CD36* and *CPT1B* between WY14643-treated and untreated hiPSC-CMs (Figure 5.9). In addition, the expression of fatty acid oxidation enzyme *HADHA1* and *ACADVL* showed no significant difference whether cells were treated with WY14643 or not (Figure 5.10).



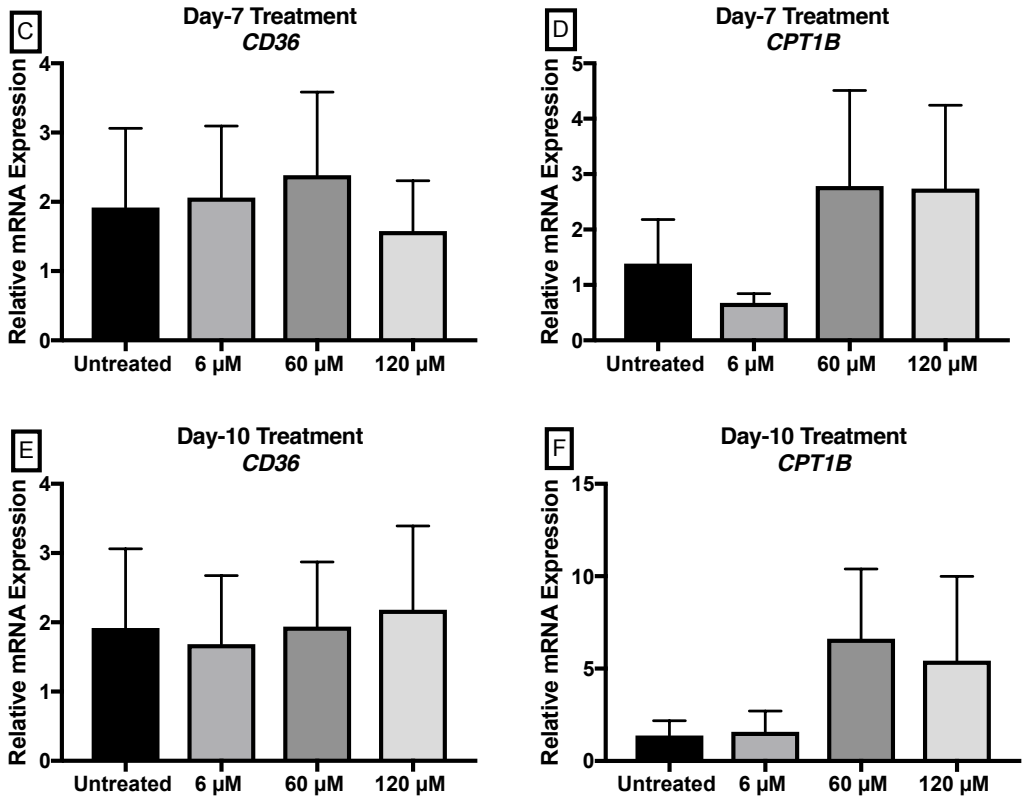
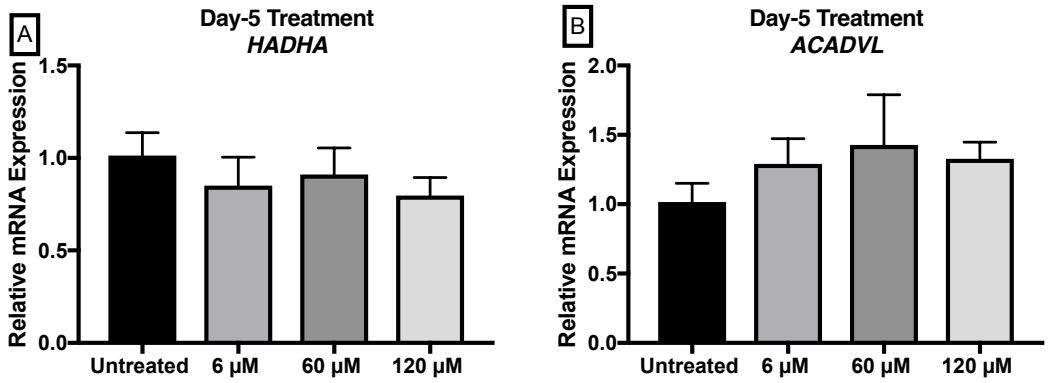


Figure 5.9: The Relative Gene Expression of CD36 and CPT1B. (A, C, E) the relative gene expression of CD36 and (B, D, F) the relative gene expression of CPT1B. WY14643 was added either on day 5, 7, or 10 of the differentiation. In each of these time points, different concentration of WY14643 was tested (6 µM, 60 µM, 120 µM). Abbreviations: CD36: cluster of differentiation 36 (fatty acid transporter), CPT1B: carnitine palmitoyltransferase 1B. Data are present as mean ± SEM, and analysed using a one-way ANOVA with (Tukey post hoc) test (n=3).



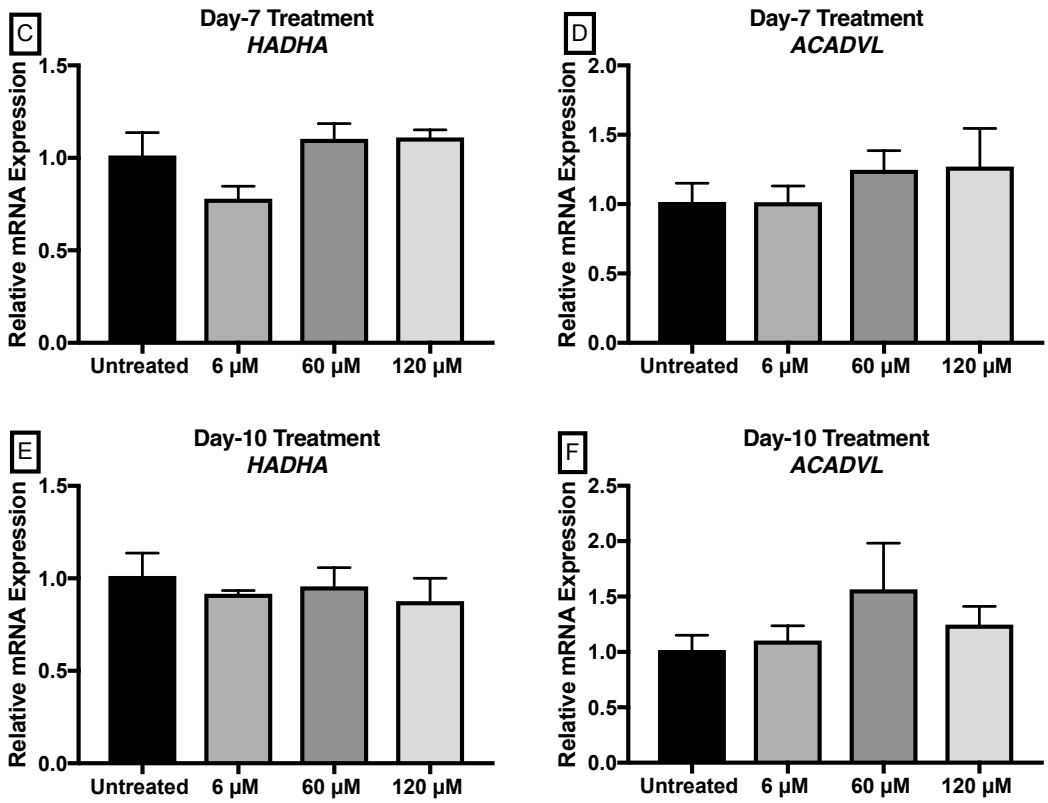


Figure 5.10: The relative gene expression of *HADHA* and *ACADVL*. WY14643 was added either on day 5 (A, B), 7 (C, D), or 10 (E, F) of the differentiation. In each of these time points, different concentration of WY14643 was tested (6 µM, 60 µM, 120 µM). Abbreviations: HADHA: hydroxyacyl-CoA dehydrogenase, alpha-subunit, ACADVL: acyl CoA dehydrogenase very long-chain. Data are present as mean ± SEM, and analysed using a one-way ANOVA with (Tukey post hoc) test (n=3).

5.5.3.3 TCA Cycle:

The expression of two TCA cycle enzymes was measured, and data showed no significant difference in citrate synthase (*CS*) expression between WY14643-treated and untreated cells. In addition, no difference in the expression of *OGDH* was reported between treated and untreated hiPSC-CMs (Figure 5.11).

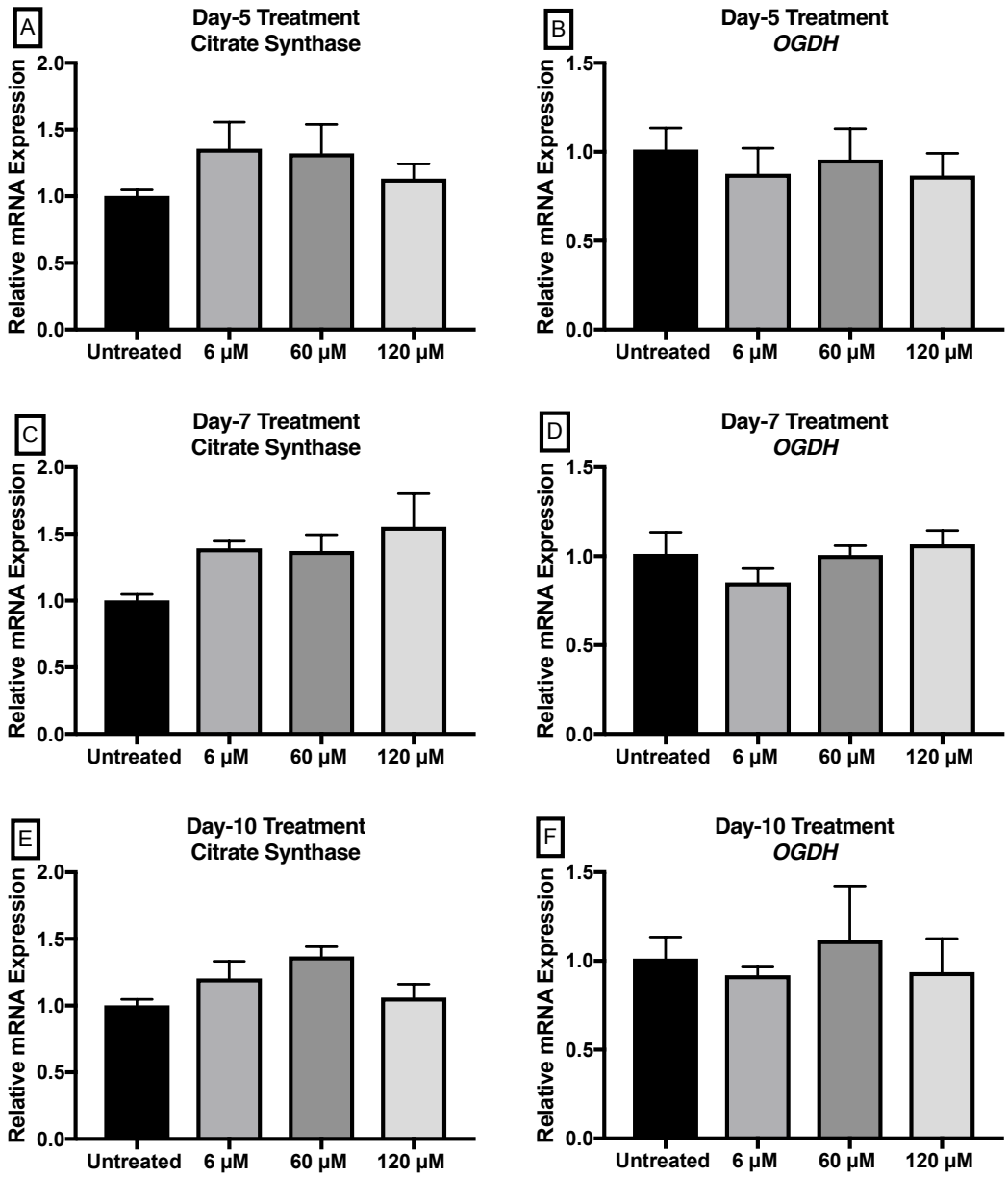


Figure 5.11: The Relative Gene Expression of TCA cycle enzymes (*CS* and *OGDH)*. Day-15 hiPSC-CMs were collected for analysis. WY14643 was used at the following concentration (6 µM, 60 µM, 120 µM) on days 5, 7, and 10 of differentiation. Abbreviations: CS: Citrate Synthase, OGDH: oxoglutarate dehydrogenase. Data are present as mean ± SEM and analysed using a one-way ANOVA with Tukey post hoc test (n=3).

5.6 Discussion

PPAR-α is expressed and activated during heart development[196,197] and during cardiac differentiation in murine[186,187] and mouse[188] embryonic stem cells (ESCs). Also, the PPAR-α agonist (WY14643) has been shown to enhance cardiac differentiation from mouse embryonic stem cells by upregulating cardiac gene expression such as, MHC-β, MHC2*a*, and MLC2*v*[188]. Therefore, it was hypothesised that PPAR-α activation using WY14643 during hiPSCs differentiation into beating cardiomyocytes (hiPSC-CMs) might enhance the differentiation by upregulating expression of cardiac genes. In addition, PPAR-α regulates the metabolic shift during heart development from glycolysis towards fatty acid oxidation[61,148,175–177,210,167–174]. Therefore, we hypothesised that WY14643 treatment might enhance this metabolic shift by upregulating the expression of fatty acid oxidation enzymes. However, we found that WY14643 treatment did not enhance cardiac differentiation nor enhance the metabolic shift towards fatty acid oxidation in hiPSC-MCs.

5.6.1 The Effect of WY14643 on the Expression of *PPARA*, *PGC1A*, and *PDK4*

During murine and mouse embryonic stem cell cardiac differentiation, it was reported that the gene expression and protein levels of PPAR-α and PGC1-α appeared on day 5 - 6 and started to increase sharply by day 7 of differentiation, peaking on day 10 - 12 of differentiation[186,188]. PPAR-α expression, started to reduce gradually to reach it lowest expression on day 17[188]. Therefore, in this project WY14643 treatment was started on day 5, 7, or 10 of the hiPSC-CMs differentiation. Our data showed no difference in the relative gene expression of *PPARA* and *PGC1A* between WY14643-treated and untreated hiPSC-CMs. The failure of WY14643 treatment to increase the expression of *PPARA* might be

due to the fact that WY14643 is a PPAR-α activator, therefore it is not necessary that it will increase the expression of the PPAR-α gene. Another explanation could be that by day 15 of differentiation, when hiPSC-CMs were collected, the expression of *PPARA* and *PGC1A* had already decreased, as seen by others[186,188]. It has been reported that PDK4 expression is upregulated by PPAR-α activation via WY14643, a PPAR-α agonist[163,164,180–183]. Our data showed there was no significant difference in the relative gene expression of *PDK4* between WY14643-treated and untreated hiPSC-CMs, although, there was a trend towards an increased expression of *PDK4* in WY14643-treated hiPSC-CMs in a dose-dependent manner. This might be due to the large variability, which might be due to the fact that the rate of differentiation varies between cells and so at day-15 hiPSC-CMs are at different maturity levels. This was emphasised by the fact that some samples had more beating areas than others and therefore in future work we decided to mature only spontaneously beating hiPSC-CMs, that had similar beating areas to avoid differences caused by differentiation efficiency.

5.6.2 The Effect of WY14643 on the Expression of Cardiac Genes (*MYH6* and *MYL7*)

From chapter 3.1, hiPSC-CMs differentiation alone upregulated cardiac genes such as *MYH6*. Activating PPAR-α by WY14643 was used here with the aim of further enhancing the upregulation of cardiac genes, however, our data showed no difference in the relative expression of *MYH6* and *MYL7* between WY14643-treated and untreated hiPSC-CMs. It might be that any increase was masked by variability between samples, or that other factors might play a more important role in enhancing cardiac differentiation than PPAR-α activation alone. Although, it has been reported that PPAR-α is the predominate isoform

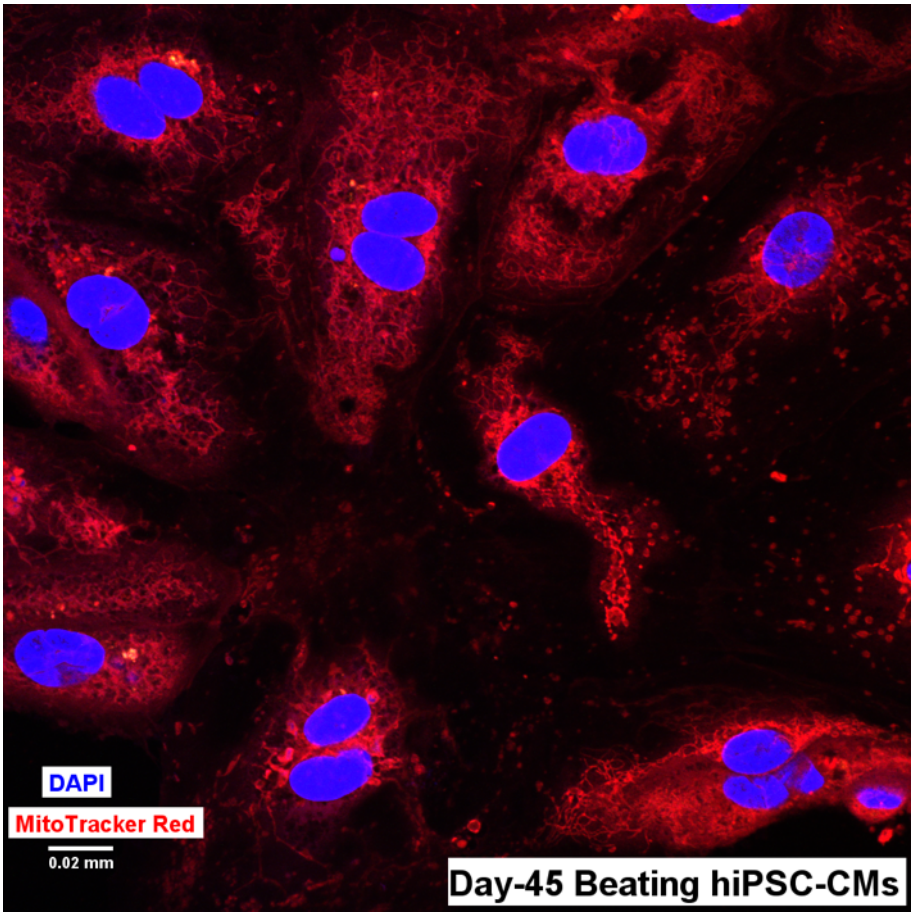
in the adult heart[179,189–195,197,211], other PPAR isoforms, such as PPAR-β/δ have been reported to be expressed during heart development[196,197] and during cardiac differentiation from mESCs[188].

5.6.3 The Effect of WY14643 on the Expression of Metabolic Genes

As the heart develops, there is a shift in metabolism from glycolysis in the foetal heart to fatty acid in adult heart and it is believed that PPAR-α activation plays a major role in the shift[61,167,176,177,168–175]. Therefore, it was hypothesised that activating PPAR-α using WY14643 during hiPSC-CMs differentiation might enhance the metabolic shift from glycolysis towards a fatty acid oxidation profile. However, our data showed no significant difference in the expression of most metabolic genes studied between WY14643-treated and untreated hiPSC-CMs. Our data suggest that PPAR-α activation alone during hiPSC differentiation into beating hiPSC-CMs is not sufficient to enhance fatty acid oxidation and other factors might play an important role. One important factor can be the availability of substrates in the culturing media. Roswell Park Memorial Institute (PRMI) media is high in glucose and lacks fatty acid. After birth, there is a change in the energy substrate levels in the circulation, which is not taken into account when hiPSCs are differentiated into beating hiPSC-CMs. This will be covered in more details in the following chapter. Another important factor might be the time at which PPAR-α was activated in the differentiation, which might be not equivalent to the time when PPAR-α is activated in the developing heart. So, we decided to use WY14643 at a later time point, after spontaneous beating occurs.

5.7 Conclusion

In conclusion, the activation of PPAR-α during differentiation of hiPSCs into beating hiPSC-CMs did not appear to enhance cardiac differentiation or affect the metabolic switch that occurs as a result of differentiation alone. However, gene expression in these cell populations was variable, as cells within the wells may have been at different points in the differentiation cycle. Therefore, it was proposed to investigate whether activation of PPAR-α in young beating hiPSC-CMs was stimulated by addition of oleic acid, to mimic the metabolic changes that occur in the heart after birth such as the changes in substrate availability.



Chapter 6

Metabolic Maturation of Young Beating hiPSC-CMs via PPAR-α Activation using WY14643 and Oleic Acid

6 Metabolic Maturation of Young Beating hiPSC-CMs via PPAR-α Activation using WY14643 and Oleic Acid

6.1 Abstract

There is a change in energy substrate availability and metabolism during heart development from the embryo into the adult stage. However, this change in metabolism is not mimicked in most published differentiation protocols. Therefore, in this chapter we aimed to investigate the concept of metabolic substrate change by adding the fatty acid, oleic acid, into the culturing conditions of the current protocol to enhance fatty acid oxidation in immature beating hiPSC-CMs at a later-stage of differentiation (> day 15). In addition, we took into consideration the role of PPAR-α activation during this metabolic shift as fatty acids are known to be natural ligands for PPAR-α. To enhance the effect of PPAR-α activation further, WY14643 was added in combination with oleic acid into the culturing media. The results showed that fatty acid alone can help in enhancing the metabolic shift, however, beating hiPSC-CMs that were treated with fatty acid and WY14643 showed mitochondria maturation and a further enhancement in fatty acid oxidation. Therefore, changing the culturing environment of immature beating hiPSC-CMs at a later-stage of differentiation enhances metabolic maturation via PPAR-α activation.

6.2 Introduction

The work in this chapter continues the studies introduced in the previous chapter, where we found that addition of the PPAR-α agonist during differentiation did not increase the

expression of cardiac or mitochondrial oxidative metabolism genes. We deduced that changes could have been masked by variability in the differentiation between batches of cells, and/or that the beneficial effect of PPAR-α activation may have been lost due to the limited availability of fatty acid substrates in the culture medium. Beating hiPSC-CMs are routinely cultured in high-glucose media, which contains 1% of the cocktail of additives B27, both during differentiation and for as long as they stay in culture. The composition of commercial B27 is not disclosed but some groups report that they make an equivalent to B27 containing around 0.2 mM oleic acid, suggesting a final concentration of 2 μM. This low concentration of oleic acid might contribute to the slow maturation of hiPSC-CMs.

6.2.1 Maturation Methods of Human Induced Pluripotent Stem Cells Derived Cardiomyocytes

Even with all these protocols, differentiated cardiomyocytes were found to be immature[33–37]. Metabolically, hiPSC-CMs have fewer mitochondria that occupy only a small fraction of the cell volume, forming irregular reticular network in the cytoplasm, whereas, adult mature cardiomyocytes have regular mitochondrial networks that occupy ≈ 20 – 40% of the cell volume[33–37]. Therefore, the main energy substrate used in immature hiPSC-CMs is glucose, whereas adult mature cardiomyocytes depends more on fatty acid oxidation[33,34]. Table 6.1 shows studies where hESC and hiPSC-CMs have been matured over time and in general these papers measure expression of cardiac proteins and electrophysiological characteristics of hESC and hiPSC-CMs. Yang *et al*[212]matured hiPSC-CMs by the addition of the growth hormone tri-iodothyronine (T3) and showed morphological changes, increased contractile force and rates of calcium release. They measured mitochondrial

metabolism in a Seahorse Analyser and observed increased oxygen consumption in treated hiPSC-CM but only measured glucose oxidation. Others have reported that long-term culture increases activity of ETC complex I and II in hiPSC-CMs, but no oxidation data was reported[41].

Table 6.1: Maturation methods for human induced pluripotent stem cell-derived cardiomyocytes

Paper	Cell Model and Differentiation Protocol	Media	Maturation Method	Effect of Maturation Method
Yang *et al* (2013)[212]	hiPSC-CMs (>d20) differentiated using Activin A and BMP4	Serum-free RPMI-B27 + L-glutamine	• 20 ng/ml T3 for one week	• Increased cardiomyocyte size and sarcomere length • Increase in rates of calcium release and reuptake • Glucose Oxidation: increased in maximal mitochondrial respiratory capacity and RRC
Ivashchenko *et al* (2013)[40]	Purified (MYH6-enriched) – hiPSC-CMs (d30) from CD1	DMEM, sodium pyruvate, galactose, FBS, P/S	• Long-term culture (up to 80 days in culture)	• Increased gene expression (Cx43, Nav1.5, Cav1.2, and KiR2.1) • Increased ratio of MYH6/MYH7 • Electrophysiology Characteristics: [current of Na^+ and Ca^+ (L-type and T-type)-channels increase with time] • Increased expression of the sarcomeric calcium handling proteins (SERCA2A and RYR2)
			• Maturation Media (serum-free media, IMDM, with T3) • T3 100nM for 24 hours on d45 hiPSC-CMs	• Increased expression of MYH6

Lundy *et al* (2013)[39]	hESC-CMs and hiPSC-CMs differentiated using Activin A, BMP4	RPMI-B27 + L-glutamine	• Maturation Media on d20 hPSC-CMs (serum-free-RPMI-B27 + L-glutamine) • Only >75% ($cTnT^{+}$) cultures were used • Long-term culture • Early-stage hPSC-CMs (20-40 days in culture) • Late-stage hPSC-CMs (80-120 days in culture)	• Morphology: d20-40 hPSC-CMs [round and irregular subcellular organization and low myofibril density] and d80-120 hPSC-CMs [increase in length and high degree of myofibril density, alignment, and z-disk registration] • Contraction performance [increased contractile magnitude] • Increase in gene expression of MYH6 and MYH7 • $[Ca^{2+}]_i$- transient kinetics [increased maximal transient upstroke and decay velocities, reduction of time to peak and decay] • Action potential [increase in maximal upstroke velocity, more hyperpolarization maximal diastolic potential, and larger action potential amplitude] • Respond to adrenergic stimulation [increased spontaneous frequency, but reduction in contraction magnitude]

Dai *et al* (2017)[41]	hESC-CMs and hiPSC-CMs differentiated using Activin A, BMP4	RPMI-B27 + L-glutamine	• Maturation Media on d20 hPSC-CMs (serum-free-RPMI-B27 + L-glutamine) • Only >90% CMs were used • Purification for hESC-CMs – CMs expressing MCK7 • Early-stage hPSC-CMs (25-40 days in culture) • Late-stage hPSC-CMs (> 100 days in culture)	• Morphology [longer cell perimeter, larger cell area, more elongation and less circularity] • Increase in both Mitochondrial indicator (using MitoTracker Green FM) and Mitochondrial membrane potential (using TMRM dye) • Increase in mitochondria abundance, but not change in mitochondria size • Increase in citrate synthase and respiratory complex activity assays (when normalised to cell number-not protein)

BMP4: Bone morphogenetic protein 4, T3: Tri-iodothryonine, FBS: Fetal bovine serum, P/S: Penicillin/Streptomycin, Cx43: Connexin 43, Nav1.5: Sodium voltage-gated channel alpha subunit 5, Cav1.2: Calcium channel voltage-dependent L-type alpha 1c subunit, Kir2.1: inward-rectifier potassium ion-channel, MYH6: Myosin heavy chain 6, MYH7: Myosin heavy chain 7, SERCA2A: Sarco/endoplasmic reticulum Ca^{2+}-ATPase, RYR2: Ryanodine receptor 2, cTnT: Cardiac troponin T, MCK7: Muscle-specific muscle creatine kinase

6.2.2 Oleic Acid

Oleic acid (OA), is a monounsaturated fatty acid, which has been reported to activate PPAR-α[62,199–201,213,214] and thereby contribute to the metabolic shift from glycolysis to oxidative phosphorylation in the heart[61,62,148]. OA also has a protective role against inflammation and insulin resistance in tissues such as the heart, skeletal muscle, and neurons[213,215–218]. Plasma concentration of oleic acid ranges between 0.03 – 3.2 mmol/L in healthy young humans[219]. Culturing rat neonatal cardiomyocytes with OA in combination with palmitic acid for 48 hours caused an increase in the expression of FABP, FAT, ACS, LCAD, UCP2, and M-CPT1[168,174,175] and increased the rate of fatty acid oxidation[175]. In another study, culture of 1-day old rat cardiomyocytes with 500 µM OA for 90 hours induced a 4.5-fold increase in the expression of muscle-type CPTI[170]. Oleic acid also resulted in the reduction of GLUT4, HKII, and GAPDH expression[168,174,175]. In addition, OA has been shown to upregulate the expression of PDK4 in muscle cells[220].

6.3 Aims of Chapter

The aims of this chapter were to promote metabolic maturation of already differentiated and beating hiPSC-CMs by addition the fatty acid, oleic acid, to the culture media, with or without the pharmacological PPAR-α activator (WY14643).

This chapter investigates:

1. The addition of fatty acid (oleic acid) to the culturing media of beating hiPSC-CMs, to fit with the metabolic shift that occurs during heart development
2. Activating PPAR-α using natural (oleic acid) and synthetic (WY14643) ligands for 8 and 24 hours

3. The effect of oleic acid and WY14643 treatment on the activation of PPAR-α in beating hiPSC-CMs, by measuring the relative gene expression of PPAR-α target genes (*UCP3* and *PDK4*)
4. The effect of oleic acid and WY14643 treatment on fatty acid oxidation in beating hiPSC-CMs, by measuring the relative gene expression of enzymes involved in fatty acid uptake and oxidation (*CD36*, *ACSL1*, *CPT1B*, *ACADM*, *HADHA*, and *ECI1*) and measuring the oxygen consumption rate of cells while respiring on oleic acid.
5. The effect of oleic acid and WY14643 treatment on glycolysis and pyruvate oxidation in beating hiPSC-CMs, by measuring the relative gene expression of (*GLUT1*, *GLUT4*, *PFKM*, *PDHA1*, and *PDK4*), measuring extracellular glucose consumption and lactate production, measuring glycolytic flux, and measuring the oxygen consumption rate of cells while respiring on pyruvate and malate
6. The effect of long-term treatment (1 week) of oleic acid and WY14643 on the metabolic shift of beating hiPSC-CMs, by measuring the relative gene expression of fatty acid and glucose metabolism markers and measuring glycolytic flux.

6.4 Materials and Methods

6.4.1 Differentiation of Human Induced Pluripotent Stem Cells into Beating Cardiomyocytes

HiPSCs were differentiated into beating cardiomyocytes using the Wnt-modulation protocol with the alterations introduced in previous chapters (Figure 6.1). Under this protocol, hiPSC-CMs normally start to spontaneously beat on day 11 – 12 of differentiation. On day 15 of differentiation, beating hiPSC-CMs were either treated with 400 µM oleic acid (OA) alone or

in combination with 120 µM WY14643 for 24 hours (Figure 6.1). Untreated beating hiPSC-CMs were used as control group.

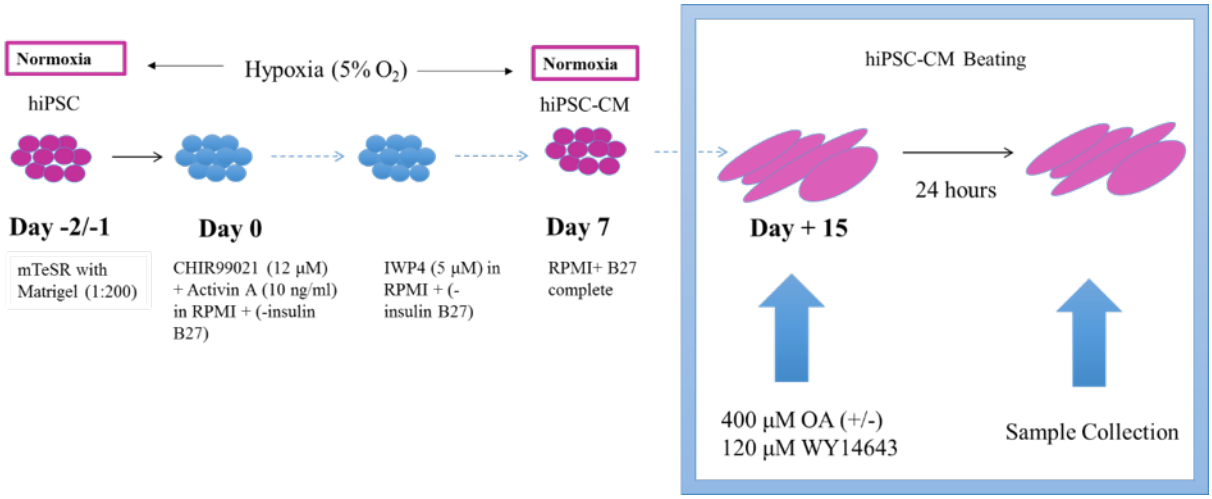


Figure 6.1: Timeline of hiPSCs differentiation to beating hiPSC-CMs using the altered Wnt-modulation protocol.

6.4.2 Oleic Acid Treatment

Oleic acid was purchased already conjugated to albumin (Sigma). Immature beating hiPSC-CMs were treated with 400 µM oleic acid on day 15 of the differentiation. For the 8 and 24 hours treatments, oleic acid was added to the RPMI+B27 media. For long term treatment (1 week), oleic acid was added to RPMI+B27 every time the media was changed.

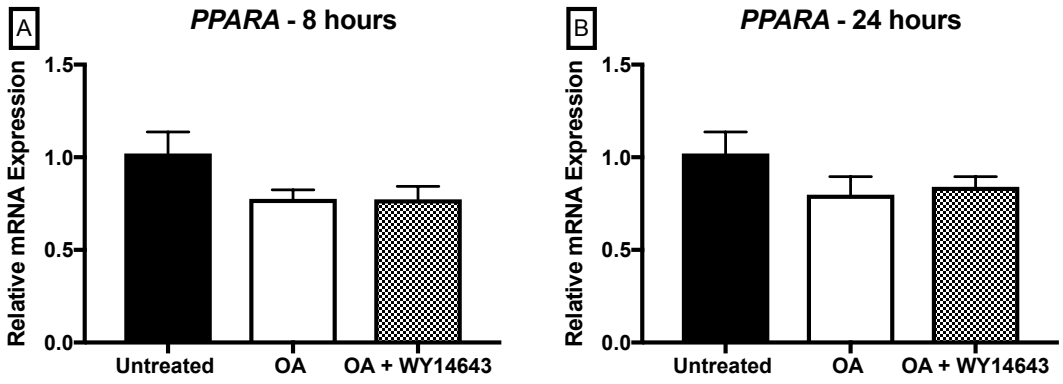
6.4.3 WY14643 Treatment

WY14643 treatment on immature beating hiPSC-CMs was used at a concentration of 120 µM and it was added in combination with 400 µM oleic acid into the RPMI+B27 culturing media at day 15 of the differentiation. For long term treatment (1 week), WY14643 was added in combination with 400 µM oleic acid to the RPMI+B27 media every time the media was changed.

6.5 Results

6.5.1 Effect of OA alone or OA and WY14643 Treatment on the Activation of PPAR-α in Beating hiPSC-CMs by Measuring the Relative Gene Expression of *PPARA*, *PGC1A*, *UCP3*, and *PDK4*

The relative gene expression of *PPARA*, *PGC1A, UCP3,* and *PDK4* were measured following 8 and 24 hours of treatment. There was no significant difference in the relative mRNA expression of *PPARA* after 8 nor 24 hours of treatment (Figure 6.2 A-B). There was no significant difference in the relative mRNA expression of *PGC1A* between treated and untreated beating hiPSC-CMs (Figure 6.2 A-B). Expression of *UCP3*, a PPAR-α target gene, showed no significant difference between treated and untreated hiPSC-CMs at either time point (Figure 6.3 A-B), however the expression of *PDK4* gene, another important PPAR-α target gene, was significantly upregulated in each treated group compared with untreated hiPSC-CMs (Figure 6.4 A-B). In addition, treatment with OA + WY14643 upregulated *PDK4* significantly compared with OA alone at both time points (Figure 6.4 A-B). Treatment for 24 hours upregulated PDK4 to a greater extent than 8 hours for both OA alone ($p = 0.03$) and OA + WY14643 ($p < 0.0001$). Although, gene expression of *PPARA* was not upregulated in treated hiPSC-CMs, the increased expression of *PDK4* indicated that OA alone or in combination with WY14643 activated PPAR-α in a time-dependent manner.



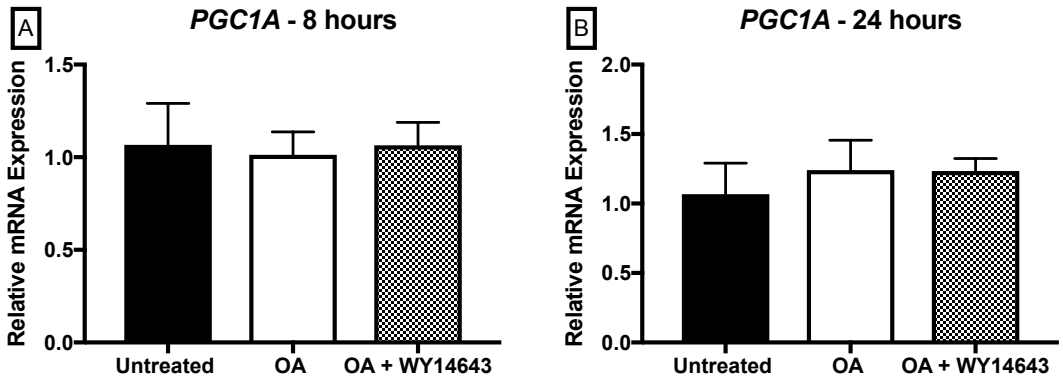


Figure 6.2: The relative mRNA expression of *PPARA* and *PGC1A* using qRT-PCR. Immature beating hiPSC-CMs were treated with 400 μM oleic acid (OA) alone or in combination with 120 μM WY14643 for (A) 8 hours or (B) 24 hours. Untreated beating hiPSC-CMs were used as control. Abbreviations: OA: Oleic acid; PPARA: Peroxisome proliferator-activated receptor alpha; PGC1A: Peroxisome proliferator-activated receptor gamma coactivator 1-alpha. Data are presented as mean ± SEM, and analysed using a one-way ANOVA with Tukey post hoc test (n=4).

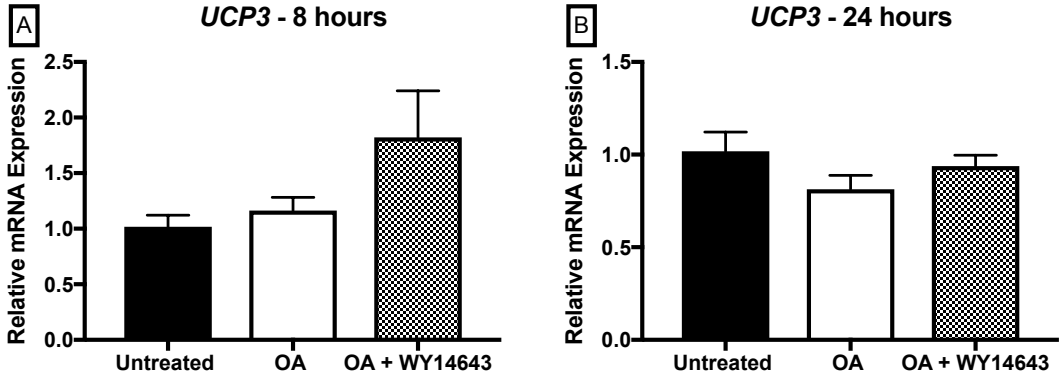


Figure 6.3: The relative mRNA expression of *UCP3* using qRT-PCR. Immature beating hiPSC-CMs were treated with 400 μM oleic acid (OA) alone or in combination with 120 μM WY14643 for (A) 8 hours or (B) 24 hours. Untreated beating hiPSC-CMs were used as control. Abbreviations: OA: Oleic acid; UCP3: Uncoupling protein 3. Data are presented as mean ± SEM, and analysed using a one-way ANOVA with Tukey post hoc test (n=4).

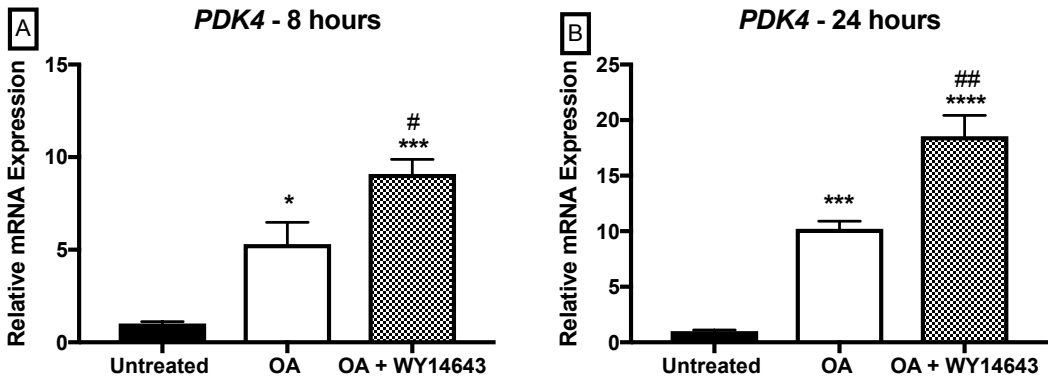


Figure 6.4: The relative mRNA expression of *PDK4* using qRT-PCR. Immature beating hiPSC-CMs were treated with 400 µM oleic acid (OA) alone or in combination with 120 µM WY14643 for (A) 8 hours or (B) 24 hours. Untreated beating hiPSC-CMs were used as control. Abbreviations: OA: Oleic acid; *PDK4*: Pyruvate dehydrogenase kinase 4. Data are presented as mean ± SEM, and analysed using a one-way ANOVA with Tukey post hoc test. P value ≤ 0.05 (*), ≤ 0.001 (***), and ≤ 0.0001 (****) compared with untreated beating hiPSC-CMs. P value ≤ 0.05 (#) and ≤ 0.0001 (##) comparing OA + WY14643 with OA treated hiPSC-CMs (n=4).

6.5.2 Effect of OA alone or OA and WY14643 Treatment on Fatty Acid Oxidation in Beating hiPSC-CMs

6.5.2.1 Relative Gene Expression of Genes Involved in Fatty Acid Oxidation

The expression levels of enzymes involved in fatty acid oxidation, *CD36*, *ACSL*, *CPT1B*, and *MCAD*, which are known to be upregulated by PPAR-α activation were measured. There was no significant difference in the relative mRNA expression of *CD36* and *ACSL1* after 8 hours of either treatment (Figure 6.5A and 6.6A) but treatment with OA + WY14643 for 8 hours significantly upregulated the expression of *CPT1B* when compared to untreated beating hiPSC-CMs, by 2-fold ($p \leq 0.05$) (Figure 6.7A). Treatment with both OA alone and OA + WY14643 also upregulated the expression of *ACADM* at 8 hours (Figure 6.8A). Treatment with OA + WY14643 for 24 hours showed no difference in the expression of FAO genes, whereas there was a small downregulation in the expression of *ACSL1* (Figure 6.6B) and *ACADM* (Figure 6.8B) in OA treated hiPSC-CMs compared to untreated hiPSC-CMs. There was no difference

in the relative mRNA expression of *HADHA* between treated and untreated hiPSC-CMs at any time point (Figure 6.8C-D).

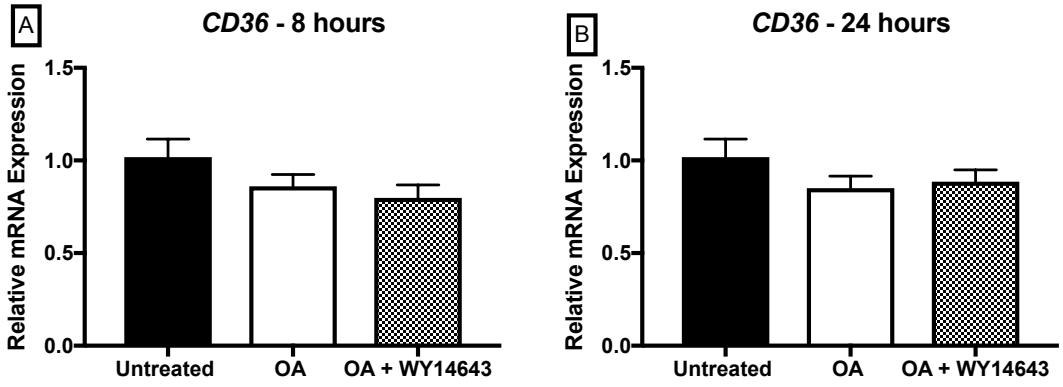


Figure 6.5: The relative mRNA expression of *CD36* using qRT-PCR. Immature beating hiPSC-CMs were treated with 400 µM oleic acid (OA) alone or in combination with 120 µM WY14643 for (A) 8 hours or (B) 24 hours. Untreated beating hiPSC-CMs were used as control for treated groups. Abbreviations: OA: Oleic acid. Data are presented as mean ± SEM, and analysed using a one-way ANOVA with Tukey post hoc test (n=4).

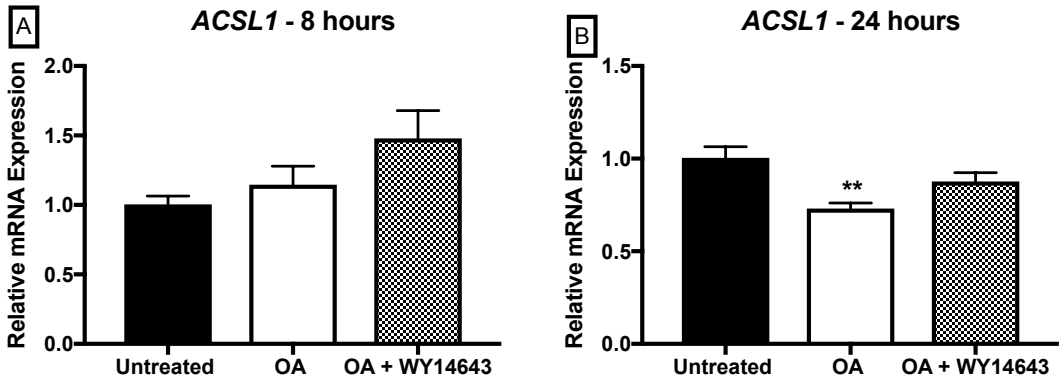


Figure 6.6: The relative mRNA expression of *ACSL1* using qRT-PCR. Immature beating hiPSC-CMs were treated with 400 µM oleic acid (OA) alone or in combination with 120 µM WY14643 for (A) 8 hours or (B) 24 hours. Untreated beating hiPSC-CMs were used as control. Abbreviations: OA: Oleic acid; *ACSL1*: Acyl CoA synthetase long-chain. Data are presented as mean ± SEM, and analysed using a one-way ANOVA with Tukey post hoc test. P value ≤ 0.01 (**) compared to untreated beating hiPSC-CMs (n=4).

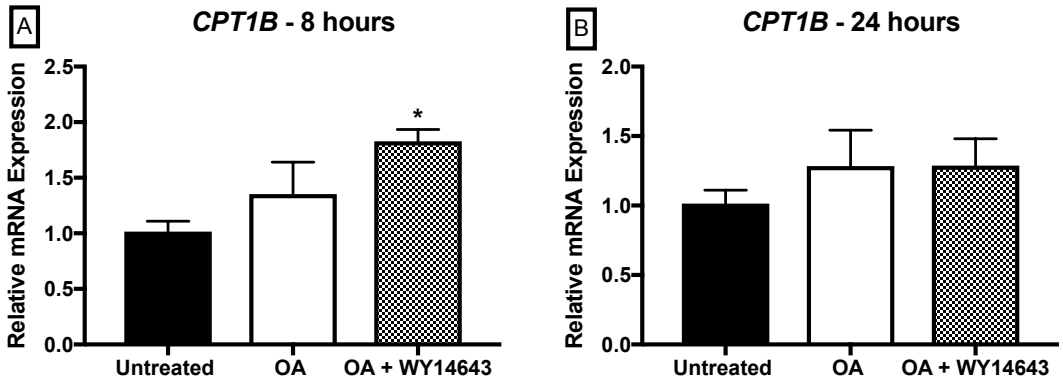


Figure 6.7: The relative mRNA expression of *CPT1B* using qRT-PCR. Immature beating hiPSC-CMs were treated with 400 µM oleic acid (OA) alone or in combination with 120 µM WY14643 for (A) 8 hours or (B) 24 hours. Untreated beating hiPSC-CMs were used as control. Abbreviations: OA: Oleic acid; *CPT1B*: Carnitine palmitoyltransferase 1B (muscle-type). Data are presented as mean ± SEM, and analysed using a one-way ANOVA with Tukey post hoc test. P value = 0.03 (*) compared with untreated beating hiPSC-CMs (n=4).

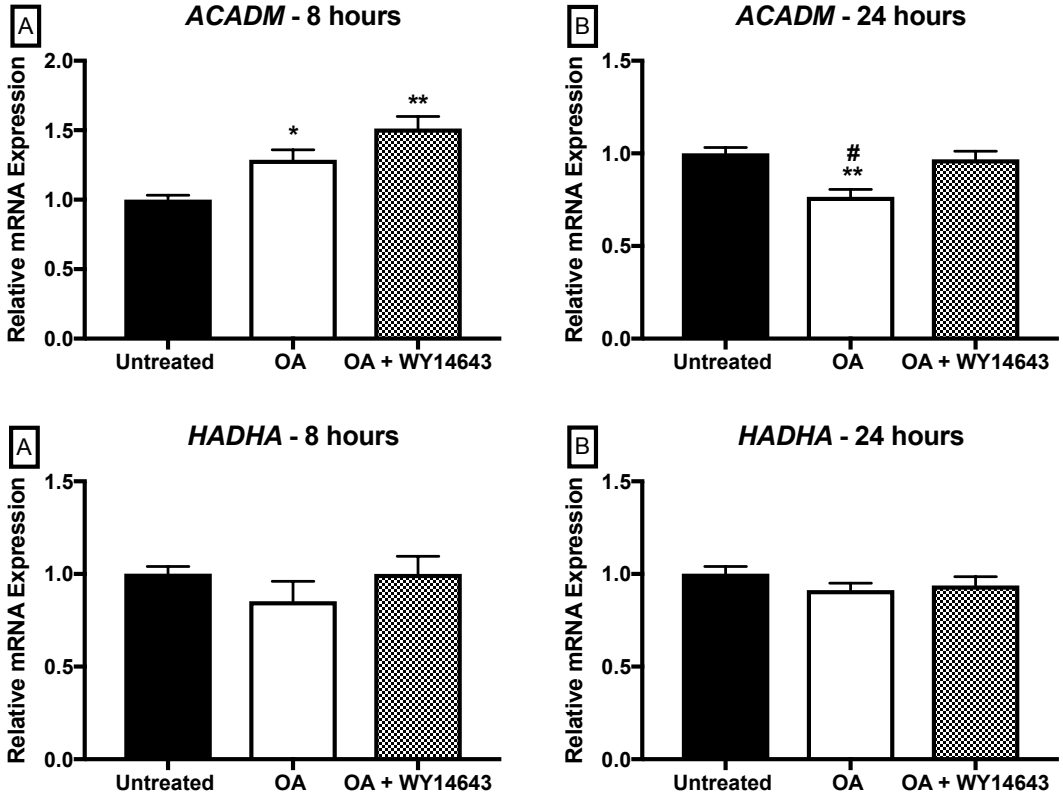


Figure 6.8: The relative mRNA expression of *ACADM* and *HADHA* using qRT-PCR. Immature beating hiPSC-CMs were treated with 400 µM oleic acid (OA) alone or in combination with 120 µM WY14643 for (A) 8 hours or (B) 24 hours. Untreated beating hiPSC-CMs were used as control. Abbreviations: OA: Oleic acid; *ACADM*: Acyl-CoA dehydrogenase medium-chain specific; *HADHA*: Hydroxyacyl-CoA dehydrogenase, alpha subunit. Data are presented as mean ± SEM, and analysed using a one-way ANOVA with Tukey post hoc test.

P value ≤ 0.05 (*) and ≤ 0.01 (**) compared with untreated beating hiPSC-CMs. P value = 0.01 (#) comparing OA with OA + WY14643 treated hiPSC-CMs (n=4).

Oleic acid is an unsaturated fatty acid, therefore, the relative gene expression of enoyl CoA isomerase (*ECI*) was measured and data showed that *ECI1* was upregulated only when WY14643 was combined with OA for both 8 (Figure 6.9A) and 24 hours (Figure 6.9B).

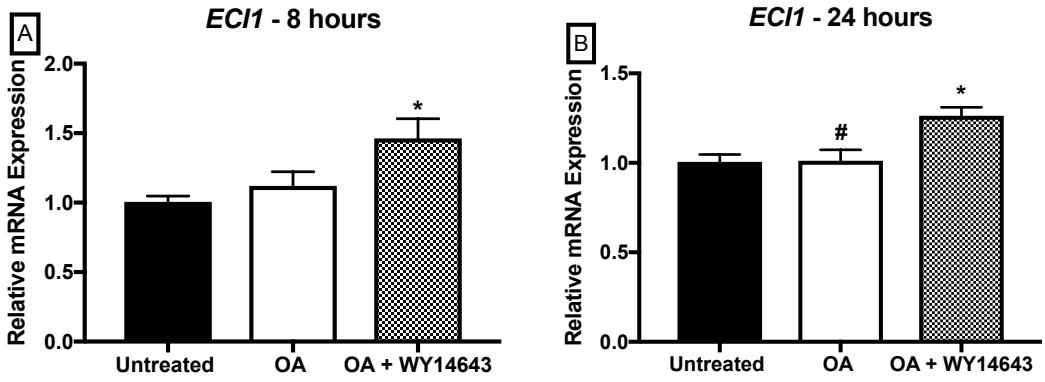


Figure 6.9: The relative mRNA expression of *ECI1* using qRT-PCR. Immature beating hiPSC-CMs were treated with 400µM oleic acid (OA) alone or in combination with 120µM WY14643 for (A) 8 hours or (B) 24 hours. Untreated beating hiPSC-CMs were used as control. Abbreviations: OA: Oleic acid; *ECI1*: Enoyl CoA isomerase 1. Data are presented as mean ± SEM, and were analysed using a one-way ANOVA with Tukey post hoc test. P value ≤ 0.05 (*) compared with untreated hiPSC-CMs. P value = 0.02 (#) comparing OA + WY14643 with OA treated hiPSC-CMs (n=4).

6.5.2.2 Fatty Acid Metabolism in OA alone or OA and WY14643 Pre-Treated Beating Human Induced Pluripotent Stem Cells-Derived Cardiomyocytes using the Clark-Type Oxygen Electrode

The rate of oxygen consumption (OCR) was measured in beating hiPSC-CMs pre-treated for 24 hours, while respiring on 400 µM oleic acid. OCR was measured at baseline, after oligomycin treatment, and maximal respiration (after FCCP treatment). There was no difference in the rate of O_2 consumption at baseline or with oligomycin, between treated and untreated hiPSC-CMs (Figure 6.10). Comparing OCR at maximal respiration (FCCP) between treated and untreated hiPSC-CMs, OCR was significantly higher in 400 µM OA + 120 µM

WY14643 pre-treated hiPSC-CMs compared with untreated and OA pre-treated hiPSC-CMs (Figure 6.10).

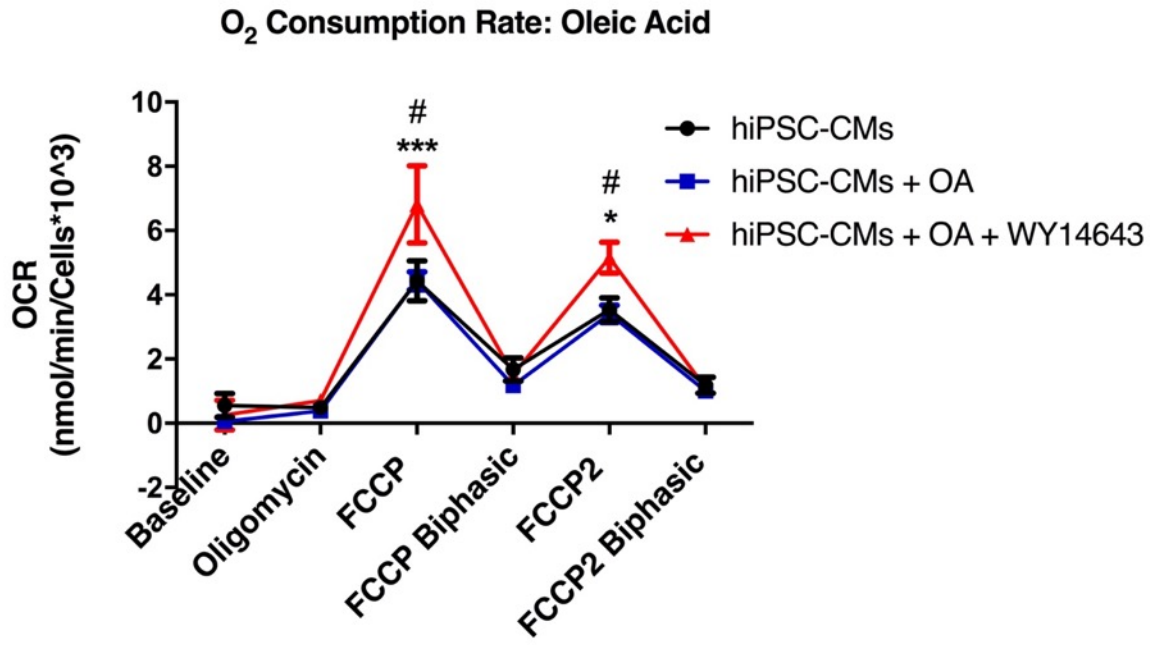


Figure 6.10: O_2 consumption rate (OCR) using the Clark-type oxygen electrode. Immature beating hiPSC-CMs were pre-treated with 400 μM oleic acid (OA) alone (blue line) or in combination with 120 μM WY-14643 (red line) for 24 hours. Untreated beating hiPSC-CMs (black line) were used as control. Two million cells from each group were used for each run and they were supplement with 400 μM OA as the respiring substrate. OCR was measured at baseline, after oligomycin treatment, at maximal respiration, and after allowing cells to rest from FCCP treatment. FCCP treatment was applied twice. Data are presented as mean ± SEM, and analysed using a one-way ANOVA with Tukey post hoc test. P value ≤ 0.05 (*) and ≤ 0.001 (***) compared with untreated hiPSC-CMs. P value ≤ 0.05 (#) compared with OA pre-treated hiPSC-CMs (n=4).

Reserve Respiratory Capacity (RRC) was determined by subtracting OCR of maximal respiration from baseline respiration while cells were respiring on 400 μM oleic acid. Our data showed that there was no difference in RRC between OA pre-treated hiPSC-CMs and untreated hiPSC-CMs (Figure 6.11). However, 24 hours treatment with OA + WY14643 was sufficient to increase the RRC of hiPSC-CMs by 2-fold compared to untreated hiPSC-CMs (Figure 6.11).

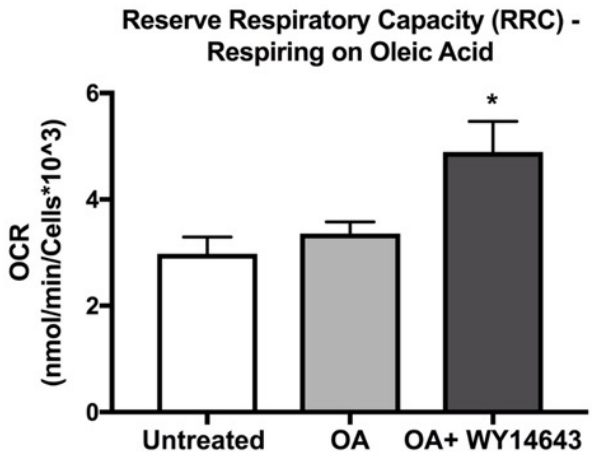


Figure 6.11: Reserve respiratory capacity (RRC) during oleic acid respiration on pre-treated hiPSC-CMs. RRC was calculated as the difference of maximal respiration to baseline respiration in 400 µM OA ± 120 µM WY-14643 pre-treated hiPSC-CMs respiring on oleic acid. Untreated hiPSC-CMs were used as control. Data are presented as mean ± SEM and analysed using a one-way ANOVA with Tukey post doc test. P value ≤ 0.05 (*) comparing OA + WY14643 with untreated hiPSC-CMs (n=4).

6.5.3 Effect of OA alone or OA and WY14643 Treatment on Glucose Metabolism

6.5.3.1 Relative Gene Expression of Genes Involved in Glucose Utilization

The relative gene expression of glucose transporter *GLUT1* was measured after 8 hours of treatment and our data showed no significant difference in the expression between treated and untreated hiPSC-CMs (Figure 6.12A), However OA alone or in combination with WY14643 significantly downregulated the expression of *GLUT4* by around 50% (Figure 6.12A). After 24 hours of treatment, the expression of *GLUT1* was downregulated in OA alone treated hiPSC-CMs when compared to OA + WY14643 treated hiPSC-CMs (Figure 6.12B) whereas, the expression of *GLUT4* in treated hiPSC-CMs returned to levels similar to those in untreated hiPSC-CMs (Figure 6.12B).

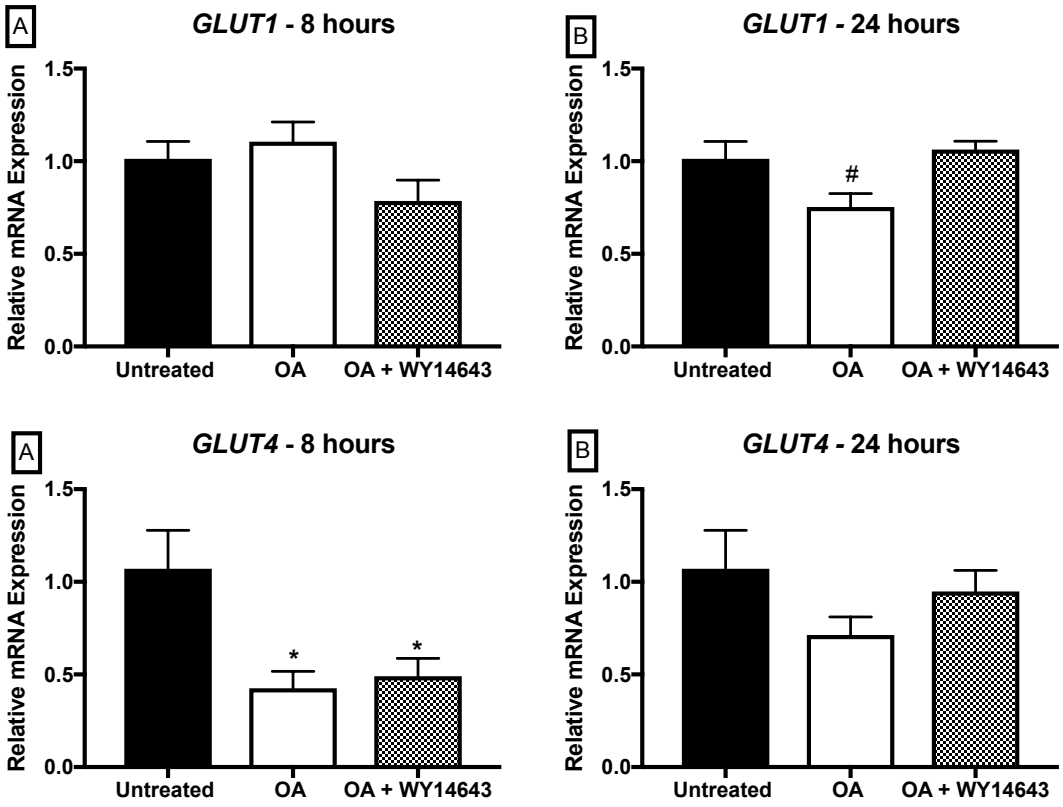


Figure 6.12: The relative mRNA expression of *GLUT1* and *GLUT4* using qRT-PCR. Immature beating hiPSC-CMs were treated with 400 μM oleic acid (OA) alone or in combination with 120 μM WY14643 for (A) 8 hours or (B) 24 hours. Untreated beating hiPSC-CMs were used as control. Abbreviations: OA: Oleic acid. Data are presented as mean ± SEM, and were analysed using a one-way ANOVA with (Tukey post doc) test. P-value ≤ 0.05 (*) compared with untreated hiPSC-CMs. P-value ≤ 0.05 (#) comparing OA treated hiPSC-CMs with OA + WY14643 treated hiPSC-CMs (n=4).

Phosphofructokinase, muscle-type *(PFKM*), an enzyme that catalyses a rate-limiting, irreversible step in glycolysis was measured. Our data showed that OA alone or in combination with WY14643 for 8 hours significantly downregulated the expression of *PFKM* in hiPSC-CMs (Figure 6.13A-B). In addition, after 24 hours OA treatment showed significant downregulation in *PFKM* expression compared with untreated hiPSC-CMs.

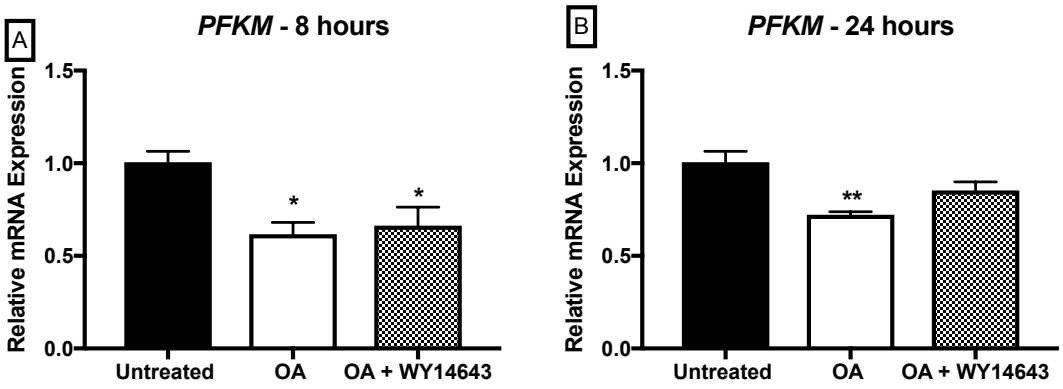
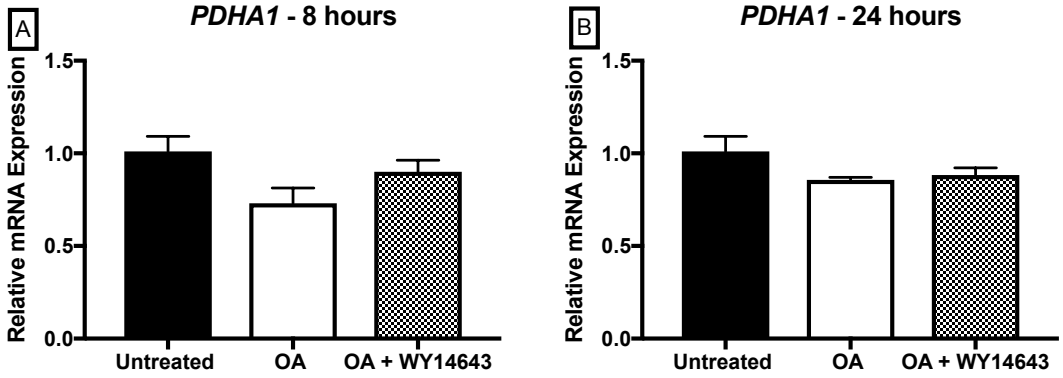


Figure 6.13: The relative mRNA expression of *PFKM* using qRT-PCR. Immature beating hiPSC-CMs were treated with 400 µM oleic acid (OA) alone or in combination with 120 µM WY14643 for (A) 8 hours or (B) 24 hours. Untreated beating hiPSC-CMs were used as control. Abbreviations: OA: Oleic acid; *PFKM*: Phosphofructokinase, muscle-type. Data are presented as mean ± SEM, and analysed using a one-way ANOVA with Tukey post doc test. P value ≤ 0.05 (*) and ≤ 0.01 (**) compared with untreated controls (n=4).

Pyruvate fate is regulated by the enzyme pyruvate dehydrogenase (PDH), which itself is regulated by PDH kinase (PDK) and PDH phosphatase (PDP). The relative gene expression of both *PDHA1* and *PDK4* were measured. Our data showed that neither 8 hours nor 24 hours of OA +/- WY14643 treatment had an effect on the expression of *PDHA1* (Figure 6.17 A-B). The relative gene expression of *PDK4* was upregulated 5- and 10-fold in hiPSC-CMs treated with 400 µM OA alone or in combination with 120 µM WY14643 for 8 hours, respectively, and 12- and 20-fold after treatment for 24 hours, respectively (Figure 6.17 A-B).



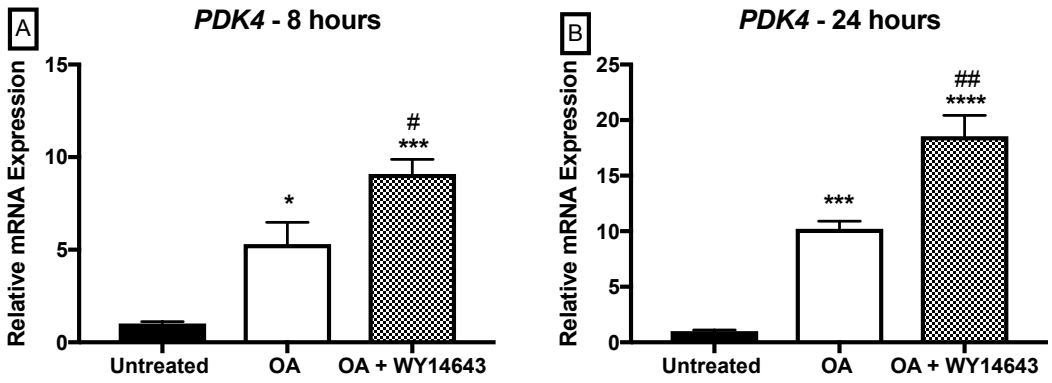


Figure 6.17: The relative mRNA expression of *PDHA1* and *PDK4* using qRT-PCR. Immature beating hiPSC-CMs were treated with 400 µM oleic acid (OA) alone or in combination with 120 µM WY14643 for (A) 8 hours or (B) 24 hours. Untreated beating hiPSC-CMs were used as control. Abbreviations: OA: Oleic acid; *PDHA1*: Pyruvate dehydrogenase type A1; *PDK4*: Pyruvate dehydrogenase kinase 4. Data are presented as mean ± SEM, and analysed using a one-way ANOVA with Tukey post doc test. P-value ≤ 0.05 (*), ≤ 0.01 (**), ≤ 0.001 (***), and ≤ 0.0001 (****) compared with untreated hiPSC-CMs. P-value ≤ 0.05 (#), and ≤ 0.01 (##) comparing OA + WY14643 treated with OA treated hiPSC-CMs (n=4).

6.5.3.2 Extracellular Glucose Consumption and Lactate Production

Glycolysis yields two molecules of pyruvate, which can be converted to either lactate or acetyl CoA. In this experiment, immature beating hiPSC-CMs were pre-treated with 400 µM OA alone or in combination with 120 µM WY14643 for 24 hours. After 24 hours incubation, culturing media were collected for the measurement of extracellular glucose and lactate. A ratio of glucose consumption to lactate production that equals two was used as an indicator of exclusively anaerobic glycolysis, whereas, a ratio less than two was used as an indicator of some utilisation of pyruvate in oxidative metabolism. Our data showed that there was no significant difference in the amount of glucose consumed (Figure 6.18A) and lactate produced (Figure 6.18B) between treated and untreated beating hiPSC-CMs. However, the ratio of glucose consumed to lactate produced showed that during 24 hours treatment with OA, less glucose was converted to lactate (Figure 6.19), suggesting an increase in glucose oxidation.

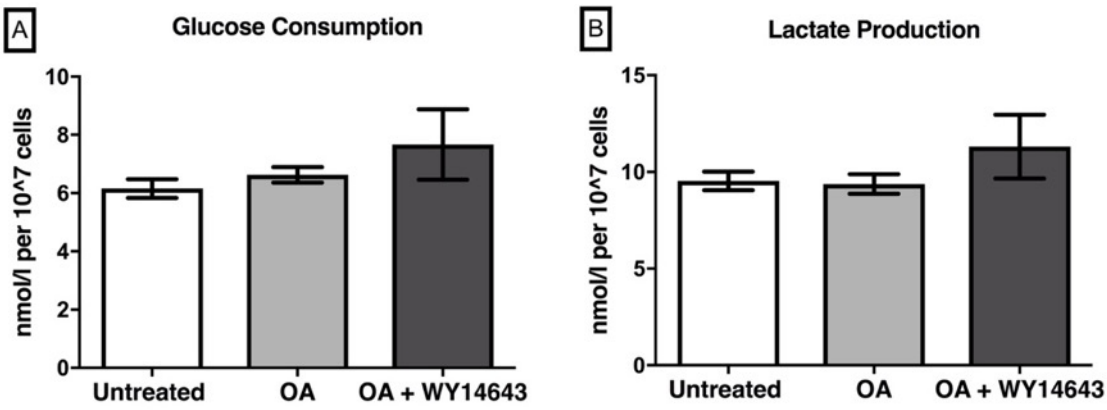


Figure 6.18: Glucose consumption and lactate production in beating hiPSC-CMs. Immature beating hiPSC-CMs were pre-treated with 400 µM OA alone or in combination with 120 µM WY14643 for 24 hours. After 24 hours of incubation, culturing media were collected for measurement of extracellular (A) glucose and (B) lactate. Untreated hiPSC-CMs were used as control. Data are presented as mean ± SEM, and analysed using a one-way ANOVA with Tukey post doc test (n=3).

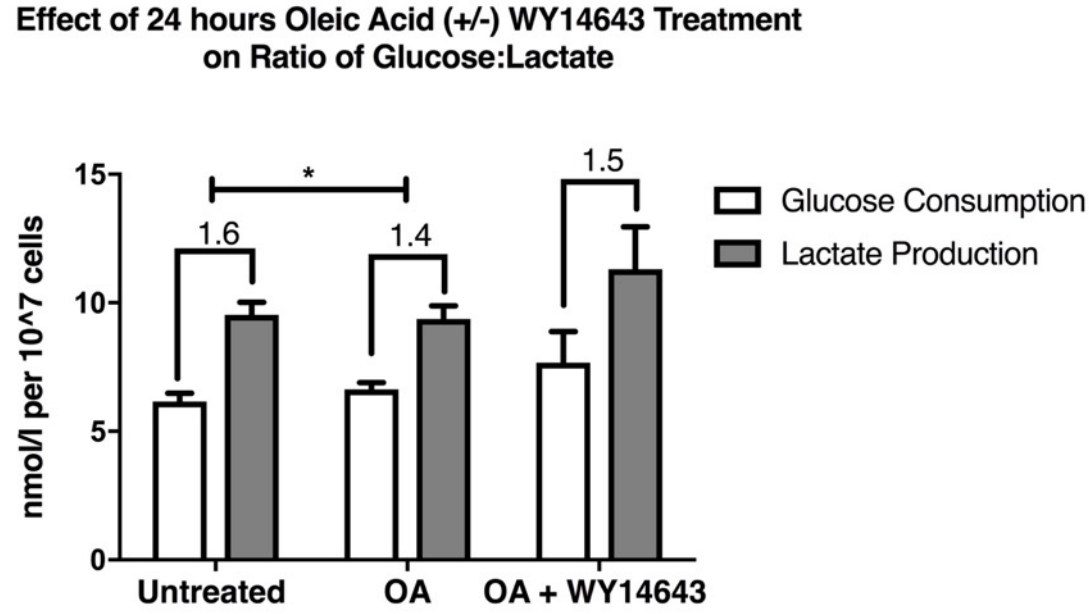


Figure 6.19: Ratio of glucose consumption to lactate production in beating hiPSC-CMs. Immature beating hiPSC-CMs were pre-treated with 400 µM OA alone or in combination with 120 µM WY14643 for 24 hours. After 24 hours of incubation, culturing media were collected for measurement of extracellular glucose and lactate. Ratio of glucose consumption to lactate production equal 2 represent anaerobic glycolysis, whereas, ratio less than 2 represent oxidation. Untreated hiPSC-CMs were used as control. Data are presented as mean ± SEM, and analysed using a one-way ANOVA with Tukey post doc test. P-value ≤ 0.05 (*) comparing OA pre-treated hiPSC-CMs with untreated hiPSC-CMs (n=3).

6.5.3.3 Glycolytic Flux Measurement via in Vitro ^{3}H-Glucose Utilization

Immature beating hiPSC-CMs were pre-treated with 400 µM OA alone or in combination with 120 µM WY14643 for 24 hours. Untreated and pre-treated beating hiPSC-CMs were cultured with fresh media containing 0.00148 MBq of [5-^{3}H]-glucose per well of a 6-well plate to measure glycolytic rates. Our data showed that 24 hours of OA ± WY14643 treatment had no effect on glycolytic rates (Figure 6.20).

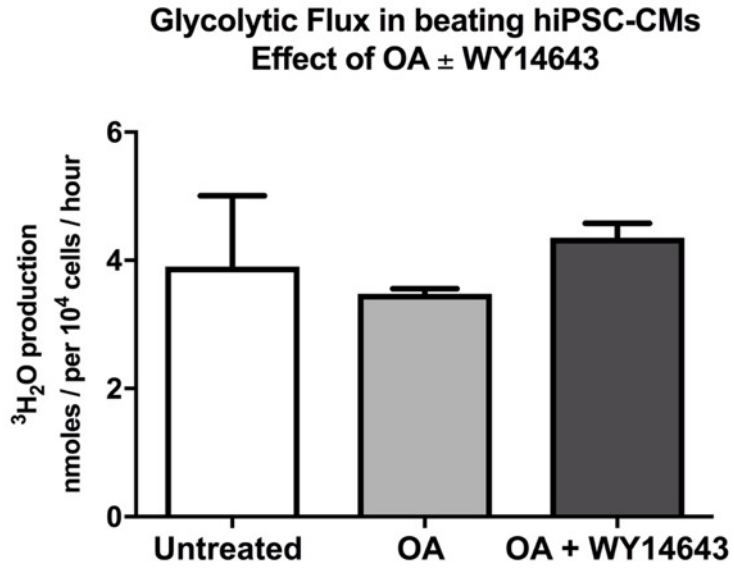


Figure 6.20: Glycolytic flux in beating hiPSC-CMs pre-treated for 24 hours with OA ± WY14643. Immature beating hiPSC-CMs were pre-treated with 400 µM OA ± 120 µM WY14643 for 24 hours. After 24 hours, beating hiPSC-CMs were cultured with fresh media containing 0.00148 MBq of [5-^{3}H]-glucose supplemented with 400 µM OA ± 120 µM WY14643 for 8 hours. Untreated beating hiPSC-CMs were cultured with fresh media (RPMI + B27) containing 0.00148 MBq of [5-^{3}H]-glucose and used as control. Data are presented as mean ± SEM, and were analysed using a one-way ANOVA with Tukey post doc test (n=3).

6.5.3.4 Pyruvate Oxidation in Pre-Treated Beating Cardiomyocytes

Immature beating hiPSC-CMs were pre-treated with 400 µM OA alone or in combination with 120 µM WY14643 for 24 hours. Two million hiPSC-CMs from each group were used to measure the oxygen consumption rate (OCR) while respiring on pyruvate and malate. Our data showed that OCR at maximal respiration of OA pre-treated hiPSC-CMs was significantly

higher than untreated and OA + WY14643 pre-treated hiPSC-CMs (Figure 6.21). However, there was no difference in the RRC between treated and untreated hiPSC-CMs while respiring on pyruvate and malate (Figure 6.22).

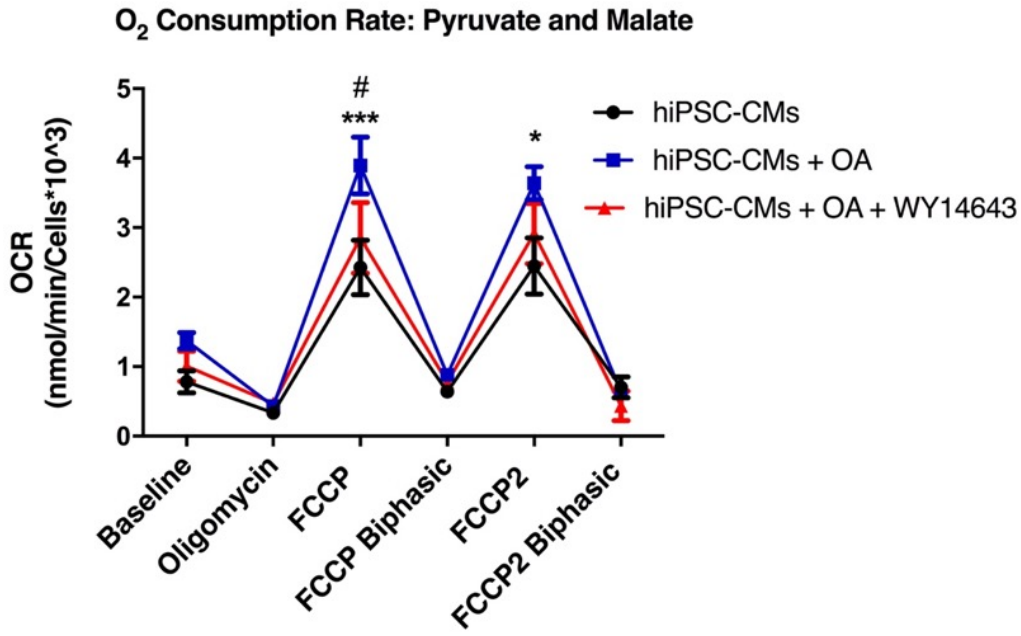


Figure 6.21: O_2 consumption rate (OCR) using the Clark-type oxygen electrode. Young beating hiPSC-CMs were pre-treated with 400 µM oleic acid (OA) alone (blue line) or in combination with 120 µM WY-14643 (red line) for 24 hours. Untreated beating hiPSC-CMs (black line) were used as control. After 24 hours of treatment, cells were dissociated and counted. Two million cells were used for each run and they were supplement with 10 mM pyruvate and 5 mM malate as the respiring substrates. OCR was measured at baseline, after oligomycin treatment, at maximal respiration, and after allowing cells to rest from FCCP treatment. FCCP treatment was applied twice. Data are presented as mean ± SEM, and analysed using a one-way ANOVA with Tukey post hoc test. P value ≤ 0.05 (*) and ≤ 0.001 (***) compared with untreated controls. P value ≤ 0.05 (#) compared with OA + WY14643 pre-treated hiPSC-CMs (n=4).

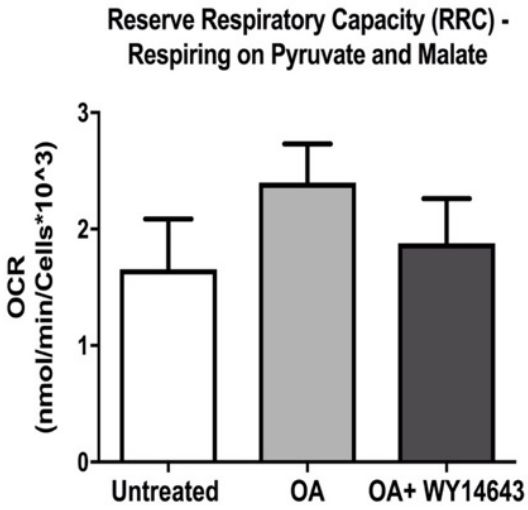


Figure 6.22: Reserve respiratory capacity (RRC) during pyruvate and malate respiration on pre-treated hiPSC-CMs. RRC was calculated as the difference of maximal respiration to baseline respiration in 400 µM OA ± 120 µM WY-14643 pre-treated hiPSC-CMs respiring on pyruvate and malate. Untreated hiPSC-CMs were used as control. Data are presented as mean ± SEM and analysed using a one-way ANOVA with Tukey post doc test (n=4).

6.5.4 Effect of Long-term Treatment with OA alone or OA and WY14643 on Metabolism in Beating Human Induced Pluripotent Stem Cells-Derived Cardiomyocytes

Immature beating hiPSC-CMs were pre-treated with 400 µM OA alone and 400 µM OA + 120 µM WY14643 for 1 week (long-term) to check the effect of treatment on metabolism. For 1 week treatment, fresh OA and OA + WY14643 were added every time the media was changed. Media was changed routinely every 2 days.

6.5.4.1 Effect of Long-term Treatment on Fatty Acid Metabolic Gene Expression

6.5.4.1.1 Relative Gene Expression of *CD36* and *ACSL1*

Long-term 400 µM OA and 400 µM OA + 120 µM WY14643 treatment had no significant effect on the relative expression of the fatty acid transporter (*CD36*) (Figure 6.23A). In

addition, no change was reported in the expression of *ASCL1* after 1 week of either treatment (Figure 6.23B).

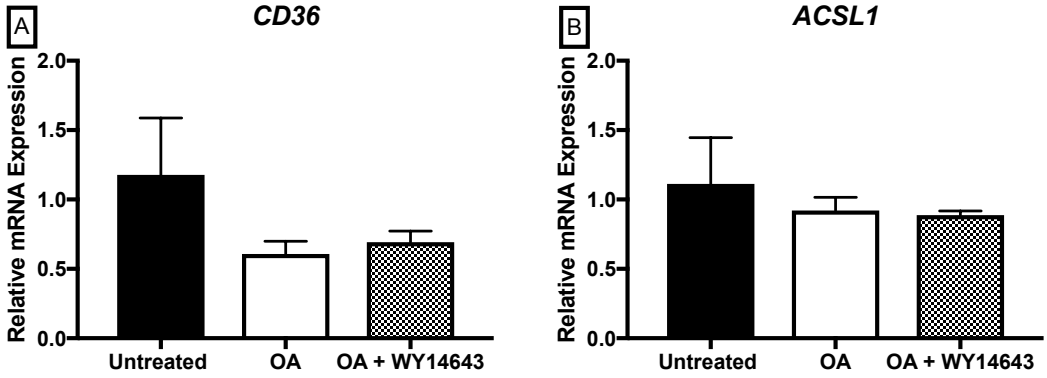
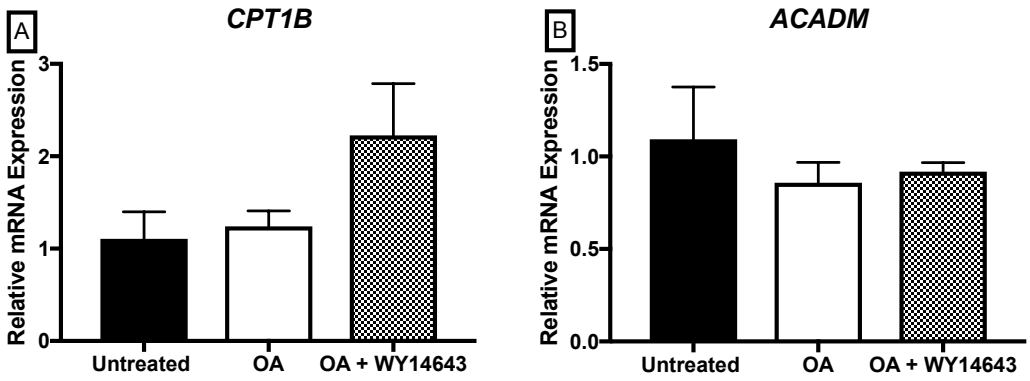


Figure 6.23: The relative mRNA expression of *CD36* and *ACSL1* using qRT-PCR. Immature beating hiPSC-CMs were treated with 400µM oleic acid (OA) alone or in combination with 120 µM WY14643 for 1 week. Untreated hiPSC-CMs were used as control. Abbreviations: OA: Oleic acid; ACSL1: Acyl CoA synthetase long-chain. Data are presented as mean ± SEM, and were analysed using a one-way ANOVA with Tukey post hoc test. P-value ≤ 0.05 (*) and ≤ 0.01 (**) compared with untreated hiPSC-CMs (n=4). Data was collected with the help of Colleen Lopez.

6.5.4.1.2 Relative Gene Expression of *CPT1B*, *MCAD*, *HADHA* and *ECI1*

One week treatment with 400 µM OA or 400 µM OA + 120 µM WY14643 did not increase the expression of *CPT1B*, *ACADM*, and *HADHA* (Figure 6.24A-C). In addition, 400 µM OA +/- 120µM WY14643 for 1 week had no effect on the expression of *ECI1* (Figure 2.24D).



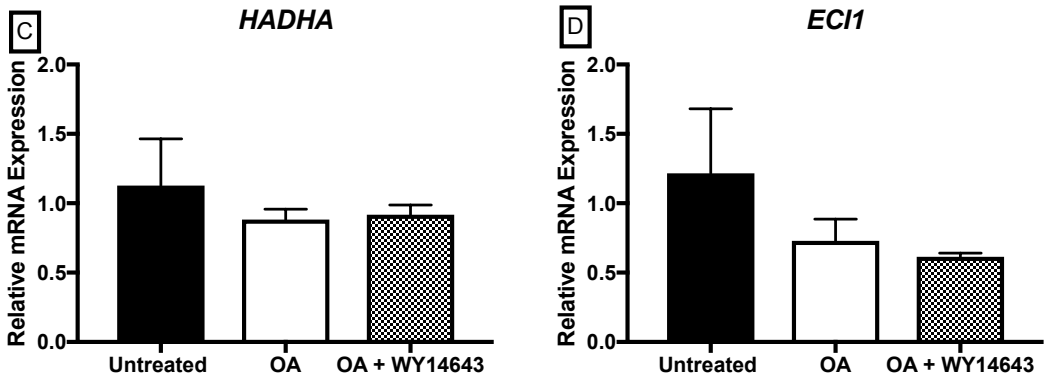


Figure 6.24: The relative mRNA expression of *CPT1B, ACADM, HADHA,* and *ECI1* using qRT-PCR. Immature beating hiPSC-CMs were treated with 400 µM oleic acid (OA) alone or in combination with 120 µM WY14643 for 1 week. Untreated hiPSC-CMs were used as control. Abbreviations: OA: Oleic acid; CPT1B: Carnitine palmitoyltransferase 1B (muscle-type); ACADM: Acyl CoA dehydrogenase medium-chain; HADHA: Hydroxyacyl CoA dehydrogenase alpha-subunit; ECI1: Enoyl CoA isomerase 1. Data are presented as mean ± SEM, and were analysed using a one-way ANOVA with Tukey post hoc test (n=4). Data was collected with the help of Colleen Lopez.

6.5.4.2 Effect of Long-term Treatment on Glucose Metabolism

6.5.4.2.1 Relative Gene Expression of Glucose Transporters (*GLUT1* and *GLUT4*) and *PFKM*

Our data showed that 1 week treatment with 400 µM OA alone or in combination with 120 µM WY14643 had no effect on the expression of *GLUT1* and *GLUT4* (Figure 6.25A-B). In addition, there was no difference in the expression of *PFKM* between treated and untreated hiPSC-CMs (Figure 6.26).

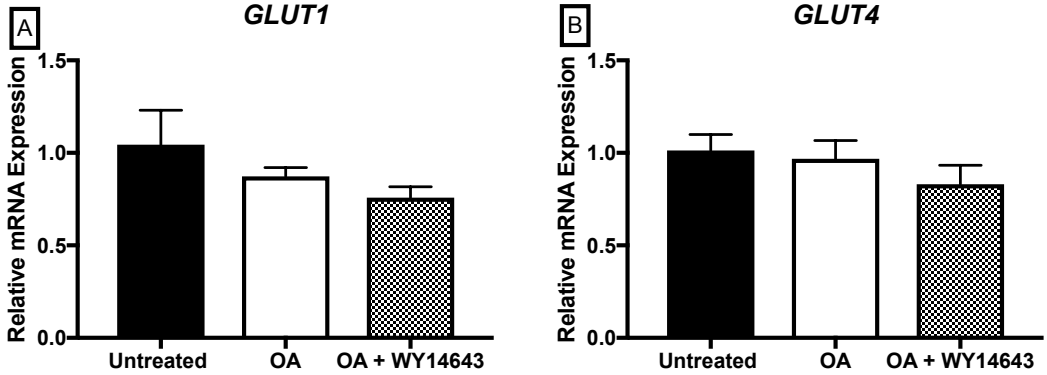


Figure 6.25: The relative mRNA expression of *GLUT1* and *GLUT4* using qRT-PCR. Immature beating hiPSC-CMs were treated with 400 µM oleic acid (OA) alone or in combination with 120 µM WY14643 for 1 week. Untreated hiPSC-CMs were used as control. Abbreviations: OA: Oleic acid. Data are presented as mean ± SEM, and were analysed using a one-way ANOVA with Tukey post hoc test (n=4). Data was collected with the help of Colleen Lopez.

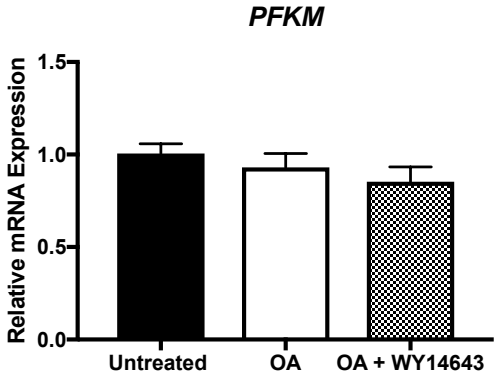


Figure 6.26: The relative mRNA expression of *PFKM* using qRT-PCR. Immature beating hiPSC-CMs were treated with 400 µM oleic acid (OA) alone or in combination with 120 µM WY14643 for 1 week. Untreated hiPSC-CMs were used as control. Abbreviations: OA: Oleic acid; PFKM: Phosphofructokinase, muscle-type. Data are presented as mean ± SEM, and were analysed using a one-way ANOVA with Tukey post hoc test (n=4). Data was collected with the help of Colleen Lopez.

6.5.4.2.2 Relative Gene Expression of *PDH* and *PDK4*

One week of 400 µM OA and 400 µM OA + 120 µM WY1464 had no effect on the expression of *PDHA1* (Figure 6.27A). Whereas, *PDK4* expression continued to be significantly upregulated in both treatment regimens (Figure 6.27B).

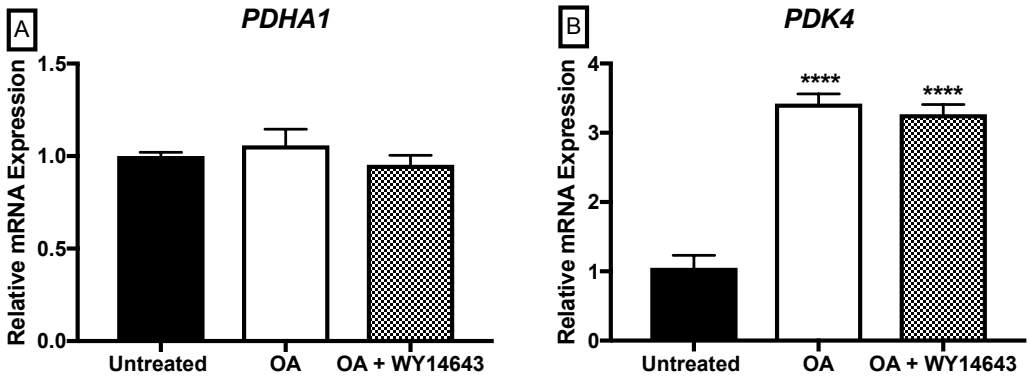


Figure 6.27: The relative mRNA expression of *PPDA1* and *PDK4* using qRT-PCR. Immature beating hiPSC-CMs were treated with 400 µM oleic acid (OA) alone or in combination with 120 µM WY14643 for 1 week. Untreated hiPSC-CMs were used as control. Abbreviations: OA: Oleic acid; *PDHA1*: Pyruvate dehydrogenase type A1; *PDK4*: Pyruvate dehydrogenase kinase 4. Data are presented as mean ± SEM, and were analysed using a one-way ANOVA with Tukey post hoc test. P-value ≤ 0.0001 (****) compared with untreated hiPSC-CMs (n=4). Data was collected with the help of Colleen Lopez.

6.5.4.2.3 In Vitro ^{3}H-Gluocose Utilization

Immature beating hiPSC-CMs were pre-treated with 400 µM OA alone or in combination with 120 µM WY14643 for 1 week. Pre-treating hiPSC-CMs with OA for 1 week significantly lowered glycolytic rates compared with untreated hiPSC-CMs and OA + WY14643-treated hiPSC-CMs (Figure 6.28).

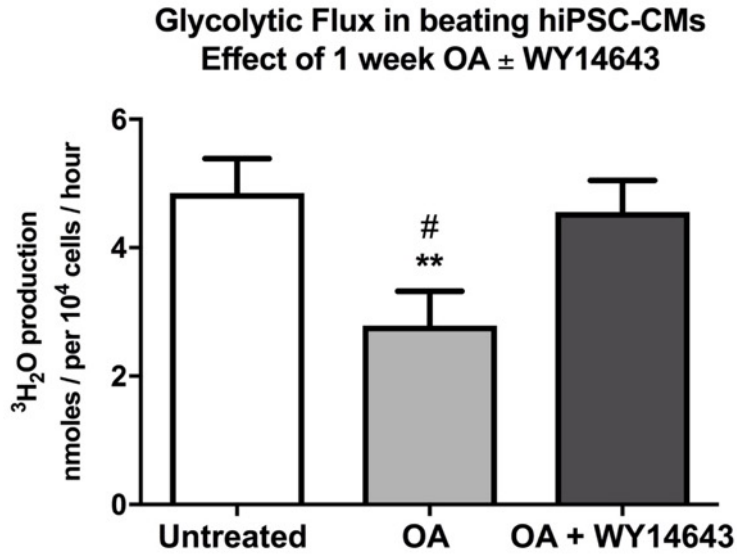


Figure 6.28: Glycolytic flux in beating hiPSC-CMs pre-treated for 1 week with OA ± WY14643. Immature beating hiPSC-CMs were pre-treated with 400 µM OA ± 120 µM WY14643 for 1 week. After 24 hours, beating hiPSC-CMs were cultured with fresh media containing 0.00148 MBq of [5-^{3}H]-glucose supplemented with 400 µM OA ± 120 µM WY14643 for 8 hours. Untreated beating hiPSC-CMs were cultured with fresh media (RPMI + B27) containing 0.00148 MBq of [5-^{3}H]-glucose and used as control. Data are presented as mean ± SEM, and were analysed using a one-way ANOVA with Tukey post doc test. P-value ≤ 0.01 (**) compared with untreated hiPSC-CMs and p-value ≤ 0.05 (#) comparing OA treated hiPSC-CMs with OA + WY14643 treated hiPSC-CMs (n=3). Data was collected with the help of Colleen Lopez.

6.6 Discussion

6.6.1 Effect of OA alone or OA and WY14643 Treatment on Beating Human Induced Pluripotent Stem Cells-Derived Cardiomyocytes

Changes in heart metabolism occur during the transition period after-birth. Changes include the levels of energy substrate, hormone concentrations such as insulin, thyroid hormone, adiponectin and leptin, and increased availability of oxygen[48,52,57,58]. Levels of glucose, lactate and free fatty acids change soon after birth. It has been reported that the measurement of arteriovenous glucose across the coronary circulation of new-born dogs showed a big reduction in glucose/O_2 quotient from new-borns to adults[58]. In addition, lactate concentration in foetal rats is around 10 mmol/L, and within hours of birth it falls to levels seen in adult rats (1-2 mmol/L)[48]. Similar reductions in lactate concentration and uptake has been reported in new-born lambs[56] and new-born pigs[54], whereas, the levels of fatty acids increase after birth, for example, in human, the concentration of plasma free fatty acids is very low during the foetal life (0.025 mmol/L), and just after birth it rises rapidly to levels seen in adults[48], which range from 0.2 to 0.8 mM[46]. Despite changes in the level of energy substrates, the same culturing media is used for hiPSC-CMs throughout the differentiation and as long as the cells are kept in culture. Most media used for culturing hiPSC-CMs are high in glucose and lack substantial amounts of fatty acids, therefore it was hypothesised that the addition of the fatty acid (Oleic Acid) into the culturing media would enhance fatty acid oxidation in immature beating hiPSC-CMs via PPAR-α activation, resulting in a more mature hiPSC-CMs. In addition, the activation of PPAR-α using WY14643 in the presence of oleic acid was hypothesised to enhance metabolic maturation in immature beating hiPSC-CMs by upregulation fatty acid oxidation, which in turn will mature the mitochondria in beating hiPSC-CMs.

6.6.2 Effect of OA alone or OA and WY14643 Treatment on the Activation of PPAR-α in Beating hiPSC-CMs: Gene Expression of *PPARA*, *PGC1A*, *UCP3*, and *PDK4*

Oleic acid treatment, with or without WY14643, did not increase the relative gene expression of *PPARA* and *PGC1A*, which is a PPAR-α co-activator and known to play an important role in mitochondria biogenesis[62]. Oleic acid and WY14643 are PPAR-α natural and synthetic ligands and they might not increase *PPARA* expression. Therefore, the effect of oleic acid alone or in combination with WY14643 on the expression of some PPAR-α target genes such as *UCP3*[62,204,205] and *PDK4*[62,163,181] was measured. Previously, it has been reported that increased fatty acid levels in the circulation or WY14643 treatment increased UCP3 levels in cardiac mitochondria via PPAR-α activation[204]. In addition, others showed that the addition of oleic acid to culturing media increased the expression of UCP3 in muscle cells such as myotubes, suggested to be via activation of PPAR-α[205]. WY14643 treatment in cultured rat neonatal cardiomyocytes also increased the expression of UCP3[167]. Also, it has been reported that UCP3 has a role in regulating the rate of fatty acid oxidation in the heart[62]. When fatty acyl CoA levels in the mitochondrial matrix exceed that needed to maintain the rate of fatty acid oxidation, fatty acyl CoA is hydrolysed to free CoA and fatty acid anions, which are exported to the cytoplasm by UCP3[62]. However, the relative mRNA expression of *UCP3* was not increased in neither treated hiPSC-CMs comparing them to untreated hiPSC-CMs. Therefore, the expression of another important PPAR-α target gene, *PDK4,* was measured and used as an indicator for PPAR-α activation. Our data showed a significant increase in *PDK4* expression in hiPSC-CMs treated with oleic acid alone and in combination with WY1643. The expression of *PDK4* continued to be upregulated with time as OA alone or in combination with WY14643 was added into the culture. Similar data has been reported previously, with activation of PPAR-

α via treatment with fatty acid or WY14643 increasing levels of PDK4[163,167,180–182]. Therefore, it was concluded that treatment with oleic acid alone or in combination with WY14643 did activate PPAR-α in our cells, which in turn initiates the transcription of *PDK4*.

6.6.3 Effect of OA alone or OA and WY14643 Treatment on Fatty Acid Metabolism

6.6.3.1 Gene Expression

PPAR-α activation upregulates genes involved in fatty acid oxidation such as CD36[61,62,68,169,175,179], ACSL1[61,179], CPT1B[61,62,168,170,176], MCAD[61,62,173,179]. Therefore, we hypothesised that PPAR-α activation by oleic acid with or without WY14643 would increase fatty acid uptake and oxidation by upregulate the expression of *CD36*, *ACSL1*, *CPT1B*, *ACADM*, and *HADHA* in our immature hiPSC-CMs. However, there was no effect on the expression of *CD36* in our treated immature beating hiPSC-CMs. Interestingly, there was a significant downregulation of *ACSL1* in OA treated hiPSC-CMs after 24 hours of treatment. In comparison, *ACSL1* expression in neonatal rat cardiomyocytes was upregulated 4-fold after culture with a combination of fatty acids (palmitic and oleic acid) and 10-fold after treatment with WY14643, compared to glucose-treated cardiomyocytes[168]. In another study, WY14643 treatment on cultured neonatal rat cardiomyocytes, upregulated *ACSL1* by 2-3-fold compared to control (DMSO treated cardiomyocytes)[167]. In these studies, WY14643 was used for 48 hours but at a much lower concentration (10 μM)[167,168] than that used in this project (120 μM), and the upregulation of *PDK4* seemed to indicate that the dose we used induced activation of PPAR-α. Therefore, the reason behind these conflicting results is not due to lack of PPAR-α activation. In their study, oleic acid (250 μM) was used in combination with palmitic acid (250 μM), whereas, with our cells we only used oleic acid. Therefore, the upregulation in *ACSL1*

they reported might be due to the effect of palmitic acid[168]. An important enzyme regulating fatty acid oxidation is the muscle-type of CPT1 (CPT1B), which has been reported to be the predominate isoform in the heart[46] CPT1B expression has been shown to be upregulated by PPAR-α activation[46,61,62,168,170,176] and to increase dramatically after birth[221]. Our data showed that treatment with 400 μM OA and 120 μM WY14643 for 8 hours was sufficient to upregulate *CPT1B* mRNA expression. It has been reported that WY14643 treatment upregulated muscle CPT1 expression in cultured rat neonatal cardiomyocytes[167,168], in cardiac α myosin heavy chain specific (MHC)-PPARα transgenic mice[210], and in hESC-derived ventricular cardiomyocytes[134]. In addition, the addition of FA to cultured rat neonatal cardiomyocytes upregulated the expression of muscle CPT1[168]. Similarly, treatment of hiPSC-CM with 400 μM OA and 120 μM WY14643 for 8 hours increased expression of *ACADM* mRNA, which is expressed at low levels in the heart during the foetal life, starts to increase after birth, and peaks at around day14-17 of age[61,221–224]. When liver cells were transfected with the PPAR expression vector, oleic acid increased *ACADM* promoter activity[173], indicating a role of fatty acid-induced PPAR activation in mediating *ACADM* expression, and *ACADM* was upregulated after WY14643 treatment in cultured rat neonatal cardiomyocytes[167] and in hESC-derived ventricular cardiomyocytes[134]. Interestingly, as with *ACSL1,* treatment with OA for 24 hours did have the same effect and caused downregulation of *ACADM* expression. More as expected, *e*xpression of *ECI1* was significantly upregulated in hiPSC-CMs treated with OA + WY14643 for 8 and 24 hours. In summary, although we did not see the expected upregulation in all fatty acid enzymes, our data showed the OA + WY14643 upregulated the expression of *CPT1B* and *ACADM*.

6.6.3.2 Fatty Acid Metabolism by Measuring Oxygen Consumption Rate using the Clark-Type Oxygen Electrode

OCR was measured in pre-treated beating hiPSC-CMs and compared to untreated beating hiPSC-CMs. Although our data showed no significant difference in OCR at baseline, treatment with both OA and WY14643 increased the maximal respiration in hiPSC-CMs respiring on OA by around 2-fold compared with untreated and OA-treated hiPSC-CMs. Pfleger *et al* measured OCR of neonatal rat cardiomyocytes and hiPSC-CMs while respiring on glucose alone, palmitate alone, or glucose and palmitate using the Seahorse XF24-3 Analyzer[184]. The cells were pre-treated for 24 hours with the same substrates used during OCR measurement[184]. They showed that neonatal rat cardiomyocytes respired better on glucose and palmitate and that hiPSC-CMs respired better on palmitate[184]. Our data agree that hiPSC-CMs respire better on fatty acid than pyruvate and malate, however, we found that treatment with OA alone did not increase OCR and that WY14643 administration was required for the increase in OCR in our cells. That was confirmed by determining the reserve respiratory capacity (RRC) of these cells, which showed that OA and WY14643 pre-treated hiPSC-CMs had an increased RRC while respiring on OA. Pfleger *et al* found that in neonatal rat cardiomyocytes both glucose and palmitate were important to generate a RRC, but in hiPSC-CMs palmitate alone generated the highest RRC which was reduced by 80% in the presence of glucose alone[184]. RRC enables cardiac cells to respond to increased energetic demands[225–227], therefore, our data suggested that PPAR-α activation via fatty acid and a specific agonist induced mitochondrial maturation in immature beating hiPSC-CMs and that the agonist WY14643 was required to induce the affect. Previously, it has been reported that WY14643 treatment increased mitochondrial membrane potential, which is an indication of a mature ETC[134].

6.6.4 Effect of OA alone or OA and WY14643 Treatment on Glucose Metabolism

Activation of PPAR-α downregulates glucose uptake and glucose utilization[198210], however it is not known whether this effect is due to direct activation of PPAR-α or secondary to increased fatty acid oxidation. PPAR-α knockout mice showed increased glucose uptake and oxidation[203] and PPAR-α overexpression reduced the gene expression of glucose transporter and glucose uptake[203]. Therefore, we expected to see a downregulation in glucose uptake and utilization as a result of OA ± WY14643 treatment.

6.6.4.1 Gene Expression after OA alone or OA and WY14643 Treatment

After birth, there is a switch in the predominant glucose transporter (GLUT) isoform in the heart[52,53,161]. GLUT1, which is predominant in the foetal heart becomes downregulated in adulthood, whereas GLUT4 becomes the predominant isoform in the adult heart[52,53,147,161]. Therefore, the switch in GLUT isoform in young beating hiPSC-CMs was used to measure the degree of maturity in these cells as a result of PPAR-α activation. Our data showed that the relative gene expression of *GLUT1* did not change after 8 hours of treatment with OA ± WY14643, whereas the relative gene expression of *GLUT4* was downregulated in 8 hours treated hiPSC-CMs. In addition, *PFKM* gene expression was significantly downregulated after 8 hours of OA ± WY14643 treatment. In MHC-PPARα mice that were treated with WY14643, there was no change in the expression of GLUT1 but downregulation in the expression of GLUT4 and PFK[210]. Others showed that culturing rat neonatal cardiomyocytes with fatty acids (palmitic and oleic acids) downregulated GLUT4 expression[168]. PDK4 was upregulated after 8 hours treatment with OA ± WY14643 and continued to be upregulated after 24 hours treatment. It has been reported that adding palmitate or palmitate and glucose into basal media

of neonatal rat cardiomyocytes increased the expression of PDK4, but not PDK1-3[184]. In addition, it has been reported that WY14643 upregulated the relative gene expression of PDK4 in control and MHC-PPARα mice[210].

6.6.4.2 Anaerobic Glycolysis and Glycolytic Flux in Young Beating Human Induced Pluripotent Stem Cells Derived Cardiomyocytes

Analysis of extracellular media showed that after 24 hours treatment with OA, there was less glucose converted into lactate suggesting that glucose oxidation was higher in these cells compared to untreated hiPSC-CMs. We saw no difference in glycolytic rates between treated and untreated hiPSC-CMs. RPMI media contains glucose, therefore treated hiPSC-CMs had the choice between using glucose or OA for energy production. These data showed that even if OA + WY14643 pre-treated hiPSC-CMs have more mature mitochondria when the cells are cultured with high concentration of glucose and fatty acid, the cells will continue to use glucose as an energy substrate. For that reason, it may be that in order to enhance the usage of fatty acid in OA + WY14643 pre-treated hiPSC-CMs, the cells should be cultured in media with a lower glucose concentration.

6.6.4.3 Pyruvate Oxidation by Measuring Oxygen Consumption Rate using the Clark-Type Oxygen Electrode

The measurement of OCR while respiring on pyruvate and malate was used to measure the potential for glucose oxidation. During respiration, untreated and treated hiPSC-CMs did not have to choose between different substrates and what was measured was the capacity of untreated and pre-treated hiPSC-CMs to oxidise pyruvate and malate. Our data showed that pre-treatment with OA for 24 hours was sufficient to increase the mitochondrial capacity to oxidise pyruvate and malate compared to untreated and OA + WY14643 pre-treated hiPSC-CMs, indicating an increase in the mitochondrial oxidation pathway. In contrast, pre-treatment

with OA + WY14643 did not also increase the mitochondrial capacity to oxidise pyruvate and malate. Previously, it has been reported that PPAR-α overexpression reduces myocardial glucose oxidation[210] and that PPAR-α activation using WY14643 led to a reduction in glucose oxidation[228]. However, in our cells WY14643 increased the expression of PDK4 by 10-fold comparing it to OA treatment, which will have inhibited PDH and therefore blocked the conversion of pyruvate into acetyl CoA and its entry into the TCA cycle.

6.6.5 Effect of Long-term OA alone or OA and WY14643 Treatment (1 week) on Metabolism in Beating hiPSC-CMs

We studied the effect of long-term treatment (1 week) in order to enhance fatty acid oxidation further. In general, our data showed that 1 week treatment had no effect on the relative gene expression of genes involved in FAO. The effect of long-term treatment on glucose uptake and metabolism was tested at a transcriptional level by measuring the relative gene expression of *GLUT1, GLUT4, PFKM, PDH, and PDK4. PDK4* expression continued to be upregulated as a result of PPAR-α activation by OA alone or in combination with WY14643. Treating hiPSC-CMs with OA ± WY14643 showed no effect on the expression of *GLUT1, GLUT4*, nor *PFKM* despite the reduction in glycolytic rate after 1 week of treatment with OA but, interestingly, not after 1 week of treatment with OA and WY14643. Without data for oxygen consumption rates or use of other substrates such as oleic acid oxidation, it is difficult to determine why there is no change in glycolytic flux in beating cardiomyocytes treated with OA and WY14643. Data from one week treatment are not sufficient to conclude that longer treatment time will further enhance the maturation of young hiPSC-CMs. More functional assays are necessary to make a conclusion whether longer treatment might be more beneficial to hiPSC-CMs than 24 hours treatment.

6.8 Conclusion

In conclusion, the late activation of PPAR-α in immature beating hiPSC-CMs enhanced metabolic maturation by upregulating mitochondrial oxidative respiration. Treating immature beating hiPSC-CMs with OA alone increased pyruvate oxidation but not fatty acid oxidation, suggesting that changing the culturing media for beating hiPSC-CMs is not sufficient to enhance metabolic maturation, whereas, pharmacological activation of PPAR-α using WY14643 in the presence of oleic acid enhanced metabolic maturation in immature beating hiPSC-CMs by upregulating fatty acid oxidation at a transcriptional and functional level.

7 General Discussion

Although, hiPSC-derived cardiomyocytes have been used extensively, they lack maturity at various levels, as has been reported by many groups[34,134,143,144]. A study comparing hESC-CMs with human foetal and adult ventricular cardiomyocytes, showed immaturity in both cardiac and metabolic markers[134]. If hiPSC-CM are to be used for disease modelling or to test the effect of drug compounds, it is essential that they express the full range of proteins, enzymes and ion channels that are found in the adult cardiomyocyte. Metabolic maturation can be achieved via long-term culture (> 100 days)[39–41], but is both time and money consuming. A range of techniques are being explored to mature hiPSC-CMs, including application of mechanical stretch them or constraining them into lines [37,43]. Few groups have considered the metabolic phenotype of hiPSC-CM. Yang *et al*[212] measured oxygen consumption in cells treated with the growth hormone T3 but they only used glucose as a substrate. This thesis sought to investigate the maturation of hiPSC-CM by upregulation of mitochondrial oxidation.

The first step was to differentiate hiPSC into beating cardiomyocytes. There are various cardiac differentiation protocols[22,80,126,81,82,114,121–125], and we wanted to find a reproducible and efficient differentiation protocol that consistently resulted in a high number of spontaneously beating hiPSC-CMs. Line-to-line variation in yield and purity of hiPSC-CMs, and reproducibility of protocol have been reported previously[33,128,229,230], and in this project, we were faced with the same problem. Alterations introduced to the Wnt-modulation protocol improved the efficiency of cardiac differentiation, accompanied by upregulation in cardiac genes such as *MYH6* and *TNNT2*, however, throughout this project we did have a range from extremely successful differentiations (hiPSC-CMs beating as one sheet in synchrony), through partial success with unsynchronised scattered beating areas, to non-beating hiPSC-CMs, all using the same cell line and conditions. One reason for this variation may be due to using

different stocks of growth factors and martigel, as they may exhibit a lot-to-lot variation in their bioactivity and protein concentration. Variation may also have been introduced during the enzymatic dissociation step of hiPSCs in preparation for cardiac differentiation. Although, the same reagents were used for the same duration of time, we did notice days where cells did not detach as fast as they would normally do, which would require manual disassociation of the cells using a cell scraper which would have been an added stress to the cells. Therefore, we suspect that technical/practical variation that occurs during the differentiation might have larger effect on the efficiency than perhaps expected.

In chapter 4 we investigated the changes in oxidative metabolism in beating hiPSC-CMs as they were differentiated from hiPSC. There are studies that compared hiPSCs with human fibroblasts[88,149,152], or hiPSC-CMs with human fibroblasts[155], however, there are few studies comparing the differentiated beating hiPSC-CMs with their corresponding hiPSCs[41]. We found an increase in fatty acid and glucose metabolism at a transcriptional and functional level. This metabolic shift from hiPSCs to hiPSC-CMs mirrors the metabolic shift that occurs during foetal heart development[52,231].

Having acquired a better understanding of the metabolic state of beating hiPSC-CMs, we sought to mature the differentiation by increasing mitochondrial metabolism. It is well known that PPAR-α drives metabolic maturation in hearts after birth[198,232], therefore, we hypothesised that PPAR-α activation, using WY14643, at early stages of cardiac differentiation would enhance the metabolic shift further. However, we found that activation of PPAR-α using WY14643 treatment on day 5, 7, and 10 of the differentiation did not enhance metabolic maturation nor enhance cardiac differentiation. It might be that the time we chosen to activate PPAR-α was too early as by these days cells were still not beating. In the embryonic development, PPAR-α is not activated until relatively late E13.5 – E15.5 in the rodent heart[197]

and Ding *et al* showed that PPAR-α was induced in differentiating mouse ESCs at the time that the cells formed beating clusters[187]. Alternatively, it might be that we did not add fatty acids with WY14643, which does not mimic what happens during normal heart development. Immediately after birth, there is an increase in the levels of fatty acids in the circulation, which activates PPAR-α and therefore, upregulates fatty acid oxidation in the heart. Therefore, we decided to activate PPAR-α at a later-stage in the differentiation and add fatty acid into the culturing media.

Immature beating hiPSC-CMs (> day 15) were cultured with oleic acid alone or were treated with WY14643 in combination with oleic acid to mimic what happens during normal heart development. We found that culturing immature beating hiPSC-CMs with oleic acid alone increased the potential for mitochondrial oxidation as it enhanced pyruvate oxidation, but it did not increase fatty acid oxidation. Therefore, we can conclude that the presence of high levels of fatty acid alone were not sufficient to drive the metabolic maturation. This make sense, since the metabolic shift during normal heart development is caused by a net effect from many variables and one of them is the increased levels of fatty acid. The activation of PPAR-α in the presence of oleic acid enhanced fatty acid metabolism genes and oxidation, therefore, enhancing mitochondrial maturation. Treated hiPSC-CMs showed evidence of the metabolic flexibility seen in the adult heart by upregulation of PDK4 which plays a pivotal role in the balance between glucose and fatty acid metabolism[181]. From these data, we concluded that we need a step in cardiac differentiation which mimics what happens to the metabolic shift during normal heart and this step should be mediated via PPAR-α activation in the presence of fatty acids. This approach will provide us with a better *in vitro* cell-based model for human cardiomyocytes that can be used for modelling late-onset disease or metabolic-related diseases of the heart. This metabolic maturation in immature beating hiPSC-CMs was achieved after 24

hours of WY14643 and oleic acid treatment. It would be interesting to compare these treated cells with those matured after long-term culture maturation (> 100 days)[41], although if cells are kept in high glucose medium for the whole culture period they may have no need to upregulate fatty acid metabolism. The short time of our maturation method makes this method more cost effective but other aspects of cell maturation, such as calcium handling and contractility need to be characterised in this model to determine its applicability to the field of disease modelling.

8 Conclusion

Since the discovery of hiPSCs, they have been used extensively as an *in vitro* cell-based model to study disease. In the field of cardiovascular research, hiPSC-CMs have been used to model rare diseases. This has become particularly valuable with the advent of the CRISPR/Cas9 gene editing system which can be used to correct a genetic mutation and therefore generate genetically corrected control cells which are otherwise genetically identical to the parent cells[233]. A large area of research has concentrated on finding efficient cardiac differentiation protocols and now is looking for ways to mature the hiPSC-CMs. Although metabolic manipulation has been used to enrich ventricular hiPSC-CMs in cell culture populations, the field was lacking studies into ways to metabolically mature the hiPSC-CMs. In this project, we proposed a model to metabolically mature hiPSC-CMs by targeting transcription factors known to play an important role in cardiac metabolism. We based our model on knowledge about what happens during heart development and the metabolic shift, which occurs just after birth. We found that the time point when PPAR-α is activated during differentiation to hiPSC-CMs is very important, as is the presence of available substrates for mature cardiac metabolism. With our model, we are a step forward towards generating mature hiPSC-CMs.

References

1. British Heart Foundation. BHF CVD Statistics Factsheet - UK. *BHF Factsheet* (2016). doi:10.1017/CBO9781107415324.004
2. Opie, L. H. *Heart Physiology From Cell to Circulation*. (Lippincott Williams & Wilkins, 2004).
3. R., L. J. *An Introduction to Cardiovascular Physiology*. (Hodder Arnold, 2011).
4. Breckenridge, R. A. *et al.* Hypoxic Regulation of Hand1 Controls the Fetal-Neonatal Switch in Cardiac Metabolism. *PLoS Biol.* **11,** 4–7 (2013).
5. Pasumarthi, K. B. S. & Field, L. J. Cardiomyocyte cell cycle regulation. *Circ. Res.* **90,** 1044–1054 (2002).
6. Puente, B. N. *et al.* The Oxygen Rich Postnatal Environment Induces Cardiomyocyte Cell Cycle Arrest Through DNA Damage Response. *Cell* **157,** 565–579 (2014).
7. Nakada, Y. *et al.* Hypoxia induces heart regeneration in adult mice. *Nature* **541,** 222–227 (2017).
8. Lalit, P. A., Hei, D. J., Raval, A. N. & Kamp, T. J. Induced pluripotent stem cells for post-myocardial infarction repair: Remarkable opportunities and challenges. *Circ. Res.* **114,** 1328–1345 (2014).
9. Bruyneel, A. A. N., Sehgal, A., Malandraki-Miller, S. & Carr, C. Stem Cell Therapy for the Heart: Blind Alley or Magic Bullet? *J. Cardiovasc. Transl. Res.* **9,** 405–418 (2016).
10. Tomita, S. *et al.* Autologous Transplantation of Bone Marrow Cells Improves Damaged Heart Function. *Circulation* **100,** 247–256 (1999).
11. Makino, S. *et al.* Cardiomyocytes can be generated from marrow stromal cells in vitro. *J. Clin. Invest.* **103,** 697–705 (1999).
12. Orlic, D. *et al.* Bone marrow cells regenerate infarcted myocardium. *Nature* **410,** 701–705 (2001).
13. Beltrami, A. P. *et al.* Adult Cardiac Stem Cells Are Multipotent and Support Myocardial Regeneration. *Cell* **114,** 763–776 (2003).
14. Oh, H. *et al.* Cardiac progenitor cells from adult myocardium: homing, differentiation, and fusion after infarction. *Proc. Natl. Acad. Sci.* **100,** 12313–12318 (2003).
15. Messina, E. *et al.* Isolation and expansion of adult cardiac stem cells from human and murine heart. *Circ. Res.* **95,** 911–921 (2004).
16. Carr, C. A. *et al.* Cardiosphere-derived cells improve function in the infarcted rat heart for at least 16 weeks - an mri study. *PLoS One* **6,** (2011).
17. Smart, N. *et al.* De novo cardiomyocytes from within the activated adult heart after injury. *Nature* **474,** 640–4 (2011).
18. Laflamme, M. a *et al.* Cardiomyocytes derived from human embryonic stem cells in pro-survival factors enhance function of infarcted rat hearts. *Nat. Biotechnol.* **25,** 1015–1024 (2007).
19. Fernandes, S. *et al.* Human embryonic stem cell-derived cardiomyocytes engraft but do not alter cardiac remodeling after chronic infarction in rats. *J. Mol. Cell. Cardiol.* **49,** 941–949 (2010).
20. Shiba, Y. *et al.* Human ES-cell-derived cardiomyocytes electrically couple and suppress arrhythmias in injured hearts. *Nature* **489,** 322–325 (2012).
21. Chong, J. J. H. *et al.* Human embryonic-stem-cell-derived cardiomyocytes regenerate non-human primate hearts. *Nature* **510,** 273–7 (2014).
22. Carpenter, L. *et al.* Efficient Differentiation of Human Induced Pluripotent Stem Cells Generates Cardiac Cells That Provide Protection Following Myocardial Infarction in the

Rat. *Stem Cells and Development* **21,** 977–986 (2012).
23. Kadota, S., Pabon, L., Reinecke, H. & Murry, C. E. In Vivo Maturation of Human Induced Pluripotent Stem Cell-Derived Cardiomyocytes in Neonatal and Adult Rat Hearts. *Stem Cell Reports* **7,** 1–12 (2017).
24. Murry, C. E. *et al.* Haematopoietic stem cells do not transdifferentiate into cardiac mycocytes in myocardial infarcts. *Nature* **428,** 664–668 (2004).
25. Balsam, L. B. *et al.* Haematopoietic stem cells adopt mature haematopoietic fates in ischaemic myocardium. *Nature* **428,** 668–673 (2004).
26. Thomson, J. A. *et al.* Embryonic Stem Cell Lines Derived from Human Blastocysts. *Science (80-.).* **282,** 1145–1147 (1998).
27. Takahashi, K. *et al.* Induction of Pluripotent Stem Cells from Adult Human Fibroblasts by Defined Factors. *Cell* **131,** 861–872 (2007).
28. Ahfeldt, T. *et al.* Programming human pluripotent stem cells into white and brown adipocytes. *Nature Cell Biology* **14,** 209–219 (2012).
29. Lan, F. *et al.* Abnormal calcium handling properties underlie familial hypertrophic cardiomyopathy pathology in patient-specific induced pluripotent stem cells. *Cell Stem Cell* **12,** 101–113 (2013).
30. Sun, N. *et al.* Patient-specific induced pluripotent stem cells as a model for familial dilated cardiomyopathy. *Sci. Transl. Med.* **4,** 130ra47 (2012).
31. Liang, P. *et al.* Drug screening using a library of human induced pluripotent stem cell-derived cardiomyocytes reveals disease-specific patterns of cardiotoxicity. *Circulation* **127,** 1677–91 (2013).
32. Banyasz, T. *et al.* Transformation of adult rat cardiac myocytes in primary culture. *Exp. Physiol.* **93,** 370–382 (2008).
33. Mummery, C. L. *et al.* Differentiation of Human ES and iPS Cells to Cardiomyocytes: A Methods Overview. *Circ. Res.* **111,** 344–358 (2012).
34. Yang, X., Pabon, L. & Murry, C. E. Engineering adolescence: Maturation of human pluripotent stem cell-derived cardiomyocytes. *Circ. Res.* **114,** 511–523 (2014).
35. Karakikes, I., Ameen, M., Termglinchan, V. & Wu, J. C. Human Induced Pluripotent Stem Cell-Derived Cardiomyocytes: Insights into Molecular, Cellular, and Functional Phenotypes. *Circ. Res.* **117,** 80–88 (2015).
36. Bedada, F. B., Wheelwright, M. & Metzger, J. M. Maturation status of sarcomere structure and function in human iPSC-derived cardiac myocytes. *Biochim. Biophys. Acta - Mol. Cell Res.* **1863,** 1829–1838 (2016).
37. Kolanowski, T. J., Antos, C. L. & Guan, K. Making human cardiomyocytes up to date: Derivation, maturation state and perspectives. *Int. J. Cardiol.* **241,** 379–386 (2017).
38. Drawnel, F. M. *et al.* Disease modeling and phenotypic drug screening for diabetic cardiomyopathy using human induced pluripotent stem cells. *Cell Rep.* **9,** 810–820 (2014).
39. Lundy, S. D., Zhu, W.-Z., Regnier, M. & Laflamme, M. A. Structural and functional maturation of cardiomyocytes derived from human pluripotent stem cells. *Stem Cells Dev.* **22,** 1991–2002 (2013).
40. Ivashchenko, C. Y. *et al.* Human induced pluripotent stem cell derived cardiomyocytes exhibit temporal changes in phenotype. *Am. J. Physiol. Hear. Circ. Physiol.* **6,** ajpheart.00819.2012- (2013).
41. Dai, D.-F., Danoviz, M. E., Wiczer, B., Laflamme, M. A. & Tian, R. Mitochondrial Maturation in Human Pluripotent Stem Cell Derived Cardiomyocytes. *Stem Cells Int.* 1–10 (2017). doi:5153625
42. Piccini, I., Rao, J., Seebohm, G. & Greber, B. Human pluripotent stem cell-derived

cardiomyocytes: Genome-wide expression profiling of long-term in vitro maturation in comparison to human heart tissue. *Genomics Data* **4,** 69–72 (2015).
43. Zhu, R. *et al.* Physical developmental cues for the maturation of human pluripotent stem cell-derived cardiomyocytes. *Stem Cell Res. Ther.* **5,** 117 (2014).
44. Salway, J. G. *Metabolism at a Glance*. (Blackwell Publishing, 2004).
45. Roach, J. O. & Benyon, S. *Metabolism and Nutrition*. (Mosby, 2003).
46. Stanley, W. W. C., Recchia, F. a & Lopaschuk, G. D. Myocardial Substrate Metabolism in the Normal and Failing Heart. *Physiol. Rev.* **85,** 1093–1129 (2005).
47. Mansor, L. S. *et al.* Cardiac metabolism in a new rat model of type 2 diabetes using high-fat diet with low dose streptozotocin. *Cardiovasc. Diabetol.* **12,** 136 (2013).
48. Lopaschuk, G. D., Collins-Nakai, R. L. & Itoi, T. Developmental changes in energy substrate use by the heart. *Cardiovasc Res* **26,** 1172–1180 (1992).
49. Jones, C. T. & Rolph, T. P. Metabolism during fetal life: a functional assessment of metabolic development. *Physiol Rev* **65,** 357–430 (1985).
50. Battaglia, F. C. & Meschia, G. Principal substrates of fetal metabolism. *Physiol Rev* **58,** 499–527 (1978).
51. Mota-Rojas, D. *et al.* Foetal and neonatal energy metabolism in pigs and humans: A review. *Vet. Med. (Praha)*. **56,** 215–225 (2011).
52. Onay-Besikci, A. Regulation of cardiac energy metabolism in newborn. *Mol. Cell. Biochem.* **287,** 1–11 (2006).
53. Depre, C., Vanoverschelde, J. L. & Taegtmeyer, H. Glucose for the heart. *Circulation* **99,** 578–88 (1999).
54. Werner, J. C. & Sicard, R. E. Lactate metabolism of isolated, perfused fetal, and newborn pig hearts. *Pediatr. Res.* **22,** 552–556 (1987).
55. Chalovich, J. M. & Eisenberg, E. Return to the fetal gene program: A suggested metabolic link to gene expression in the heart. *Biophys. Chem.* **257,** 2432–2437 (2005).
56. Bartelds, B. *et al.* Myocardial Lactate Metabolism in Fetal and Newborn Lambs. *Circulation* **99,** 1892–97 (1999).
57. Jones, C. T. & Rolph, T. P. Metabolism during fetal life: a functional assessment of metabolic development. *Physiol. Rev.* **65,** 357–430 (1985).
58. Battaglia, F. C. & Meschia, G. Principal Substrates of Fetal Metabolism. *Physiol. Rev.* **58,** 499–527 (1978).
59. Breckenridge, R. Molecular Control of Cardiac Fetal/Neonatal Remodeling. *J. Cardiovasc. Dev. Dis.* **1,** 29–36 (2014).
60. Narravula, S. & Colgan, S. P. Hypoxia-Inducible Factor 1-Mediated Inhibition of Peroxisome Proliferator-Activated Receptor Expression During Hypoxia. *J. Immunol.* **166,** 7543–7548 (2001).
61. Barger, P. M. & Kelly, D. P. PPAR Signaling in the Control of Cardiac Energy Metabolism. *Trends Cardiovasc. Med* **10,** 238–45 (2000).
62. Lopaschuk, G. D., Ussher, J. R., Folmes, C. D. L., Jaswal, J. S. & STANLEY, W. C. Myocardial Fatty Acid Metabolism in Health and Disease. *Physiol. Rev.* **90,** 207–258 (2010).
63. Martin, O. J. *et al.* A Role for PGC-1 Coactivators in the Control of Mitochondrial Dynamics during Postnatal Cardiac Growth. *Circ Res* **114,** 626–636 (2014).
64. Rustan, A. C. & Drevon, C. A. Fatty Acids : Structures and Properties. *Encycl. Life Sci.* 1–7 (2005).
65. Standing Committee on the Scientific Evaluation of Dietary Reference Intakes. *Dietary Reference Intakes*. *Nutrition reviews* **55,** (1997).
66. Kaneko, F. *et al.* Structure and Crystallization Behavior of the β Phase of Oleic Acid. *J.*

Phys. Chem. B **101,** 1803–1809 (1997).
67. Frayn, K. N. *Metabolic Regulation A Human Perspective*. (Wiley-Blackwell, 2014).
68. Glatz, J. A. N. F. C., Luiken, J. J. F. P. & Bonen, A. Membrane Fatty Acid Transporters as Regulators of Lipid Metabolism : Implications for Metabolic Disease. *Physiol Rev* **90,** 367–417 (2010).
69. Mathews, C. K., Van Holde, K. E., Appling, D. R. & Anthony-Cahill, S. J. *Biochemistry*. (Pearson, 2012).
70. Luiken, J. J. F. P. *et al.* Insulin Stimulates Long-Chain Fatty Acid Utilization by Rat Cardiac Myocytes Through Cellular Redistribution of FAT/CD36. *Diabetes* **51,** 3113–3119 (2002).
71. Campbell, F. M. *et al.* A Role for Peroxisome Proliferator-activated Receptor a (PPAR a) in the Control of Cardiac Malonyl-CoA Levels. *Biochemistry* **277,** 4098–4103 (2002).
72. Folmes, C. D. L., Dzeja, P. P., Nelson, T. J. & Terzic, A. Metabolic plasticity in stem cell homeostasis and differentiation. *Cell Stem Cell* **11,** 596–606 (2012).
73. Zhang, J., Nuebel, E., Daley, G. Q., Koehler, C. M. & Teitell, M. a. Metabolic regulation in pluripotent stem cells during reprogramming and self-renewal. *Cell Stem Cell* **11,** 589–95 (2012).
74. Shyh-Chang, N., Daley, G. Q. & Cantley, L. C. Stem cell metabolism in tissue development and aging. *Development* **140,** 2535–47 (2013).
75. Folmes, C. D. L. *et al.* Somatic oxidative bioenergetics transitions into pluripotency-dependent glycolysis to facilitate nuclear reprogramming. *Cell Metab.* **14,** 264–271 (2011).
76. Folmes, Clifford, D., Nelson, timothy, J. & Terzic, A. Energy metabolism in nuclear reprogramming. *biomark Med.* **5,** 715–729 (2011).
77. Xu, X. *et al.* Mitochondrial regulation in pluripotent stem cells. *Cell Metab.* **18,** 325–332 (2013).
78. Burridge, P. W. *et al.* Chemically defined generation of human cardiomyocytes. *Nat. Methods* **11,** 855–60 (2014).
79. van Wilgenburg, B., Browne, C., Vowles, J. & Cowley, S. A. Efficient, Long Term Production of Monocyte-Derived Macrophages from Human Pluripotent Stem Cells under Partly-Defined and Fully-Defined Conditions. *PLoS One* **8,** (2013).
80. Lian, X. *et al.* Robust cardiomyocyte differentiation from human pluripotent stem cells via temporal modulation of canonical Wnt signaling. *Proc. Natl. Acad. Sci. U. S. A.* **109,** E1848-57 (2012).
81. Lian, X., Zhang, J., Zhu, K., Kamp, T. J. & Palecek, S. P. Insulin inhibits cardiac mesoderm, not mesendoderm, formation during cardiac differentiation of human pluripotent stem cells and modulation of canonical Wnt signaling can rescue this inhibition. *Stem Cells* **31,** 447–457 (2013).
82. Lian, X. *et al.* Directed cardiomyocyte differentiation from human pluripotent ste cells by modulating Wnt/beta-catenin signaling under fully defined conditions. *Nat. Protoc.* **8,** 162–175 (2013).
83. Lin, B. *et al.* Modeling and studying mechanism of dilated cardiomyopathy using induced pluripotent stem cells derived from Duchenne Muscular Dystrophy (DMD) patients. *Dis. Model. Mech.* **8,** 457–66 (2015).
84. Gavet, O. & Pines, J. Progressive activation of CyclinB1-Cdk1 coordinates entry to mitosis. *Dev Cell* **18,** 533–43 (2010).
85. Britton Chance and G. R. Williams. Respiratory Enzymes in Oxidative Phosphorylation. *J Biol Chem* **217,** 409–428 (1955).
86. Brand, M. D. & Nicholls, D. G. Assessing mitochondrial dysfunction in cells. *Biochem.*

J. **435,** 297–312 (2011).
87. Gerencser, A. A. *et al.* Quantitative Microplate-Based Respirometry with Correction for Oxygen Diffusion. *Anal. Chem.* **81,** 6868–78 (2009).
88. Zhang, J. *et al.* Measuring energy metabolism in cultured cells, including human pluripotent stem cells and differentiated cells. *Nat. Protoc.* **7,** 1068–1085 (2012).
89. Clarke, L. C. J. Monitor and Control of Blood and Tissue Oxygen tensions. *Trans. Am. Soci. Artif Intern. Organs* **2,** 41–48 (1956).
90. Neely, B. J. R., Denton, R. M., England, P. J. & Randle, P. J. The Effects of Increased Heart Work on the Tricarboxylate Cycle and its Interactions with Glycolysis in the Perfused Rat Heart. *Biochem. J* **128,** 147–159 (1972).
91. Teslaa, T. & Teitell, M. A. Techniques to Monitor Glycolysis. *Methods Enzym.* **542,** 91–114 (2014).
92. Russell, R. W. & Young, J. W. A review of metabolism of labeled glucoses for use in measuring glucose recycling. *J. Dairy Sci.* **73,** 1005–16 (1990).
93. Onay-besikci, A. Radioactive Measurements as an Indicator of Metabolic Fluxes in Myocytes. *Open Chem. Biomed. Methods J.* **3,** 128–131 (2010).
94. Liedtke, a. J., Renstrom, B. & Nellis, S. H. Correlation between [5-3H]glucose and [U-14C]deoxyglucose as markers of glycolysis in reperfused myocardium. *Circ. Res.* **71,** 689–700 (1992).
95. Heather, L. C. *et al.* Differential translocation of the fatty acid transporter, FAT/CD36, and the glucose transporter, GLUT4, coordinates changes in cardiac substrate metabolism during ischemia and reperfusion. *Circ. Hear. Fail.* **6,** 1058–1066 (2013).
96. Støttrup, N. B. *et al.* Inhibition of the malate-aspartate shuttle by pre-ischaemic aminooxyacetate loading of the heart induces cardioprotection. *Cardiovasc. Res.* **88,** 257–266 (2010).
97. Walborg, E. F. & Lantz, R. S. Separation and quantitation of saccharides by ion-exchange chromatography utilizing boric acid / glycerol buffers. *Anal. Biochem.* **22,** 123–133 (1968).
98. Hammerstent, R. H. The Use of Dowex-l-Borate from to Separate 3HOH from 2-3h-glucose. *Anal. Biochem.* **56,** 292–293 (1973).
99. Lopaschuk, G. D. Advantages and limitations of experimental techniques used to measure cardiac energy metabolism. *J. Nucl. Cardiol.* **4,** 316–28 (1997).
100. Barr, R. L. & Lopaschuk, G. D. Methodology for measuring in vitro/ex vivo cardiac energy metabolism. *J. Pharmacol. Toxicol. Methods* **43,** 141–152 (2000).
101. Gray C. Schoenwolf, Steven B. Bleyl, Philip R. Brauer, P. H. F.-W. *Larsen's Human Embryology*. (Elsevier Churchill Livingstone, 2015).
102. T.W.Sadler. *Langman's Medical Embryology*. (Wolters Kluwer, 2015).
103. Keith L. Moore, T.V.N. Persaud, M. G. T. *The Developing Human: Clinically Oriented Embryology*. (Elsevier, 2016).
104. Xin, M., Olson, E. N. & Bassel-Duby, R. Mending broken hearts: cardiac development as a basis for adult heart regeneration and repair. *Nat. Rev. Mol. Cell Biol.* **14,** 529–541 (2013).
105. Wu, S. M., Chien, K. R. & Mummery, C. Origins and Fates of Cardiovascular Progenitor Cells. *Cell* **132,** 537–543 (2008).
106. Brade, T., Pane, L. S., Moretti, A., Chien, K. R. & Laugwitz, K. L. Embryonic heart progenitors and cardiogenesis. *Cold Spring Harb. Perspect. Med.* **3,** 1–17 (2013).
107. McFadden, D. G. The Hand1 and Hand2 transcription factors regulate expansion of the embryonic cardiac ventricles in a gene dosage-dependent manner. *Development* **132,** 189–201 (2004).

108. Burridge, P. W., Keller, G., Gold, J. D. & Wu, J. C. Production of de novo cardiomyocytes: Human pluripotent stem cell differentiation and direct reprogramming. *Cell Stem Cell* **10,** 16–28 (2012).
109. Dunwoodie, S. L. The role of hypoxia in development of the Mammalian embryo. *Dev. Cell* **17,** 755–73 (2009).
110. Patterson, A. . & Zhang, L. Hypoxia and Fetal Heart Development. *curr Mol Med.* **10,** 653–666 (2010).
111. Simon, M. C. & Keith, B. The role of oxygen availability in embryonic development and stem cell function. *Nat. Rev. Mol. Cell Biol.* **9,** 285–96 (2008).
112. Carreau, A., Hafny-Rahbi, B. El, Matejuk, A., Grillon, C. & Kieda, C. Why is the partial oxygen pressure of human tissues a crucial parameter? Small molecules and hypoxia. *J. Cell. Mol. Med.* **15,** 1239–1253 (2011).
113. Medley, T. L. *et al.* Effect of oxygen on cardiac differentiation in mouse iPS cells: role of hypoxia inducible factor-1 and Wnt/beta-catenin signaling. *PloS one* **8,** e80280 (2013).
114. Kattman, S. J. *et al.* Stage-specific optimization of activin/nodal and BMP signaling promotes cardiac differentiation of mouse and human pluripotent stem cell lines. *Cell Stem Cell* **8,** 228–240 (2011).
115. Ezashi, T., Das, P. & Roberts, R. M. Low O2 tensions and the prevention of differentiation of HES cells. *Nat. Methods* **2,** 325 (2005).
116. Semenza, G. L. Regulation of mammalian O2 homeostasis by hypoxia-inducible factor 1. *Annu. Rev. Cell Dev. Biol* **15,** 551–78 (1999).
117. Wang, G. L., Jiang, B. H., Rue, E. A. & Semenza, G. L. Hypoxia-inducible factor 1 is a basic-helix-loop-helix-PAS heterodimer regulated by cellular O2 tension. *Proc. Natl. Acad. Sci.* **92,** 5510–5514 (1995).
118. Berra, E., Roux, D., Richard, D. E. & Pouysségur, J. Hypoxia-inducible factor-1 alpha (HIF-1 alpha) escapes O(2)-driven proteasomal degradation irrespective of its subcellular localization: nucleus or cytoplasm. *EMBO Rep.* **2,** 615–20 (2001).
119. Krishnan, J. *et al.* Essential role of developmentally activated hypoxia-inducible factor la for cardiac morphogenesis and function. *Circ. Res.* **103,** 1139–1146 (2008).
120. Krishnan, J. *et al.* Essential role of developmentally activated hypoxia-inducible factor 1alpha for cardiac morphogenesis and function. *Circ. Res.* **103,** 1139–46 (2008).
121. Kehat, I. *et al.* Human embryonic stem cells can differentiate into myocytes with structural and functional properties of cardiomyocytes. *J. Clin. Invest.* **108,** 407–414 (2001).
122. Paige, S. L. *et al.* Endogenous wnt/beta-Catenin signaling is required for cardiac differentiation in human embryonic stem cells. *PLoS One* **5,** (2010).
123. Xu, C., Police, S., Rao, N. & Carpenter, M. K. Characterization and enrichment of cardiomyocytes derived from human embryonic stem cells. *Circ. Res.* **91,** 501–508 (2002).
124. Laflamme, M. A. *et al.* Formation of human myocardium in the rat heart from human embryonic stem cells. *Am J Pathol* **167,** 663–671 (2005).
125. Yang, L. *et al.* Human cardiovascular progenitor cells develop from a KDR 1 embryonic-stem-cell-derived population. *Nature* **453,** 524–528 (2008).
126. Zhang, J. *et al.* Extracellular Matrix Promotes Highly Efficient Cardiac Differentiation of Human Pluripotent Stem Cells: The Matrix Sandwich Method. *Circ Res* **111,** 1125–1136 (2012).
127. Kim, M. *et al.* Cardiomyogenesis in pluripotent cells is enhanced by modulating Wnt-induced endogenous signaling with exogenous activin a and bmp4 protein. in

Symposium on Cardiovascular Regenerative Medicine 71–72 (2013).
128. Osafune, K. *et al.* Marked differences in differentiation propensity among human embryonic stem cell lines. *Nat. Biotechnol.* **26,** 313–315 (2008).
129. Bock, C. *et al.* Reference maps of human es and ips cell variation enable high-throughput characterization of pluripotent cell lines. *Cell* **144,** 439–452 (2011).
130. Ohi, Y. *et al.* Incomplete DNA methylation underlies a transcriptional memory of somatic cells in human iPS cells. *Nat. Cell Biol.* **13,** 541–549 (2011).
131. Närvä, E. *et al.* Continuous hypoxic culturing of human embryonic stem cells enhances SSEA-3 and MYC levels. *PLoS One* **8,** e78847 (2013).
132. Forristal, C. E. *et al.* Environmental Oxygen Tension Regulates the Energy Metabolism and Self-Renewal of Human Embryonic Stem Cells. *PLoS One* **8,** e62507 (2013).
133. Marsboom, G. *et al.* Glutamine Metabolism Regulates the Pluripotency Transcription Factor OCT4. *Cell Rep.* **16,** 323–332 (2016).
134. Poon, E. *et al.* Proteomic Analysis of Human Pluripotent Stem Cell–Derived, Fetal, and Adult Ventricular Cardiomyocytes Reveals Pathways Crucial for Cardiac Metabolism and Maturation. *Circ Cardiovasc Genet* **8,** 427–436 (2015).
135. Nagao, K. *et al.* HIF-1a Signaling Upstream of NKX2.5 Is Required for Cardiac Development in Xenopus. *J. Biol. Chem.* **283,** 11841–11849 (2008).
136. Ng, K.-M. *et al.* Exogenous expression of HIF-1 alpha promotes cardiac differentiation of embryonic stem cells. *J. Mol. Cell. Cardiol.* **48,** 1129–37 (2010).
137. Tulenko, T. & Dimuzio, P. J. The Role of Hypoxia in Stem Cell Differentiation and Therapeutics. *J. Surg. Res.* **165,** 112–117 (2012).
138. Wang, Z. *et al.* Activin A can induce definitive endoderm differentiation from human parthenogenetic embryonic stem cells. *Biotechnol. Lett.* **37,** 1711–1717 (2015).
139. McLean, A. B. *et al.* Activin a efficiently specifies definitive endoderm from human embryonic stem cells only when phosphatidylinositol 3-kinase signaling is suppressed. *Stem Cells* **25,** 29–38 (2007).
140. Naujok, O., Diekmann, U. & Lenzen, S. The generation of definitive endoderm from human embryonic stem cells is initially independent from activin A but requires canonical Wnt-signaling. *Stem Cell Rev.* **10,** 480–493 (2014).
141. Loh, K. M. *et al.* Efficient endoderm induction from human pluripotent stem cells by logically directing signals controlling lineage bifurcations. *Cell Stem Cell* **14,** 237–252 (2014).
142. Xu, X., Browning, V. L. & Odorico, J. S. Activin, BMP and FGF pathways cooperate to promote endoderm and pancreatic lineage cell differentiation from human embryonic stem cells. *Mech. Dev.* **128,** 412–427 (2011).
143. Robertson, C., Tran, D. & George, S. Concise Review: Maturation Phases of Human Pluripotent Stem Cell-Derived Cardiomyocytes. *Stem Cells* **31,** 1–17 (2013).
144. Veerman, C. C. *et al.* Immaturity of Human Stem-Cell-Derived Cardiomyocytes in Culture: Fatal Flaw or Soluble Problem? *Stem Cells Dev.* **24,** 1035–1052 (2015).
145. Ito, K. & Suda, T. Metabolic requirements for the maintenance of self-renewing stem cells. *Nat. Rev. Mol. Cell Biol.* **15,** 243–56 (2014).
146. Kolwicz, S. C., Purohit, S. & Tian, R. Cardiac metabolism and its interactions with contraction, growth, and survival of cardiomyocytes. *Circ. Res.* **113,** 603–16 (2013).
147. Doenst, T., Nguyen, T. D. & Abel, E. D. Cardiac metabolism in heart failure: Implications beyond atp production. *Circ. Res.* **113,** 709–724 (2013).
148. Chung, S. *et al.* Mitochondrial oxidative metabolism is required for the cardiac differentiation of stem cells. *Nat Clin Pr. Cardiovasc* **4,** s60–s67 (2007).
149. Zhang, J. *et al.* UCP2 regulates energy metabolism and differentiation potential of

human pluripotent stem cells. *EMBO J.* **30,** 4860–4873 (2011).
150. Gaspar, J. A. *et al.* Unique metabolic features of stem cells, cardiomyocytes, and their progenitors. *Circ. Res.* **114,** 1346–1360 (2014).
151. Folmes, C. D. L., Ma, H., Mitalipov, S. & Terzic, A. Mitochondria in pluripotent stem cells: Stemness regulators and disease targets. *Curr. Opin. Genet. Dev.* **38,** 1–7 (2016).
152. Panopoulos, A. D. *et al.* The metabolome of induced pluripotent stem cells reveals metabolic changes occurring in somatic cell reprogramming. *Cell Res.* **22,** 168–177 (2012).
153. Zhu, S. *et al.* Brief Report Reprogramming of Human Primary Somatic Cells by OCT4 and Chemical Compounds. *Stem Cell* **7,** 651–655 (2010).
154. Prigione, A., Fauler, B., Lurz, R., Lehrach, H. & Adjaye, J. The senescence-related mitochondrial/oxidative stress pathway is repressed in human induced pluripotent stem cells. *Stem Cells* **28,** 721–733 (2010).
155. Varum, S. *et al.* Energy metabolism in human pluripotent stem cells and their differentiated counterparts. *PLoS One* **6,** e20914 (2011).
156. Zhou, W. *et al.* HIF1α induced switch from bivalent to exclusively glycolytic metabolism during ESC-to-EpiSC/hESC transition. *EMBO J.* **31,** 2103–16 (2012).
157. Shyh-Chang, N., Zheng, Y., Locasale, J. W. & Cantley, L. C. Human pluripotent stem cells decouple respiration from energy production. *EMBO J.* **30,** 4851–2 (2011).
158. Angin, Y. *et al.* CD36 inhibition prevents lipid accumulation and contractile dysfunction in rat cardiomyocytes. *Biochem. J.* **448,** 43–53 (2012).
159. Mobasheri, A. *et al.* Glucose transporter expression and regulation in embryonic and mesenchymal stem cells. *Adv. Anat. Embryol. Cell Biol.* **200,** 57–66 (2008).
160. Montessuit, C. & Lerch, R. Regulation and dysregulation of glucose transport in cardiomyocytes. *Biochim. Biophys. Acta - Mol. Cell Res.* **1833,** 848–856 (2013).
161. Young, L. H., Coven, D. L. & Russell, R. R. Cellular and molecular regulation of cardiac glucose transport. *J Nucl Cardiol* **7,** 267–276 (2000).
162. Scheepers, A., Joost, H. & Schurmann, A. The glucose transporter families SGLT and GLUT: molecular basis of normal and aberrant function. *J. Parenter. Enter. Nutr.* **28,** 364–371 (2004).
163. Jeong, J. Y., Jeoung, N. H., Park, K. G. & Lee, I. K. Transcriptional regulation of pyruvate dehydrogenase kinase. *Diabetes Metab J* **36,** 328–335 (2012).
164. Sugden, M. C. & Holness, M. J. Recent advances in mechanisms regulating glucose oxidation at the level of the pyruvate dehydrogenase complex by PDKs. *Am. J. Physiol. Endocrinol. Metab.* **284,** E855–E862 (2003).
165. Kodiha, M. *et al.* Detecting changes in the mitochondrial membrane potential by quantitative fluorescence microscopy. *Protoc. Exch.* (2015).
166. Chung, S., Arrell, D. K., Faustino, R. S., Terzic, A. & Dzeja, P. P. Glycolytic network restructuring integral to the energetics of embryonic stem cell cardiac differentiation. *J. Mol. Cell. Cardiol.* **48,** 725–34 (2010).
167. Cheng, L. *et al.* Peroxisome proliferator-activated receptor δ activates fatty acid oxidation in cultured neonatal and adult cardiomyocytes. *Biochem. Biophys. Res. Commun.* **313,** 277–286 (2004).
168. Van Der Leij, G. J. *et al.* Peroxisome Proliferator-Activated Receptor (PPAR) a and PPARb/c, but not PPARg, Modulate the Expression of Genes Involved in Cardiac Lipid Metabolism. *Circ Res* **92,** 518–524 (2003).
169. Motojima, K., Passilly, P., Peterst, J. M., Gonzalezt, F. J. & Latruffe, N. Expression of Putative Fatty Acid Transporter Genes Are Regulated by Peroxisome Proliferator-activated Receptor a and c Activators in a Tissue-and Inducer-specific Manner. *J Biol*

Chem **273,** 16710–14 (1998).
170. Brandt, J. M., Djouadi, F. & Kellyţ, D. P. Fatty Acids Activate Transcription of the Muscle Carnitine Palmitoyltransferase I Gene in Cardiac Myocytes via the Peroxisome Proliferator-activated Receptor α. *J. Biol. Chem.* **273,** 23786–92 (1998).
171. Djouadi, F. *et al.* A Gender-related Defect in Lipid Metabolism and Glucose Homeostasis in Peroxisome Proliferator–activated Receptor a–deficient Mice. *J. Clin. Invest.* **102,** 1083–1091 (1998).
172. Djouadi, F. *et al.* The role of the peroxisome proliferator-activated receptor a (PPARa) in the control of cardiac lipid metabolism. *Prostaglandins, Leukot. Essent. Fatly Acids* **60,** 339–343 (1999).
173. Gulick, T., Crescitt, S., Cairatt, T., Moore, D. D. & Kellyt, D. P. The peroxisome proliferator-activated receptor regulates mitochondrial fatty acid oxidative enzyme gene expression. *Biochemistry* **91,** 11012–11016 (1994).
174. Van Bilsen, M., De Vries, J. E. & Van Der Vusse, G. J. Long-term effects of fatty acids on cell viability and gene expression of neonatal cardiac myocytes. *Prostaglandins Leukot. Essent. Fat. Acids* **57,** 39–45 (1997).
175. J M van der Lee, K. A. *et al.* Long-chain fatty acid-induced changes in gene expression in neonatal cardiac myocytes. *J. Lipid Res.* **41,** 41–47 (2000).
176. Mascaró, C. *et al.* Control of Human Muscle-type Carnitine Palmitoyltransferase I Gene Transcription by Peroxisome Proliferator-activated Receptor. *J. Biol. Chem.* **273,** 8560–63 (1998).
177. Barrero, M., Camarero, N., Marrero, P. F. & Haro, D. Control of human carnitine palmitoyltransferase II gene transcription by peroxisome proliferator-activated receptor through a partially conserved peroxisome proliferator-responsive element. *Biochem. J* **369,** 721–729 (2003).
178. Cole, M. A. *et al.* On the pivotal role of PPARα in adaptation of the heart to hypoxia and why fat in the diet increases hypoxic injury. *FASEB J.* **30,** 2684–2697 (2016).
179. Mandard, S., Müller, M. & Kersten, S. Peroxisome proliferator-activated receptor a a target genes. *C. Cell. Mol. Life Sci* **61,** 393–416 (2004).
180. Huang, B., Wu, P., Bowker-Kinley, M. M. & Harris, R. A. Regulation of Pyruvate Dehydrogenase Kinase Expression by Peroxisome Proliferator–Activated Receptor-α Ligands, Glucocorticoids, and Insulin. *Diabetes* **51,** 276–283 (2002).
181. Wu, P., Peters, J. M. & Harris, R. A. Adaptive Increase in Pyruvate Dehydrogenase Kinase 4 during Starvation Is Mediated by Peroxisome Proliferator-Activated Receptor alpha. *Biochem. Biophys. Res. Commun.* **287,** 391–396 (2001).
182. Holness, M. J. *et al.* Evaluation of the role of peroxisome-proliferator-activated receptor α in the regulation of cardiac pyruvate dehydrogenase kinase 4 protein expression in response to starvation, high-fat feeding and hyperthyroidism. *Biochem. J* **364,** 687–694 (2002).
183. Zungu, M., Young, M. E., Stanley, W. C. & Essop, M. F. Chronic treatment with the peroxisome proliferator-activated receptor a agonist Wy-14,643 attenuates myocardial respiratory capacity and contractile function. *Mol. Cell. Biochem.* **330,** 55–62 (2009).
184. Pfleger, J., He, M. & Abdellatif, M. Mitochondrial complex II is a source of the reserve respiratory capacity that is regulated by metabolic sensors and promotes cell survival. *Cell Death Dis.* **6,** 1–14 (2015).
185. DeBerardinis, R. J., Lum, J. J., Hatzivassiliou, G. & Thompson, C. B. The Biology of Cancer: Metabolic Reprogramming Fuels Cell Growth and Proliferation. *Cell Metab.* **7,** 11–20 (2008).
186. Ding, L., Liang, X., Zhu, D. & Lou, Y. Peroxisome proliferator-activated receptor a is

involved in cardiomyocyte differentiation of murine embryonic stem cells in vitro. *cell Biol. Int.* **31,** 1002–1009 (2007).
187. Ding, L., Liang, X.-G. & Lou, Y.-J. Time-dependence of cardiomyocyte differentiation disturbed by peroxisome proliferator-activated receptor alpha inhibitor GW6471 in murine embryonic stem cells in vitro. *Acta Pharmacol. Sin.* **28,** 634–642 (2007).
188. Sharifpanah, F., Wartenberg, M., Hannig, M., Piper, H.-M. & Sauer, H. Peroxisome Proliferator-Activated Receptor a Agonists Enhance Cardiomyogenesis of Mouse ES Cells by Utilization of a Reactive Oxygen Species-Dependent Mechanism. *Stem Cell* **26,** 64–71 (2008).
189. Kota, B. P., Huang, T. H. W. & Roufogalis, B. D. An overview on biological mechanisms of PPARs. *Pharmacol. Res.* **51,** 85–94 (2005).
190. Ferré, P. The Biology of Peroxisome Proliferator–Activated Receptors Relationship With Lipid Metabolism and Insulin Sensitivity. *Diabetes* **53,** s43-50 (2004).
191. Berger, J. P., Akiyama, T. E. & Meinke, P. T. PPARs: Therapeutic targets for metabolic disease. *Trends Pharmacol. Sci.* **26,** 244–251 (2005).
192. Grygiel-Górniak, B. Peroxisome proliferator-activated receptors and their ligands: nutritional and clinical implications – a review. *Nutr. J.* **13,** (2014).
193. Schoonjans, K., Staels, B. & Auwerx, J. Role of the peroxisome proliferator-activated receptor (PPAR) in mediating the effects of fibrates and fatty acids on gene expression. *J. Lipid Res.* **37,** 907–25 (1996).
194. Bishop-Bailey, D. Peroxisome proliferator-activated receptors in the cardiovascular system. *Br. J. Pharmacol.* **129,** 823–834 (2000).
195. Rakhshandehroo, M., Knoch, B., Müller, M. & Kersten, S. Peroxisome Proliferator-Activated Receptor Alpha Target Genes. *PPAR Res.* (2010). doi:612089
196. Braissant, O. & Wahli, W. Differential Expression of Peroxisome Proliferator-Activated Receptor-a ,-b , and -g during Rat Embryonic Development. *Endocr. Soc.* **139,** 2748–2754 (1998).
197. Michalik, L. *et al.* PPAR expression and function during vertebrate development. *Int. J. Dev. Biol* **46,** 105–114 (2002).
198. Finck, B. N. The PPAR regulatory system in cardiac physiology and disease. *Cardiovasc. Res.* **73,** 269–277 (2007).
199. Krey, G. *et al.* Fatty Acids, Eicosanoids, and Hypolipidemic Agents Identified as Ligands of Peroxisome Proliferator- Activated Receptors by Coactivator-Dependent Receptor Ligand Assay. *Mol. Endocrinol.* **11,** 779–91 (1997).
200. Xu, H. E. *et al.* Molecular Recognition of Fatty Acids by Peroxisome Proliferator–Activated Receptors that activate the PPARs in vitro have pharmacological effects similar to those reported for the synthetic PPAR. *Mol. Cell* **3,** 397–403 (1999).
201. Kliewer, S. A. *et al.* Fatty acids and eicosanoids regulate gene expression through direct interactions with peroxisome proliferator-activated receptors a and g. *Proc. Natl. Acad. Sci. USA* **94,** 4318–4323 (1997).
202. Forman, B. M., Chen, J. & Evans, R. M. Hypolipidemic drugs, polyunsaturated fatty acids, and eicosanoids are ligands for peroxisome proliferator-activated receptors a and d. *Biochemistry* **94,** 4312–4317 (1997).
203. Lee, W.-S. & Kim, J. Peroxisome Proliferator-Activated Receptors and the Heart: Lessons from the Past and Future Directions. *PPAR Res.* (2015). doi:271983
204. Murray, A. J., Panagia, M., Hauton, D., Gibbons, G. F. & Clarke, K. Plasma Free Fatty Acids and Peroxisome Proliferator–Activated Receptor a in the Control of Myocardial Uncoupling Protein Levels. *Diabetes* **54,** 3496–3502 (2005).
205. Thompson, M. P. & Kim, D. Links between fatty acids and expression of UCP2 and

UCP3 mRNAs. *FEBS Lett.* **568,** 4–9 (2004).
206. Wu, P. *et al.* Starvation and diabetes increase the amount of pyruvate dehydrogenase kinase isoenzyme 4 in rat heart. *Biochem. J.* **329,** 197–201 (1998).
207. Santilli, A. A., Scotese, A. C. & Tomarelli, R. M. A potent antihypercholesterolemic agent: [4-chloro-6-(2,3-xylidino)-2-pyrimidinylthio]acetic acid (Wy-14643). *Experientia* **30,** 1110–1111 (1974).
208. Keller, H., Devchand, P. R., Perroud, M. & Wahli, W. PPAR alpha structure-function relationships derived from species-specific differences in responsiveness to hypolipidemic agents. *J. Control. Release* **378,** 651–655 (1997).
209. Bernardes, A. *et al.* Molecular mechanism of peroxisome proliferator-activated receptor a activation by WY14643: A new mode of ligand recognition and receptor stabilization. *J. Mol. Biol.* **425,** 2878–93 (2013).
210. Finck, B. N. *et al.* The cardiac phenotype induced by PPARα overexpression mimics that caused by diabetes mellitus. *J. Clin. Invest.* **109,** 121–130 (2002).
211. Mukherjee, R., Jow, L., Croston, G. E. & Paterniti, J. R. Identification, Characterization, and Tissue Distribution of Human Peroxisome Proliferator-activated Receptor (PPAR) Isoforms PPARg2 versus PPARg1 and Activation with Retinoid X Receptor Agonists and Antagonists. *J. Biol. Chem.* **272,** 8071–8076 (1996).
212. Yang, X. *et al.* Tri-iodo-l-thyronine promotes the maturation of human cardiomyocytes-derived from induced pluripotent stem cells. *J. Mol. Cell. Cardiol.* **72,** 296–304 (2014).
213. Coll, T. *et al.* Oleate reverses palmitate-induced insulin resistance and inflammation in skeletal muscle cells. *J. Biol. Chem.* **283,** 11107–11116 (2008).
214. Hostetler, H. A., Petrescu, A. D., Kier, A. B. & Schroeder, F. Peroxisome proliferator-activated receptor α interacts with high affinity and is conformationally responsive to endogenous ligands. *J. Biol. Chem.* **280,** 18667–18682 (2005).
215. Kwon, B., Lee, H. K. & Querfurth, H. W. Oleate prevents palmitate-induced mitochondrial dysfunction, insulin resistance and inflammatory signaling in neuronal cells. *Biochim. Biophys. Acta - Mol. Cell Res.* **1843,** 1402–1413 (2014).
216. Salvadó, L. *et al.* Oleate prevents saturated-fatty-acid-induced ER stress, inflammation and insulin resistance in skeletal muscle cells through an AMPK-dependent mechanism. *Diabetologia* **56,** 1372–1382 (2013).
217. Perdomo, L. *et al.* Protective role of oleic acid against cardiovascular insulin resistance and in the early and late cellular atherosclerotic process. *Cardiovasc. Diabetol.* **14,** 75 (2015).
218. Soriguer, F. *et al.* Oleic acid from cooking oils is associated with lower insulin resistance in the general population (Pizarra study). *Eur. J. Endocrinol.* **150,** 33–39 (2004).
219. Abdelmagid, S. A. *et al.* Comprehensive profiling of plasma fatty acid concentrations in young healthy canadian adults. *PLoS One* **10,** 1–16 (2015).
220. Hessvik, N. P. *et al.* Metabolic switching of human myotubes is improved by n-3 fatty acids. *J. Lipid Res.* **51,** 2090–2104 (2010).
221. Lehman, J. J. *et al.* Peroxisome proliferator-activated receptor gamma coactivator-1 promotes cardiac mitochondrial biogenesis. *J. Clin. Invest.* **106,** 847–56 (2000).
222. Disch, D. L. *et al.* Transcriptional control of a nuclear gene encoding a mitochondrial fatty acid oxidation enzyme in transgenic mice: role for nuclear receptors in cardiac and brown adipose expression. *Mol Cell Bio* **16,** 4043–51 (1996).
223. Nagaos, M., Parimoo, B. & Tanaka, K. Developmental, Nutritional, and Hormonal Regulation of Tissue-specific Expression of the Genes Encoding Various Acyl-CoA Dehydrogenases and a-Subunit of Electron Transfer Flavoprotein in Rat. *J. Biol. Chem.* **268,** 24114–24124 (1993).

224. Kelly, D. P., Gordon, J. I., Alpers, R. & Strauss, a W. The tissue-specific expression and developmental regulation of two nuclear genes encoding rat mitochondrial proteins. Medium chain acyl-CoA dehydrogenase and mitochondrial malate dehydrogenase. *J. Biol. Chem.* **264,** 18921–18925 (1989).
225. Hill, B., Dranka, B., Zou, L., Chatham, J. & Darley-Usmar, V. Importance of the bioenergetic reserve capacity in response to cardiomyocyte stress induced by 4-hydroxynonenal. *Biochem. J* **424,** 99–107 (2010).
226. Sansbury, B. E., Jones, S. P., Riggs, D. W. & Darley-usmar, V. M. Bioenergetic function in cardiovascular cells: the importance of the reserve capacity and its biological regulation. *Chem. Biol. Interact.* **191,** 288–295 (2011).
227. Desler, C. *et al.* Is there a link between mitochondrial reserve respiratory capacity and aging? *J. Aging Res.* (2012). doi:192503
228. Young, M. E., Laws, F. A., Goodwin, G. W. & Taegtmeyer, H. Reactivation of Peroxisome Proliferator-activated Receptor a Is Associated with Contractile Dysfunction in Hypertrophied Rat Heart. *Biochemistry* **276,** 44390–44395 (2001).
229. Burridge, P. W. *et al.* Improved Human Embryonic Stem Cell Embryoid Body Homogeneity and Cardiomyocyte Differentiation from a Novel V-96 Plate Aggregation System Highlights Interline Variability. *Stem Cells* **25,** 929–938 (2007).
230. Burridge, P. W., Keller, G., Gold, J. D. & Wu, J. C. Production of de novo cardiomyocytes: Human pluripotent stem cell differentiation and direct reprogramming. *Cell Stem Cell* **10,** 16–28 (2012).
231. Lavrentyev, E. N., He, D. & Cook, G. A. Expression of genes participating in regulation of fatty acid and glucose utilization and energy metabolism in developing rat hearts. *Am J Physiol Hear. Circ Physiol* **287,** H2035-42 (2004).
232. Buroker, N. E., Ning, X. H. & Portman, M. Cardiac PPARa protein expression is constant as alternate nuclear receptors and PGC-1 coordinately increase during the postnatal metabolic Transition. *PPAR Res.* (2008). doi:279531
233. Wang, G. *et al.* Efficient, footprint-free human iPSC genome editing by consolidation of Cas9/CRISPR and piggyBac technologies. *Nat. Protoc.* **12,** 88–103 (2016).